INDC(CCP)-71/U

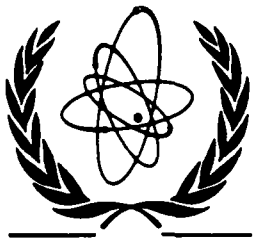

International Atomic Energy Agency

INDC INTERNATIONAL NUCLEAR DATA COMMITTEE

ANISOTROPY OF ELASTIC SCATTERING OF NEUTRONS

Survey of Experimental Data and their Analysis

M.N. Nikolaev, N.O. Bazazyants

January 1976

IAEA NUCLEAR DATA SECTION, KÄRNTNER RING 11, A-1010 VIENNA

INDC(CCP)-71/U

ANISOTROPY OF ELASTIC SCATTERING OF NEUTRONS

Survey of Experimental Data and their Analysis

M.N. Nikolaev, N.O. Bazazyants

January 1976

This book was translated from Russian by A. Schett (NEA/CCDN, Saclay) in collaboration with J. Weil (IAEA, Vienna) who translated the first 11 pages, F. Froehner (Karlsruhe, Germany) who checked the first 34 pages of the translation and L. Truran (NEA/CCDN, Saclay) who corrected the English.

The translation was suggested and directed by J.J. Schmidt (IAEA, NDS, Vienna) and undertaken with the permission of the authors.

NIKOLAEV, M.N., BAZAZYANTS, N.O.

Anisotropy of Elastic Scattering of Neutrons
Moscow, Atomizdat, 1972

Results and a critical review of all published data on angular distributions of elastic neutron scattering are given. Problems on the sufficiency of experimental and theoretical information and the compatability of results by different authors are considered, and the possible causes of divergencies are discussed. The data up to 15 MeV are represented in the form of graphs. A review of the main characteristics of the experimental methods and practically the whole bibliographic information on the problems considered are given.

150 figures, 33 tables and 237 references are contained in this book.

Introduction

The angular distributions of elastically scattered neutrons are interesting from several points of view.

In nuclear physics, data on angular distributions (together with the scarcity of information on neutron polarization due to scattering) are employed to determine the scattering phases of neutron waves with different orbital angular momenta and parity and to establish the spins of the individual resonances. Knowledge of how the scattering anisotropy depends on the energy of neutrons and on the atomic weight of the scattering nuclei is used to select the parameters of the nuclear optical model.

In reactor physics, a correct description of neutron fluxes in various media necessitates knowledge of the angular distributions of

elastically scattered neutrons. If the flux gradient in the medium is high, approximations which describe the anisotropy of the neutron flux accurately enough must be used to describe neutron transport. If, however, in this case the neutron scattering is strongly anisotropic, an increase in the accuracy with which the anisotropy of the neutron flux is taken into account must go along with an increase in the accuracy with which allowance is made for scattering anisotropy (despite the fact that the influence of the latter on the results of the neutron field calculations is smaller than that of flux anisotropy). Thus, in describing the propagation of a group of fission neutrons able to induce U-238 fission in an extended uranium or U-238-oxide medium, use of the P_5- approximation gives rise to an appreciable increase in accuracy over the P_3- approximation. In doing so, however, scattering anisotropy must be taken into account with an accuracy of, at least, up to three terms of angular moments , since the error due to the use of the ordinary transport approximation is in this case equal to or even greater than the increase in accuracy caused by using the P_5- instead of the P_3-approximation. Especially important is the role of angular distributions in calculations of radiation protection of nuclear reactors. Mainly neutrons scattered through small angles in the shields penetrate through the thick shielding layers. It is in just this range of angles that the most penetrating and dangerous fast neutrons have a pronounced diffraction peak in the cross-section, which must be taken into account in the calculations.

Allowance for scattering anisotropy also plays a very important role in shadow shielding calculations. In this case, the character of the angular distribution of the neutrons scattered in the surrounding medium determines, to a substantial extent, the optimum thickness of the shielding cone.

Therefore, data on angular distributions of elastically scattered neutrons are of great interest to a wide range of specialists.

Until very recently, the Atlas on Angular Distributions of Neutron Reaction Products compiled by M.D. Goldberg, V.M. May and T.R. Stehn of the Brookhaven National Laboratory (BNL-400) was the most complete compilation of data on elastically scattered neutron angular distributions. The second edition of this atlas was published at the end of 1962 [1, 2].

The majority of data obtained later on is collected in the bulletins of the Information Centre on Nuclear Data [3].

As a rule, the information on scattering anisotropy in the compilations mentioned is given in the form of curves showing the angular dependence of differential scattering cross-sections for different energies. This representation has several disadvantages. In particular, interpolation and extrapolation of the experimental results with respect to energy is very difficult.

In reactor physics as well as in nuclear physics, angular distributions are usually employed in the form of Legendre polynomial expansions. It was, therefore, very useful to set up the scattering anisotropy data compilation in the form of energy dependent Legendre polynomial expansion coefficients of angular distributions. This compilation - as well as a discussion of its results - is the purpose of this book. Information on angular distributions of elastically scattered neutrons obtained and published up to the middle of 1967 is presented. There are no data given on the anisotropy of inelastic scattering and the angular distributions of products of other neutron reactions.

The angular dependence of differential elastic-scattering cross-sections is described by an expression of the form

$$\sigma_s(\mu) = \frac{1}{4\pi} \sum_{l=0}^{N_s} B_l P_l(\mu), \qquad (1)$$

where μ is the cosine of the scattering angle in the laboratory system; and P_l is the l th-order Legendre polynomial. A sufficient number of terms in the expansion (1) was taken for fitting the experimental data with an accuracy up to the errors in their determination.

The B_l coefficients are connected with the frequently used angular momentum coefficients, $\omega_l = (2l + 1) \cdot \bar{P}_l$ (where the bar denotes averaging over the angle with the weight of the differential scattering cross-section) by the simple relation

$$B_l = B_0 \omega_l. \qquad (2)$$

The values of the expansion coefficients calculated from the experimental data on differential elastic neutron scattering cross-sections are plotted as points in the graphs representing the energy dependence of these coefficients. This representation permits easy comparison of the results of different authors, energy interpolation and extrapolation and energy averaging (which is necessary, for example, in setting up group constants for reactor calculations).

In many cases, the authors of original work themselves represent their data in the form of energy dependent Legendre coefficients of their angular distributions. Such a representation is, in particular, used in practically all modern works where the angular distributions are measured with a high energy resolution for a large number of energies. This is natural since the number of expansion terms needed for a description of the angular distribution is nearly always substantially smaller than the number of experimental points with respect to the angles. Thus, the representation of angular distributions with the help of Legendre coefficients is more compact.

However, in those experimental papers where the angular distributions are measured only for a small number of neutron energies, the data on scattering anisotropy are, as a rule, plotted as graphs showing the angular dependence of the differential scattering cross-section for each one of the energies investigated. In these cases, the data on scattering anisotropy presented in this book cannot be immediately compared with the data of the original papers, which is of course, a drawback of our representation, especially since the values of the expansion coefficients generally depend on the method of their determination. We hope, however, that this disadvantage is compensated by the convenience with which our representation can be used in practical work.

Processing of experimental and theoretical information as well as a good deal of work in setting up the tables and figures in this book was carried out by A.F. Larina, A.S. Zabrodskaya, K.I. Nesterova, N.A. Nikolayeva and V.V. Mikryukova, to whom the authors are deeply indebted.

Legendre Polynomial Expansion of Angular Distributions

We have determined the values of the Legendre coefficients of experimental angular distributions either by the method of least squares or by a second method described below. In this method, the optimum number of Legendre polynomials N_o needed for a description of the experimental data with an accuracy consistent with the uncertainties in the measured differential cross-sections was obtained from the Gauss (least-squares) criterion.

In the least-squares method the experimental data measured for, say, M angles were described by formula (1) with a varying number of expansion terms, N. For each number N, the coefficients which minimize the weighted sum of squared deviations of the experimental data from the theoretical curve, were determined :

$$S(N) = \sum_{m=1}^{M} \left[\sigma_s(\mu_m) - \frac{1}{4\pi} \sum_{l=0}^{N} B_l P_l(\mu_m) \right]^2 w_m. \qquad (3)$$

Quantities inversely proportional to the squares of the experimental errors were used as the statistical weights, W_m. (In those cases where in the original work the errors are not given, the errors of the differential cross-sections were taken to be equal to the square roots of the cross-section values). The weights were normalized to unity :

$$\sum_{m=1}^{M} w_m = 1. \qquad (4)$$

The System of equations for determining the B_l and minimizing (3) is obtained by differentiating (3) with respect to all B_l and setting the partial derivatives equal to zero :

$$\sum_l B_l T_{ln} = C_n, \tag{5}$$

where

$$T_{ln} = \frac{1}{(4\pi)^2} \sum_{m=1}^{M} P_l(\mu_m) w_m P_n(\mu_m); \tag{6}$$

$$C_n = \frac{1}{4\pi} \sum_{m=1}^{M} \sigma_s(\mu_m) w_m P_n(\mu_m). \tag{7}$$

Let T^{-1} be the inverse of the matrix T. Then,

$$B_l = \sum_n C_n T_{nl}^{-1}. \tag{8}$$

The variances of the expansion coefficients thus obtained are determined by the diagonal elements of the inverse matrix

$$D(B_l) = \delta T_{ll}^{-1},$$

where δ is the so-called general dispersion, for which the larger of the two following estimates

$$\sigma(N_0) = S_{min}(N_0)/(M - N_0 - 1) \tag{9}$$

$$\delta = \frac{1}{\sum_{m=1}^{M} 1/[\delta\sigma_s(\mu_m)]^2}, \tag{10}$$

was used, $\delta\sigma(\mu_m)$ being the error in the measurement of $\sigma_s(\mu_m)$. In those cases where these errors were not known or could not be determined accurately (which, for example, occurred when the experimental points had to be taken from small-scale graphs), the latter estimate only served as a control.

The optimum number of Legendre polynomials N_o in formula (1) was determined from the condition that δ (N) be minimal (Gauss criterion).

In some cases, several (two or three) minima were observed in δ as a function of N. In such cases the minimum for which δ (N) was comparable with the estimate of δ based on the experimental errors (10), was chosen.

Sometimes the minimum in the δ (N) curve was very flat. In this case, N_o was chosen as the smallest number N in the region of this minimum for which δ (N) proved to be sufficiently close to the estimate (10), i.e., did not differ from it by more than a factor of 1.5 or 2.

The application of the Gauss criterion is practically equivalent to the requirement that, in expansion (1), one should restrict oneself to those terms which can be determined with an error of less than 100%.

For a sufficiently large number of experimental points M - depending on the complexity of the shape of the angular distribution (i.e. on N_o) and on the angular spacing of experimental points - the angular distribution obtained by the method described above usually reproduced the experimental data well and met the a-priori physical requirements (e.g., it did not vanish anywhere). A typical example of such an expansion is shown in Fig. 1 .

In those cases, however, where the number of experimental points was not large enough, the solution obtained by the least-squares method becomes unstable with increasing N : the values of even the first expansion coefficients with $\ell \ll N$ obtained by this method prove to be too large and vary strongly even if N increased only by one; the angular distribution constructed from the coefficients - although passing close to the given experimental points - greatly deviates elsewhere from a smooth curve plotted through these points; for some angles, the calculated differential cross-section even becomes negative (Fig. 2). The non-diagonal elements of the inverse matrix which determine the correlations between the errors of the values found, prove to be comparable to the diagonal elements in these cases : the correlation coefficients determined from

$$\rho_{ln} = T_{ln}^{-1} / \sqrt{T_{ll}^{-1} T_{nn}^{-1}} < 1,$$

are close to unity.

The correlation coefficients show the extent to which the coefficients B_ℓ vary (relative to the estimated error in their determination) if the coefficients B_n vary by the value of the error in their determination. If the $\rho_{\ell n}$ are close to unity, the variation of one expansion coefficient gives rise to substantial variations of the other coefficients which also explains the instability of the solution. The fact that the correlation coefficients are close to unity indicates that the system of equations (5) is nearly degenerate. In other words, if we try to determine a large number of expansion coefficients rather exactly from experimental data, we expect to extract more information from the data than they contain. On the other hand, a smaller number of Legendre polynomials does not guarantee a sufficiently close approximation of the data either (i.e., the Gauss criterion is not fulfilled). In these cases, the a-priori physical information that the solution is positive and relatively smooth must be used in processing the data. For this purpose, there exist several mathematical methods whose application, however, makes the solution of the problem much more difficult. On the other hand, all these methods are not and cannot be rigorous since the problem itself is mathematically incorrect. Therefore, instead of working out computer codes on the basis of these methods, we have, in order to take into account the necessary a-priori information, deemed it possible to apply the following simple method which allows complicated calculations to be replaced by the direct use of our experience and common sense.

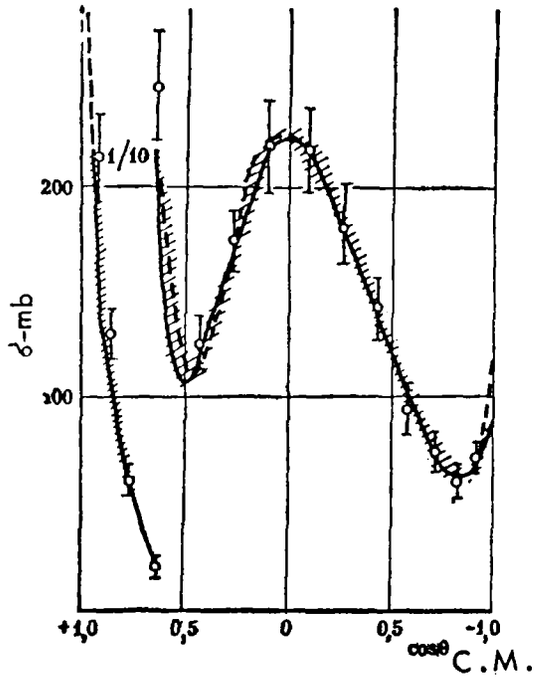

Figure 1. Angular distribution of neutrons with an energy of 2.0 MeV scattered elastically from Pu-239. The circles are experimental data taken from Ref. /C-6/. The full curve is drawn by hand through the experimental data. The dotted curve has been obtained by the least-squares method ($N_o = 6$). The error range of this curve is indicated by bars.

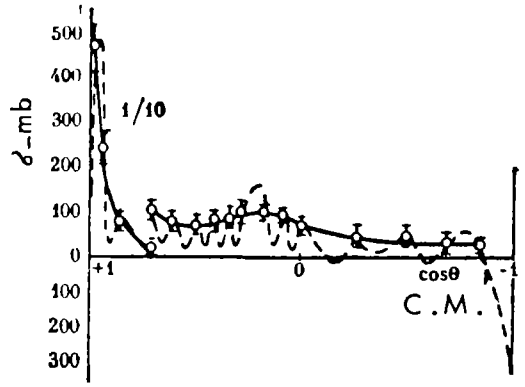

Figure 2. Angular distribution of neutrons with an energy of 7 MeV scattered elastically from U-238. The circles are experimental data from Ref. [W-8]. The full curve was drawn by hand. The dotted curve was obtained by the least-squares method for $N = N_o = 11$.

A smooth curve was drawn by hand through the experimental points. In those cases where the peaks of angular distribution were insufficiently measured in the experiments, information on the angular distributions of neutrons of similar energies scattered from the nucleus under consideration and from its neighbouring nuclei was used (subjectively). In some cases, the behaviour of the differential cross-section in the region of the scattering maximum was chosen so as to ensure that the integral scattering cross-section be equal to the known difference between the total cross-section and the cross-section of the nonelastic processes.

The results of many checks showed that in cases where the least-squares solution of the problem was stable, the curves drawn by hand do not substantially differ from those generated by the least-squares method : the difference between them is less than the accuracy with which the form of the elastic distribution estimated by the least-squares method was determined (see Fig. 1).

After the smooth curve had been plotted, points were taken from it at values of the scattering angle cosine which divide the interval (-1, +1) into an even number of parts. Then these points were used as input for the ordinary least-squares programme, in which case the weights were taken either inversely proportional to the square of the cross-section or estimated on the basis of the accuracy of the experimental data.

Two versions of subdivision were adopted : 20 and 40 intervals, depending on the complexity of the angular distribution.

The expansion coefficients determined in this way were used to calculate the values of the differential cross-sections at those scattering angles for which experimental data were available. In doing so, various numbers N of expansion coefficients were taken into account in the Legendre expansion.

For each of these numbers a sum of squared deviations (3) was found, after which the same criteria as in the usual application of the least-squares method were applied to determine N_o.

Since for a sufficiently large number of points the differences between results obtained by the methods described were insignificant (Table 1), the second method was often used to expand experimental data which could also be processed directly by the normal least-squares method. In particular, we prefer to use this method in those cases where the experimental data are given graphically in the publication in question : reading off data from a smooth curve for chosen standard values of the scattering angle cosine may be performed substantially faster and more accurately than reading off an even essentially smaller number of direct experimental data at, as a rule, nonstandard cosine values.

Table 1: Expansion coefficients of the angular distribution of neutrons with an energy of 2 MeV scattered elastically from Pu-239 as calculated by different methods.

Input data in least-squares method	B_0	B_1	B_2	B_3	B_4	B_5	B_6
Experimental points	4,33± ±0,09	7,15± ±0,23	8,09± ±0,33	9,04± ±0,32	7,84± ±0,31	3,66± ±0,25	1,22± ±0,18
Points from hand-drawn curve	4,26	7,10	7,96	9,03	7,66	3,53	1,17

In processing series of such data the method of least squares was directly applied to the experimental points only as a check to some typical angular distributions.

When the curve is drawn by hand, it is not possible to calculate (with the help of the calculation program available to us) the error matrix of the expansion coefficients to be determined. In the present compilation, however, this drawback does not apply since, because of the following facts, we have decided not to carry out an estimation of the errors of the B_ℓ values :

1. The scatter of the experimental data obtained by different authors, as a rule, substantially exceeds the estimates based on the errors in the values of B_ℓ obtained from the accuracies of differential cross-sections given in individual publications. It is, therefore, more justified to base error estimates on the magnitude of this scatter. If there are only a few experimental points in the diagram and their comparison is difficult, the error in these data can, in most cases, be estimated from the discrepancy of the results given in the same papers for other elements from the smooth curves drawn through the ensemble of all experimental points available for these elements.

2. Owing to the rather strong correlation usually present between the values of B_ℓ , the errors of these quantities alone only yield insufficient information on the accuracy of the results.

3. In many cases, presentation of the errors would make the diagrams less clear.

The Calculation of Angular Distributions of Neutrons Scattered Elastically by means of the Nuclear Optical Model

In the energy range above 5 MeV for the majority of nuclei, angular distributions are measured only for one or two energy points. For interpolation between these points, results obtained by optical-model calculations have been used whenever angular distribution data were unavailable.

In recent years the optical model of the nucleus has been qualitatively confirmed and quantitatively refined to such an extent that it has become a very important source of information on cross sections which complements the experimental data. The accuracy of optical-model calculations based on a single set of potential parameters for all nuclei is not very high. Between these results and the experimental data there are usually systematic discrepancies whose magnitude depends on which nucleus and which energy is considered. The calculated values, however, correctly describe the general behaviour of the cross-section as a function of the energy and of the mass number of the nucleus. They are, therefore, very useful for interpolation and extrapolation of the available data of, as yet uninvestigated, nuclei and energy ranges.

As is well known one can calculate, by means of the optical model, that part of the elastic scattering which does not lead to compound nucleus formation. This cross section approximates the total elastic cross section measured in an experiment only if the number of open channels for decay of the compound nucleus is high and consequently, because of the competition between them, the probability for compound elastic scattering is low. Therefore we use results of optical-model calculations only in energy ranges where this condition is fulfilled.

In the calculations a local optical potential given by Björklund and Fernbach /4/ is used :

$$V(r) = -V_{CR} f(r) - iV_{CI} g(r) + V_{so}\left(\frac{\hbar}{\mu_c}\right)^2 \frac{1}{r} \cdot \frac{\partial f(r)}{\partial r} (\sigma l),$$

where

$$f(r) = \left[1 + \exp\left(\frac{r-R}{a}\right)\right]^{-1}, \qquad g(r) = \exp\left[-\left(\frac{r-R}{b}\right)^2\right]$$

($R = r_o A^{1/3}$; A is the mass number; r_o = 1.25 Fermi; b = 0.98 Fermi)

The individual properties of nuclei were in a certain way taken into account by introducing a dependence of the parameter V_{CR} on the isotopic spin of the nucleus,

$$V_{CR} = V_0\left(1 - \frac{N-Z}{2A}\right),$$

where N and Z are the numbers of neutrons and protons in the nucleus. The energy dependence of the parameters V_o, V_{CI} and a was assumed as follows :

$$V_o = \begin{cases} 52 \text{ MeV} & \text{for } E \leqslant 1 \text{ MeV} \\ (52 - 0.35E) \text{ MeV} & \text{for } E > 1 \text{ MeV} \end{cases}$$

$$V_{CI} = \begin{cases} 6 \text{ Mev} & \text{for } E \leqslant 0.1 \text{ MeV} \\ (6 + 0.75E) \text{ MeV} & \text{for } 0.1 < E \leqslant 4 \text{ MeV} \\ (8.2 + 0.2E) \text{ MeV} & \text{for } E \geqslant 4 \text{ MeV} \end{cases}$$

$$a = \begin{cases} 0.65 \text{ Fermi} & \text{for } E \leqslant 4 \text{ MeV} \\ 0.70 \text{ Fermi} & \text{for } E > 4 \text{ MeV} \end{cases}$$

The spin-orbit parameter V_{SO}, which has little influence on the cross-section, was assumed in the form

$$V_{so} = 0{,}2 V_{CR}.$$

This set of parameters was derived by I.K. Averyanov, B.Ya. Guzhovskii and V. A. Saraeva as optimally describing the totality of experimental cross-section values obtained until 1963. Since data which were obtained later do not change the energy and mass number dependence of the cross-section qualitatively, their utilization for the selection of optical-model parameters cannot significantly influence these parameters.

Calculations with a spherical potential are inadequate for nuclei with $A \sim 150$-190 and $A > 222$, which are considerably deformed, and the nuclei with A~60-80, which have a large dynamical surface deformation. In the high energy range of interest to us, however, the influence of this particularity seems to be weak.

Characteristics of Experimental Methods *

Geometry of Experiment

For the measurement of angular distributions two geometries are used for the arrangement of the source, the scatterer and the detector. The first, which is called ring geometry, is represented in Figure 3. The source neutrons (1) emitted under an angle and symmetrical around the axis are scattered on a ring (2) of the material under study, and finally registered by the detector (3).

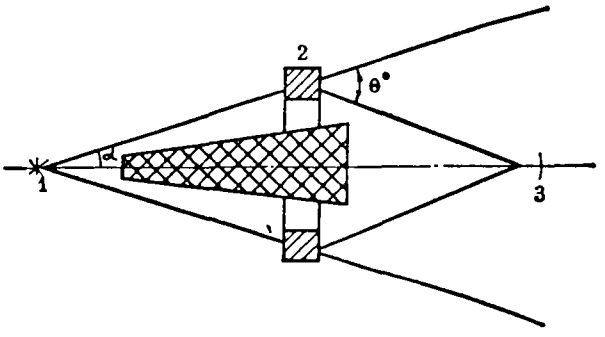

Figure 3. Ring geometry arrangement : 1 source, 2 scatterer, 3 detector

The advantage of the ring geometry is the possibility of arranging a rather large quantity of material in a sufficiently thin layer, so that the multiple scattering corrections are small and easy to calculate. This method therefore provides a comparatively high scattering yield.

The disadvantage of the ring geometry is the rapidly decreasing scattering yield if one moves to small or large scattering angles. When the angular distribution has a comparatively simple form, the measurement at very small and very high angles is not important. In the case of strong anisotropic neutron angular distribution at high energies, the decrease of the scattering yield at small angles is compensated by the increase of the differential cross section.

---

* The essential characteristics of the experiments, the results of which have been used in the present compilation, are tabulated (page 250) at the end of the book. Here we give a short review of these characteristics.

A principal disadvantage of ring geometry is the strong dependence of the scattering angle on the position of the scatterer and the detector, which makes automation of the experimental procedure difficult.

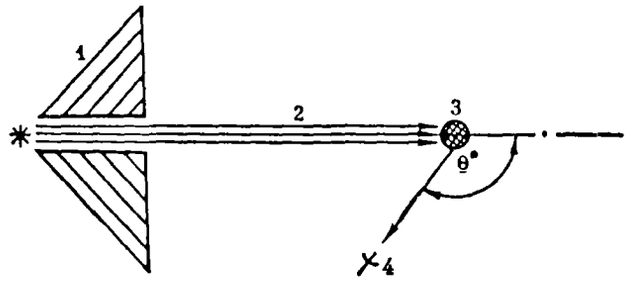

Figure 4 : Central Geometry : 1 Kollimator, 2 neutron beam, 3 target, 4 detector

The second geometry used is the central geometry (Fig. 4). By means of a collimator (1) neutrons (2) of a given energy are selected, and those which are scattered through the appropriate angle in target (3) of the material studied hit the detector (4), positioned at a given angle relative to the neutron beam.

Most of the recent data on neutron elastic angular distribution are obtained by the central geometry.

Neutron Sources

In the majority of the experiments below 14 MeV monochromatic sources with neutrons from the reactions T(p,n), Li(p,n), D(d,n) have been used. Usually, a Van de Graaff accelerator has been employed as a monochromatic source of the protons and deuterons which induce these reactions. This permits variation of the energy of the charged particles, and as a consequence, the energy of neutrons, over a wide range (up to some MeV). As a neutron source for neutrons with 14-15 MeV the exothermic reaction T(d,n) is used. The deuterons inducing this reaction are in the majority of cases accelerated with an ordinary cascade generator.

In some old experiments photoneutrons have been utilized. For instance, in the work /L-1/, a Na-γ-Be source was used to obtain neutrons with an energy of 0.9 MeV.

For studying neutron angular distributions in the low energy range (up to 0.5 keV) monochromatic neutrons were also obtained with the time-of-flight method /A-13/. For this purpose the pulsed fast reactor IBR was employed as neutron source.

Neutron Detectors

For measuring the angular distributions of neutrons elastically scattered in the relatively low energy range, where inelastic scattering is absent or small, no spectrometric properties are needed. In this case boron counters in a hydrogenous moderator can be used as detector.

The efficiency of such a detector is high and depends little on the energy. Such detectors have, for example, been used by the group of experimentalists at the Argonne Laboratory /L-2, L-4, L-6 et al./, which has obtained extremely rich and detailed information on the anisotropy of neutrons scattered at energies below 1.5 MeV for a great number of nuclei. With this method neutron angular distributions have also been measured in energy regions where inelastic scattering is significant. In these cases the results of the original work have been corrected accordingly. The way in which this correction has been made will be discussed below.

Above the inelastic scattering threshold one has to use spectrum-sensitive detectors which permit the separation of elastically, from inelastically, scattered neutrons. Different types of proton recoil detectors have been widely applied for this purpose: hydrogen ionization chambers, proportional counters and scintillation detectors with organic scintillators of different types.

In a great number of publications, where the task was to study only elastic scattering, a complete spectral analysis of the scattered neutrons was not carried out. Single registered neutrons with energies higher than some threshold, gave a well-defined minimum proton recoil pulse, registered by the electronic circuit. Since the efficiency of counting elastically scattered neutrons decreases with increasing detector threshold, one cannot always set the electronic bias so high that all inelastically scattered neutrons are cut off. This leads to a distortion of the angular distribution and

a measured scattering cross section which is too large.

Unfortunately, the authors of the original papers have rarely applied corrections for this effect. The characteristics of the experimental device, like the form of the pulse height distribution and the determination of the energy response of the detector at energies above the threshold are usually not given in the publication. One has, however, to point out that the correction for the inelastic scattering contribution is usually not big. Our estimates indicate that in the majority of cases these corrections are smaller than the uncertainty of B_ℓ estimated from the scatter between the data from different authors. Wherever this is not true, we discuss it in the comments to the graphs showing the energy dependence of B_ℓ .

The best way to separate elastic and inelastic scattering is to use the time-of-flight method with high resolution. This method permits not only angular distributions for elastically scattered neutrons, but also neutrons scattered inelastically to individual levels (if the number of excited levels is not too large) to be obtained. Owing to the complexity of the instrumentation necessary for this method, the number of such measurements is still relatively small. Nevertheless, the data on neutron elastic angular distributions obtained by this method represents a considerable part of all available data. It is an established fact that the time-of-flight method is suitable in the energy region where the structure of the inelastically scattered neutron spectra are sufficiently simple and can be resolved for separated levels.

Measurement of Angular Distributions of Neutrons Scattered by Light, Gaseous Elements by means of the Energy Spectrum of the Recoiling Nuclei

Angular distributions of neutrons scattered by nuclei such as helium, nitrogen, oxygen , are often determined using a method which is based on the measurement of the recoil nucleus energy spectra by means of ionization chambers filled with the gas to be studied.

The energy of the recoil nucleus E' is related to the cosine of the scattering angle $\mu_{C.M.}$ in the centre-of-mass system by the following linear relation

$$E' = \frac{2AE_n}{(A+1)^2}(1-\mu_{c.m.}).$$

E_n is the incident neutron energy. A is the mass of the scattering nucleus in units of the neutron mass.

In this way the calculation of the angular distribution of elastically scattered neutrons from the energy spectra of the recoil nucleus is very easy.

The disadvantage of the method is the difficulty of measuring the scattering at small angles : the corresponding recoil energy of the nucleus is small and its pulse is likely to be lost in the background. This makes it difficult to obtain sufficiently complete data on the form of the angular distribution of neutrons with high energy : the maximal diffraction at small angles is very difficult to measure with this method.

Application of this method to the measurement of elastic scattering of oxygen is further complicated by the fact that because of the high probability for electron attachment to oxygen molecules one must operate the ionization chamber in the ion-collection mode. In this mode it is difficult to achieve a low noise level.

The energy resolution required is defined by the character of the cross-section structure in the energy range to be studied.

In the range of relatively low energies the resolution reached in recent experiments permits a sufficiently large number of energy points to be measured so that the resonance structure of the angular distribution is obtained. It is clear that in order to judge such experimental results a still higher resolution is required.

In a series of papers high resolution has been employed only at some energies, at the resonances and one or two energy points in regions between the resonances. If it is true that all resonances in the energy interval considered have been measured, then the data obtained in these experiments are in principle sufficient for a representation of the energy dependence of the angular distribution between the energies investigated. For narrow resonances this can be done with the Blatt-Biedenharn formula /5/. The resonance widths and the resonance energies appearing in this formula are obtainable from data on the energy dependence of the total cross-section. Such an analysis, however, is very difficult and because of the limited accuracy of the experimental data, its results are usually not quite reliable. A full analysis is complicated by the fact that the influence of a resonance is still considerable at rather great distances, as follows from calculations of the interference between resonances and potential scattering (the interference term at great distances from the resonance is proportional to $\Gamma/(E-E_o)$, where Γ is the total width; E_o is the resonance energy). Consequently, the range of influence of separated resonances is generally quite large, and a measurement in regions between resonances cannot be represented simply as the angular distribution of the potential scattering. The correction of the influence of nearby resonances by means of the Blatt-Biedenharn theory is, in this case, not correct : it is necessary to account for the interference between resonances appearing in the shape of angular distributions, even when the spins and parities of the resonances are different.

Due to the difficulties pointed out we did not perform such an analysis of experimental data.

It should be stressed that in the range of unresolved resonances, relatively high energy resolution and the small number of energy points measured is a still more unfavourable factor. The results of such experiments can neither be interpreted as an average over a large number of resonances, nor as angular distributions of separated resonances. This is often the cause of the discrepancies of data from different authors.

As already pointed out, in nuclear physics, data on angular distributions of elastically scattered neutrons are usually used only for fitting optical model parameters. This model does not describe the energy dependence of the average cross-section in all details.

One has, however, to use it since the experimental studies of the energy dependence of the angular distributions averaged over many resonances are unsatisfactory in large energy regions (despite the fact that carrying out such measurements is technically much simpler than measuring angular distributions of separated resonances which require a high resolution). It is true that recently the interest of nuclear physicists in such measurements increased in connection with the discovery of the so-called intermediate structure of cross-sections. The first publication in which a detailed measurement of the unresolved resonance region is given appeared in reference /C-15/.

Nevertheless, the energy dependence of the coefficients B_ℓ in the energy region above 1.5 MeV (i.e. for those energies where the anisotropy of scattering is particularly high!) is at present measured with an accuracy which is far from sufficient for nuclear reactor design.

Measurement of Average Characteristics of Resonance Structure in Angular Distributions.

For understanding neutron transport in a medium with resonance cross-sections and anisotropic scattering one has to study the influence of the resonance structure of the cross-section not only on the values of the mean effective cross-sections, but also for the mean effective angular distribution. As shown in references /6 - 8/, the n-th harmonic should be averaged over the spectrum of the n-th harmonic of the neutron flux, which in first approximation is directly proportional to the (n + 1) - th degree of the total cross-section. In this way, averaging over the peak regions one obtains a decrease, and in the regions of interference minima, a more pronounced increase the higher harmonics of the neutron flux one considers. Starting from experimental data taken with thin samples one can thus derive an excellent average over resonances for the scattering anisotropy that can noticeably affect the integral characteristics of neutron transport in bulk media.

In shielding layers far from the source, the role of energy regions with low total cross-sections is even more pronounced than in the above-mentioned approximation, and the influence of resonance self-shielding is greater.

For consideration of this effect it is not necessary to know the exact energy dependence of the angular distribution. It is sufficient to measure the average parameters of the resonance structure which can be determined by a method outlined in refs. /6, 7/. This method can be explained as follows (Figure 5).

One measures the scattering anisotropy of neutrons belonging to an energy interval ΔE which contains a sufficiently large number of resonances. Then, the measurement is repeated with the neutron beam passing through a filter of the investigated material. If the conditions of "good geometry" are fulfilled, so that each collision in the filter leads to neutron removal from the beam, then the neutron spectrum incident on the sample has the form

$$f(E)e^{-\Sigma_t(E)t}, \qquad (11)$$

where $\Sigma_t(E)$ is the total macroscopic cross-section, t is the thickness of the filter and f(E) is the source spectrum. It is obvious that neutrons with energies corresponding to resonance peaks will be suppressed in the spectrum of the filtered beam.

If the measurement is performed with a wide range of filter thicknesses one can deduce from the results the correlation function between the probability for scattering by a given angle and the total cross-section, i.e., the conditional probability density $S(\mu, \sigma_t)$ for scattering by an angle $\arccos\mu$ in the case where the cross-section has the value σ_t.

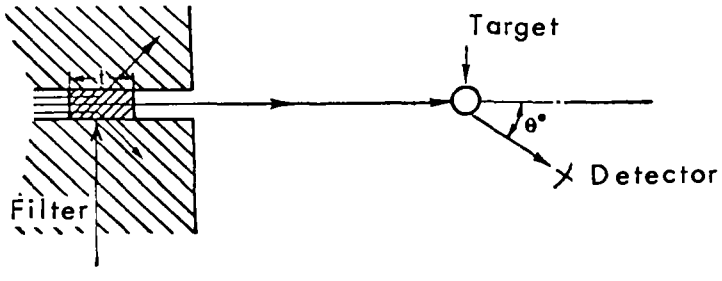

Figure 5. Scheme of measurement of the influence of the resonance structure on the average effective angular distribution.

In fact, the differential scattering cross-section for the filtered beam can be written as follows :

$$\sigma_s(\mu, t) = \int_{\Delta E} f(E)\,\sigma_s(\mu, E)\,e^{-\Sigma_t(E)t}\,dE = \bar{f}\int_{\Delta\sigma_t} \sigma_t S(\mu, \sigma_t)\,p(\sigma_t)\,e^{-\Sigma_t t}\,d\sigma_t. \quad (12)$$

Here, $p(\delta_t)$ is the distribution function of the total cross-section in the interval ΔE (weighted with $f(\bar{E})$), which can be determined from transmission experiments (when the detector is placed at the position of the scatterer); $\bar{f}$, owing to the lack of correlation between the source spectrum and the cross-section of the sample, is simply the (energy) average of the neutron intensity in the incident beam.

The experimentally determined transmission $T(t)$ through a filter with thickness t is related to $p(\delta_t)$ as follows :

$$T(t) = \int_{\Delta\sigma_t} p(\sigma_t)\,e^{-\Sigma_t t}\,d\sigma_t, \quad (13)$$

where $\Delta\delta_t$ is the range of total cross-sections in the energy interval ΔE.

The function $S(\mu, \delta_t)$ is determined by simultaneously solving the integral equations (12) and (13).

The average value of any function of the scattering- and the total cross-section can be given as follows :

$$\langle \varphi[\sigma_s(\mu), \sigma_t] \rangle = \int_{-1}^{+1} d\mu \int_{\Delta\sigma_t} \varphi[\sigma_s(\mu), \sigma_t]\,p(\sigma_t)\,S(\mu, \sigma_t)\,\frac{\sigma_t}{\sigma_s(\mu)}\,d\sigma_t. \quad (14)$$

In particular, the value

$$\bar{B}_l = \frac{\langle B_l/\sigma_t^{l+1} \rangle}{\langle 1/\sigma_t^{l+1} \rangle}, \quad (15)$$

which occurs in the transport theory of resonance neutrons is equal to :

$$\overline{B}_l = \frac{\int_{-1}^{+1} d\mu \int_{\Delta\sigma_t} \sigma_t^{-l} P_l(\mu)\, S(\mu, \sigma_t)\, p(\sigma_t)\, d\sigma_t}{\int_{\Delta\sigma_t} \sigma_t^{-(l+1)}\, p(\sigma_t)\, d\sigma_t} . \qquad (16)$$

In spite of the rather large uncertainty of the procedure for solving the system of integral equations, the resulting estimates for the functions S and p turn out to be sufficient for determining, with tolerable accuracy, the scattering anisotropy required for reactor calculations.

The method described was applied to the estimation of the average characteristics of the resonance structure in the angular distribution of neutrons scattered from iron /9/. The experiment has integral character : the energy distribution of incoming neutrons was similar to a fission spectrum above approximately 1.5 MeV. Nevertheless, the influence of the resonance structure in the cross-section appeared sufficiently clear. The data obtained allowed us to estimate the influence of resonance self-shielding of the angular distribution on the relaxation length of fast neutrons in iron. This effect was shown to be approximately 5%, which is roughly five times the uncertainty in the determination of the relaxation length which could be considered tolerable in shielding calculations.

Unfortunately, other more detailed measurements of the average characteristics of resonance structure in neutron angular distribution do not exist. One has to point out that experimental data on the resonance structure in angular distributions are clearly not sufficient for an accurate calculation of the resonance self-shielding, even for the energy range where the resolution is good enough to resolve the resonances. The problem is that the experimental accuracy in the regions of cross-section interference minima is rather low. Moreover, owing to the finite resolution, these minima show rather considerable contributions from the "smeared out" wings of the resonance peak. However, as already mentioned, just those regions with low cross-sections give the main contribution to the spectrum-averaged cross-section. Therefore, a calculation of resonance self-shielding of the cross-section requires a higher resolution than, say, the phase analysis of experimental data.

Angular Resolution

In the majority of the experiments the angular resolution is sufficiently high, and it is not necessary to take it into account in the calculation of B_ℓ from experimental data. An exception is the angular distributions at high energies, where the finite angular resolution causes a diffraction peak of small-angle scattering to be somewhat smeared out. Calculations show (Table 2), that the influence of this effect is comparatively low (only for high harmonic amplitudes is it not negligible).

Table 2:

Influence of the angular resolution on the coefficients of the expansion of angular distribution of neutrons with an energy of 14 MeV, scattered on Ni . The angular resolution $\Delta\theta = \pm 5^\circ$. The resolution function is assumed to be rectangular.

Expansion coefficients of neutron angular distribution	B_0	B_1	B_2	B_3	B_4	B_5	B_6	B_7	B_8	B_9	B_{10}
Correction for angular resolution : done	1,28	2,95	4,56	4,88	5,47	4,43	3,99	2,62	2,22	0,95	0,47
not done	1,25 ±0,03	2,90 ±0,06	4,50 ±0,12	4,87 ±0,11	5,50 ±0,16	4,54 ±0,11	4,11 ±0,15	2,78 ±0,08	2,38 ±0,10	1,06 ±0,03	0,50 ±0,04

In most publications the resolution function is not given. At best, the angular spread, knowledge of which is not sufficient for a real correction for finite angular resolution, is given (but, not always). Therefore we have to bear in mind that these corrections are, as a rule, smaller than the accuracy with which the values of B_ℓ are known, and in the published experimental values this correction has not been taken into account. Where the correction for angular resolution has been applied by the authors themselves, this is mentioned in the table (page 250) under the heading "Remarks".

Determination of the Absolute Cross-Section

For a determination of the differential cross-section from the detector count rate the experimental angular distribution has to be suitably normalized. The detector count rate, corrected for multiple scattering, geometrical factors, etc., is related to the differential cross-section as follows :

$$N(\mu) = \Phi \varepsilon N \sigma_s(\mu)/R^2,$$

where Φ is the neutron flux at the target; ε is the efficiency of the detector; N is the number of nuclei in the scatterer; and R is the distance between target and detector. For determining $\Phi\varepsilon$ one normally uses a calibrated detector. If this detector is placed at the scatterer position the count rate is just equal to this product.

If the experiment is performed with ring geometry then, to calibrate the count rate of the detector, the incoming beam is measured, i.e., without shielding conus and without scatterer (see Fig. 3). The difference between the neutron flux reaching the detector and the neutron flux bombarding the ring can be obtained from geometrical considerations and the known angular distribution of the neutrons emitted from the source. If the neutrons emitted from the source in the direction of the detector, and from the source in the direction of the ring have different energies, then correction for this difference using the energy dependence of the detector efficiency has to be made.

Another method widely used to normalize the differential cross-section is normalization to a well-known standard cross-section. In most cases hydrogen is used as a standard; its scattering cross-section being well-known, and its angular distribution of scattered neutrons being isotropic in the centre-of-mass system up to an energy of approximately 10 MeV. In the publications /L-2, L-6/ the angular distribution of neutrons scattered on carbon is used as a standard.

Finally, in those cases where elastic scattering is practically the

only open channel for neutron-induced nuclear reactions, the angular distribution is often normalized to the value of the integrated scattering cross-section, which in this case is equal to the easily measured total cross-section.

In the table (page 250), the method of normalizing the angular distributions given in the publication is mentioned under the heading "remarks". In those cases where the normalization method is not mentioned in the publication, the procedure of detector calibration in the incident beam described above was usually applied.

Correction for Instrumental Effects

The experimental angular distribution has, generally, to be corrected for a whole series of different instrumental effects such as multiple scattering in the ring; angular dependence of the detector efficiency caused by the dependence of neutron energy on scattering angle; different angular resolution at different angles, etc. The corrections made are given in the table (see page 250) only when stated by individual authors. In some cases the influence of instrumental effects is described in the comments to the graphs in order to explain the differences between data from different authors.

Calculation of the Contribution of the Inelastic Neutron Scattering

In the energy range below 1.5 MeV the neutron scattering angular distribution of a whole series of nuclei was measured at many energies by Langsdorf, Elwyn, Monahan et al. /L-2, L-4, L-6, L-7/. The detector employed in these measurements was an array of boron counters placed in a water moderator. As mentioned above, such a detector has a flat energy response and therefore registers, not only the elastically scattered neutrons, but also the inelastically scattered neutrons. The correction for the latter is made for sufficiently heavy nuclei (heavier than boron) assuming isotropy of the inelastic scattering in the laboratory system. An estimation of the accuracy of such an assumption based on available anisotropic inelastic scattering data

has shown that a more rigorous correction is not justified in view of the accuracy of the available experimental data. In this approximation the contribution of the inelastic scattering appears only in the quantity B_o - the integrated scattering cross-section; the higher-order Legendre coefficients remain unchanged. In fact, in this approximation the angular distribution of elastic (e) and inelastic (in) scattering in the laboratory system can be represented as follows :

$$4\pi\sigma_{s(e)}(\mu) = B_{0(e)} + \sum_{l=1} B_{l(e)} P_l(\mu);$$
$$4\pi\sigma_{s(in)}(\mu) = B_{0(in)}\, g,$$

where g is the ratio of the efficiency of registering elastically and inelastically scattered neutrons, the value of which can be obtained from the graph in /L-6/ which represents the detector efficiency as a function of energy.

The energy dependence of the inelastic scattering cross-section used for corrections is given in a separate graph in the comments on the graphs showing the energy dependence of B_ℓ .

In the case of fluorine which has low-lying energy levels, the inelastic neutron scattering contribution particularly strongly distorts the form of the angular distribution. The correction for inelastic events has, therefore, been carried out more precisely : the inelastic scattering has been assumed to be isotropic in the centre-of-mass system.

The neutrons, inelastically scattered to a level with energy E_{ok} in the laboratory system have an angular distribution given by the relation :

$$\sigma^k_{s(in)}(\mu) = \frac{1}{4\pi} \sum_l B_{l\,(in)}(E_{0,k})\, P_l(\mu).$$

The quantity $B_\ell(E_{o,k})$ is determined from the kinematics of inelastic scattering :

$$B_{l\,(in)}(E_{0,k}) = \sigma_{in,k}\,(2l+1)\int_{-1}^{+1} f_{in}(E_{0,k},\,\mu)\,P_l(\mu)\,d\mu.$$

The values of $B_{\ell\,(e)}$ shown in the graphs were obtained by subtracting from the expansion coefficients of the angular distribution of all scattered neutrons the sums of the corresponding expansion coefficients of the angular distribution of neutrons inelastically scattered to all excited states for a given energy. The form of the excitation function used is given in the comment on the graphs of B_ℓ of fluorine. More detailed questions about the anisotropy of the inelastic scattering on fluorine and its influence on the measure ments of the angular distribution in reference /L-2/ are discussed in reference /10/ (see also page 75).

Representation of Experimental Data

Most of the results of the determination of Legendre coefficients for angular distributions, obtained by one of the methods described above or directly taken from the original papers, are shown as points in the graphs given below, with various symbols denoting different data sets. For energies less than 2.5 MeV , the first six non-zero expansion coefficients (i.e. up to B_5) are represented. At higher energies either six (for nuclei lighter than Al) or eight (for heavier nuclei) coefficients (i.e. up to B_7) are plotted. A greater number of expansion coefficients are required only for the description of angular distributions in the high-energy region, where experiments are usually very scarce. For this reason, and because calculations with high angular moments are rare in practice, the values of these coefficients are represented in tables (see Tables 6-31); the representation of these values in graphs would leave too much empty space.

The unit chosen for the scattering cross-section calculated with formula (1) is barn. Thus, the quantity B_o which represents the integrated scattering cross-section is expressed in barn. The remaining B_ℓ are given in

the same units. For the graphical representation two different energy scales have been used. A larger scale is used for energies below 2.5 MeV, where the number of experimental points is more considerable than for higher energies. The scale of the ordinate has been chosen according to the values to be plotted.

For some elements the angular distribution of elastic neutron scattering in the resonance region has been measured with high energy resolution at so many energies, that it was not possible to plot them all on the basic graphs. Such large data sets have been plotted on separate sheets with an enlarged energy scale, and they are summarily represented on the basic graphs in the form of broken lines, so as to permit comparison of these data with other measurements. Generally, each set of experimental data is plotted with a different symbol. The bibliographic reference that corresponds to a given symbol appears, together with the number assigned to the symbol on the plot, at the end of the comments which accompany the data for each element and isotope considered here. In several cases, where at one and the same or at only slightly differing energies the results of various papers confirm each other, these data were treated together by the least-squares method, or a smooth curve was drawn through all existing experimental points which was then expanded into Legendre polynomials. In these cases the literature references to all utilized publications are given next to the number assigned to the symbol.

An essential part of the experimental data used by us is compiled in the angular distribution atlas, BNL-400 /1,2/. Sometimes this information differs from the results of the original work. In this case we considered the data given in the atlas as more up-to-date. The reference is, therefore, given together with the atlas BNL-400.

In some cases information on angular distribution of scattered neutrons available in BNL-400 /1,2/ was extracted from this document. There the energy dependence of the cross-section at individual scattering angles are represented; in the reference citation such data are denoted by /1[a]/ and /2[a]/. The results of the experiment /L-2/, in contrast to all other references, are not given pointwise but as curves, since they are

represented in the same form in the original publication. The energy dependence of B_ℓ ($\ell > 0$), obtained in this paper is represented as a continuous line. B_o has been represented in the form of a continuous line only if no correction for inelastic scattering was required. Otherwise the corrected data are represented as dotted lines.

The results of optical model calculations (or other theoretical calculations, if their results were quoted) are represented as dash-dotted curves.

References to the experimental papers used in this compilation are given in a table (page 250) in which, together with the bibliographic information, the main characteristics of the experimental method are given : elements or isotopes studied (5th field); energy range covered in MeV (6th field) and energy resolution in MeV (7th field); neutron source and neutron detector; angular interval (in degrees) or interval of cosines of the scattering angles. Additional information is given, where appropriate, in the field "Remarks" : angular resolution, multiple-scattering correction, whether there were essential contributions from inelastic scattering, how the angular distribution was normalized, etc.

The transformation of data given in the laboratory system to the centre-of-mass system can be performed by using the matrix elements $R_{\ell n}$ (table 3), taken from reference /25/.

In this reference the coefficients $R_{\ell n}$ were given in the form of an expansion in powers of $1/A$ (A being the atomic weight of the target nucleus) up to the term of order $1/A^2$. This accuracy is adequate in view of the accuracy of existing data on the quantity B_ℓ .

We also tabulate the inverse matrix $K_{n\ell}$, which we used to transform data given in the centre-of-mass system to the laboratory system (Table 4).

In practically all cases the characteristics of the distribution of the elastically scattered neutrons are not sufficiently complete and accurate for a derivation of the energy dependence of B_ℓ over the whole energy interval considered.

Nevertheless, for many practical calculations (for example, reactor and shielding calculations) one must accept a certain energy dependence, $B_\ell(E_n)$, even if it is not fully reliable.
For a convient comparison of results from different calculations it is also desirable, that the input data, especially the data on anisotropy of elastic scattering, are the same. We give, therefore, recommended curves $B_\ell(E_n)$ for the whole energy interval considered. In the graphs these curves are represented as fine, dashed lines.

Matrix Elements Table 3

$$\left(B_{l,c.m.} = \sum_n R_{ln}\, B_{n,lab}\right)$$

l \ n	0	1	2	3	4	5	6
0	1	0	0	0	0	0	0
1	$-\frac{2}{A}$	$1-\frac{1}{5A^2}$	$\frac{2}{5A}$	$\frac{3}{35A^2}$	0	0	0
2	$\frac{3}{A^2}$	$-\frac{2}{A}$	$1-\frac{9}{7A^2}$	$\frac{6}{7A}$	$\frac{8}{21A^2}$	0	0
3	0	$\frac{16}{5A^2}$	$-\frac{12}{5A}$	$1-\frac{14}{5A^2}$	$\frac{4}{3A}$	$\frac{10}{11A^2}$	0
4	0	0	$\frac{30}{7A^2}$	$-\frac{20}{7A}$	$1-\frac{370}{77A^2}$	$\frac{20}{11A}$	$\frac{240}{143A^2}$
5	0	0	0	$\frac{40}{7A^2}$	$-\frac{10}{3A}$	$1-\frac{95}{13A^2}$	$\frac{30}{13A}$
6	0	0	0	0	$\frac{3185}{429A^2}$	$-\frac{42}{11A}$	$1-\frac{567}{55A^2}$

The recommended curves have been drawn by hand mainly based on the experimental and theoretical data given. The curves $B_\ell(E_n)$ $(\ell > 0)$ were so chosen that the reasonable energy dependent relation

$$\omega_l = B_l/B_0.$$

is fulfilled.

For determining the curve $B_o(E_n)$ the data on the total cross-section δ_t and the non-elastic cross-section have been used.

In the high energy region, where the experimental data were, as a rule, scarce, we used results from nuclear optical model calculations as a guide. The value $B_{\ell o}$ at the limit $E_n \rightarrow 0$ was obtained assuming isotropic scattering in the centre-of-mass system.

For several light nuclei some low-lying resonances were completely or partially resolved in the measured angular distribution. In the region of these resonances the recommended curve was drawn directly through the experimental points.

Hence, the recommended curves presented by us are not based strictly on all the information which could be derived from the theory. Thus, for example, in the region of unresolved resonances a more reliable energy dependence could possibly have been obtained by describing all experimental data of each nucleus by optical model calculations with specially adjusted parameters for the potential (for example, by the least-squares method).

The energy dependence of B_ℓ in the resonance region can, in principle, by calculated by : using the known resonance parameters (where they are available) and the one-level formula by Blatt and Biedenharn /5/, or, in order to take into account the interference between resonances, the use of the formula by Luk'ynov /11/.

However, carrying out such calculations represents a very difficult task because not all parameters contained in the theory can be uniquely determined from the available experimental data. In particular, a considerable difficulty is the choice of the energy-dependences for the optical parameters, and the potential scattering phase with high orbital momentum (for the calculation of angular distributions in the resonance region).

Matrix Elements

Table 4

$$\left(B_{n.lab} = \sum_{l} K_{nl}\ B_{l.c.m.}\right)$$

n \ l	0	1	2	3	4	5	6
0	1	0	0	0	0	0	0
1	$\frac{2}{A}$	$1-\frac{3}{5A^2}$	$-\frac{2}{5A}+\frac{12}{35A^3}$	$\frac{9}{35A^2}-\frac{5}{21A^4}$	$-\frac{4}{21A^3}+\frac{2}{11A^5}$	0	0
2	$\frac{1}{A^2}+\frac{1}{7A^4}$	$\frac{2}{A}-\frac{4}{7A^3}-\frac{2}{21A^5}$	$1-\frac{11}{7A^2}+\frac{3}{7A^4}$	$-\frac{6}{7A}+\frac{4}{3A^3}-\frac{82}{231A^5}$	$\frac{16}{21A^2}-\frac{272}{231A^4}$	0	0
3	0	$\frac{8}{5A^2}$	$\frac{12}{5A}-\frac{28}{15A^3}$	$1-\frac{46}{15A^2}+\frac{65}{33A^4}$	$-\frac{4}{3A}+\frac{1456}{429A^3}-\frac{868}{429A^5}$	$\frac{50}{33A^2}$	0
4	$-\frac{1}{7A^4}$	$\frac{4}{7A^3}+\frac{12}{77A^5}$	$\frac{18}{7A^2}-\frac{68}{77A^4}$	$\frac{20}{7A}-\frac{336}{77A^3}+\frac{1116}{1001A^5}$	$1-\frac{390}{77A^2}+\frac{5787}{1001A^4}$	$-\frac{20}{11A}$	$\frac{360}{143A^2}$
5	0	0	0	$\frac{80}{21A^2}$	$\frac{10}{3A}$	$1-\frac{295}{39A^2}$	$-\frac{30}{13A}$
6	0	0	0	0	$\frac{2275}{429A^2}$	$\frac{42}{11A}$	$1-\frac{581}{55A^2}$

Remark : The coefficients $K_{n\ell}$ are also represented by a series expansion in powers of 1/A to a higher accuracy.

Review of Energy Dependent Coefficients of Legendre Polynomials which Represent the Angular Distribution of Neutrons Elastically Scattered.

D E U T E R I U M

The elastic neutron scattering cross-section of deuterium is a fairly smooth function of energy and can, therefore, be easily interpolated.

Theoretical calculations of angular distribution of elastically scattered neutrons on deuterium are carried out in reference /12/. The authors of this work studied two body interactions and showed that the drawback of this approximation is that the forward-scattering differential cross-section is too low (Figure 6).

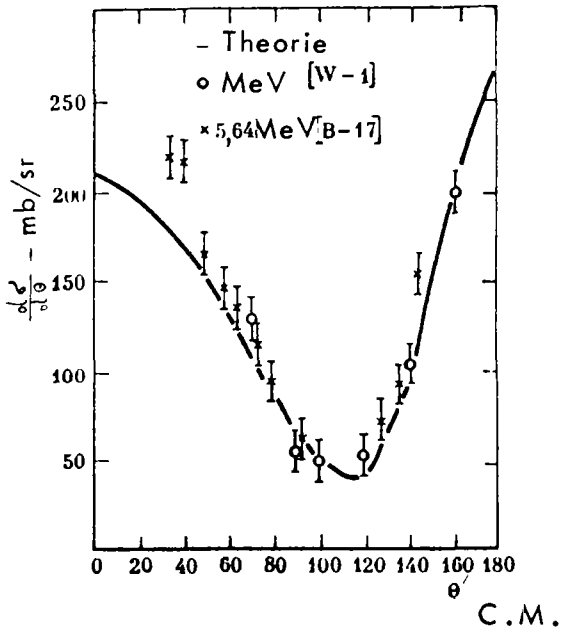

Figure 6 : Experimental and theoretical scattering angular distribution of 5.5 MeV neutrons on deuterium /W-1/.

The resulting integrated cross-section is therefore also lower (Fig. 7). The authors felt it possible to remove this drawback by improved three-body interaction calculations.

Even results of approximative calculations can be useful for the interpolation of energy dependent curves of B_ℓ . In reference /12/, however, calculations were only carried out for those energies for which experimental results were available.

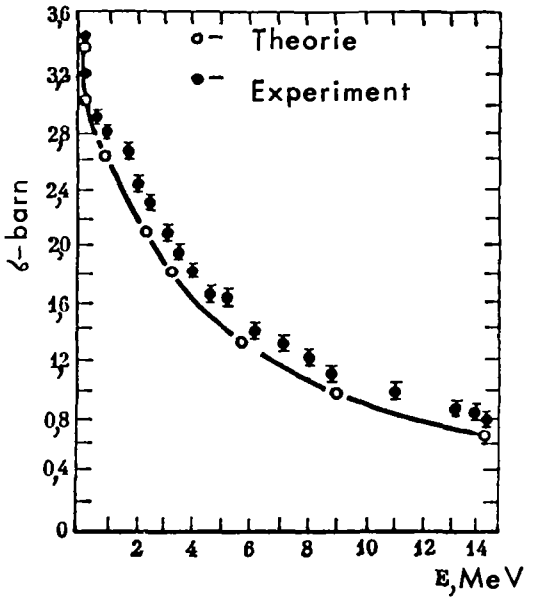

Figure 7 : Total neutron-scattering cross-section of Deuterium.

The recommended curve for B_o below the (n,2n) threshold is obtained from the available total cross-sections and, above this threshold (3.3 MeV) this curve is obtained by subtracting $\sigma_{n,2n}$ from σ_{total}.

The energy dependence of the moments B_ℓ corresponding to neutrons elastically scattered on deuterium which are represented in the form of graphs are derived from the data given in the following references (*) .

(*) For each element, a list of references is given after the comment indicating the source of the data for the corresponding graphs.

$^{2}{}_{1}D$

1 — [1];	[*W*—1] —	E. Wantuch (1951)
2 — [1];	[*A* — 2] —	R. K. Adair (1953)
3 — [1];	[*A* — 3] —	J. C. Allred (1953)
	[*S* — 4]	J. D. Seagrave (1955)
4 — [1];	[*A* — 2] —	R. K. Adair (1953)
	[*S* — 5] —	J. D. Seagrave (1957)
5 — [1];	[*A* — 4] —	W. D. Allen (1955)
6 — [1];	[*S* — 5] —	J. D. Seagrave (1957)
7 — [1];	[*E* — 2] —	A. J. Elwyn (1962)
8 — [1];	[*A* — 2] —	R. K. Adair (1953)
	[*E* — 2] —	A. J. Elwyn (1962)
9 —	[*B* — 17] —	B. E. Bonner (1965)

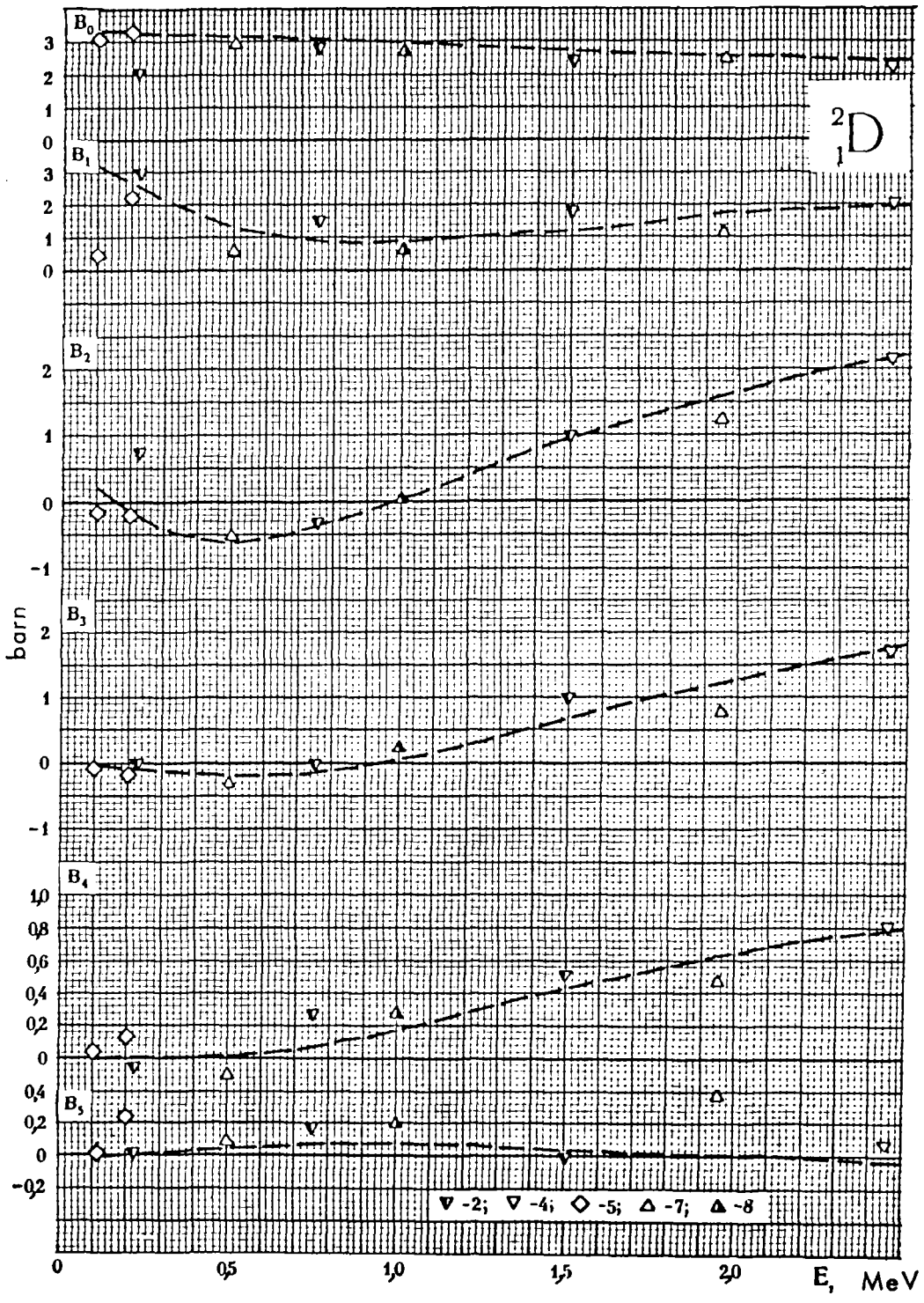
B_0
B_1
B_2
B_3
B_4
B_5
^2_1D
barn
▽ -2; ▽ -4; ◇ -5; △ -7; ▲ -8
0
0,5
1,0
1,5
2,0
E, MeV

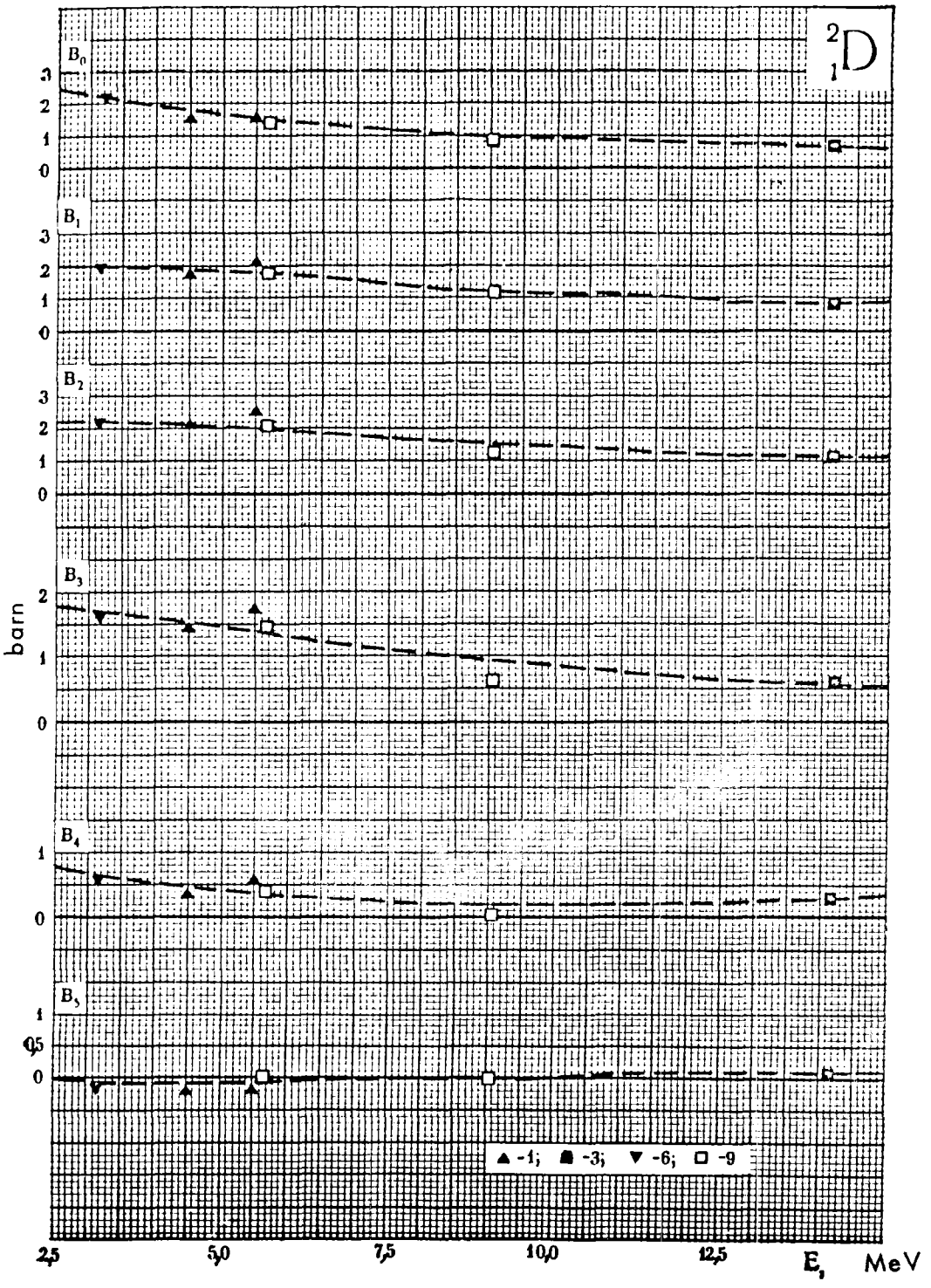
^2_1D
B_0
B_1
B_2
B_3
B_4
B_5
barn
▲ -1; ■ -3; ▼ -6; □ -9
2,5
5,0
7,5
10,0
12,5
E_n MeV

T R I T I U M

In the energy range from 1 to 6 MeV the angular distribution of tritium has only been measured in one experiment /S-7/. In spite of the application of an appropriate experimental method and a correct analysis, a comparison of these data with other experimental results would be desirable for a final judgement of their reliability.

Since no other angular distribution measurements of neutrons scattered on tritium are available, verification could only be made with the integrated cross-section values B_o and the total cross-section from reference /13/ which showed excellent agreement. As another criterion for the accuracy of the data given in reference /S-7/, the reasonable agreement of elastic neutron angular distribution cross-sections of He-3 of this work can be used in conjunction with the cross-sections published in the reference /S-9/ (see under Helium-3). Although the available data permitted a more-or-less reliable interpolation in the energy range from 1 to 6 MeV, they were still not sufficiently detailed for an extrapolation to the energy range below 1 MeV. It is preferable to extrapolate on the basis of calculations which use models for tritium.

At 14 MeV, results of two experiments are published in reference /B-22/ and reference /C-1/, respectively. The latter is an older measurement of neutron angular distribution for $0.2 \leqslant \cos\vartheta^{*}(C.M.) \leqslant -1$.

In order to estimate B_ℓ, the results of reference /C-1/ were extrapolated to small angles in such a manner that the integrated cross-section agreed with the difference of the total- minus the T(n,3n)H cross-section which was equal to 0.8 barn at this energy.

The T(n,3n)H cross-section at 14 MeV was estimated with the values given in references /14/ and /16/ assuming isotropy of the outgoing neutrons in the centre-of-mass system. This estimation gave a value equal to 0.1 barn, which is about 10% of the total cross-section. The reliability of such an extrapolation is evidently very low since it is shown that the values in the range $1.0 \geqslant \cos(\vartheta^{*}) \geqslant 0.2$, obtained by extrapolation, contribute about 80% to the integrated cross-section.

In reference /B-22/ the angular distribution in the cosine interval (C.M.) from 0.4 to 1 was measured at more angles. This permitted extrapolation to low angles by means of the least-squares method.

$^{3}_{1}T$

1 — [1]; [*C* — 1] — J. H. Coon (1951)
2 — [1]; [*S* — 7] — J. D. Seagrave (1960)
3 — [*B* — 22] — D. Blanc (1966)

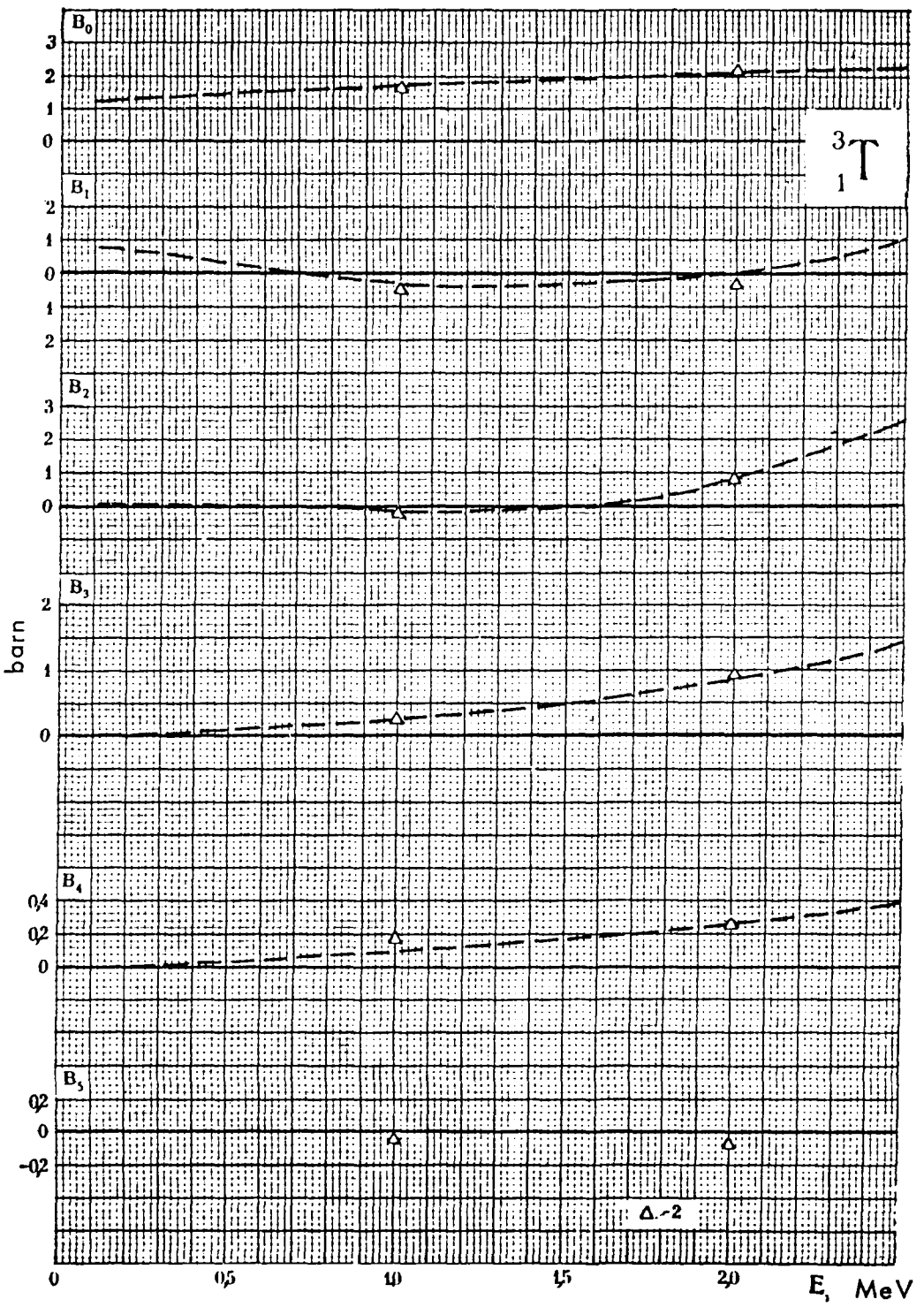
B0
B1
B2
B3
B4
B5
barn
3T
1
Δ-2
0
0,5
1,0
1,5
2,0
E, MeV

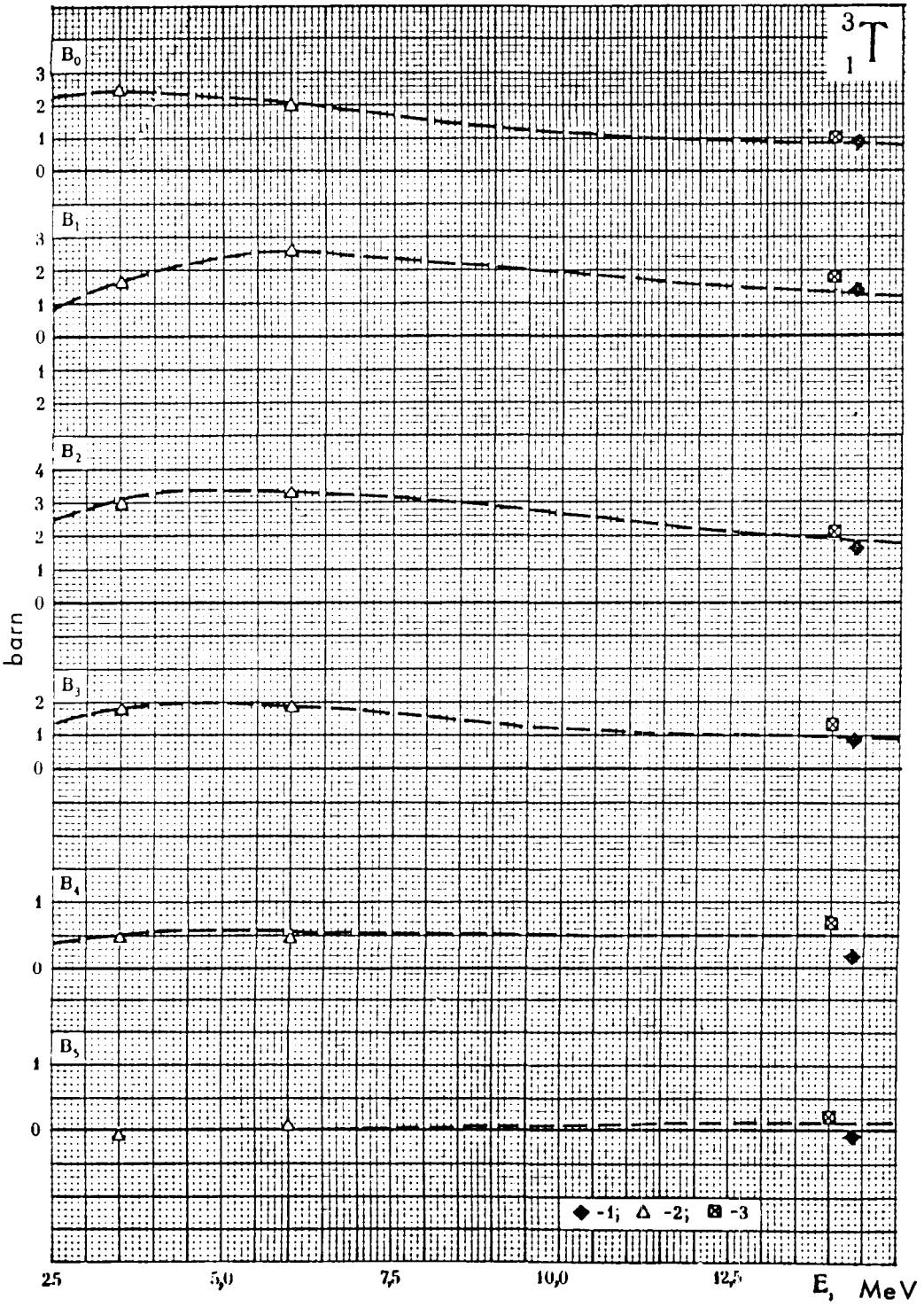
$^{3}_{1}T$
B_0
B_1
B_2
B_3
B_4
B_5
barn
◆ -1; Δ -2; ⊠ -3
2,5
5,0
7,5
10,0
12,5
E, MeV

H E L I U M - 3

In the energy range from 1 to 8 MeV data are published in the two references /S-7/(1960) and /S-9/(1961) which were measured with completely different methods (see comments in the Appendix). In the energy range from 2.5 to 8.0 MeV, where results of both measurements are given, the agreement is satisfactory.

The values B_o obtained in these works agree with the differences of the total cross-sections /13/ and the cross-sections of the reaction He-3(n,p)T-3 /16/ within the uncertainties which range from 0.1 to 0.15 barn for the differences, and from 0.06 to 0.1 barn for the B_o values.

The empirical extrapolation using the available data in the low energy region ($E_n < 1$MeV) and, particularly, in the high energy region ($E_n > 8$MeV) is not satisfactory. For this purpose it was thought preferable to use results from calculations based on models established for Helium-3.

For the extrapolation to the high energy region, the results obtained in reference /S-9/ at 17.5 MeV : $B_o = 0.82$; $B_1 = 1.8$; $B_2 = 2.1$; $B_3 = 1.7$; $B_4 = 1.0$; $B_5 = 0.5$, barn, have been used. However, the reliability of these data is not high, since, below 45 degrees, no measurements have been done in reference /S-9/. In order to obtain B_ℓ a further extrapolation of the angular distribution is required. For this extrapolation we relied on the theoretical curve obtained in reference /17/. The recommended curve $B_o(E)$ was obtained on the basis of the available total cross-sections and cross-sections of the reactions (n,p) and (n,d).

$^{3}_{2}He$

1 — [1]; [S — 7] — J. D. Seagrave (1960)
2 — [1]; [S — 9] — A. R. Sayres (1961)

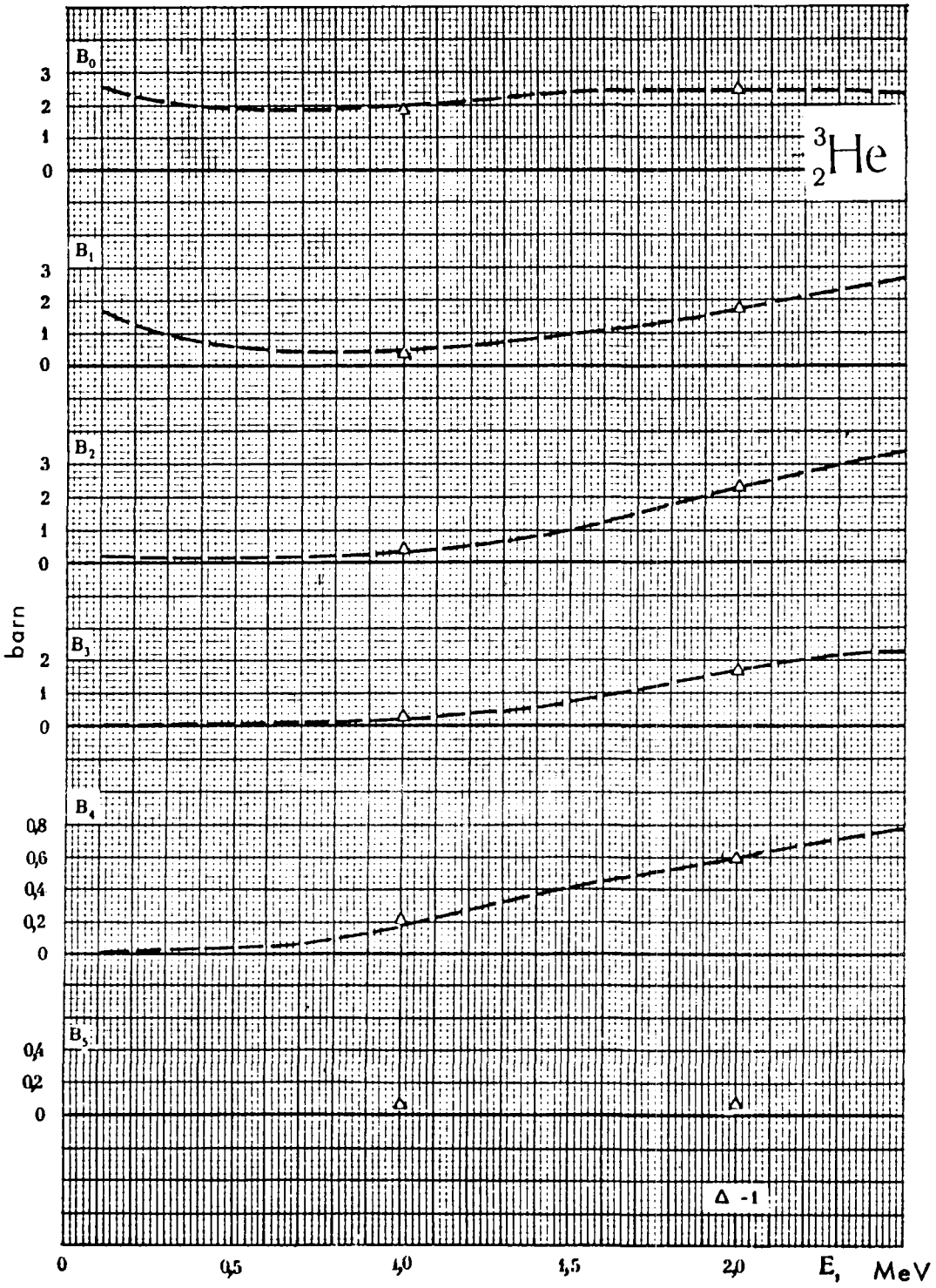
B0
B1
B2
B3
B4
B5
3
2
1
0
0,8
0,6
0,4
0,2
barn
$^{3}_{2}$He
Δ -1
0
0,5
1,0
1,5
2,0
E, MeV

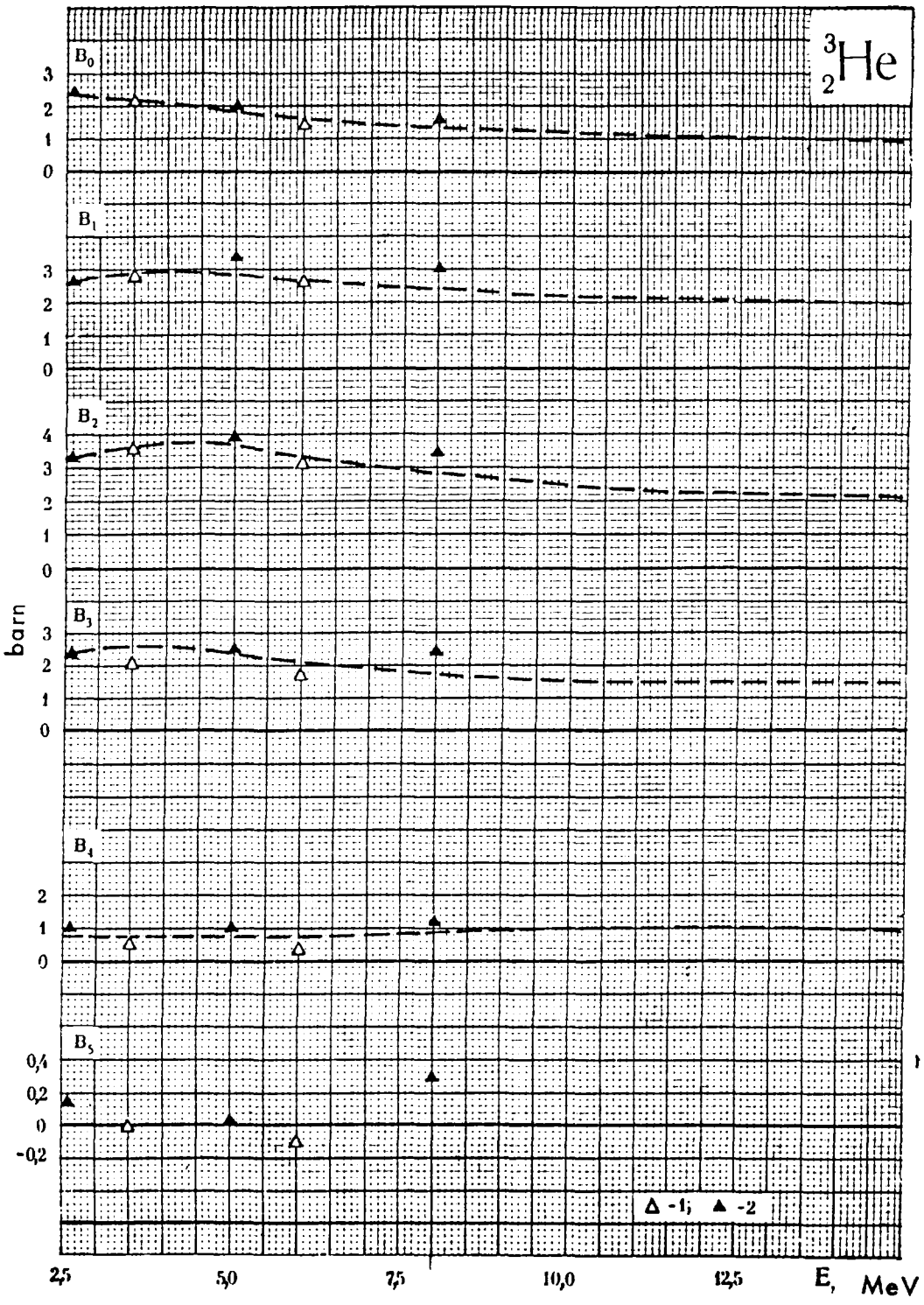
$^3_2$He
B_0
B_1
B_2
B_3
B_4
B_5
barn
Δ -1; ▲ -2
2,5
5,0
7,5
10,0
12,5
E, MeV

H E L I U M - 4

In the energy range below 2.5 MeV the most complete data for elastic neutron angular distributions of helium were determined in the work by Adair, reference /A-1/ using a helium proportional counter. The counting of Helium recoil spectra corresponding to elastic neutron scattering permitted the latter to be obtained only at angles in the range 30-70° onwards, and consequently the values B_ℓ could not be reliably determined directly from the experimental data. Therefore, in the energy range below 2.5 MeV the values of B_ℓ (solid curve) have been obtained from the expansion of the theoretical angular distribution, calculated in the cited reference and fitting, with sufficient accuracy, the measured angular distribution.

The calculation was made assuming that the interaction of neutrons with an orbital angular momentum greater than 1 can be neglected. In this case when coupling between spin and orbital angular momentum is taken into account, the neutron differential elastic scattering cross-section can be expressed by the following formula :

$$\frac{d\sigma}{d\Omega} = \lambda^2 \left| e^{i\delta_0} \sin\delta_0 + \cos\theta \left(2e^{i\delta_+} \sin\delta_+ + e^{i\delta_-} \sin\delta_-\right)\right|^2 + \\ + \lambda^2 \left| \sin\theta \left(e^{i\delta_-} \sin\delta_- - e^{i\delta_+} \sin\delta_+\right)\right|^2,$$

where δ_o is the s-wave phase shift and δ_+ and δ_- are the phase shifts for $P_{3/2}$- and $P_{1/2}$- waves respectively.

The p-wave phase shift in the single-level approximation can be calculated with the equation

$$\delta = \operatorname{arctg} \frac{k\gamma^2/(F^2+G^2)}{E_\lambda - E + \Delta} - \operatorname{arctg} \frac{F}{G},$$

where the level shift Δ is given by the equation

$$\Delta = -\frac{\gamma^2}{a}\left(\frac{d \ln \sqrt{F^2 + G^2}}{d \ln ka} + l\right).$$

F and G are the regular and irregular free particle wave functions which can be calculated using tables /18/; k = 1/2 is the wave number of the neutron; a is the nuclear radius; γ^2 is the reduced resonance width, and E_λ is the resonance energy.

The values for the parameters in the formula for δ are obtained from the analysis of the proton elastic scattering data on Helium /19/ and are uniquely determined by studies of proton polarization /20/. As a result, one has : $a = 2.9.10^{-13}$cm; $\gamma^2(P_{3/2}) = \gamma^2(P_{1/2}) = 17.6.10^{-13}$ MeV.cm; $E_\lambda(P_{3/2}) = 3.65$ MeV, and the doublet splitting $E_\lambda(P_{1/2}) - E_\lambda(P_{3/2})$ in the spin orbit coupling calculation is equal to 5 MeV.

The phase shift for s-waves were calculated by the condition that the neutron s-wave function has the same logarithm derivative at the nuclear surface as the proton s-wave.

In reference /A-1/ it is shown that, in agreement with the estimation made, the contribution of neutrons interacting with $\ell > 1$ does not influence the angular distribution for energies below ~ 3 MeV.

The difference between the calculated and the experimental angular distributions below 2 MeV is of the same order of magnitude as the statistical uncertainty of the experimental points; at energies of 2.4 and 2.73 MeV the maximal deviation is 20% for scattering angles less than 90°.

The results of Adair agree reasonably well with the results obtained by Young /Y-2/(1963) and Austin /A-10/(1962), for the energies 1.8 and 2 MeV respectively, and are close to the data at higher energies. At energies higher than 1.5 MeV the calculated values of B_o are a little

smaller than δ_T. Since scattering is practically the only reaction at these energies, the recommended curve $B_o(E)$ obtained from δ_T is in good agreement with the experimental data of B_o.

For energies higher than 2.5 MeV results from several works are available and they agree satisfactorily. They permit the derivation of smooth energy dependence of B_ℓ with sufficiently high accuracy.

We wish to point out that in processing the data of reference /S-1/, the extrapolation of the measured angular distribution to small angles has been done in such a way that a correct total cross-section could be obtained. The data by Fasoli /F-5/ were treated in the same way. However, in this case, owing to the great irregularity of the angular distribution, the extrapolation was less reliable. The over-estimated value of B_5 is probably due to this inaccurate extrapolation.

$^{4}_{2}He$

1 — [1]; [S — 1] — J. D. Seagrave (1953)
[S — 3] — D. F. Shaw (1955)
2 — [F — 5] — V. Fasoli (1963)
3 — [1]; [A — 10] — S. M. Austin (1962)
4 — [Y — 2] — P. G. Young (1963)
5 — [H — 5] — B. Hoop, Jr. (1965)

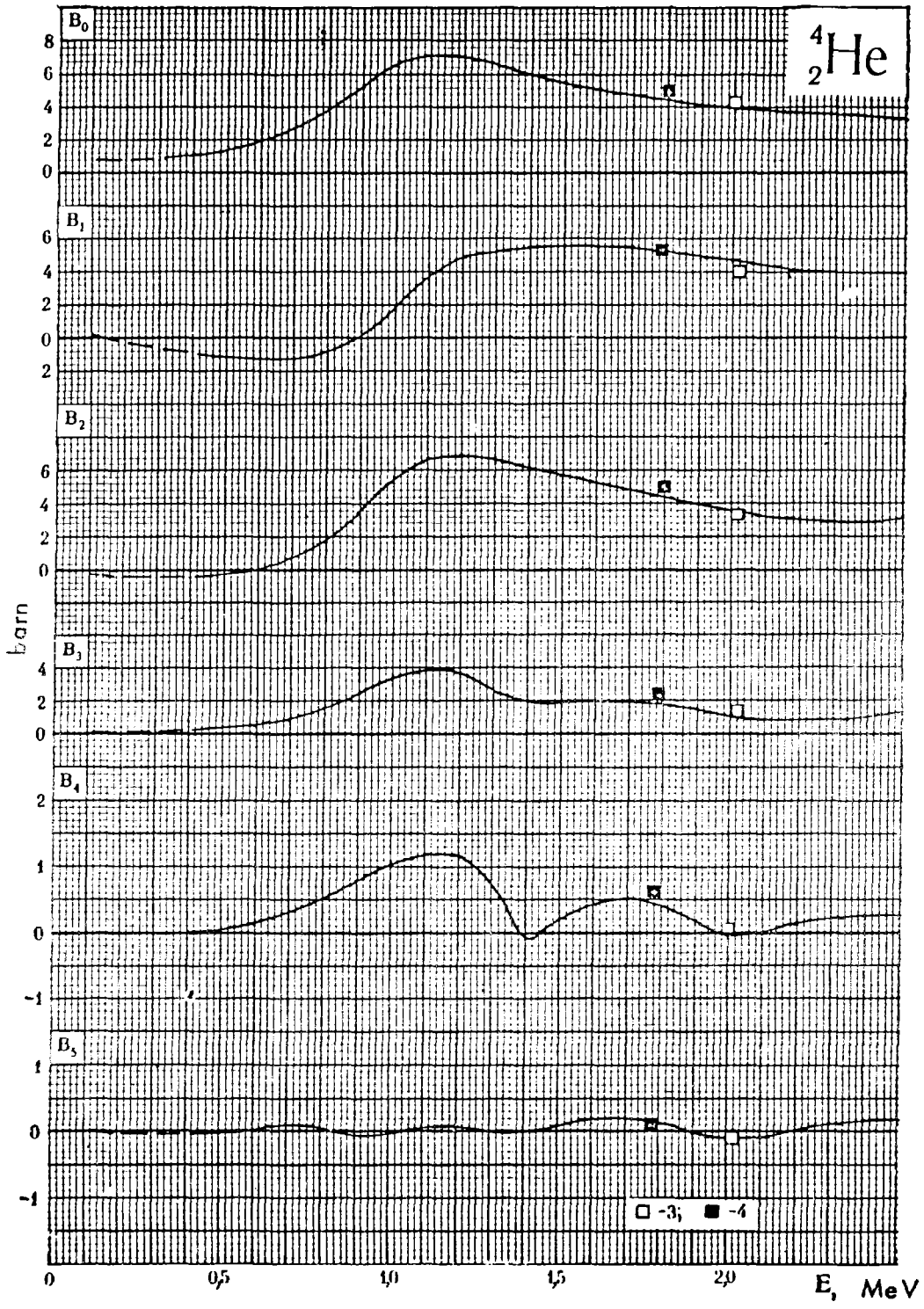
$^4_2$He
B_0
B_1
B_2
B_3
B_4
B_5
barn
□ -3; ■ -4
0
0,5
1,0
1,5
2,0
E, MeV

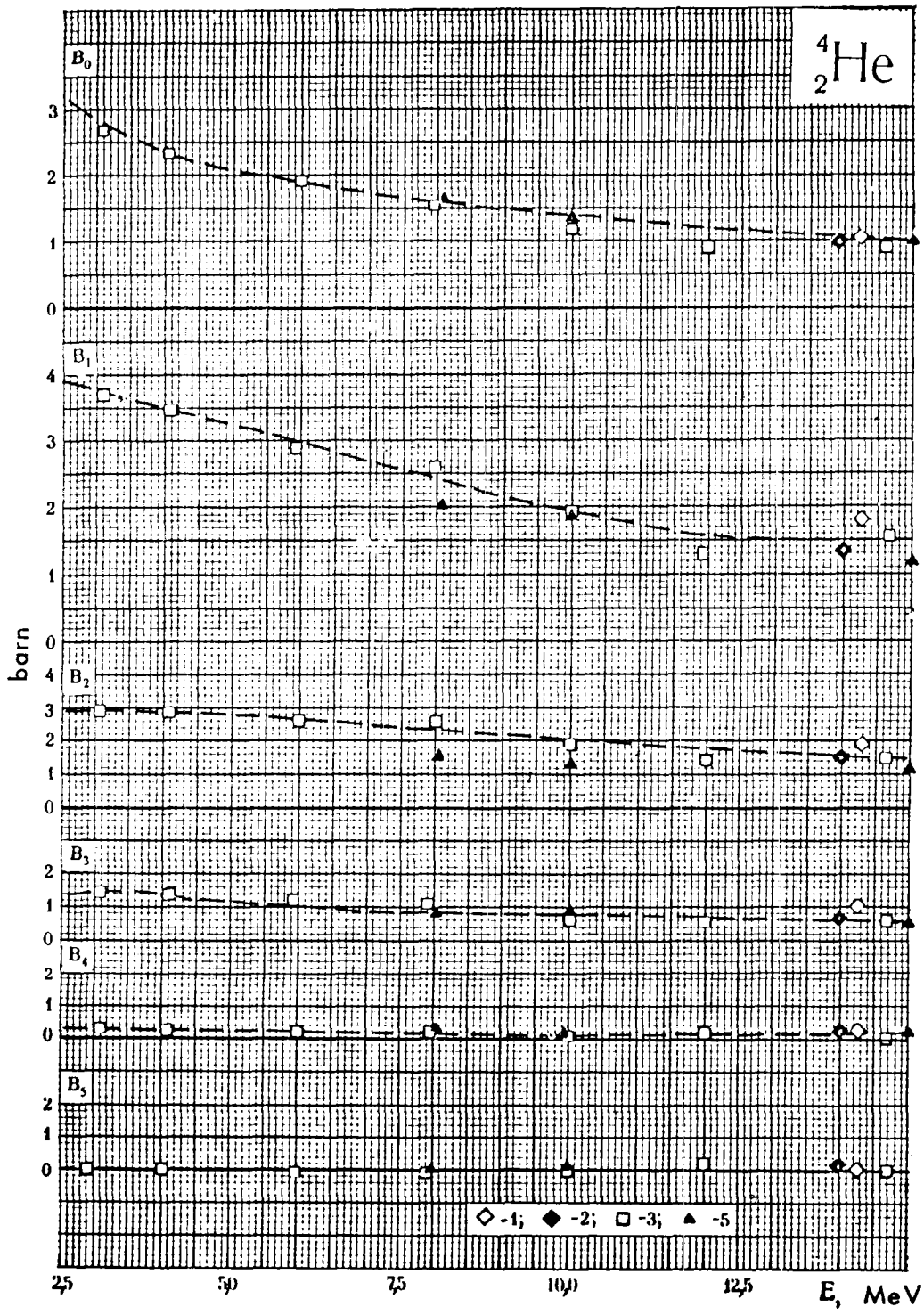
$^4_2$He
B_0
B_1
B_2
B_3
B_4
B_5
barn
◇-1; ◆-2; □-3; ▲-5
25
50
75
100
125
E, MeV

L I T H I U M - 6

In the energy range below 2.25 MeV there are many data by Langsdorf et al. /L-6/(1961) available with an energy resolution of 40 keV in the energy range from 50 to 600 keV which is sufficient for resolving the resonance at 255 keV (Γ = 125 keV, Γ_n = .88 keV, I = 5/2, ℓ = 1).

However, it is remarkable that in the resonance region the higher harmonics of all experimental results have a strong peak. The angular distribution in this resonance region has also been measured in an earlier work by Willard et al. /W-7/(1956) with a resolution of about 20 keV. These results, however, are doubtful : the value of B_o is, for example, considerably higher at the resonance energy (= 8.4 barn) than the difference $\sigma_T - \sigma_{n,\alpha} \cong 7.8$ barn /13/, /16/; the very strong disagreement between the values of B_1 of this work and those of the measurement by Langsdorf /L-6/ cannot be explained by the better energy resolution of the former. The experimental values of B_2 at energies of 0.258 and 0.3 MeV (see /W-7/) do not agree with the form of the resonance curve. However, the values of B_o obtained from the measurement presented in reference /L-6/ agree very well with the available data of $\sigma_T - \sigma_{n,\alpha}$. We based the derivation of the recommended curve for energies below 2 MeV on the data by Langsdorf et al.

In the energy range 3.3 - 7.54 MeV data are available from the very thorough measurement done by Batchelor and Towle /B-10/. The coefficients for the elastic neutron angular distribution at an energy of 4.83 MeV were not taken from this work, since the measurement was only done at a few angles and no correction for multiple scattering was undertaken; judging from measurements at other energies, this is rather essential.

At energies of 6.3 and 7.5 MeV, the values of B_o published

in /B-10/ coincide with the values =
$\sigma_t - (\sigma_{n,\alpha} + \sigma_{n,t} + \sigma_{n,p} + \sigma_{in})$, but in the range of 3 to 5 MeV the measured values of B_o lie 0.10 - 0.15 barn higher than those obtained from this relation. This difference can, however, be fully explained by the inaccuracy of the available cross-sections.

The data of reference /B-10/ agree sufficiently well with the result of the measurement by Hopkins /H-7/(1966) who measured the elastic neutron angular distribution at an energy of 4.83 MeV. The disagreement between the results of these two measurements is of the order of the experimental uncertainty.

At 10 MeV the value of B_o obtained by Cookson et al. /C-21/(1967) agrees well with the difference $\sigma_T - \sigma_{ne}$.

The results of the angular distribution measurements at 14 MeV in the references /W-11/ and /A-11/ agree well (unlike Li-7, where the results of these works differ much for high moments). The value of B_o obtained in these works is essentially lower than the value of the difference between the total- and the nonelastic cross section ($\simeq$1.2 barn). However, this value agrees very well with B_o measured in a later work by Merchez /M-9/. For obtaining the recommended curve we therefore relied on the values of the latter measurement.

$^{6}_{3}Li$

1 — [1]; [*W* — 7] — H. B. Willard (1956)
2 — [1*]; [*L* — 6] — R. O. Lane (1961)
3 — [*W* — 11] — C. Wong (1962)
4 — [*B* — 10] — R. Batchelor (1963)
5 — [*A* — 11] — A. H. Armstrong (1964)
6 — [*M* — 9] — F. Merchez (1965)
7 — [*H* — 7] — J. C. Hopkins (1966)
8 — [*C* — 21] — J. A. Cookson (1967)

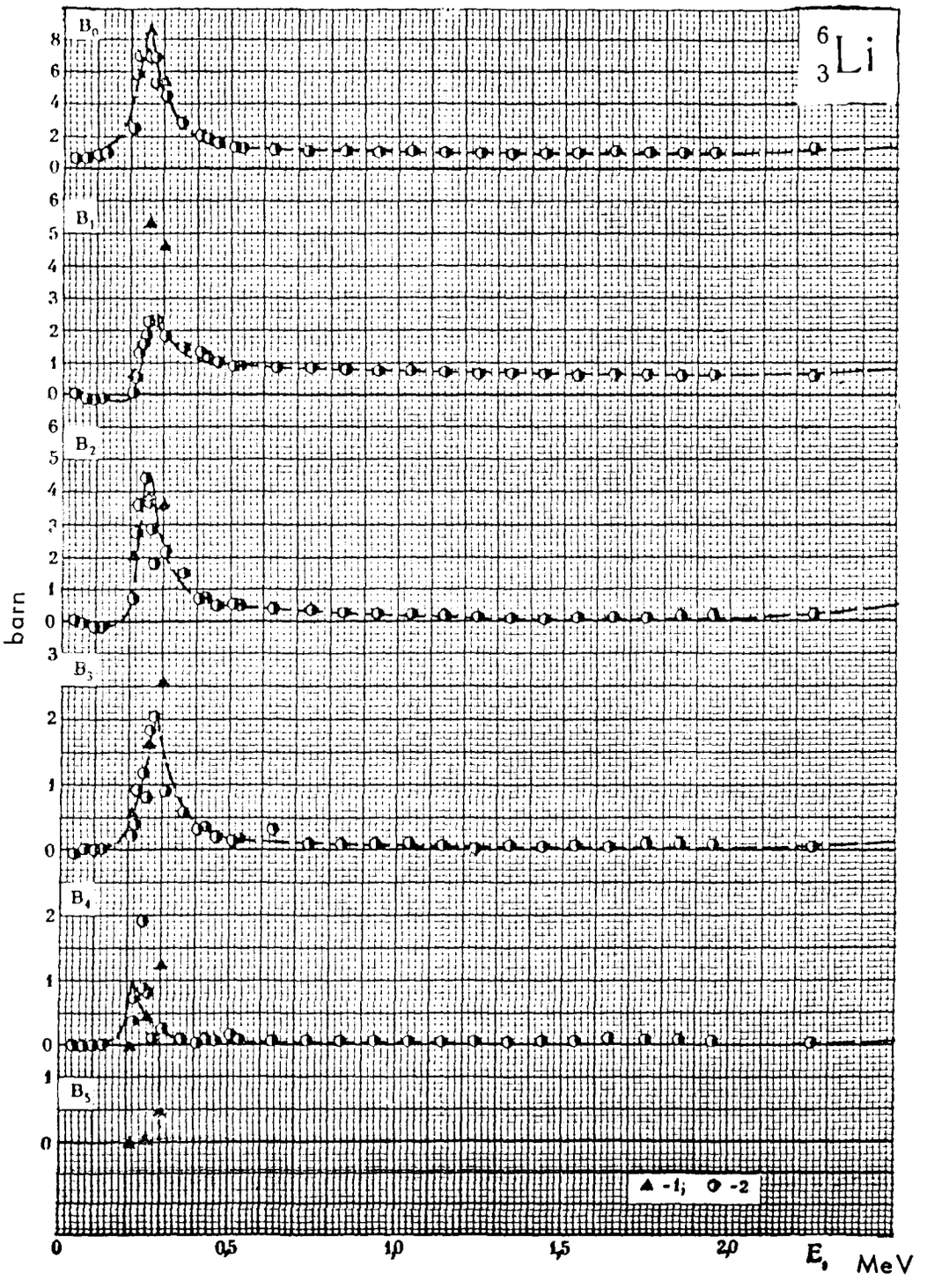
B_0
B_1
B_2
B_3
B_4
B_5
^6_3Li
barn
▲ -1; ○ -2
0
0,5
1,0
1,5
2,0
E_n MeV

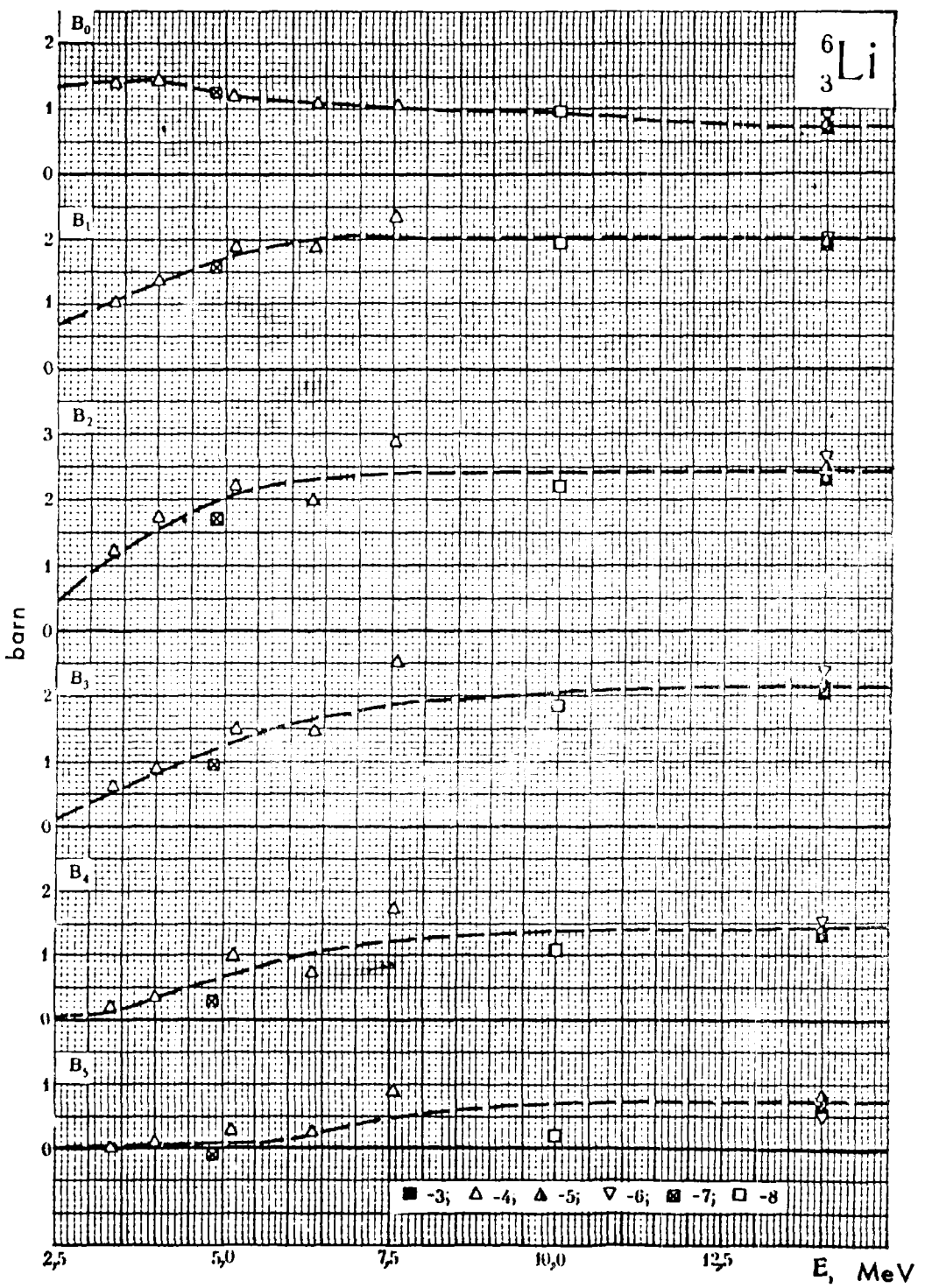
$^{6}_{3}Li$
B_0
B_1
B_2
B_3
B_4
B_5
barn
■ -3; △ -4; ▲ -5; ▽ -6; ▩ -7; □ -8
2,5
5,0
7,5
10,0
12,5
E, MeV

L I T H I U M - 7

As in the case of Li-6, there are many data measured for Li-7 below 2,25 MeV by Langsdorf et al./L-6/, and also results by Willard /W-7/ and Thomas et al. /T-1/. The energy resolutions in these measurements were 40, 20 and 10 keV respectively. As distinct from Li-6, the data of all these measurements are in sufficient agreement.

The data by Batchelor and Towle /B-10/(1963) in the interval 3 - 5 MeV are confirmed by a more recent measurement by Hopkins /H-7/(1966). At higher energies and for higher harmonics ($\ell \geq 3$) however, a fit to the data obtained in reference /B-10/ at 5 - 7 MeV and to the data of Cookson et al. /C-21/(1967) at 10 MeV as well as those by Armstrong /A-11/, Wong /W-11/ and Merchez /M-9/ is rather difficult.

One has to point out that in all experiments, except in the measurement published in reference /H-7/, the elastic scattering and the inelastic scattering to the level of 0.48 MeV have not been individually distinguished. As the inelastically scattered neutrons on such a light nucleus as Li-7 are considerably anisotropic in the laboratory system even when they are isotropic in the centre-of-mass system, not only B_o, but also the higher harmonics have to be corrected for the inelastic contribution. Let's assume that the inelastic scattering in the centre-of-mass system is isotropic. This is, in fact, not quite correct (see reference /B-10/). However, since the inelastic scattering correction is not very high even for B_1, the results are little effected by the anisotropy of the neutrons scattered inelastically in the centre-of-mass system.

At energies of 10 and 14 MeV the correction for inelastic scattering to the level of 0.48 MeV was not necessary, since the cross-secrion for this excited state is negligible at these energies.

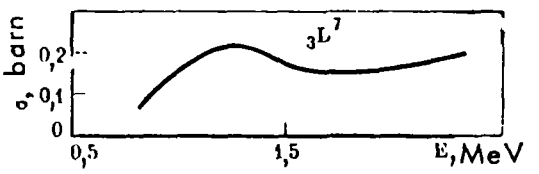

Figure 8 : Inelastic neutron scattering cross-section of Li-7 used for correcting B_o.

One can assume (Fig. 8) that it is less than 0.1 barn and, consequently, the uncertainty in connection with the insufficient resolution is very small even for B_o.

^7_3Li

1 — [1]; [*T* — 1] — R. G. Thomas (1956)
2 — [1]; [*W* — 7] — H. B. Willard (1956)
3 — [1]; [*W* — 7] — H. B. Willard (1956)
[*T* — 1] — R. G. Thomas (1956)
4 — [1a]; [*L* — 6] — R. O. Lane (1961)
5 — [1]; [*W* — 11] — C. Wong (1962)
6 — [*B* — 10] — R. Batchelor (1963)
7 — [*A* — 11] — A. H. Armstrong (1964)
8 — [*H* — 7] — J. C. Hopkins (1966)
9 — [*C* — 21] — J. A. Cookson (1967)
10 — [*M* — 9] — F. Merchez (1965)

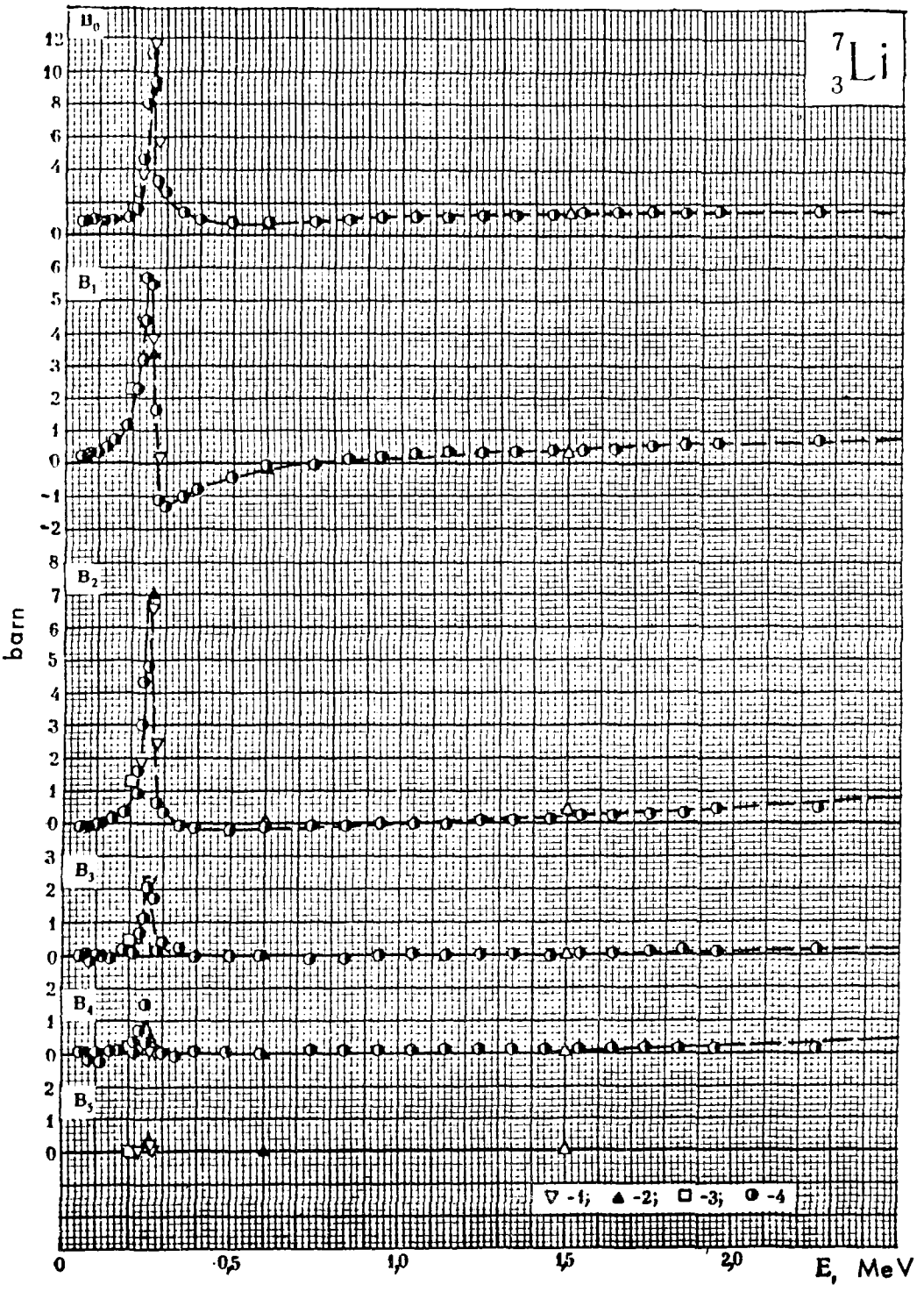
$^{7}_{3}Li$
B_0
B_1
B_2
B_3
B_4
B_5
barn
▽ -1; ▲ -2; □ -3; ◐ -4
0
0,5
1,0
1,5
2,0
E, MeV

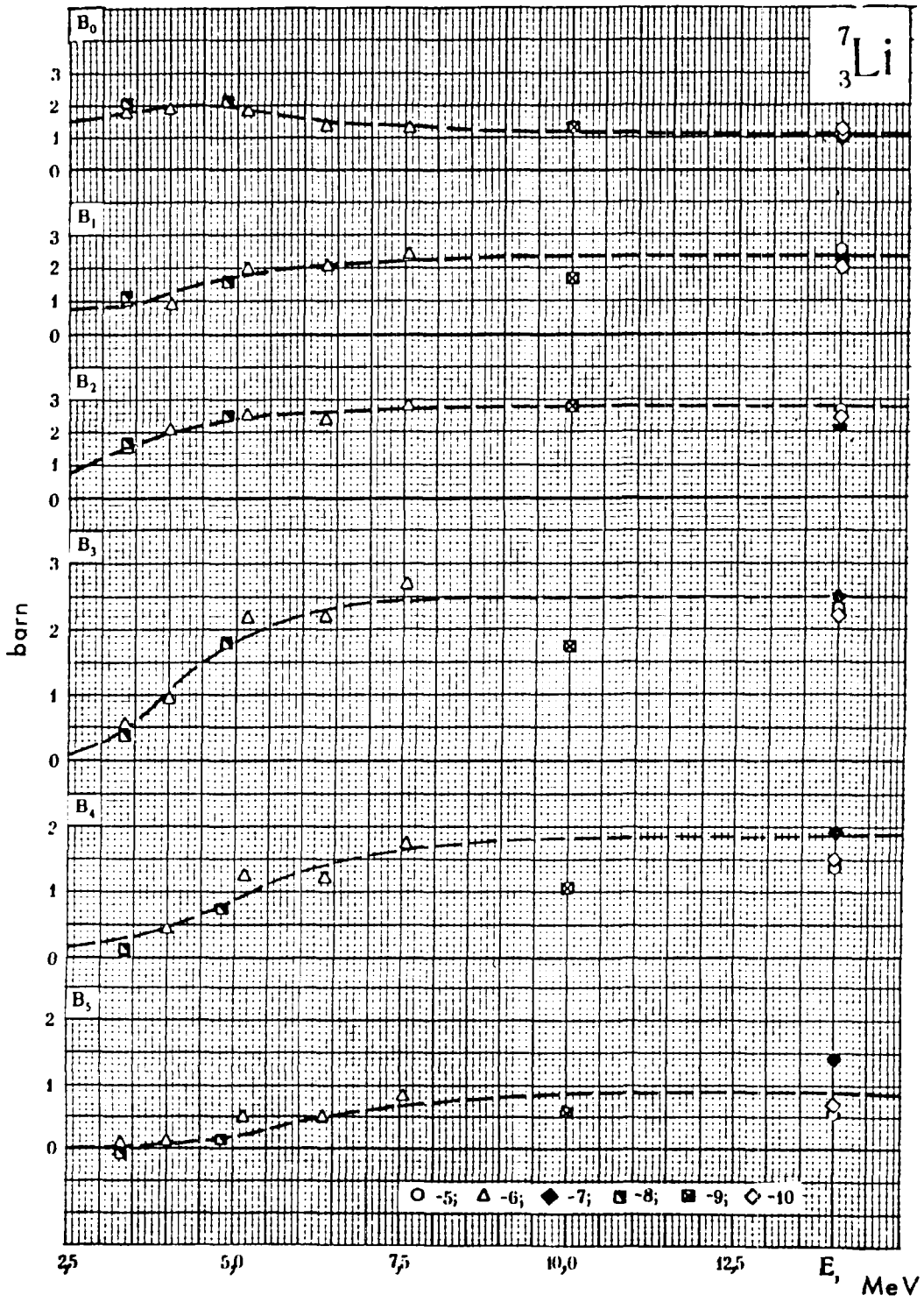
$^{7}_{3}Li$
B_0
B_1
B_2
B_3
B_4
B_5
barn
○ -5; △ -6; ◆ -7; ◪ -8; ◙ -9; ◇ -10
2,5
5,0
7,5
10,0
12,5
E, MeV

L I T H I U M

Neutron angular distribution data for natural lithium are very scarce. The coefficients of the expansion of neutron scattering angular distribution of natural lithium can, however, be derived from the available data of the isotopes with sufficient accuracy.

$_3Li$

1 — [1]; [*W* — 10] — H. B. Willard (1955)
2 — [1]; [*B* — 6] — N. A. Bostrom (1959)
3 — [1]; [*W* — 11] — C. Wong (1962)

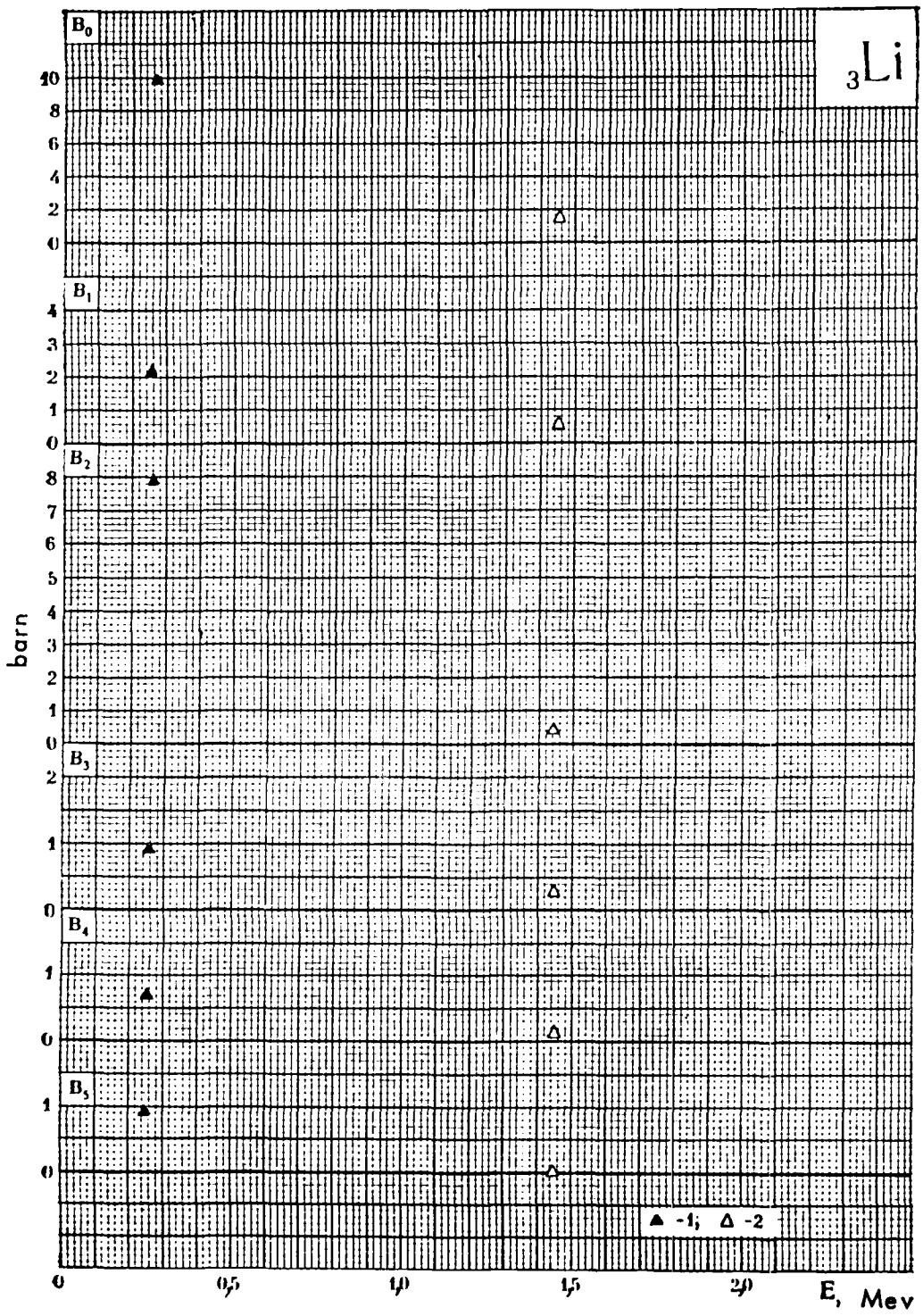
$_3$Li
B_0
B_1
B_2
B_3
B_4
B_5
barn
▲ -1; Δ -2
0
0,5
1,0
1,5
2,0
E, Mev

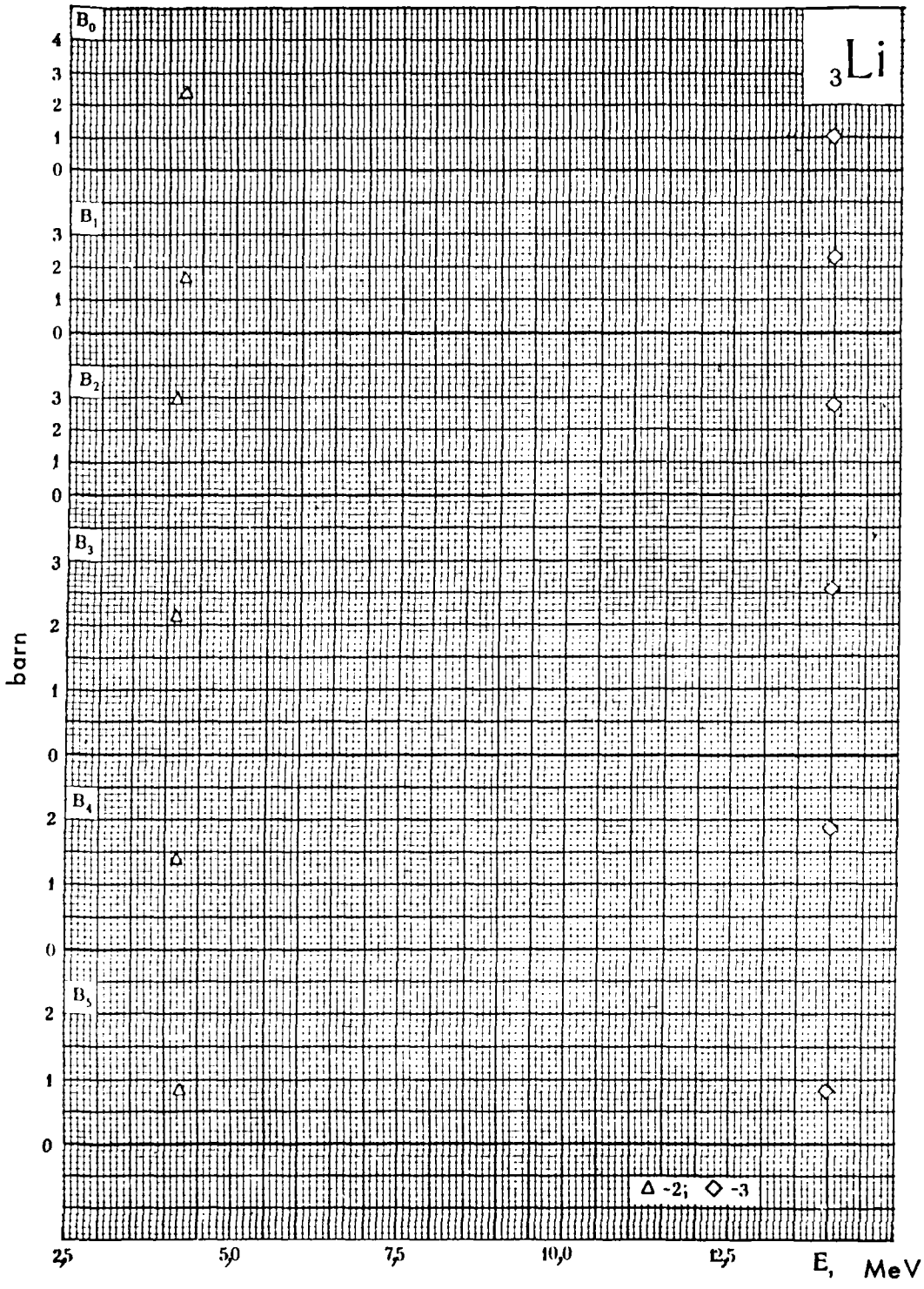
$_3$Li
B_0
B_1
B_2
B_3
B_4
B_5
barn
Δ -2; ◇ -3
2,5
5,0
7,5
10,0
12,5
E, MeV

B E R Y L L I U M

In the energy range below 1 MeV many experimental results have been obtained with different energy resolutions. The best resolutions, 8 and 10 keV, were obtained in experiments by Willard /W-6/(1955), Lane and Monahan /L-8/(1962), and Lane, Elvin and Langsdorf /L-9/(1964).*

Moreover, in the last two works there are enough points measured at sufficient energy values to permit the resonances of Beryllium, lying at 625 and 815 keV to be distinctly resolved. The discrepancies of the available data in the indicated energy range can be explained by the different energy resolutions used and the experimental uncertainties given. With the exception of the experiment by Lane /L-9/, the results of which yield - in the energy range from 0.5 to 0.7 MeV - B_1 values which are three times smaller than those from other works, particularly from those experiments published in the references /L-2/(1957), /L-6/(1961) and /L-8/(1962) which were carried out by the same author. The reasons for the discrepancy mentioned are not given in the publication /L-9/. In the latter work the experimental data have been carefully analysed for elastic angular distribution results as well as for polarization.

The authors in reference /L-9/ have determined spins, parities and resonance parameters of Be-10 states of the first two cross section resonances of Be-9 (see Table 5). Using these parameters and the Blatt-Biedenharn /5/ formula, the energy dependence of B_ℓ in the neutron energy range from 0 to 1 MeV have been calculated in reference /L-9/. In the region of the first two resonances, the results of this calculation are indicated by a dash-dotted curve. We wish to point out, that in the resonance region of 0.625 MeV, the calculated B_1 values lie just between the experimental data

---

* The results of the last two experiments are given in the graphs which represent the energy dependence of B_ℓ only in the resonance region indicated.

of reference /L-9/ and those of older publications.

Table 5:

Parameters of the first two resonances of Beryllium used for the calculation of the energy dependence of B_ℓ.

E_0, MeV	j^π	l	γ_n^2, MeV		$\Gamma_n(E_r)$	
			$s=1$	$s=2$	$s=1$	$s=2$
0,625	3−	2	0,082	0,082	0,008	0,008
0,815	2+	1	0,0008	0,0053	0,0008	0,0053

where γ_n^2 is the reduced width in the centre-of-mass system; $\Gamma_n = 2P_\ell \gamma_n^2$ is the neutron width (where P_ℓ is the penetrability); j and π indicate spin and parity of the compound nucleus Be-10 respectively; ℓ is the orbital angular momentum of neutrons having excited a given level; Eo is the resonance energy; $s = (1 \pm 1/2)$ is the spin of the channel; $I = 3/2$ is the spin of Be-9.

The phases of the potential s-wave scattering were obtained in a unique way; their values were calculated from the effective nuclear radius R = 5.6 Fermi. The phases of the potential scattering of neutrons with high orbital angular momenta are almost zero in this range.

The adopted phases of the potential scattering are not in bad agreement with the scattering cross-section shape in the range below 0.5 MeV, if one assumes the existence of interfering levels, excited by s-wave neutrons. Nevertheless, the experimental values of B_o and, in particular, the total cross sections which coincide in this range with B_o are more reliable than the calculated data. Therefore, the recommended

curve $B_o(E)$ has been derived from experimental data for energies less than 0.6 MeV.

The recommended B values in the energy range 0.9 - 1.1 MeV are not as reliable because of the uncertainty of the data due to the high and low energy resolution used. Moreover, in this energy range, the measured total cross-section (3.5 barn /16/) is considerably higher than the experimental data of B_o. To obtain the recommended curve we gave preference to the latest and more recent data which are in agreement with the theoretical results. The Be resonance at 2.7 MeV is, thanks to the work of Fowler /F-3/ and Levin /L-5/, satisfactorily resolved. The shape of B_o in this resonance range (as well as at higher energies) is in excellent agreement with the data obtained by subtracting the nonelastic cross-section from the total cross-section /16/. The very weak resonance at 4.18 MeV is unresolved. The recommended curve of B_o in this energy range was derived on the basis of the total cross-section. The anomaly of B_ℓ ($\ell > 0$) appearing at 4.2 MeV is not understood.

In the energy range above 7 MeV the total cross-section of Beryllium is a smooth function of energy /16/ and because of this the energy dependence at high energies can be interpolated with confidence between the available points at 7 and 14 MeV.

$_4$Be

1 — [1];	[*W* — 6]	— H. B. Willard (1955)
2 —	[*L* — 2]	— A. Langsdorf (1957)
3 — [1];	[*F* — 3]	— J. L. Fowler (1958)
	[*W* — 6]	— H. B. Willard (1955)
4 — [1];	[*F* — 3]	— J. L. Fowler (1958)
5 — [1];	[*N* — 2]	— M. P. Nakada (1958)
6 — [1];	[*F* — 3]	— J. L. Fowler (1958)
	[*L* — 5]	— J. S. Levin (1960)
7 — [1];	[*F* — 3]	— J. L. Fowler (1958)
	[*L* — 5]	— J. S. Levin (1960)
	[*P* — 3]	— D. D. Phillips (1961)
8 — [1];	[*M* — 5]	— J. B. Marion (1959)
9 — [1];	[*M* — 5]	— J. B. Marion (1959)
	[*W* — 5]	— M. Walt (1955)
10 — [1],	[*L* — 5]	— J. S. Levin (1960)
11 — [1];	[*P* — 3]	— D. D. Phillips (1961)
12 — [1^a];	[*L* — 6]	— R. O. Lane (1961)
13 — [1];	[*P* — 3]	— D. D. Phillips (1961)
	[*M* — 5]	— J. B. Marion (1959)
14 — [1];	[*P* — 3]	— D. D. Phillips (1961)
	[*L* — 5]	— J. S. Levin (1960)
15 — [1];	[*P* — 3]	— D. D. Phillips (1961)
	[*B* — 2]	— J. R. Beyster (1956)
16 — [1^a];	[*L* — 8]	— R. O. Lane (1962)
17 — [1^a];	[*L* — 9]	— R. O. Lane (1964)
18 —	[G — 2]	— G. V. Gorlov (1964)
	[G — 3]	— G. V. Gorlov (1965)
19 —	[*R* — 8]	— J. Roturier (1965)
20 —	[*C*—20]	— J. P. Chien (1966)

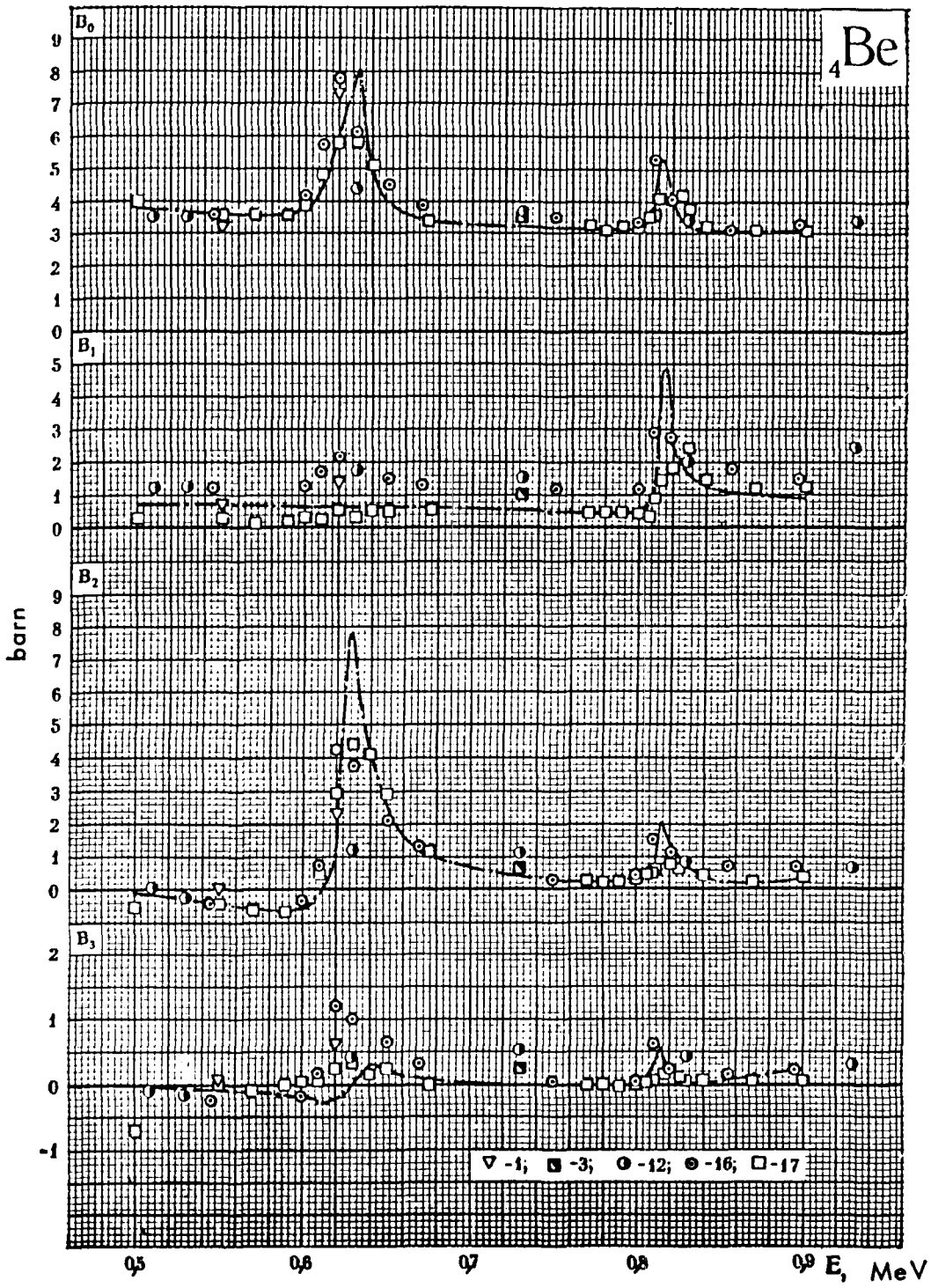
$_4$Be
B_0
B_1
B_2
B_3
barn
E, MeV
0,5
0,6
0,7
0,8
0,9
▽ -1; ■ -3; ◑ -12; ● -16; □ -17

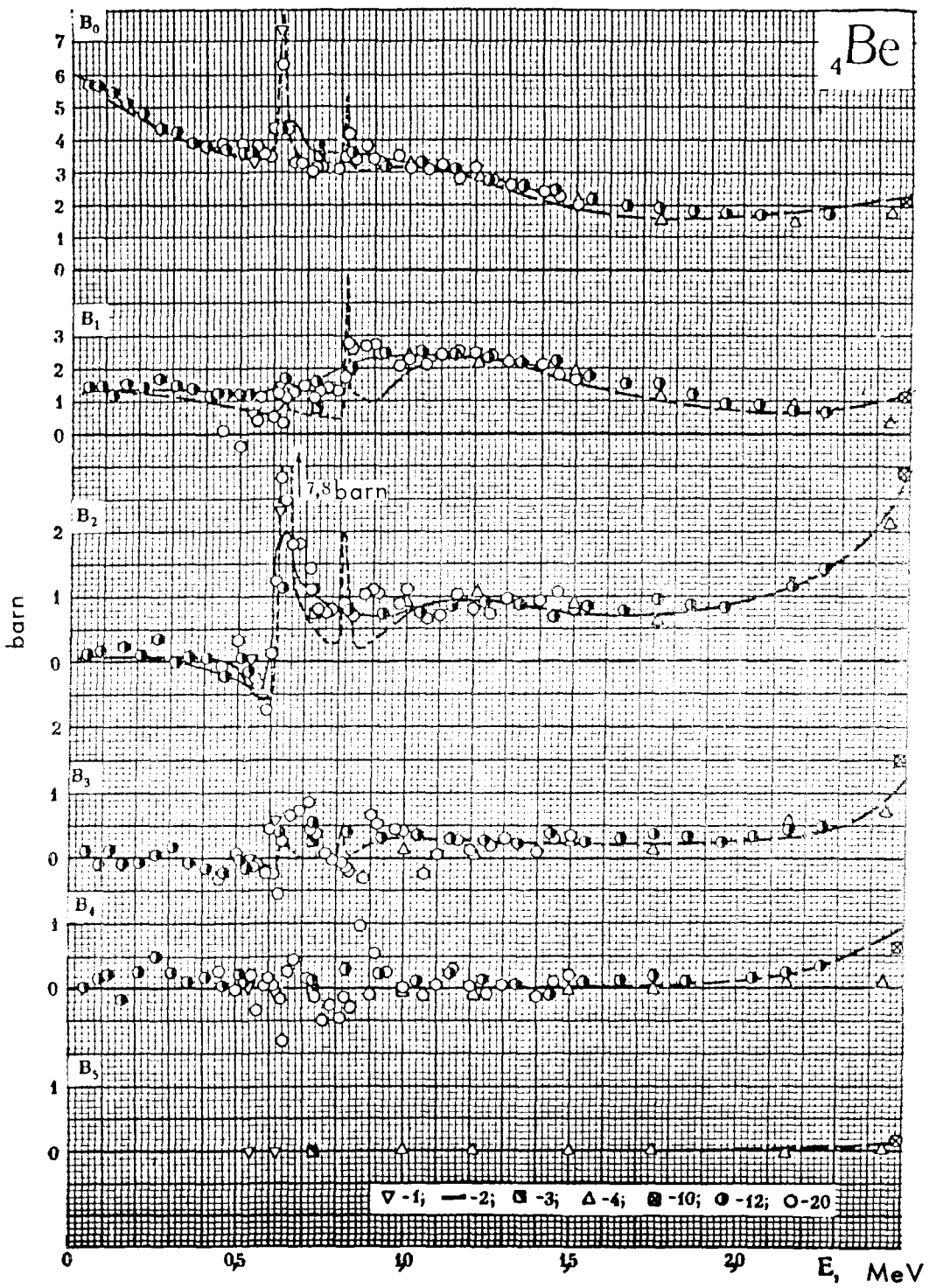
$_4$Be
B_0
B_1
B_2
B_3
B_4
B_5
7,8 barn
barn
E, MeV
0
0,5
1,0
1,5
2,0
▽ -1; — -2; ▣ -3; △ -4; ▩ -10; ● -12; ○ -20

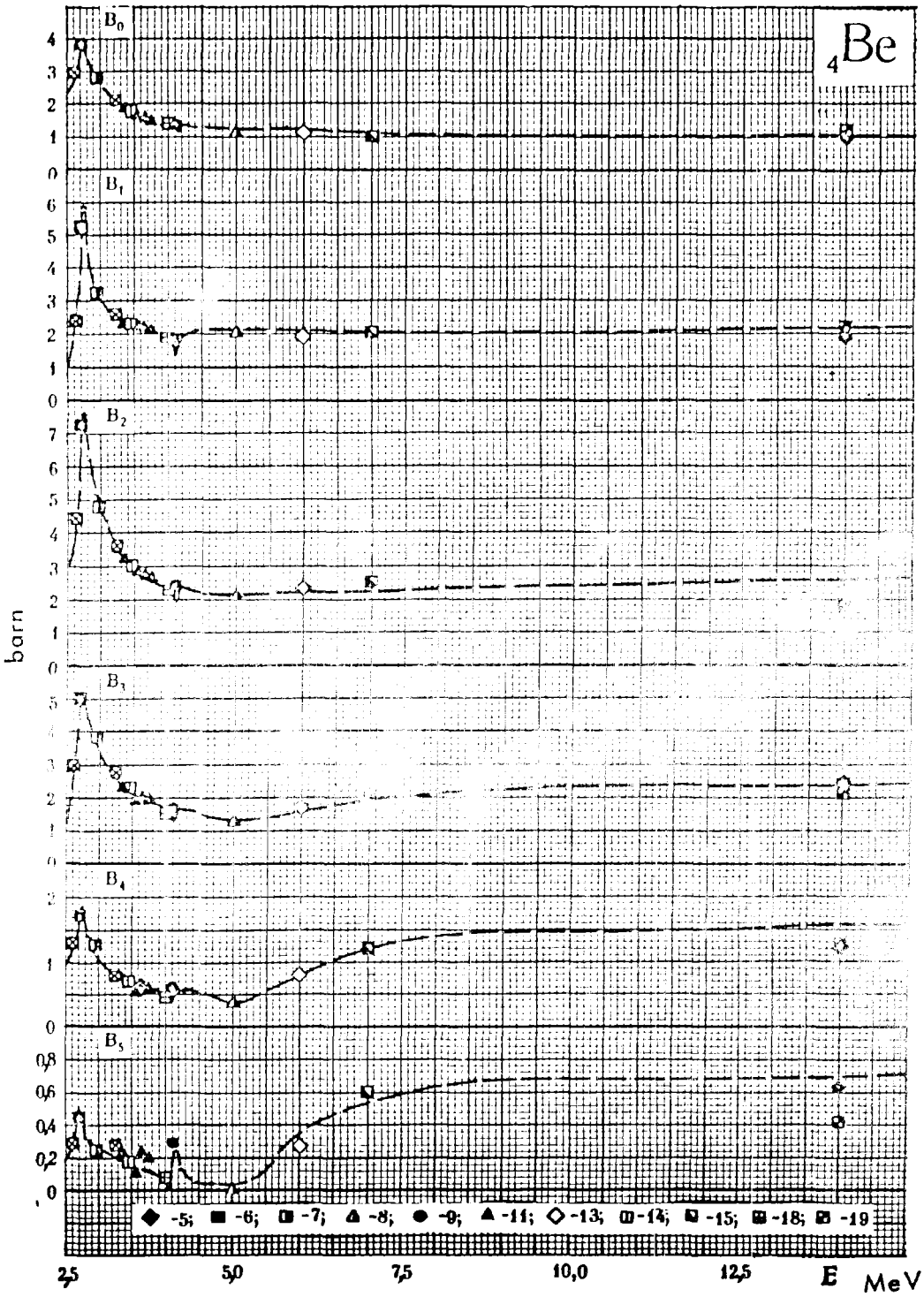
$_4$Be
B_0
B_1
B_2
B_3
B_4
B_5
barn
-5; -6; -7; -8; -9; -11; -13; -14; -15; -18; -19
2,5
5,0
7,5
10,0
12,5
E MeV

B O R O N

The available experimental data on B_ℓ are not very numerous. For natural Boron the data from the three references : /W-6/(1955), /L-2/(1957) and /P-4/(1963) are neither contradictory with one another nor with the global behaviour of the total- and the (n,α)- cross-section /16/ data.

In principle, the energy dependence of B_ℓ in this region can, apparently, be calculated with comparative reliability, as the resonance parameters of all resonance levels of B-11 : (levels, which contribute predominantly to the neutron scattering in natural boron) are well enough established /16/. The phases of the potential scattering can be estimated by fitting the theoretical results to the experimental data. As we did not have the results of such an analysis at our disposal, we derived the recommended curve $B_\ell(E)$ in the range below 1.8 MeV from the data by Langsdorf /L-2/ and, in the range from 1.8 to 3.5 MeV, from the data by Popov /P-7/.

In the energy range above 3.5 MeV only data at 14 MeV from two references /T-4/(1962) and /F-7/(1966) are available : they agree sufficiently well. The data of these measurements show, that at this energy, neutrons with an orbital momentum of 3 and even 4 contribute essentially to the scattering. In conclusion one can say that the data are not very reliable in the range from 3.5 to 14 MeV. With regard to Boron-10, there are still less data for scattering available /W-6/.

$^{10}_{5}B$

1 — [1]; [*W* — 6] — H. B. Willard (1955)

$^{}_{5}B$

1 — [1]; [*W* — 6] — H. B. Willard (1955)
2 — [*L* — 2] — A. Langsdorf (1957)
3 — [*T* — 4] — K. Tesch (1962)
4 — [P — 7] — V. I. Popov (1966)
5 — [*F* — 7] — A. J. Frasca (1966)

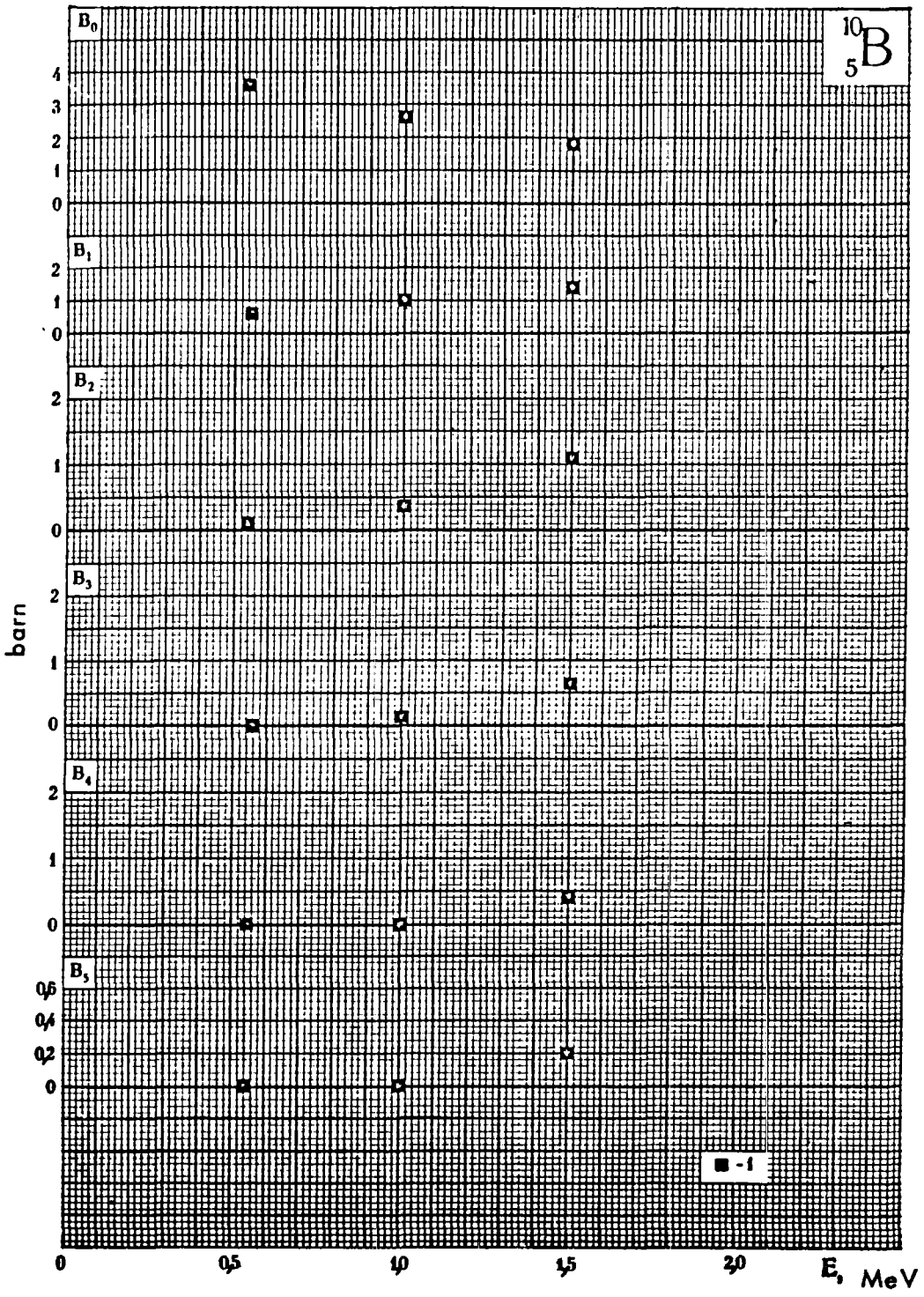
$^{10}_{5}B$
B_0
B_1
B_2
B_3
B_4
B_5
barn
■ -1
0
0,5
1,0
1,5
2,0
E, MeV

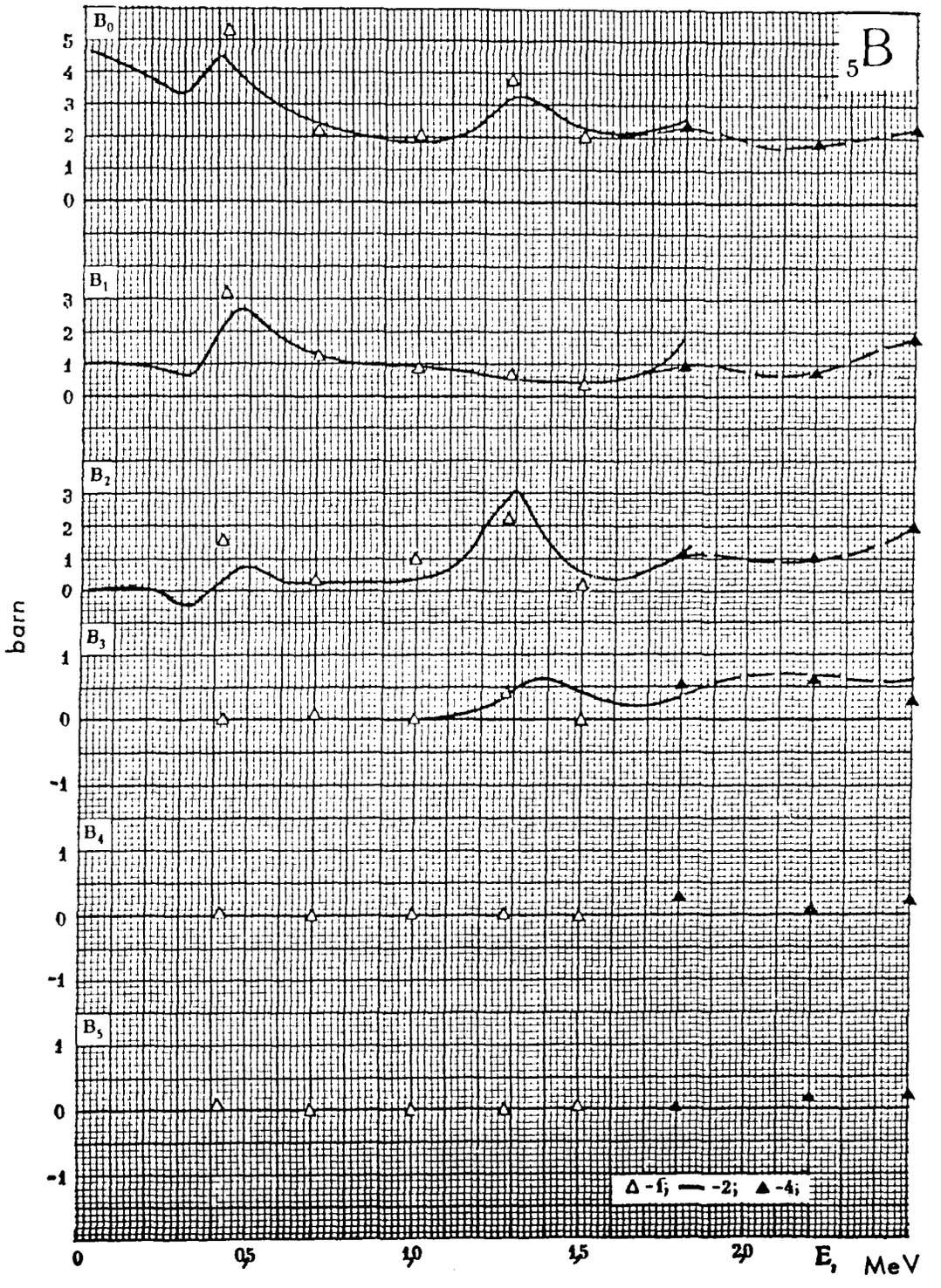
B_0
B_1
B_2
B_3
B_4
B_5
$_5B$
barn
Δ -1; — -2; ▲ -4;
0
0,5
1,0
1,5
2,0
E_n MeV

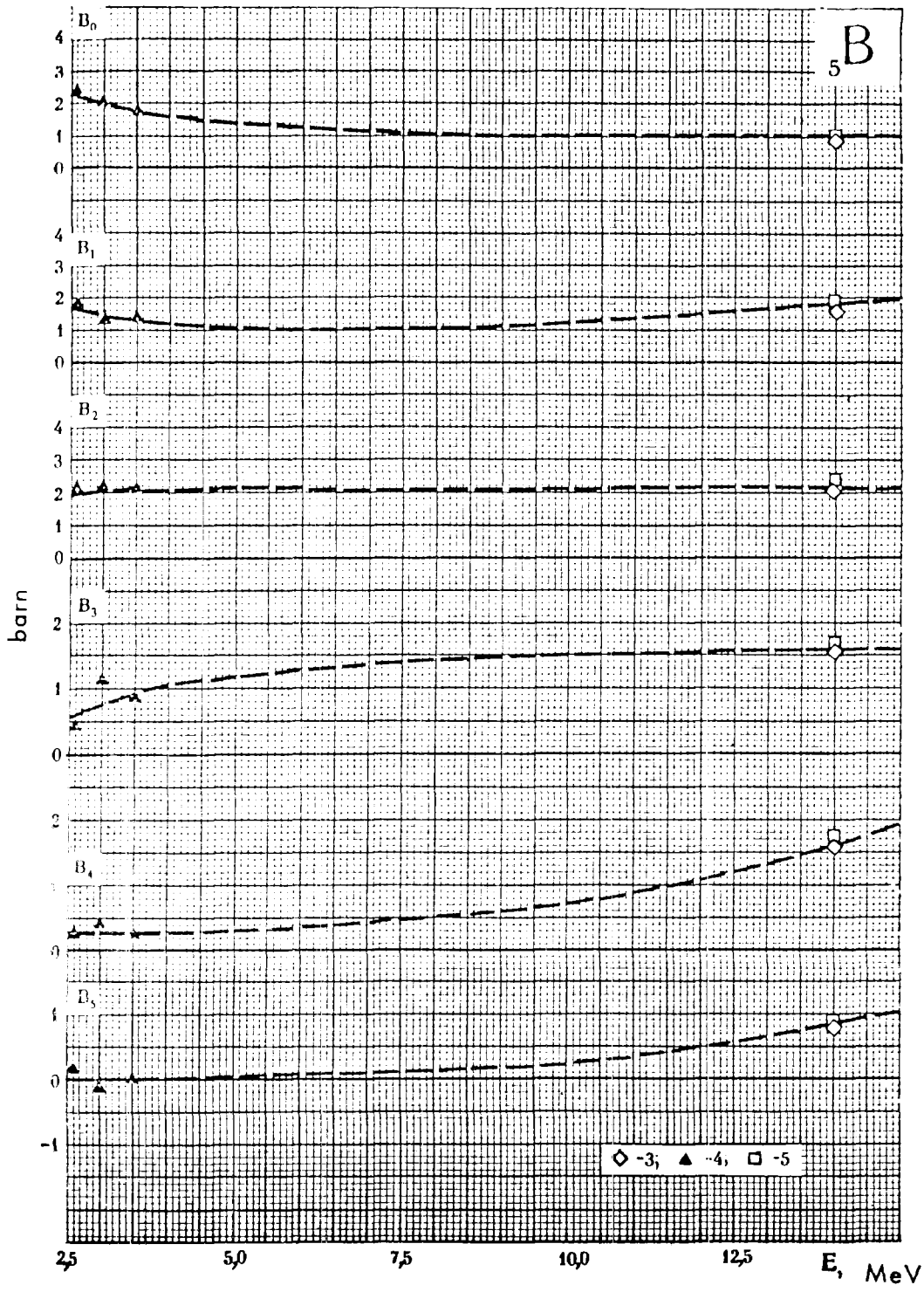
^{5}B
B_0
B_1
B_2
B_3
B_4
B_5
barn
◇ -3; ▲ -4; □ -5
2,5
5,0
7,5
10,0
12,5
E, MeV

C A R B O N

The neutron scattering angular distribution below 2.5 MeV has been measured in several works. The results of these experiments, however, show considerable disagreement. Willard /W-6/(1955) and Rogers /R-5/(1961) obtained, in the energy range from 0.5 to 1.5 MeV, isotropic angular distributions in the centre-of-mass system, while the experimental results of the references /L-2/(1957), /L-6/(1961), /K-5/(1964) and /W-9/(1958), which agree well in this energy range,are mainly forward-peaked (in the centre-of-mass system). The latter results appear to us to be more reliable. The normalization of differential scattering cross-sections in the energy range considered was performed with the help of the total cross-section of c arbon.

In the cross-section resonance region of C-12 at 2.08 MeV, the angular distribution was measured by Lane et al. /L-6/ with high resolution (9 - 10 keV), which is comparative with the resonance width equal to 7 keV. The results of reference /L-6/ are plotted on a separate sheet in the resonance region around 2.08 MeV. The normalization of the experimental angular distribution was carried out here relative to the integrated cross-section of t in, which in its turn, was normalized to the flat scattering cross-section of carbon in the non-resonance region, where it was practically energy independent and equal to the total cross-section.

The angular distribution (not normalized) in the resonance region was also measured by the time-of-flight method with a resolution of 15 keV /L-10/. The expansion coefficients represented in the graph are derived after normalizing this angular distribution to the total cross-section averaged over the resolution function (which we have assumed to be rectangular). The results of reference /L-10/ apparently agree with the more detailed results in reference /L-6/; the agreement can be improved upon, if one assumes that the mean energy in reference /L-10/ is 2.075 MeV and not 2.08. Another possible explanation for the discrepancy is that the real resolution function differs from that chosen by us.

Above 2.5 MeV there are detailed angular distribution measurements available (from 3.07 to 4.73 MeV), made by Lister and Sayres /L-11/(1965) using a proportional counter and a resolution of 25 keV. Since there are many data points they are plotted on a separate sheet. These data indicate resonances at 3.6 and 4.3 MeV, which also appear distinctly in the total cross-section (the level width at 3.6 MeV seems to indicate a single-particle resonance). The results of earlier measurements permit the shape of B_ℓ in the resonance region around 2.95 MeV to be traced too. The resonances lying at energies higher than 4.3 MeV were not resolved in the angular distribution measurements. We wish to point out that the value $B_1 \sim 1.5$ barn in reference /L-11/ at 4.2 MeV confirms the value in reference /B-6/(1959), while in the references /W-5/(1955) and /W-9/(1958) a value of ~ 0.2 barn is given. The total cross-section (B_0) at 4.7 MeV from reference /L-6/, however, shows a disagreement of 40% with B_0 from reference /L-11/, while all other coefficients agree well. Poor agreement is also observed between the low values of B_3 and B_4 obtained in /L-10/ at 4.3 MeV compared with the data of all other references.

In the range from 4.7 to 8.0 MeV only data at some energy points are available and, moreover, their energy resolutions are not at all high. Owing to this and the existence of some strong resonances in the energy range considered, it is difficult to describe the unique middle value of B_ℓ with a smooth curve, derived from experimental points.

The weak resonance at 4.93 MeV was most likely covered by the resolution function of the point measured at 5 ± 0.1 MeV /H-2/(1957), but the influence of its small width cannot affect the result. A stronger level at 5.36 MeV is on the limits of the energy spread of the above-mentioned work as well as that of /B-8/(1960), where the angular distribution was measured at 5.6 ± 0.07 MeV.

The large discrepancy of B_1 obtained in these experiments is difficult to explain.

Also, in the region between the resonances at 5.36 and 6.5 MeV,

where B_0 is almost constant (which follows from the total cross-section measurements), the establishment of the higher harmonics is not at all reliable, since the experimental values of B_ℓ at 5.6 ± 0.07 MeV and 6 ± 0.23 MeV /W-12/, /W-13/ differ strongly for $\ell > 0$ (possibly due to the influence of resonances in the neighbourhood). We wish to point out that the results of the references /W-12/ and /W-13/ agree excellently with the results of Haddad and Phillips /H-3/(1959) at 6 MeV. The energy resolution used in the latter work is, unfortunately, unknown. This circumstance also makes it difficult to use the data of these authors at 6.3 MeV (which is exactly the resonance energy) and to compare these data with the results of the experiment published in /L-10/ at 6.3 MeV, with an energy resolution of $\pm$ 80 keV which covers almost the whole resonance region, of which the width is equal to 65 keV.

The results which have been obtained in work /H-3/ at an energy of 7 MeV, almost coincide with the data by Beyster et al. /B-2/(1956). The energy resolution in the latter work was $\pm$ 0.2 MeV, therefore, the results should not have been strongly influenced by the near resonances (a group of weak levels is at 6.50; 6.57 and 6.7 MeV, and a strong resonance ($\Gamma \sim 250$ keV) at 7.4 MeV). The weak anisotropic scattering observed at 7 MeV in the experiments /H-3/ and /B-2/ is probably due to this influence. The anisotropic scattering in the 7.4 MeV region was measured by Bostrom et al. /B-6/(1959) at an energy of 7.58 ± 0.1 MeV. The character of the angular distribution at this energy differs strongly from that at 7 MeV. However, the angular distribution of the next resonance is not very much different as can be seen from the data at 7.8 MeV published in reference /L-10/. *

---

* The data of reference /L-10/ have been normalized to the total cross-section averaged over the resolution function.

For higher energies, only data in the 14 MeV region are available; in general, they agree quite well. However, since in the range from 7.5 to 14 MeV there is a great number of resonances, a more-or-less reliable interpolation of the data is not possible in this region. It would therefore be very desirable to do a series of measurements in the energy range from 5 to 15 MeV with low energy resolution which should, nevertheless, cover the whole energy interval and would at least permit the derivation of average values of B_l. Such data would be sufficient for many practical applications.

From the above considerations, it follows that the reliability of the recommended curves for energies above 4.5 MeV is low. In order to derive these curves we used, as a guide, not only the quoted data of B_l but also the total- and the nonelastic cross-sections. The values for the high moments are given in Table 6.

Table 6

Ref.	E, MeV	B_4	B_7	Ref.	E, MeV	B_4	B_7	Ref.	E, MeV	B_4	B_7
[Г—2] [Г—3]	4,0	0,099	0,101	[H—2]	5,0	0,208	0,366	[B—2] [H—3]	7,0	—0,020	—0,013
[W—5] [W—9]	4,1	0,197	—0,062	[B—8]	5,6	—0,069	—0,047	[B—6]	7,58	0,130	0,118
[B—6]	4,21	0,051	0,109	[H—3] [W— —12]	6,0	—0,042	0,049	[B— 11] [F—7]	14,6 14,0	0,206 0,350	0,024 —0,193
[B—6]	4,7	0,102	0,062	[H—3]	6,3	0,189	0,123	[1]	14,0	0,481	0,243

$_6C$

1 — [1]; [M — 2] — R. W. Meier (1954)
2 — [1]; [L — 1] — R. N. Little (1955)
3 — [1]; [W — 6] — H. B. Willard (1955)
4 — [1]; [W — 5] — M. Walt (1955)
[W — 9] — J. E. Wills (1958)
5 — [1]; [B — 2] — J. R. Beyster (1956)
[H — 3] — E. Haddad (1959)
6 — [1]; [M — 3] — C. O. Muehlhause (1956)
7 [L — 2] — A. Langsdorf (1957)
8 — [1]; [H — 2] — R. W. Hill (1958)
9 — [1]; [K — 1] — M. M. Khaletskii (1957)
[C — 5] — J. H. Coon (1958)
[N — 2] — M. P. Nakada (1958)
[S — 6] — J. B. Singletary (1959)
[S — 10] — V. I. Strizhak (1961)
[C — 16] — R. L. Clarke (1964)
10 — [1]; [W — 9] — J. E. Wills (1958)
11 — [1]; [B — 6] — N. A. Bostrom (1959)

12 — [1]; [*H* — 3] — E. Haddad (1959)
13 — [1]; [*H* — 3] — E. Haddad (1959)
[*W* — 12] — R. M. Wilenzick (1962)
[*W* — 13] — R. M. Wilenzick (1965)
14 — [1]; [*B* — 8] — J. E. Braley (1960)
15 — [*R* — 5] — W. L. Rogers (1961)
16 — [1ª]; [*L* — 6] — R. O. Lane (1961)
17 — [*B* — 11] — R. Bouchez (1963)
18 — [*K* — 5] — I.A.Korzh (1964)
19 — [G— 2] — G.V.Gorlov (1964)
[G— 3] — G.V.Gorlov (1965)
20 — [*L* — 10] — A. Langsdorf (1965)
21 — [*L* — 11] — D. Lister (1965)
22 — [*F* — 7] — A. J. Frasca (1966)

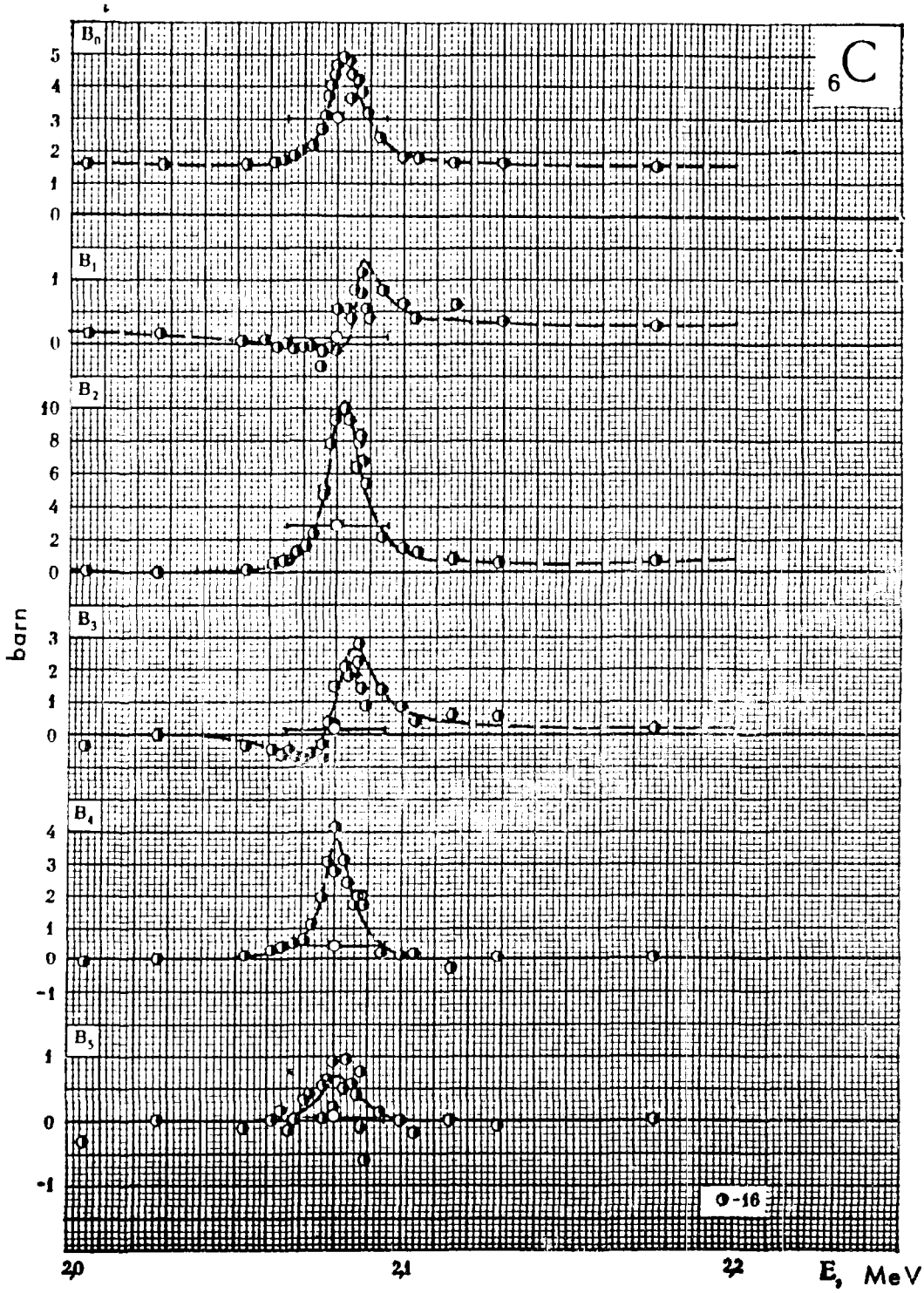
B_0
B_1
B_2
B_3
B_4
B_5
$_6C$
barn
O-16
20
21
22
E, MeV

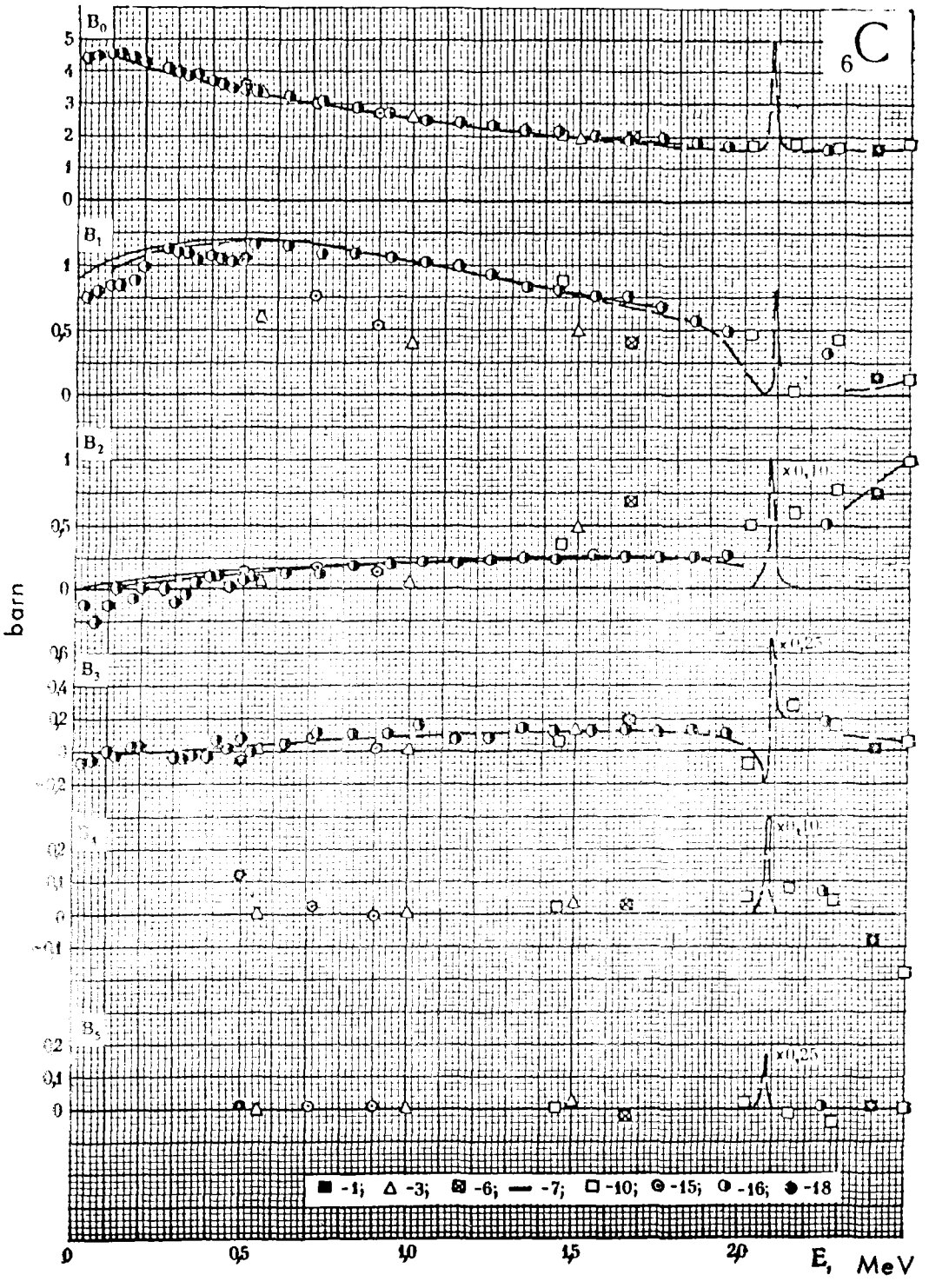
B_0
B_1
B_2
B_3
B_4
B_5
^6C
barn
E, MeV
■ -1; △ -3; ⊠ -6; — -7; □ -10; ⊙ -15; ◑ -16; ● -18

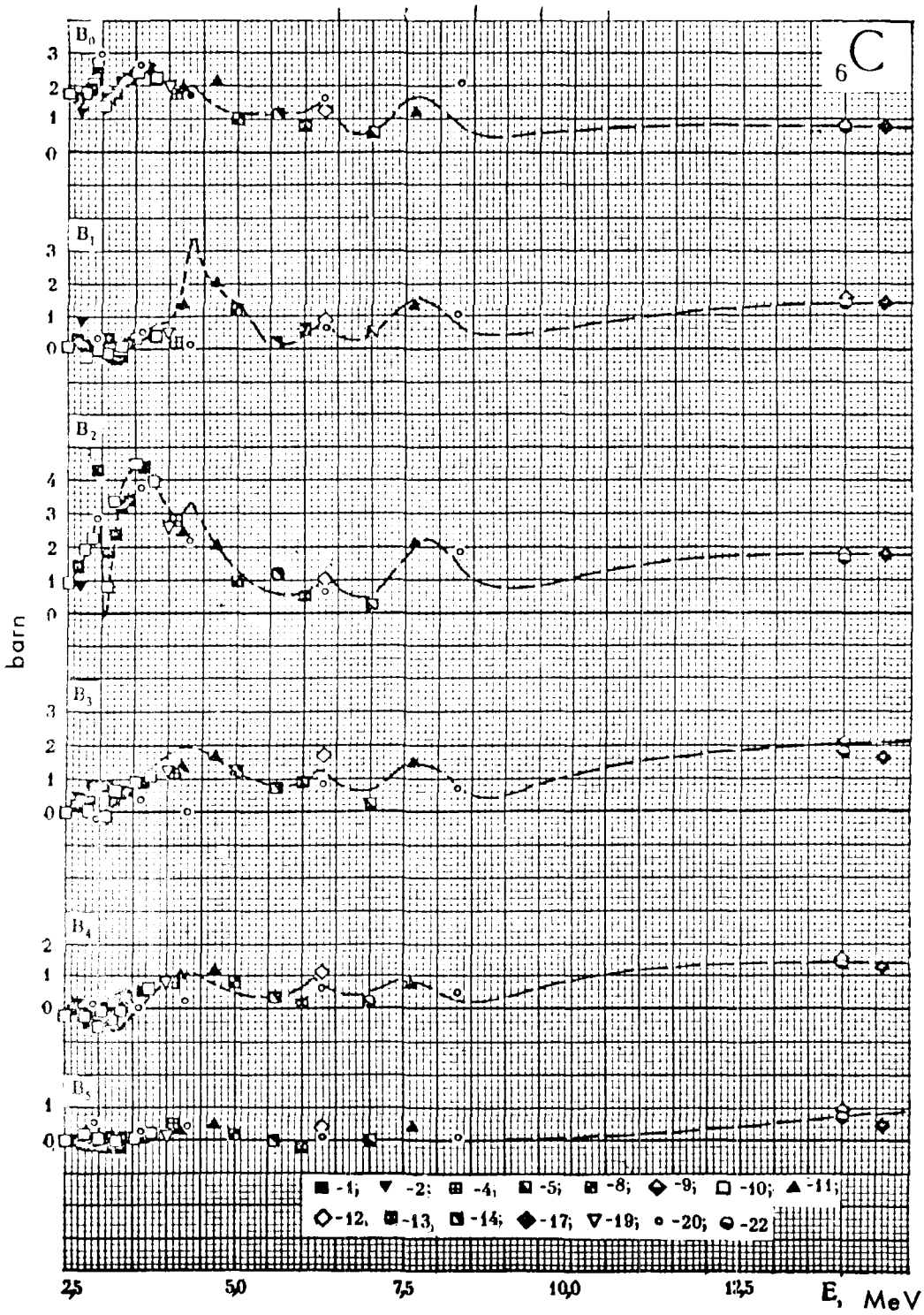
B_0
B_1
B_2
B_3
B_4
B_5
^6C
barn
■ -1; ▼ -2; ⊞ -4; ▣ -5; ▩ -8; ◆ -9; □ -10; ▲ -11;
◇ -12; ▦ -13; ◨ -14; ◆ -17; ▽ -19; ∘ -20; ⊖ -22
2,5
5,0
7,5
10,0
12,5
E, MeV

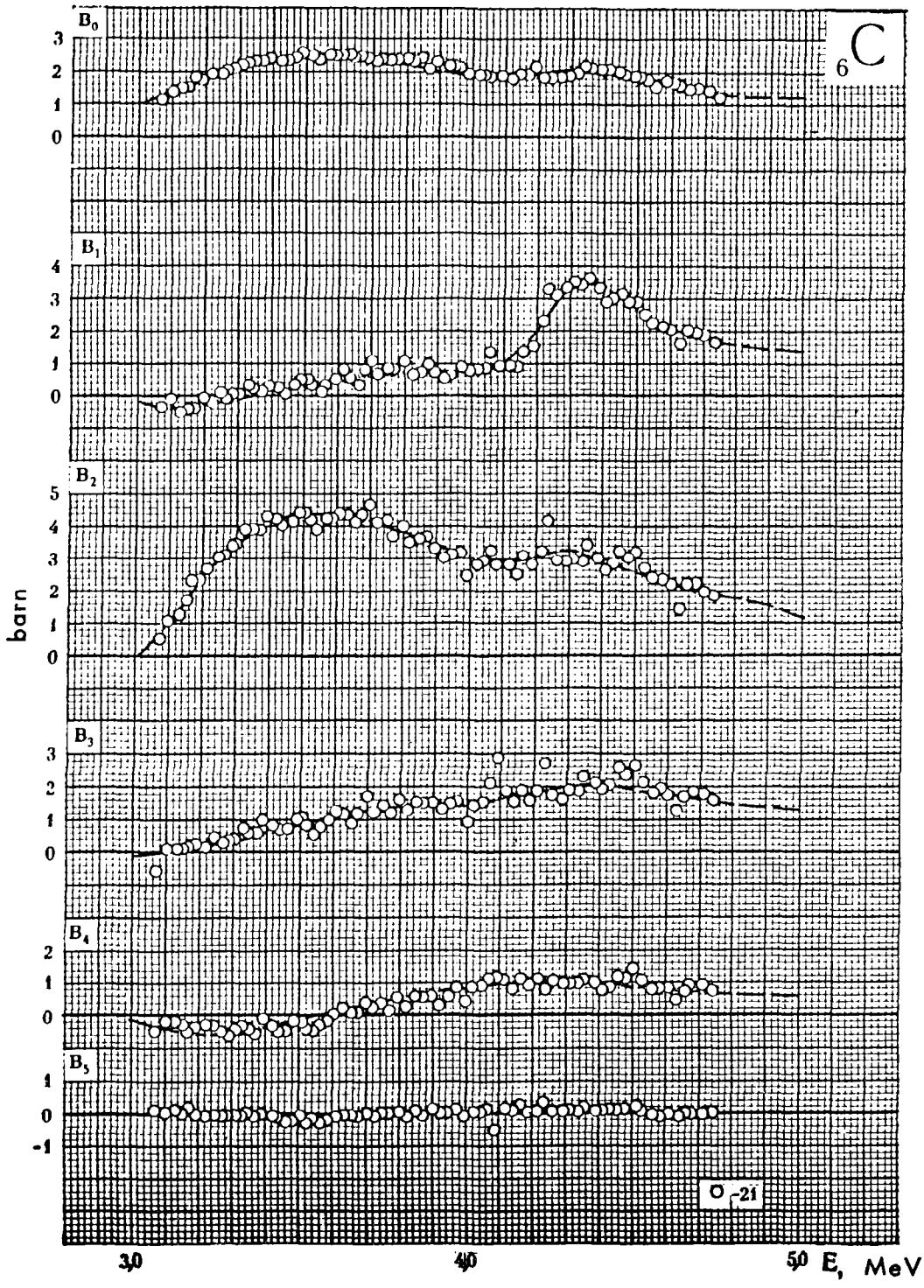
B_0
B_1
B_2
B_3
B_4
B_5
^6C
O -21
barn
E, MeV
30
40
50

N I T R O G E N

Experimental data for the angular distribution of neutrons elastically scattered on nitrogen are only available for energies higher than 0.8 MeV. At lower energies, the cross-section of nitrogen has only one rather narrow resonance which results from capture of neutrons with $\ell > 0$ at 0.43 MeV. Therefore, in this energy region, the anisotropic scattering should not be large. It can be estimated by means of linear extrapolation from the mean cosine scattering angle value available at 0.8 MeV to 0.0476 at E = 0. In the region from 0.8 to 3 MeV the data by Fowler and Johnson /F-1/(1955) agree well with the more recent data by Fowler /F-8/(1967). The results of both experiments also agree well with the total cross-section (the nonelastic cross-section is still small in this region). One has to point out that the majority of angular distributions in reference /F-1/ are only measured for $\mu < 0.45$ so that in order to derive B_ℓ from this experiment one had to extrapolate to small angles which obviously reduced the reliability of the data obtained.

For energies higher than 3 MeV there are sufficient data for the anisotropic scattering so that the energy dependence of B_ℓ could be obtained up to 15 MeV. The accuracy of the recommended curves can be estimated from the scatter of the experimental points around them. The values of the high moments are given in Table 7.

Table 7

Ref.	E, MeV	B_1	B_2	Ref.	E, MeV	B_1	B_2	Ref.	E, MeV	B_1	B_2
[B—4]	4,5	0,040	0,047	P—3	7,0	—0,069	—0,011	B—21	11,55	0,792	—
[B—4]	4,85	0,284	0,113	B—4	7,11	—0,002	—0,118	C—12	11,6	0,478	0,195
[C—12]	4,99	0,191	0,077	B—21	7,93	0,357	—	B—21	12,25	1,07	—
[B—4]	5,15	0,065	0,010	C—12	8,00	—0,018	—0,110	B—21	13,50	1,36	—
[C—12]	5,66	0,084	—	B—21	8,35	0,209	—	B—21	13,96	1,25	—
[C—12]	6,02	0,015	—	B—21	9,38	0,400	—	B—12	14,00	0,762	0,241
[C—12]	6,53	—0,026	0,102	B—21	10,10	0,575	—	C—10	14,00	0,250	0,014
[B—21]	6,78	0,095	—	B—21	10,93	0,431	—	--	—	—	—

$_{7}N$

1 — [1]; [*F* — 1] — J. L. Fowler (1955)
2 — [1]; [*S* — 10] — V. I. Strizhak (1961)
3 — [1]; [*B* — 4] — N. A. Bostrom (1957)
4 — [1]; [*C* — 12] — L. F. Chase (1961)
5 — [1]; [*P* — 3] — D. D. Phillips (1961)
6 — [*B* — 12] — R. W. Bauer (1963)
7 — [*F* — 8] — J. L. Fowler (1966)
8 — [*B* — 21] — R. W. Bauer (1967)

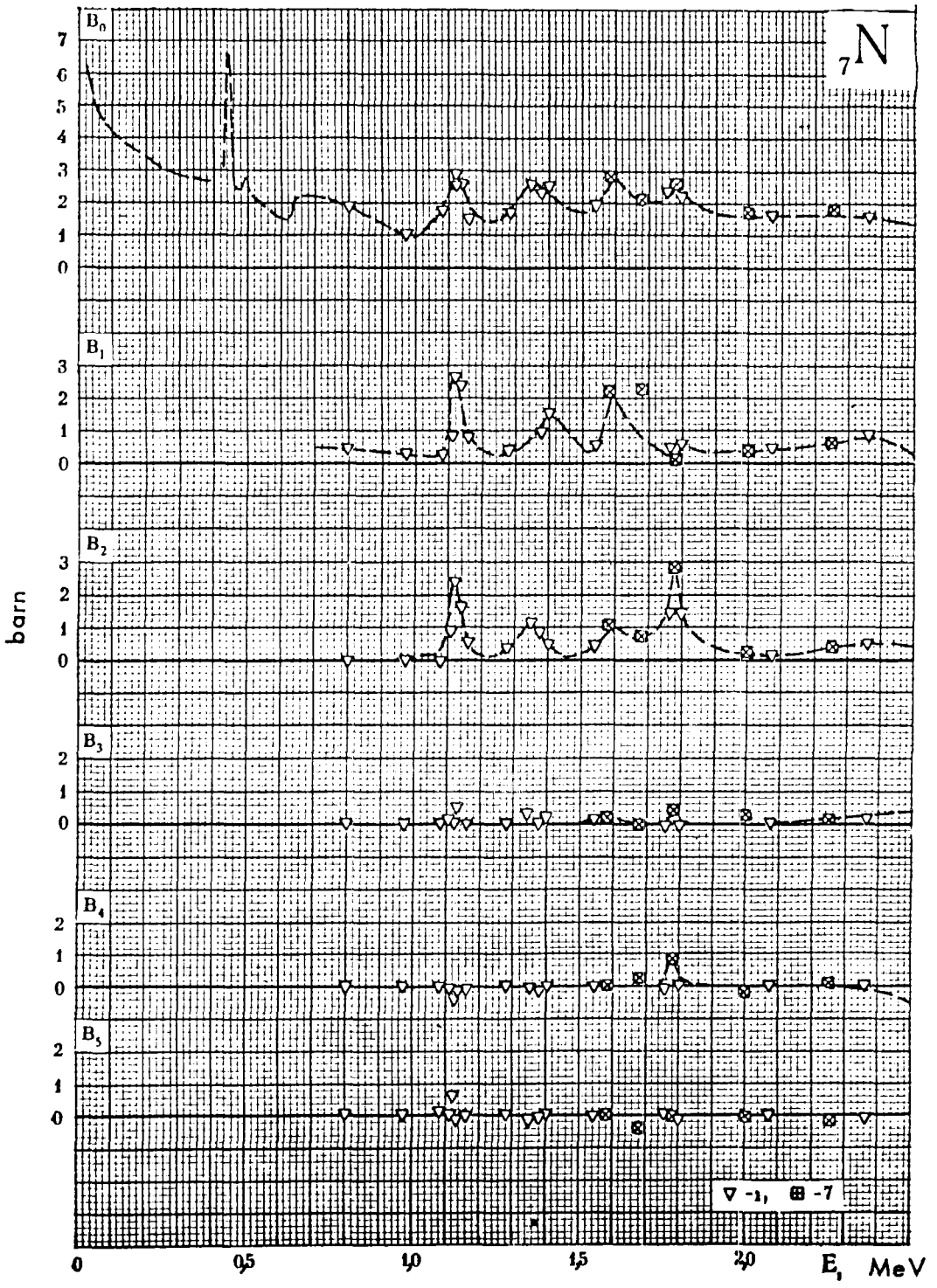
B_0
B_1
B_2
B_3
B_4
B_5
$_7N$
barn
▽ -1, ⊠ -7
0
0,5
1,0
1,5
2,0
E_1 MeV

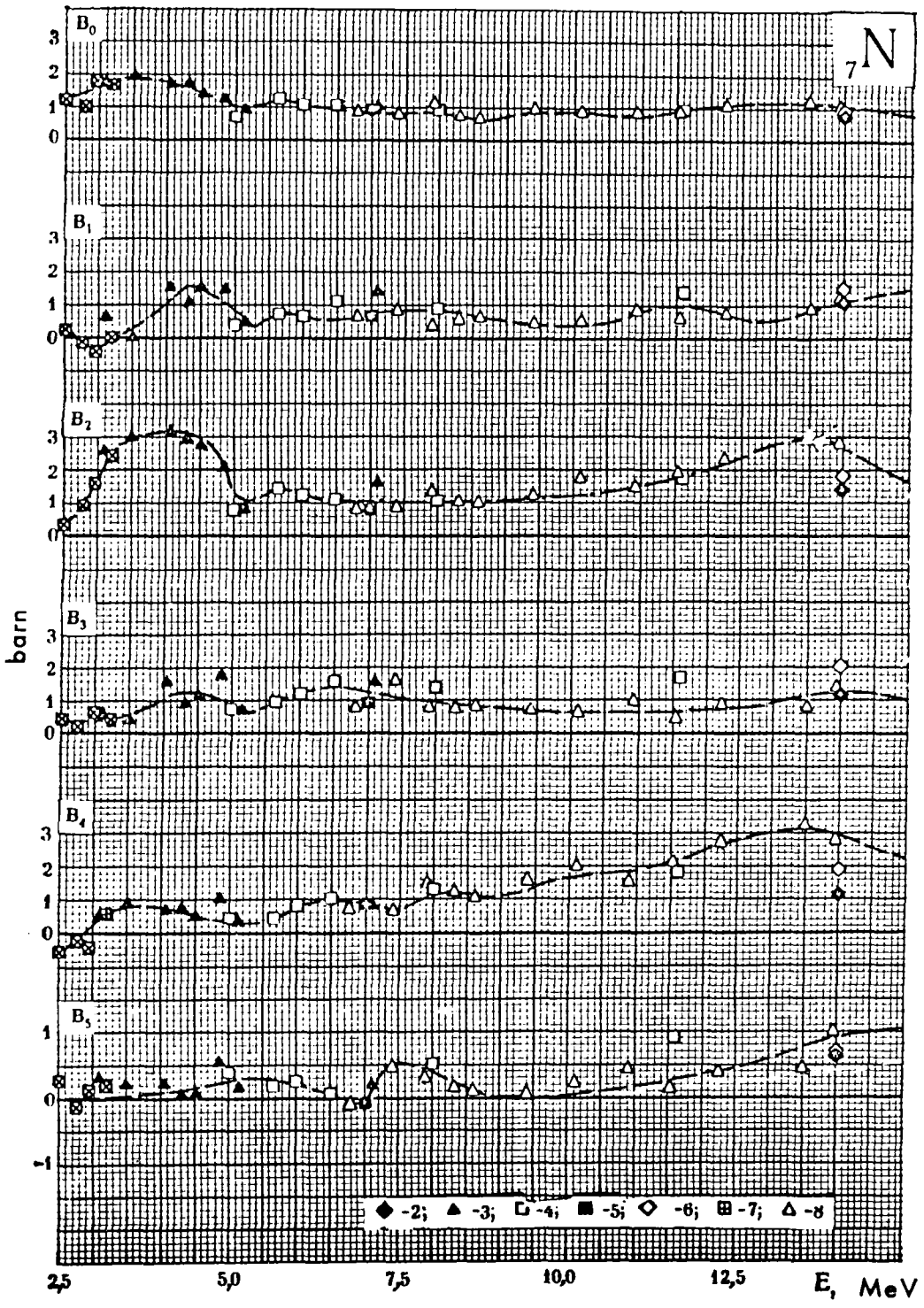
$_7N$
B_0
B_1
B_2
B_3
B_4
B_5
barn
◆ -2; ▲ -3; □ -4; ■ -5; ◇ -6; ⊞ -7; △ -8
2,5
5,0
7,5
10,0
12,5
E, MeV

O X Y G E N

From the experiment for oxygen by Lane et al. /L-6/(1961) one can obtain a well-defined energy dependence of B_ℓ in the energy range from 0.3 to 1.7 MeV. At lower energies the angular distribution is almost isotropic in the centre-of-mass system. The energy dependence of B_o is, however, not measured. Also, the total cross-section which, in this energy range, coincides with B_o, is measured with a very high uncertainty. The results of reference /L-6/ for the resonance at 0.442 MeV are in excellent agreement with earlier, detailed data by Okazaki /O-1/(1955), and with the data by Fowler /F-2/(1958) at the next resonance energy (1 MeV). The high resolution of 6 keV in the region of 1.6 MeV and about 20 keV in the region of 1 MeV obtained in reference /L-6/, permitted a clear resolution of the first four resonances of oxygen, of which the shape of the first three are slightly distorted due to the energy spread.

In the range from 1.65 to 2.5 MeV, oxygen has 3 resonances : at 1.84 MeV ($\ell > 0$), at 1.91 MeV (p-wave resonance) and, a broad s-wave resonance at 2.37 MeV where the cross-section has a deep minimum brought about by interference with the potential scattering. The angular distribution is slightly anisotropic in the neighbourhood of the latter resonance and has been carefully studied. For the resonance regions around 1.84 and 1.91 MeV where one can also expect particularities in the angular distributions (although they are not very important because of the narrowness of these resonances) there are, unfortunately, no experimental values available.

The B_ℓ - values in this region were calculated by Jona /11/ using the Blatt-Wigner formula. The phases for potential scattering have been obtained considering the conditions that, the calculated total cross-section in the range from 1.6 to 2.4 MeV and the energy dependence of B_1 and B_2 near the resonance at 1.67 MeV are in sufficiently good agreement with the experimental data. The authors did not, however, succeed in satisfying these two conditions and, as a consequence, the results obtained by them in the energy range from 1.75 to 2.0 MeV are also doubtful. For orientation we nevertheless represent these results in the plots by points. The derivation of the recommended curves in the energy range from 1.7 to 1.8 MeV are based on the fact that the energy dependence of B_o which is practically equal to the total cross-

section in this region.

We now consider the energy range from 2.5 to 5.5 MeV. The general behaviour of B_ℓ in this region is sufficiently well described by the data of D. Phillips /P-3/(1961) and H. Bostrom /B-4/(1957). The energy resolutions used in these measurements are not mentioned in the publications. However, a comparison of their energy dependence of B_o with the energy dependence of the total experimental cross-sections of oxygen, measured in the range considered with a resolution of 30 keV, permits the supposition that the resolution in the experiments /P-3/ and /B-4/ was about $\pm$100 keV. With such a resolution the resonance peak should be smoothed out : this is in fact the case.

Apart from the experiments mentioned, the angular distribution of neutrons elastically scattered by oxygen in the energy range considered has also been measured by T. Fowler et al. /F-6/(1964), Hunzinger and P. Huber /H-6/(1962), as well as D. Lister et al. /L-11/(1965). The energy resolution in reference /F-6/ was very high ($\pm$10 keV). This explains the exceptional behaviour of B_ℓ obtained from this work at the 3.77 MeV resonance as well as at its wing at 3.9 MeV. At an energy of 3.3 MeV, where the cross-section is almost constant, the data by Fowler agree well with the results by Phillips. Reference /L-11/ gives many data on the energy dependence of the coefficients B_ℓ in the energy range from $\sim$3.1 to $\sim$4.8 MeV, where two series of measurements with a resolution of 25 and 18 keV have been carried out. The results of these works are plotted on separate sheets. The latter experiment confirms the data of other authors and permits investigation of the resonances which are present in the energy range considered.

The data of reference /H-6/, which have been obtained by analysing the oxygen recoil spectra in an ionization chamber at 3 MeV, diverge appreciably from the results of the previous authors. This is possibly due to the uncertainty of the measurement of low energy recoil spectra, and also to the fact that scattering has been measured at only a few angles for cosine values less than 0.6 (centre-of-mass system). Consequently, the data of reference /H-6/ can not be used for deriving B_ℓ in the energy range (3-4 MeV) where anisotropic scattering is high.

At lower energies, where the angular distribution function is more flat, the results of this work are entirely correct.

At energies higher than 5 MeV there are the basic data of L. Chase /C-12/(1961) which have been measured with a broad resolution from 0.23 to 0.8 MeV, and which already yield comparatively good mean values over the resonances. The results obtained in this work agree well with the measurements by Phillips /P-3/ at 6 and 7 MeV and by Bostrom /B-4/ at 5 and 7 MeV.

A comparison of the values of B_o with the data obtained by subtracting the nonelastic cross-section from the total cross-section shows that there is good agreement in the energy range below 5.5 MeV and also at 8 and 11.6 MeV. At energies from 6.5 to 7.5 MeV, however, the experimental data of B_o lie essentially lower than the results obtained by the above-mentioned subtraction. Around 7 MeV this difference is 0.7 barn, which exceeds twice the nonelastic cross-section. It is, therefore, difficult to attribute this difference to the uncertainty of the latter. It is also unlikely that the total cross-section error is so large. Therefore, regardless of the low B_o-values obtained independently in all three experiments (/C-12/, /P-3/ and /B-4/) in the energy range from 6.5 to 7 MeV, we found it necessary to use the total cross-sections averaged over the resonance peaks and nonelastic cross-sections in order to derive the recommended curve $B_o(E)$ in this energy range. The curves $B_\ell(E)$ ($\ell > 0$) were derived in such a manner that, in the mean, it satisfied the values $(2\ell+1)\omega_\ell = B_\ell/B_o$, which have been obtained from measured angular distributions.

At 14 MeV there are no reliable data for the nonelastic cross-sections and B_o cannot be obtained from the difference $\sigma_T - \sigma_{nonel.}$ For the derivation of the recommended curves we were guided by the work of Bauer /B-12/(1963).

The values of high momenta are given in tables 8 and 9. The coetficients B_8 and B_9, obtained in work /B-12/ at 19 MeV are equal to 0.35 and 0.12 barn, respectively.

Table 8

Ref.	E, MeV	B_α	Ref.	E, MeV	B_α	Ref.	E, MeV	B_α
[L—6]	1,643	0,332	[L—6]	1,657	1,23	[L—6]	1,6635	1,75
	1,6463	0,504		1,658	2,48		1,6646	0,814
	1,6472	0,275		1,659	2,37		1,6655	0,830
	1,6505	0,112		1,660	2,09		1,6678	—0,024
	1,6524	0,310		1,6608	2,54		1,6695	0,160
	1,6533	0,074		1,662	1,95		1,672	0,485
	1,655	0,600		1,6627	1,17		1,673	—0,698

Table 9

Ref.	E, MeV	B_α	B_7	Ref.	E, MeV	B_α	B_7	Ref.	E, MeV	B_α	B_7
[B—4]	4,05	—	—	[B—4]	5,15			[B—4]	7,11	0,095	0,066
[B—4]	4,30	0,188	0,014	[C—12]	5,66	0,035	0,003	[C—12]	8,0	—0,106	—0,175
[B—4]	4,50	—0,185	—0,025	[C—12] }	6,00	0,078	0,019	[C—12]	11,6	1,109	0,290
				[P—3] }							
[B—4]	4,85	—	—					[B—12]	14	1,388	0,802
[C—12]	4,99	0,242	—0,043	[C—12]	6,53	0,230	0,169	[C—2]	14,1	0,441	0,085
[H—2]	5,0	0,245	0,164	[P—3]	7,0						

$_8O$

1 — [1]; [C — 2] — J. P. Conner (1953)
2 — [1]; [O — 1] — A. Okazaki (1955)
3 — [1]; [B — 4] — N. A. Bostrom (1957)
4 — [1]; [F — 2] — J. L. Fowler (1958)
5 — [1]; [H — 2] — R. W. Hill (1958)
6 — [1]; [L — 6] — R. O. Lane (1961)
7 — [1]; [P — 3] — D. D. Phillips (1961)
8 — [1]; [C — 12] — L. F. Chase (1961)
9 — [1]; [P — 3] — D. D. Phillips (1961)
[B — 4] — N. A. Bostrom (1957)
10 [1]; [C — 12] — L. F. Chase (1961)
[P — 3] — D. D. Phillips (1961)
11 — [1]; [M — 6] — J. P. Martin (1962)
12 — [1]; [M — 6] — J. P. Martin (1962)
[F — 2] — J. L. Fowler (1958)
13 — [1]; [H — 6] — W. Hunzinger (1962)
14 — [1]; [L — 3] — **G. N. Lovchikova (1962)**
15 — [B — 12] — **R. W. Bauer (1963)**
16 — [F — 6] — **J. L. Fowler (1964)**
17 — [L — 11] — **D. Lister (1965)**

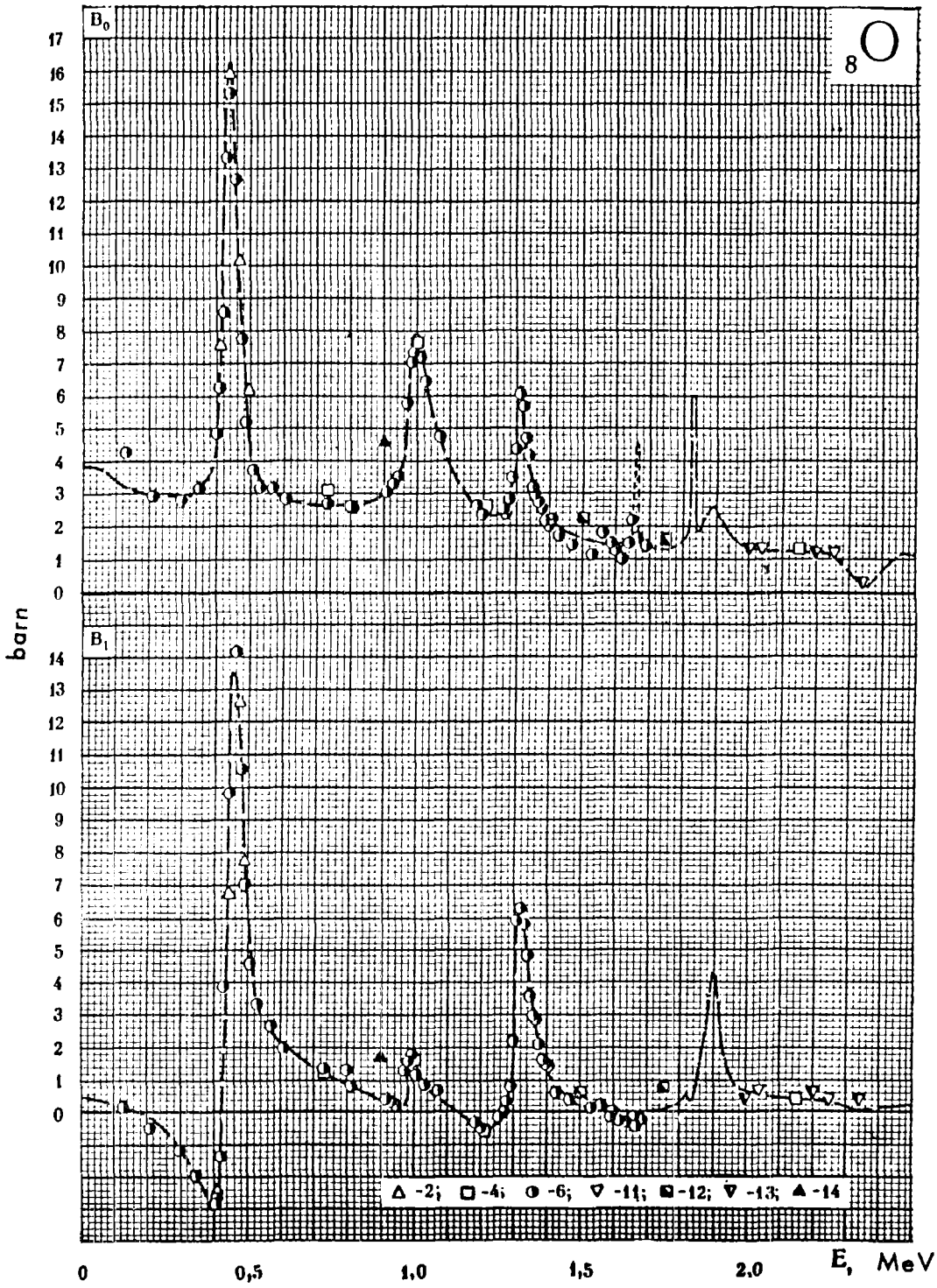
B_0
B_1
$_8O$
barn
E, MeV
0
0,5
1,0
1,5
2,0
△ -2; □ -4; ○ -6; ▽ -11; ◙ -12; ▼ -13; ▲ -14

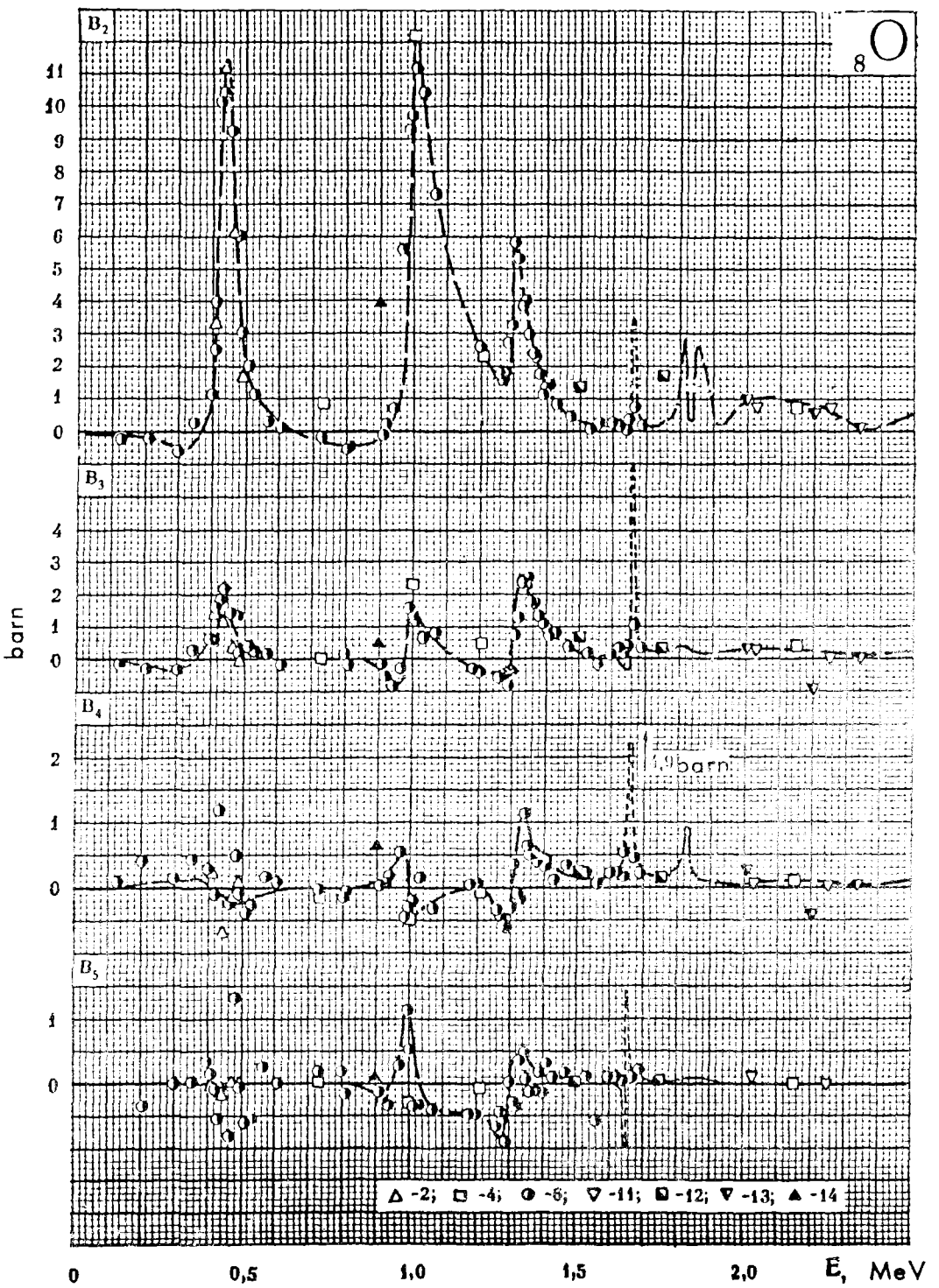
B_2
B_3
B_4
B_5
8O
barn
0,9barn
△ -2; □ -4; ◑ -6; ▽ -11; ◘ -12; ▼ -13; ▲ -14
0
0,5
1,0
1,5
2,0
E, MeV

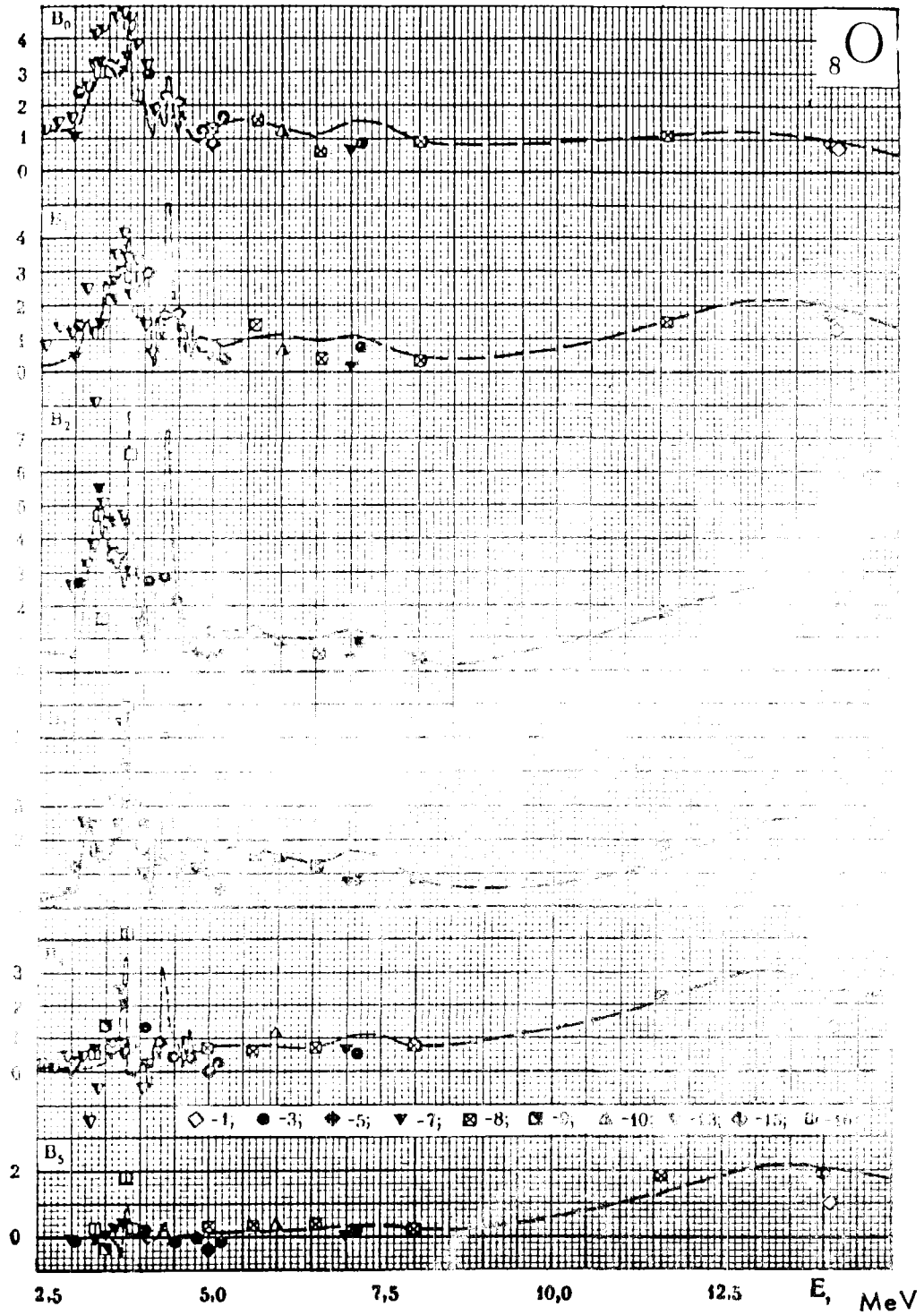
B_0
B_2
B_5
8O
◇ -1; ● -3; ◆ -5; ▼ -7; ⊠ -8;
2,5
5,0
7,5
10,0
12,5
E, MeV

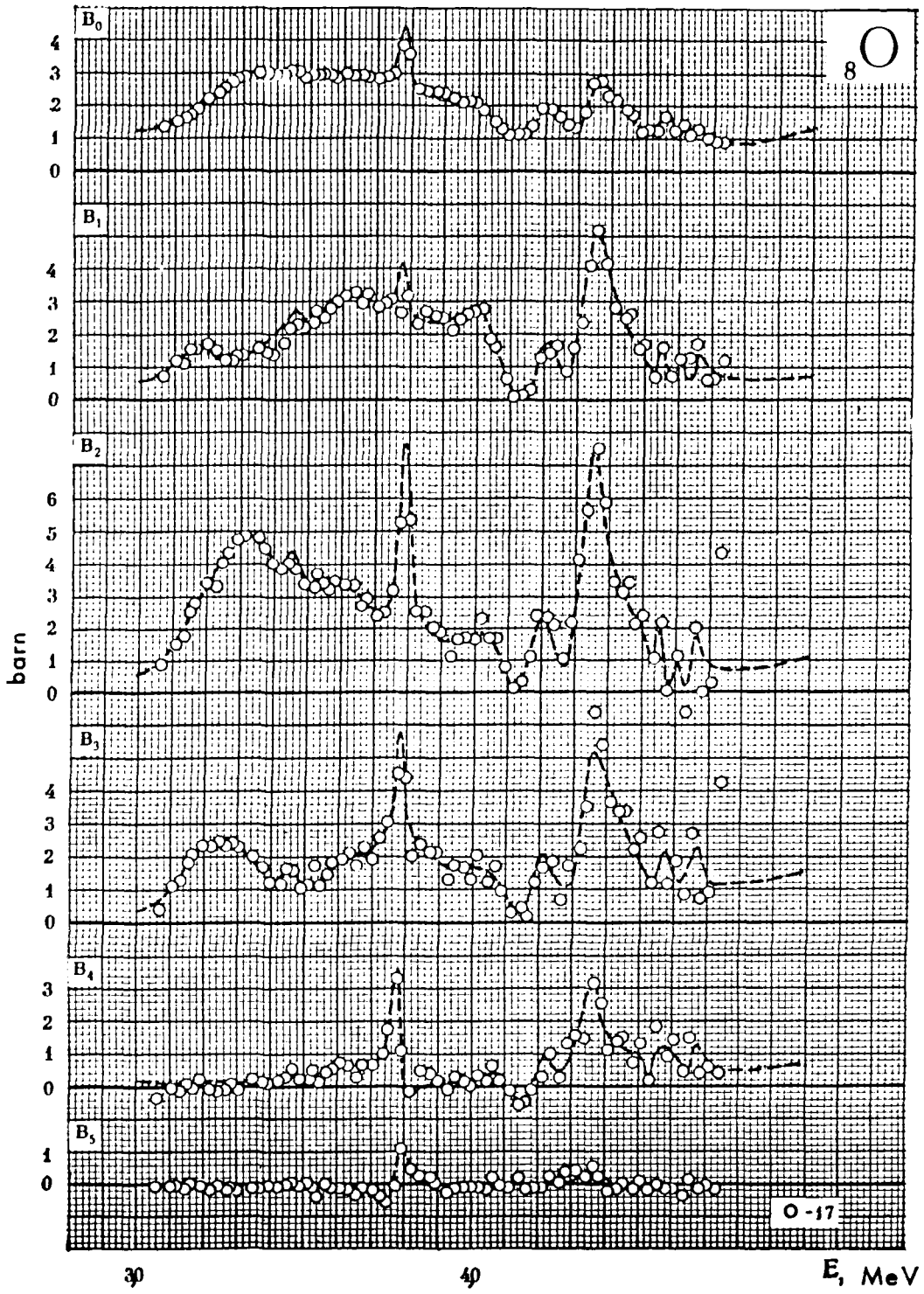
B_0
B_1
B_2
B_3
B_4
B_5
^{8}O
O -17
barn
30
40
E, MeV

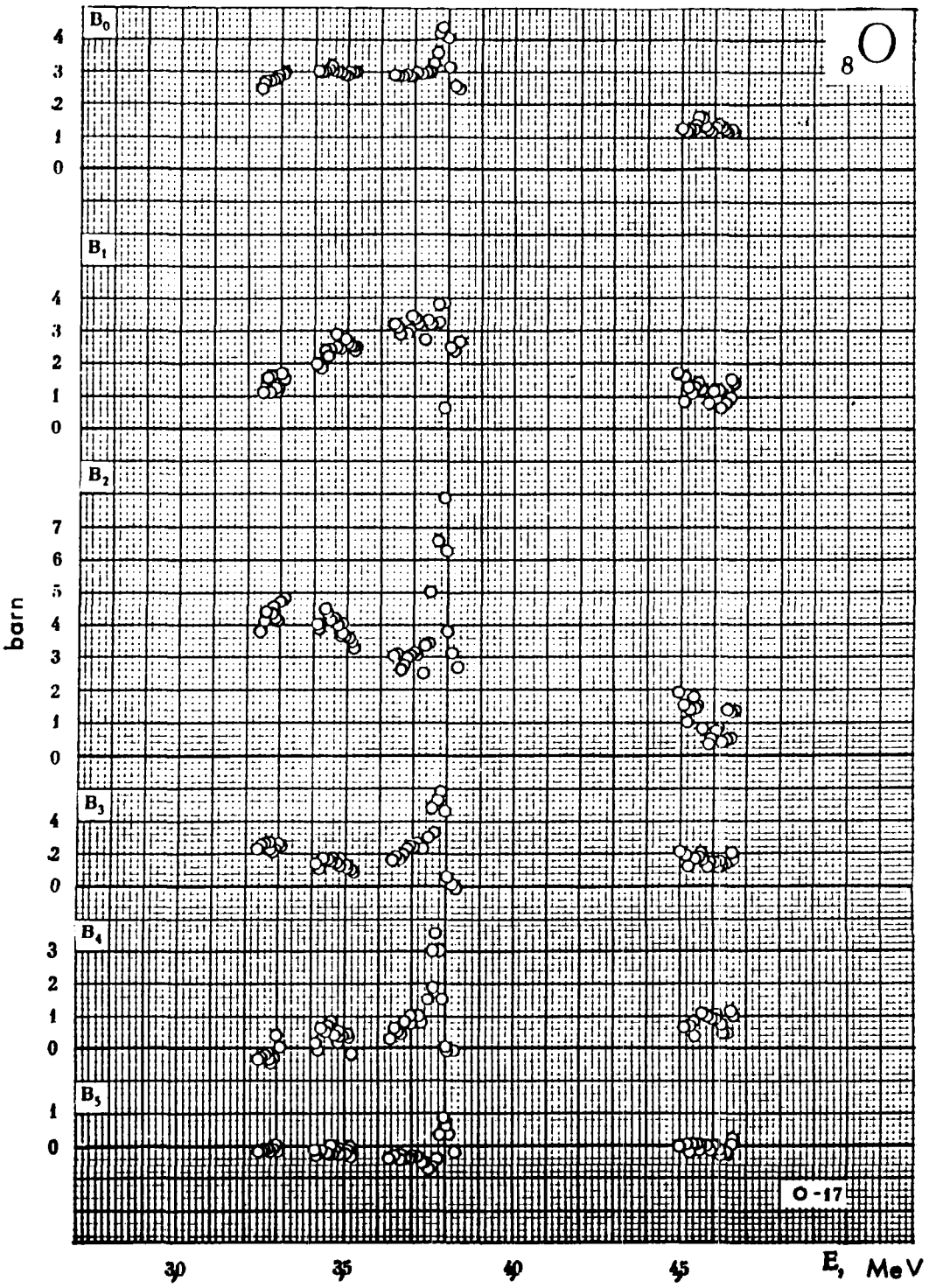
B_0
B_1
B_2
B_3
B_4
B_5
^{8}O
O-17
barn
E_γ MeV
30
35
40
45

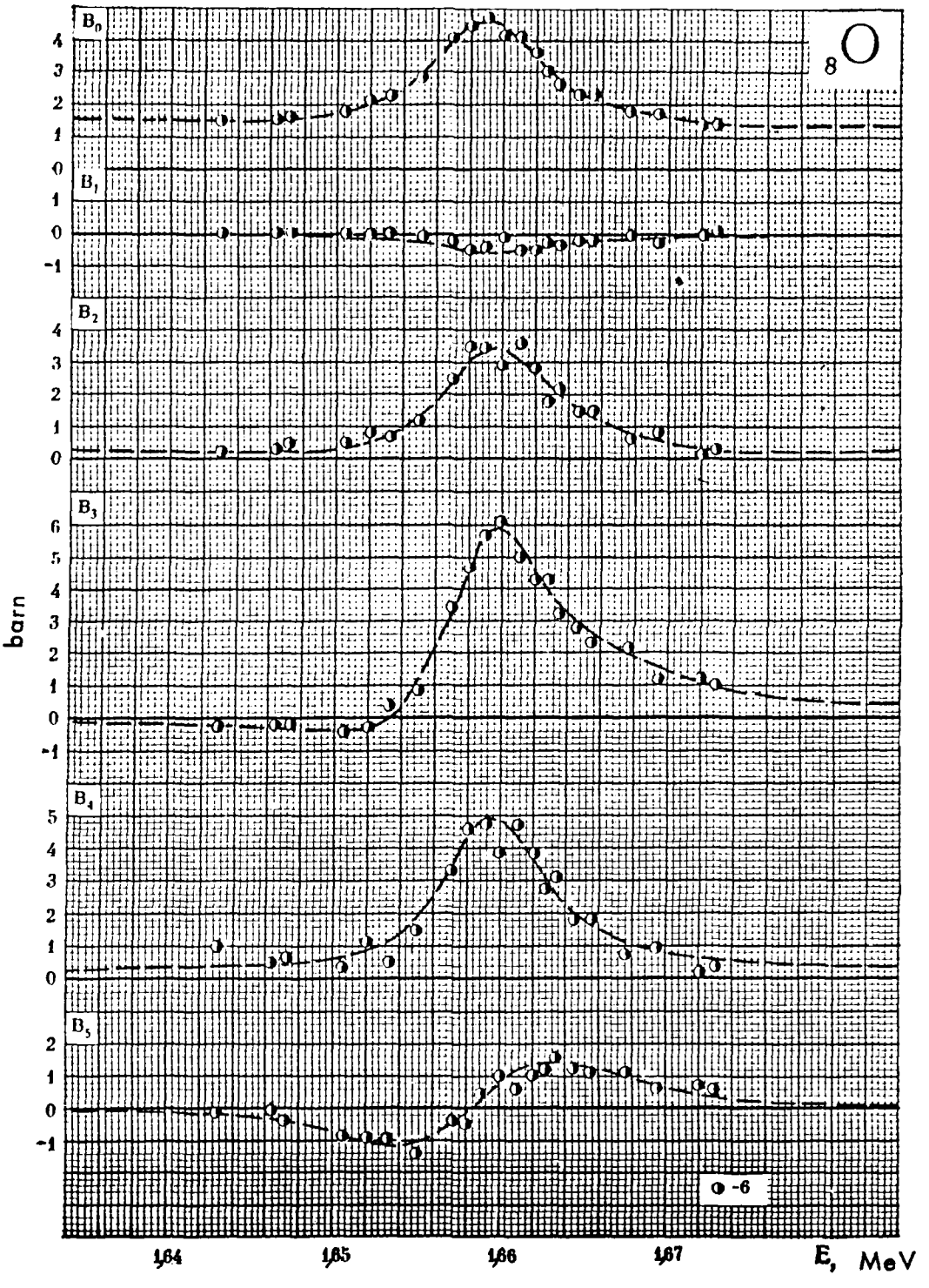
B_0
B_1
B_2
B_3
B_4
B_5
$_8O$
barn
1,64
1,65
1,66
1,67
E, MeV

F L U O R I N E

Basic angular distribution data of neutrons scattered on fluorine have been obtained in the experiments /L-2/(1957) and /E-3/(1964), and these results are in good agreement. The experimental method used in these works did not, unfortunately, permit distinction of elastic from inelastic neutron scattering. The inelastic neutron scattering of light nuclei is always considerably anisotropic in the laboratory system. Since the velocity of the centre-of-mass system is comparatively high for light nuclei, and the velocity of the inelastic scattered neutron is noticeably lower than the velocity of the incoming neutrons, it is clear that the contribution to the anisotropic angular distribution is still higher than in the case of elastic scattering.

It can be shown /10/ that, working on the assumption that the inelastic scattering is isotropic in the centre-of-mass system, the angular distribution of neutrons scattered inelastically to the levels $E_{o,k}$ can be described by the following relation in the laboratory system :

$$f[E_{0,k}, \mu]\, d\mu = \frac{d\mu}{\sqrt{a^2+1}} \left(\mu \pm \frac{2\mu^2 + a^2}{2\sqrt{\mu^2 + a^2}} \right),$$

where

$$a^2 = A^2 \left(1 - \frac{A+1}{A} \cdot \frac{E_{0,k}}{E} \right) - 1.$$

A is the mass-number of the target nucleus; E is the incoming neutron energy; μ is the cosine of the scattering angle in the laboratory system.

Inelastic scattering can occur only for $E > \frac{A+1}{A} E_{o,k}$; for $E < \frac{A+1}{A} E_{o,k}$ all neutrons inelastically scattered in the laboratory system are in the front hemisphere. In this case the angular distribution has two values corresponding to the forward and backward scattering. The more important case in practice is $E > \frac{A+1}{A} E_{o,k}$, in which the inelastically

scattered neutrons can fly in any direction also in the laboratory system. In this case the plus sign is valid in the above-mentioned formula for the angular distribution.

The coefficients of the expansion of the angular distribution of inelastically scattered neutrons by Legendre polynomials can, in the case considered, be represented in the following form :

$$B_{l,\,in} = \sum_k \sigma_{in,\,k}\,(2l+1)\int_{-1}^{+1} f(E_{0,\,k},\,\mu)\,P_l(\mu)\,d\mu,$$

where $\sigma_{in,k}$ indicates the inelastic cross-section to the levels $E_{o,k}$; the sum is over all levels excited at a given neutron energy.

Replacing $f(E_{o,k},\mu)$ by the expression given above, we obtain :

$$B_{0,\,in} = \sum_k \sigma_{in,\,k};$$

$$B_{1,\,in} = 2\sum_k \sigma_{in,\,k} \Big/ \sqrt{a_k^2+1}\;;$$

$$B_{2,\,in} = (5/16)\sum_k \sigma_{in,\,k}\left[(4-6a_k^2) + 3\left(a_k^4 \Big/ \sqrt{a_k^2+1}\right)\times\right.$$

$$\left.\times \ln\left(\sqrt{a_k^2+1}\right)\Big/\left(\sqrt{a_k^2+1}-1\right)\right]; \qquad B_{3,\,in} = 0.$$

All higher odd harmonics are also equal to zero. In order to correct for inelastic scattering the data in the references /L-2/ and /E-3/, we used the results of the excitation function of low lying levels of fluorine determined by Freeman /22/ (Figure 9). In the latter work a rather high energy resolution had been used and the data were, therefore, averaged over the interval of the energy spread (ΔE = 100 - 150 keV) corresponding to the spread used for the angular distribution measurement. A rectangular resolution function has been assumed.

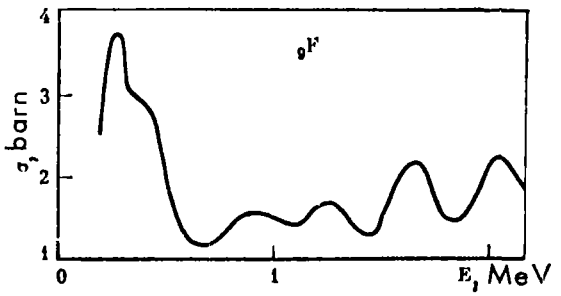

Figure 9. Inelastic neutron scattering cross-section of fluorine used for corrections of B_o.

The calculation of B_ℓ for inelastic scattering has been carried out using the above-mentioned formula, i.e., assuming that the inelastic scattering is isotropic in the centre-of-mass system. In reality this condition is not fulfilled, since a level can only be excited when the neutron forming a compound nucleus, and/or the outgoing neutron has an orbital angular momentum other than zero (which follows from the conservation of the moment and the parity). Therefore, our corrections only have qualitative character. Calculation of the anisotropic inelastic scattering, which would be more exact, is not feasible at present, since the information on the influence of different waves on the compound nucleus formation cross-section are rather incomplete and unreliable.

The correction was made by subtracting from B_ℓ^* (which contains elastic and inelastic scattering), $B_{\ell,in}$, which in its turn has been calculated by means of the above-mentioned formulae. The results of the measurements /W-9/(1958) and /R-5/(1961) are also given in the graphs, but no such corrections have been made, since the measurements are only ascribed to elastic scattering in these publications. It is true that the comparison of B_o obtained from the angular distribution of these measurements with the corresponding total cross-section /13/ apparently suggests that no contribution from inelastic neutron scattering is present.

At energies below 0.2 MeV it is difficult to recommend a curve

only on the basis of the values from /L-2/, since the strong fluorine resonances at 27, 49 and 100 keV, which determine the character of the angular distribution at these energies, were not resolved in this experiment although they have a strong influence on the results. For obtaining $B_o(E)$ it seemed suitable to us to use the energy dependence of σ_T in the energy range up to 0.11 MeV and the well-known energy dependence of $\sigma_T - \sigma_{in}$ in the energy range from 0.11 to 0.2 MeV /16/. The energy dependence of B_1 was put equal to $3\bar{\omega}_1(E)\, B_o(E)$, where $\bar{\omega}_1(E)$ is the mean cosinus angular distribution measured in reference /L-2/ averaged over the resolution function; $3\bar{\omega}_1(E) = B_1(E)/B_o(E)$, where $B_1(E)$ and $B_o(E)$ are the values given in the graphs. In the interval from 0 to 50 keV, where data for the anisotropic scattering do not exist, one can obtain a value of $\bar{\omega}_1(E) = 0.035$ at E = 0 by extrapolation. There are no experimental neutron angular distributions available in the interval from 3 to 14 MeV.

We wish to point out that for this range, the results obtained by optical model calculations (although they differ from experimental results by Wills /W-9/ at 2.9 MeV) do not contradict the extrapolation of the experimental values available at lower energies to 2.5 MeV.

We wish to mention that the total cross-section of fluorine, calculated by the optical model with adopted parameters, lies 0.1 to 0.15 barn below the experimental values everywhere.

One can, therefore, conclude that the calculated results of elastic scattering given here are one half of this value too low (since the nonelastic cross-sections in this energy range amount to 50% of the total cross-section).

$_9F$

1 — [*L* — 2] — A. Langsdorf (1957)
2 — [1]; [*W* — 9] — J. E. Wills (1958)
3 — [1]; [*R* — 5] — W. L. Rogers (1961)
4 — [*E* — 3] — A. J. Elwyn (1964)
5 — [*B* — 18] — G. C. Bonazzola (1966)

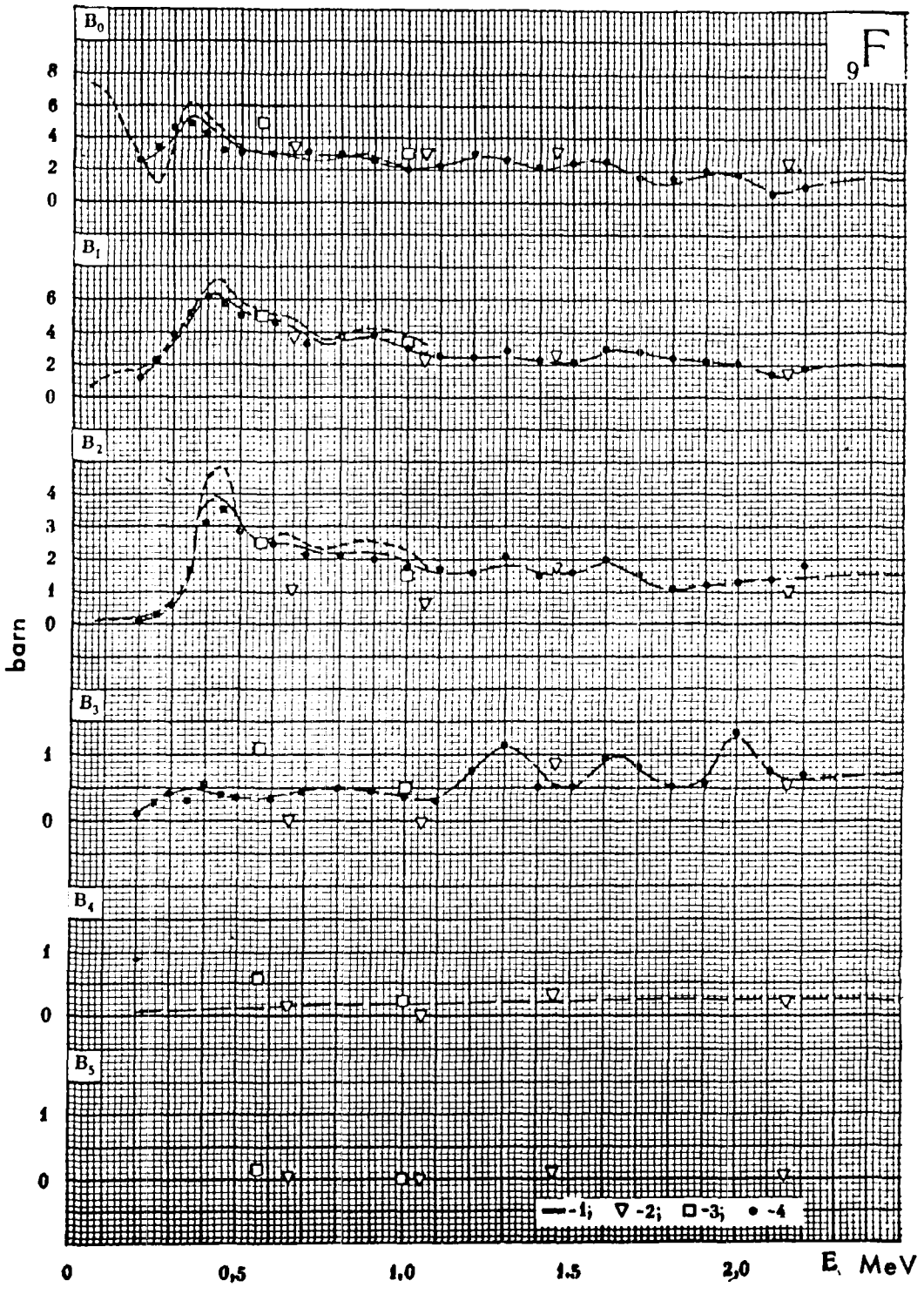
B_0
B_1
B_2
B_3
B_4
B_5
$_9F$
barn
E, MeV
0
0,5
1,0
1,5
2,0
—-1; ▽-2; □-3; •-4

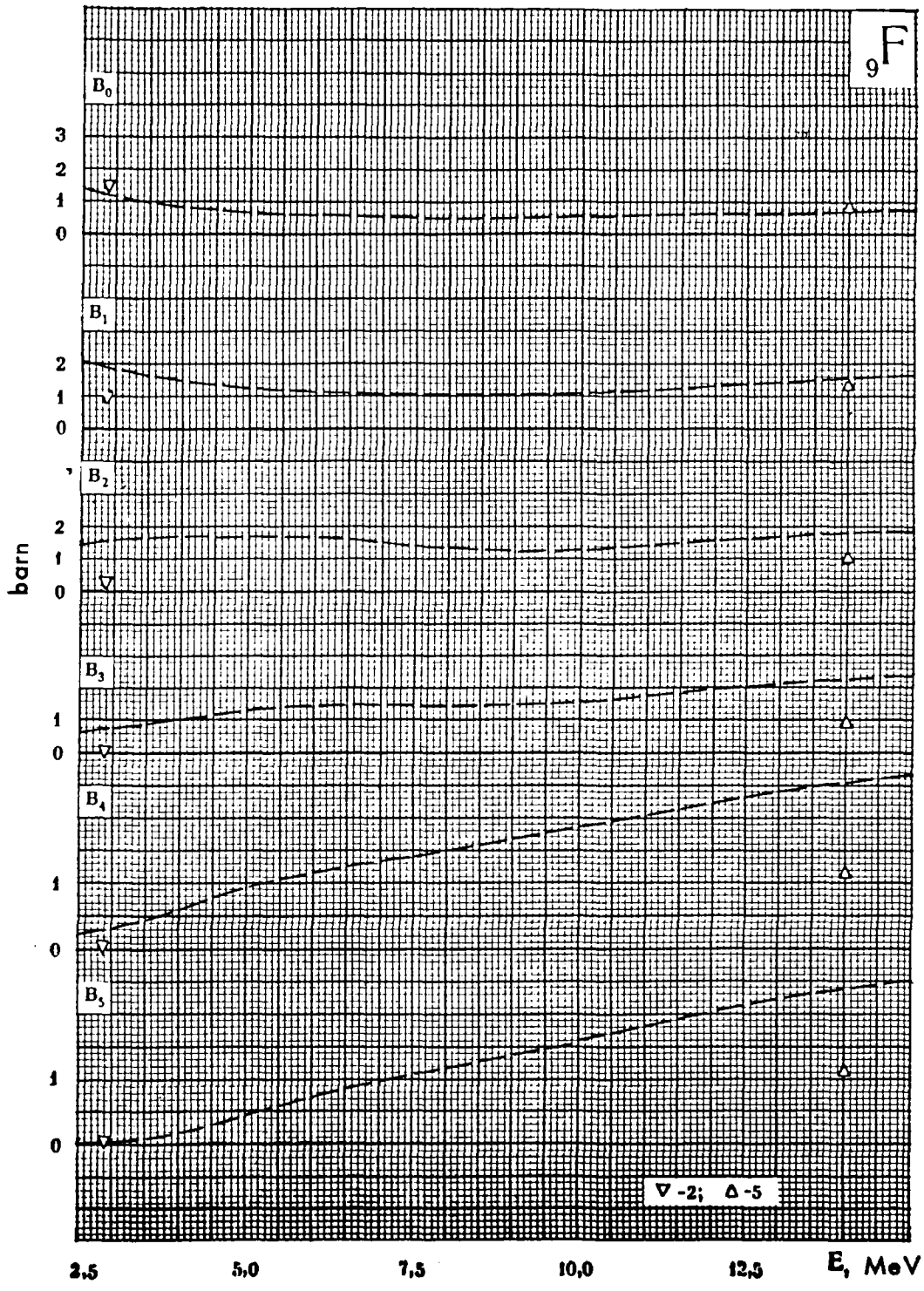
$_9F$
B_0
B_1
B_2
B_3
B_4
B_5
barn
3
2
1
0
2
1
0
2
1
0
1
0
1
0
1
0
▽ -2; △ -5
2,5
5,0
7,5
10,0
12,5
E, MeV

S O D I U M

The most detailed information on neutron angular distribution of elastic scattering are presented in the measurements by Lane and Monahan /L-4/(1960) and Elwyn et al. /E-3/(1964). After correcting B_o for inelastic scattering (Figure 10), the results of these works are in good agreement with the data obtained by means of other methods (/T-5/, /K-4/, /K-5/, /P-6/, /K-8/).

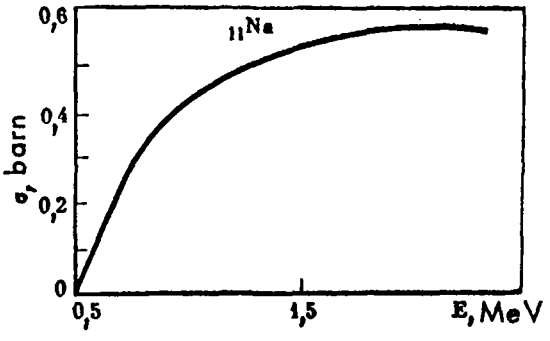

Figure 10. Inelastic neutron scattering cross-section of Sodium used for correcting B_o.

A comparison of B_ℓ derived from the angular distribution of the work /L-4/ (the data of which are plotted on a separate sheet), with the total cross-section /13/ shows that, in the range 0.2 - 0.8 MeV, practically all strong resonances have been resolved in the angular distribution measurement.

The results of this most detailed investigation confirm data of earlier works. The results obtained in reference /L-2/, in the energy range below 0.2 MeV do not, as in the case of fluorine, permit a curve to be recommended because of the undetermined influence of the resonances at 54 - 55 and 200 keV. In the range 0.2 - 0.6 MeV we derived these curves

on the basis of the total cross-sections and by extrapolating the results of reference /L-4/. At lower energies $B_o(E)$ can be derived from the total cross-section, and $B_1(E)$ can be roughly estimated assuming isotropic scattering, since the angular distribution in the resonance region of 55 keV following from the data in reference /L-2/, are very near to the isotropic distribution. A more detailed energy dependence of $B_1(E)$ has to be calculated on the basis of the parameters for the first resonances of sodium.

At energies higher than 2.5 MeV the only data available are those by Towle and Gilboy /T-5/(1962) obtained with an energy resolution of 60 keV using the time-of-flight method (E = 2.515; 3.97 MeV).

We wish to point out that the theoretical total cross-section in the range 2 - 14 MeV agrees well with the experimental data /15/.

$_{11}Na$

1 — [1]; [*L* — 2] — A. Langsdorf (1957)
2 — [1^n]; [*L* — 4] — R. O. Lane (1960)
3 — [1]; [*T* — 5] — J. H. Towle (1962)
4 — [*K* — 4] — I.A.Korzh (1963)
5 — [*K* — 5] — I.A.Korzh (1964)
6 — [*E* — 3] — A. J. Elwyn (1964)
7 — [*P* — 6] — V.I.Popov (1965)
[*K* — 8] — L.Ya.Kazakova (1965)
8 — [*C* — 20] — J. P. Chien (1966)

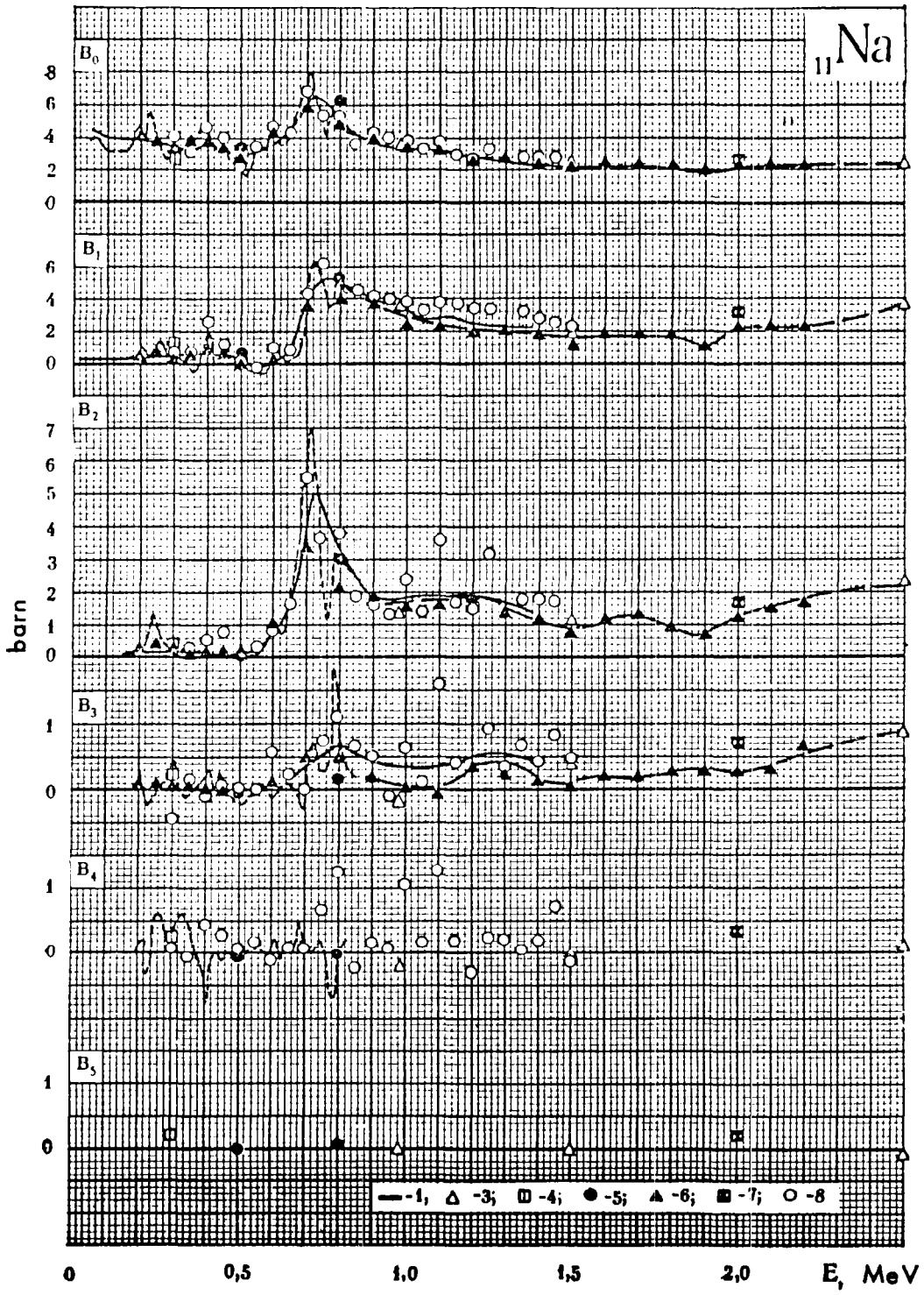
$_{11}$Na
B_0
B_1
B_2
B_3
B_4
B_5
barn
E, MeV
0
0,5
1,0
1,5
2,0
—1; Δ -3; ⊡ -4; ● -5; ▲ -6; ■ -7; ○ -8

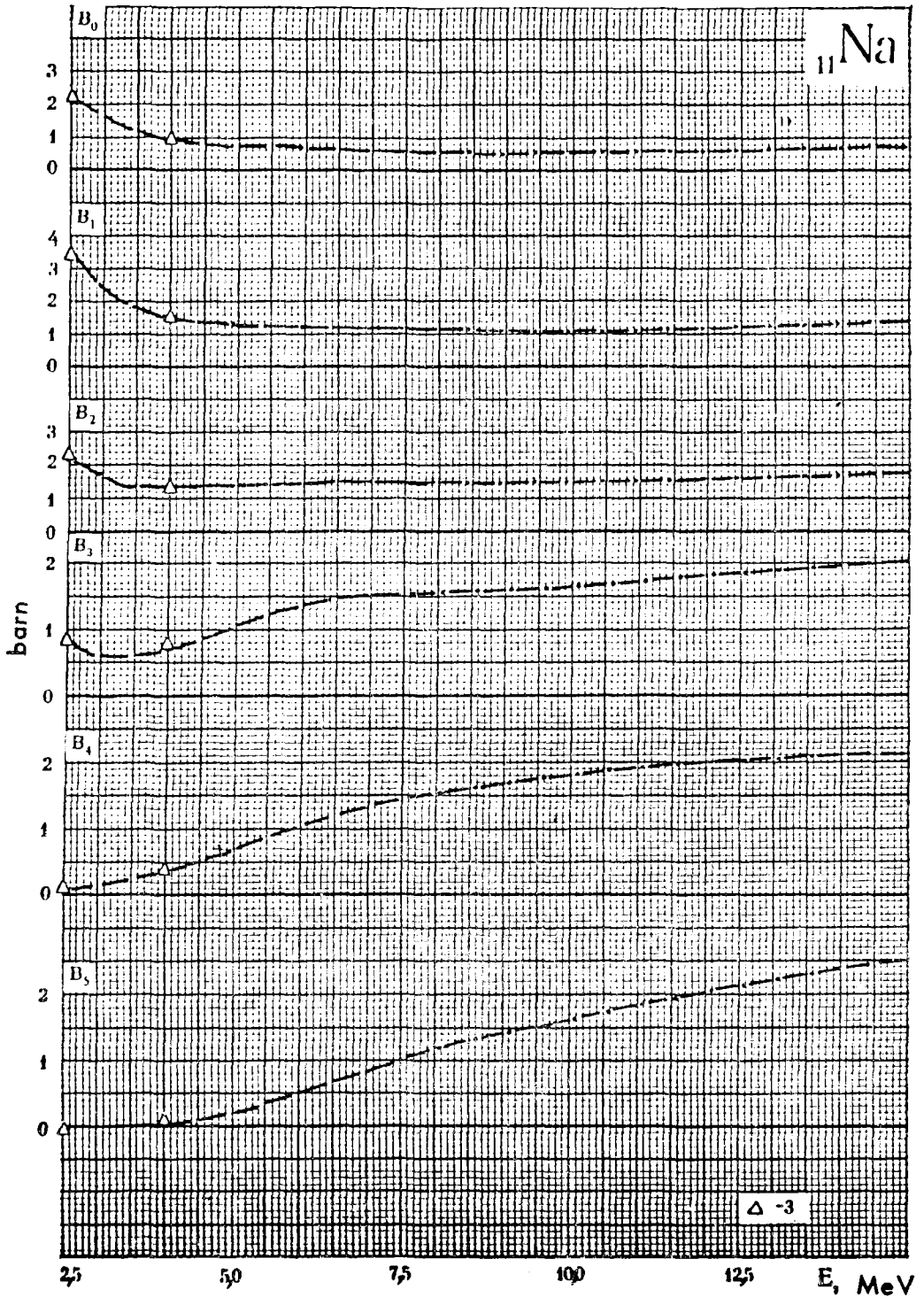
B_0
B_1
B_2
B_3
B_4
B_5
$_{11}Na$
barn
Δ -3
2,5
5,0
7,5
10,0
12,5
E, MeV

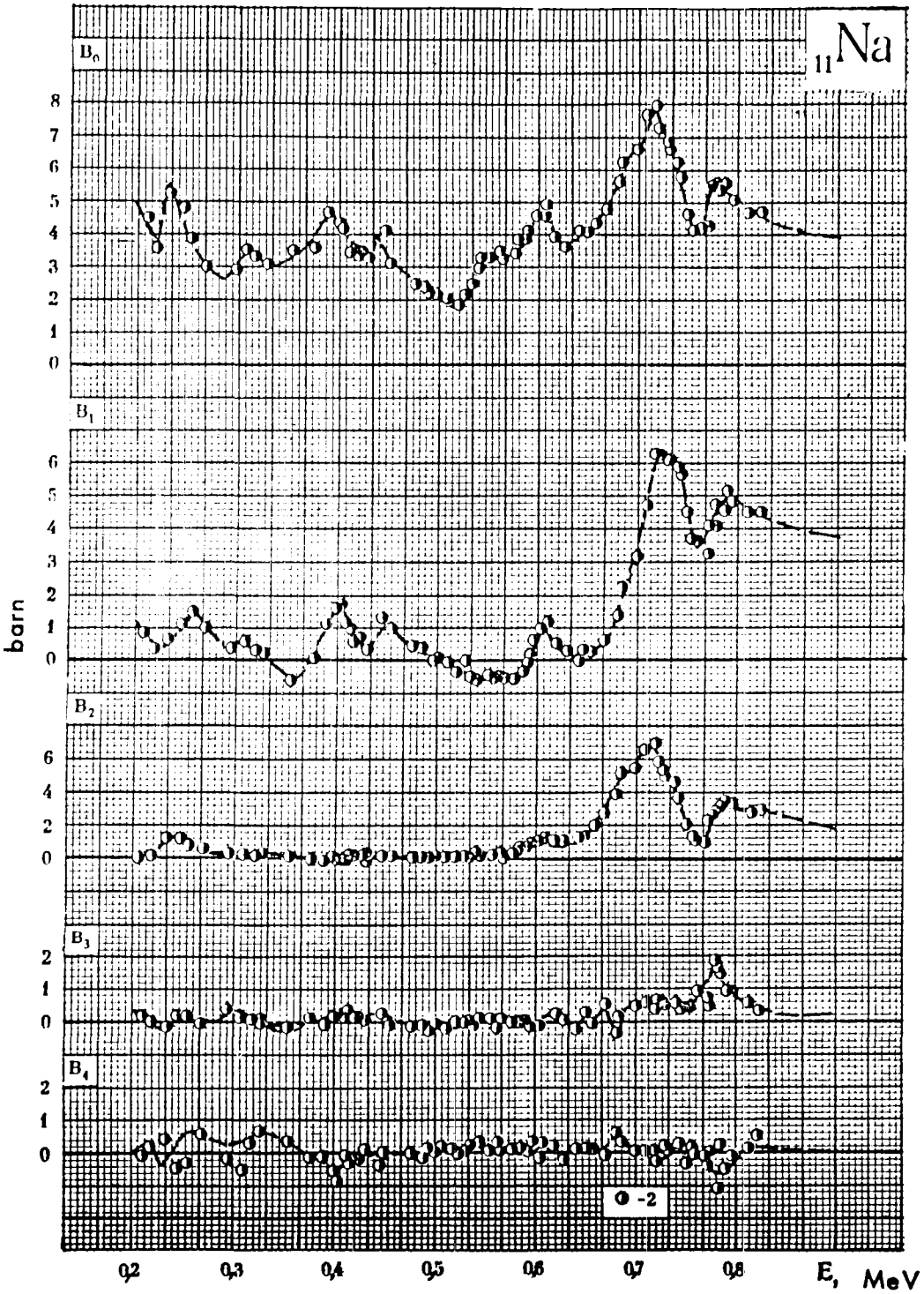
$_{11}$Na
B_0
B_1
B_2
B_3
B_4
barn
E, MeV
0,2
0,3
0,4
0,5
0,6
0,7
0,8
-2

M A G N E S I U M

In the low energy range the most detailed information on neutron angular distribution has been obtained by Langsdorf /L-2/(1957). The correction of B_o for inelastic scattering (Figure 11) obtained in this work, does not exceed 10%. Comparing the values B_ℓ from /L-2/ with the data of Korsch et al. /K-4/(1963), /K-5/(1964) shows remarkable discrepancies which can be partly explained by the different energy resolutions used : 100 keV in reference /L-2/ and 50 keV in the measurements by Korsch et al.

In the energy range from 1.5 to 5.0 MeV the only results available are those by Thomson, Cranberg and Lewin /T-6/(1962), obtained with a resolution of about 200 keV which, therefore, represents angular distributions averaged over many resonances. The results of Stuart /S-18/(1965) measured at 6.0 MeV are in good agreement with these results.

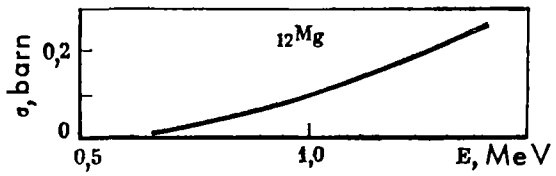

Figure 11. Inelastic neutron scattering cross-section of magnesium used for correcting B_o .

At an energy of~14 MeV there are data available by Clarke /C-6/(1962) and Cross /C-7/(1960). One has to point out that the character of the angular distribution at this energy is essentially different from that observed at energies from 4 to 6 MeV, and the absence of experimental data in the energy range from 6 to 14 MeV makes the interpolation of the existing data difficult.

The recommended curves in the energy range above 1.6 MeV were obtained using the available total- and nonelastic cross-sections. The values

of the high momenta are given in table 10.

Table 10

Ref.	E_x MeV	B_0	B_1	Ref.	E_x MeV	B_0	B_1	B_2	B_3	B_4
[T—6]	3,3	—0,003	0,111							
[T—6]	4,0	0,016	0,019	[C—16]	14	2,27	1,906	1,152	0,477	0,142
[T—6]	5,0	—0,012	0,086	[C—7]						
[S—18]	6,0	—0,127	—0,126							

$_{12}$Mg

1 — [L — 2] — A. Langsdorf (1957)
2 — [1]; [C — 16] — R. L. Clarke (1964)
[C — 7] — W. G. Cross (1960)
[C — 13] — R. L. Clarke (1962)
3 — [1]; [T — 6] — D. B. Thomson (1962)
4 — [K — 4] — I.A.Korzh (1963)
5 — [K — 5] — I.A.Korzh (1964)
6 — [S — 18] — D. T. Stewart (1965)

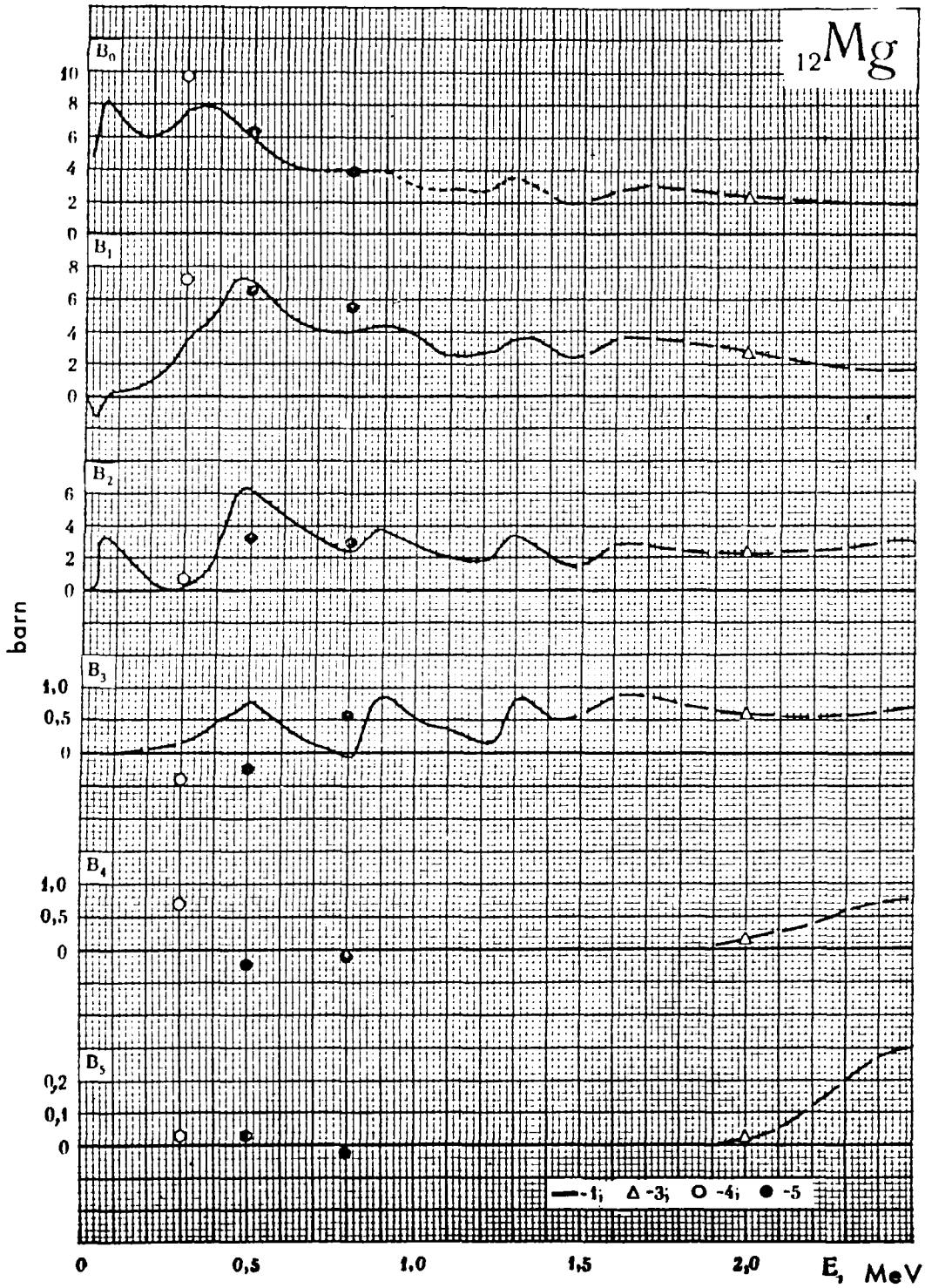
$_{12}Mg$
B_0
B_1
B_2
B_3
B_4
B_5
barn
E, MeV
—1; Δ-3; O-4; ●-5

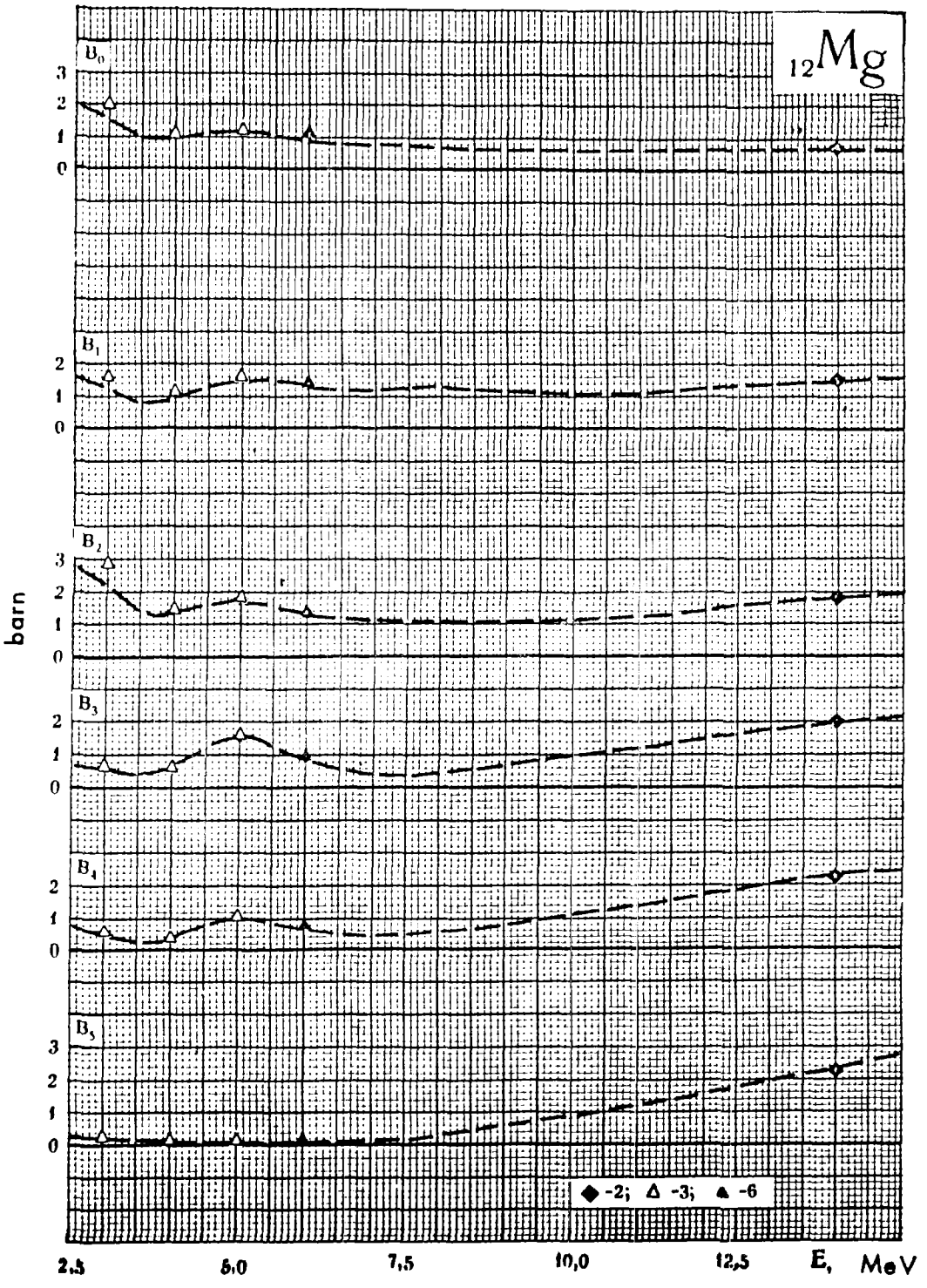
$_{12}Mg$
B_0
B_1
B_2
B_3
B_4
B_5
barn
◆ -2; Δ -3; ▲ -6
2,5
5,0
7,5
10,0
12,5
E, MeV

A L U M I N I U M

In the energy range below 2.0 MeV there are many experimental results of neutron scattering angular distributions available. However, they show considerable discrepancies due to the different energy resolutions used. One can see that, in this range, the difference of the most detailed results of B_o measured in /L-2/(1957) and /E-3/(1964) from the total cross-sections /13/ is of the same order as the difference of their data from the results of reference /S-14/(1964). The correction of B_o for inelastic scattering (Figure 12), in the works /L-2/ and /E-3/ is comparatively small (< 25%).

In the energy range higher than 2 MeV the experimental data agree, on the whole, sufficiently well.

The measurements at 5.7 and 14 MeV yield angular distributions averaged over many resonances and, since the total cross-section is sufficiently monotonic, interpolation in this range is quite acceptable.

When carrying out this interpolation we relied on the behaviour of B_ℓ, calculated by the optical model. The curve $B_o(E)$ was derived from the available experimental data on total- and nonelastic cross-sections. The values of the coefficients B_8 and B_9 at 14 MeV, obtained from the data of reference /1/, amount to 0.725 and 0.280 respectively.

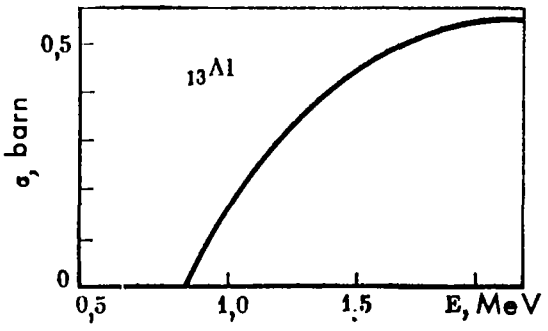

Figure 12. Inelastic neutron scattering cross-section of aluminium, used for correcting B_o.

$_{13}$Al

1 — [1]; [*W* — 3] — W. D. Whitehead (1953)
2 — [1]; [*W* — 5] — M. Walt (1955)
3 — [1]; [*L* — 1] — R. N. Little (1955)
4 — [1]; [*B* — 2] — J. R. Beyster (1956)
5 — [1]; [*B* — 2] — J. R. Beyster (1956)
[*P* — 1] — M. J. Poole (1952)
6 — [1]; [*B* — 3] — N. A. Bostrom (1956)
7 — [1]; [*L* — 2] — A. Langsdorf (1957)
8 — [1]; [*L* — 1] — G. N. Lovchikova (1957)
9 — [1]; [*H* — 2] — R. W. Hill (1958)
10 — [1]; [*P* — 2] — C. St. Pierre (1959)
[*Y* — 1] — K. Yuasa (1958)
[*C* — 5] — J. H. Coon (1958)
[*A* — 9] — J. D. Anderson (1959)
[*K* — 1] — M. M. Khaletskii (1957)
11 — [1]; [*L* — 2] — G. N. Lovchikova (1960)
12 — [*P* — 3] — V. I. Popov (1961)
13 — [1]; [*T* — 7] — J. H. Towle (1962)
14 — [1]; [*T* — 8] — K. Tsukada (1962)
[*T* — 9] — S. Tanaka (1964)
15 — [*K* — 4] — I. A. Korzh (1963)
16 — [*K* — 3] — I. A. Korzh (1963)
17 — [1]; [*S* — 14] — A. B. Smith (1964)
[*C* — 20] — J. P. Chien (1966)
18 — [*B* — 13] — D. J. Bredin (1964)
19 — [*E* — 3] — A. J. Elwyn (1964)
20 — [*K* — 5] — I. A. Korzh (1964)
21 — [*B* — 20] — R. L. Becker (1966)

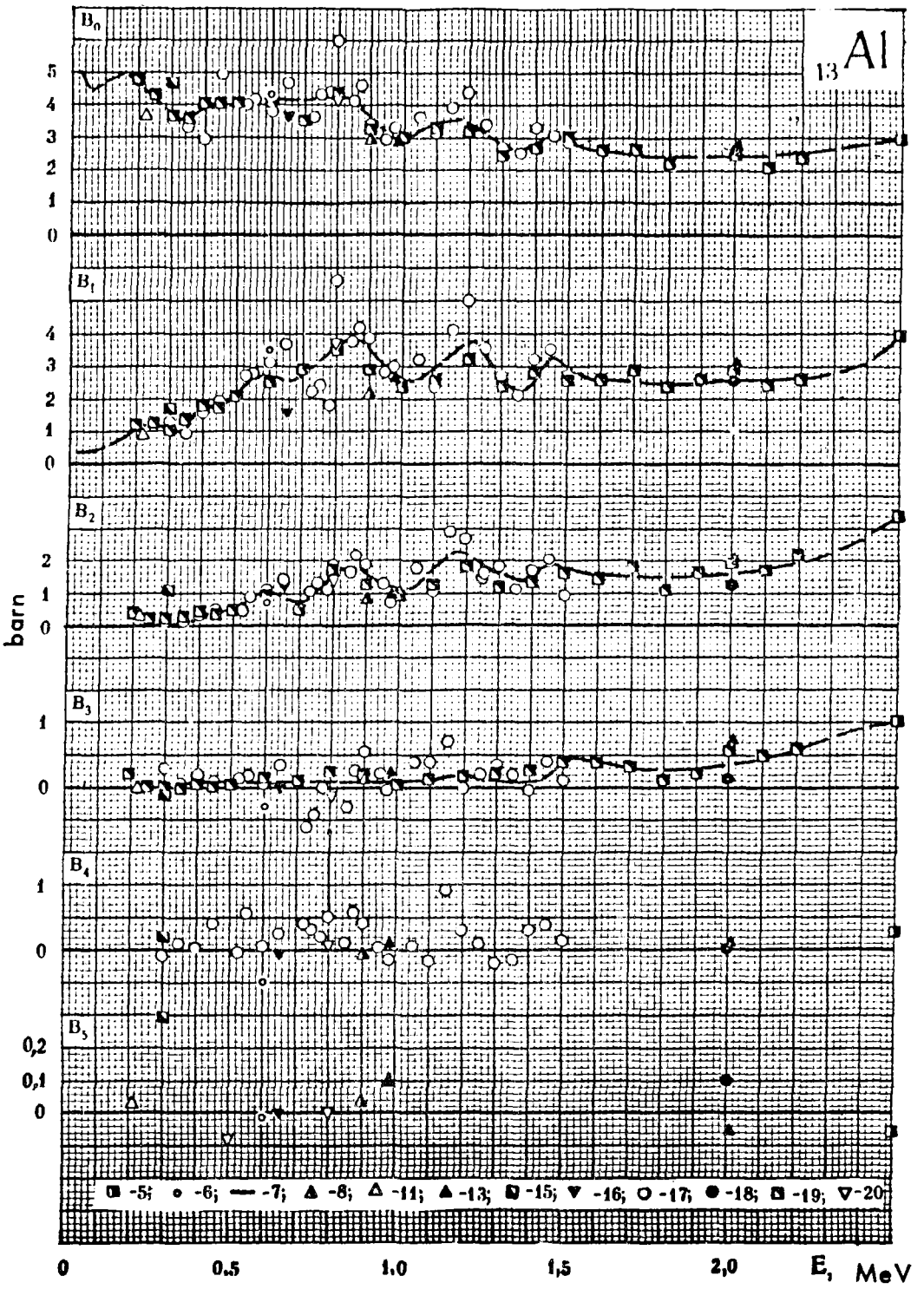
B_0
B_1
B_2
B_3
B_4
B_5
13 Al
barn
E, MeV
0
0.5
1.0
1,5
2,0
-5; -6; -7; -8; -11; -13; -15; -16; -17; -18; -19; -20

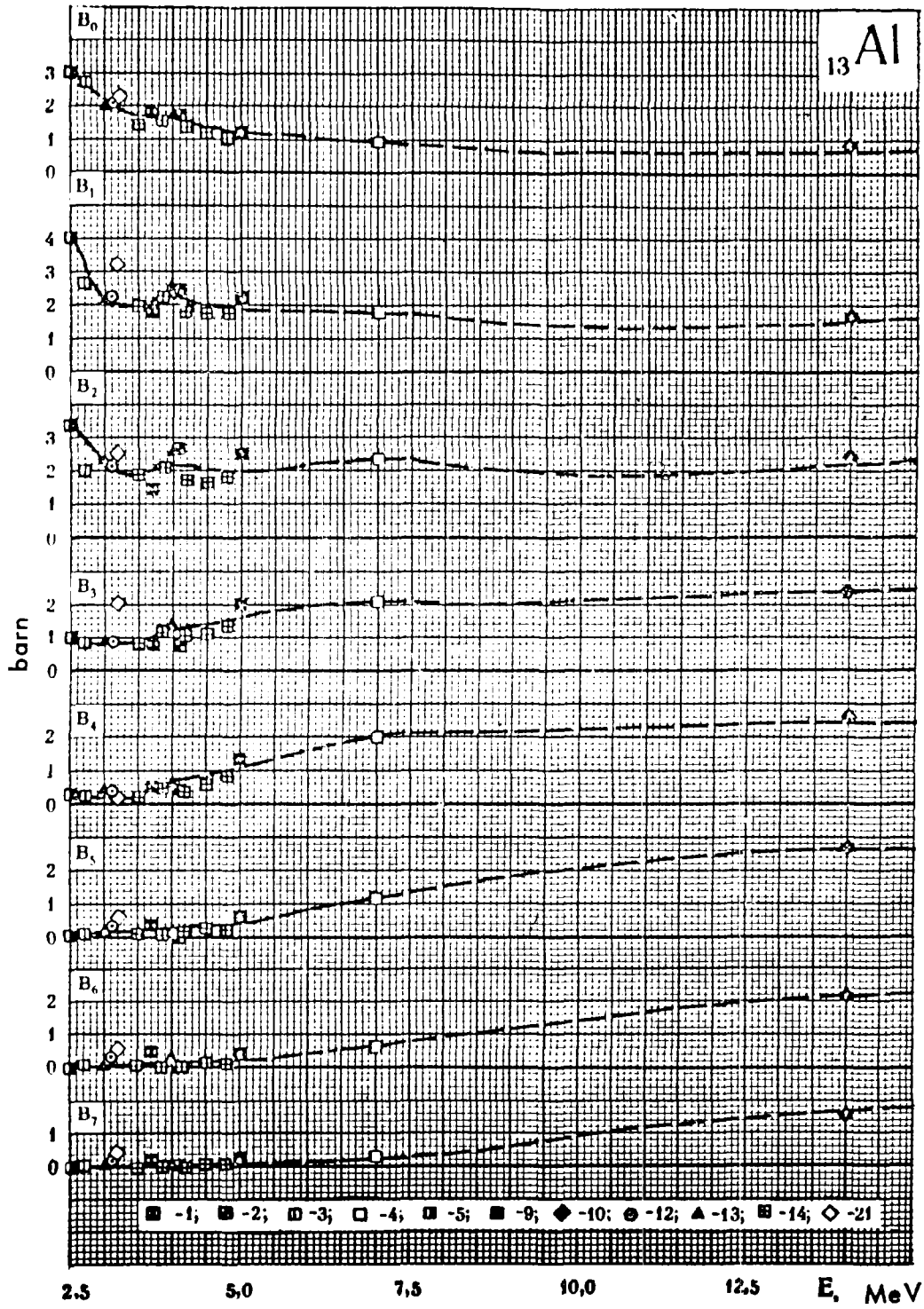
$_{13}$Al
B_0
B_1
B_2
B_3
B_4
B_5
B_6
B_7
barn
-1; -2; -3; -4; -5; -9; -10; -12; -13; -14; -21
2,5
5,0
7,5
10,0
12,5
E, MeV

S I L I C O N

In the energy range below 0.7 MeV there are detailed measurements of the angular distribution /L-6/(1961) and /L-7/(1962) which revealed strong resonances in the energy dependence of B_ℓ .

At higher energies the resonances of B_ℓ are not resolved. The existence of these resonances is manifested by the strong fluctuations observed in the energy dependence of B_ℓ . The data of different authors agree sufficiently well up to 2.5 MeV. At higher energies the agreement between results of different works is considerably worse. There are, in particular, strong differences for B_ℓ ($\ell > 0$). One has to point out that the sum of elastic and inelastic scattering measured in the works /T-8/ and /T-9/ do not agree everywhere with the total cross-section values : the sum is 0.5 - 0.3 barn lower than σ_T . There are two measurements at 14 MeV : /C-16/ and /M-8/ which agree satisfactorily between one another and they are also in good agreement with the optical model calculation. The value of B_o obtained from these works is equal to 0.64 in reference /C-16/ and 0.79 barn in reference /M-8/, which is a little lower than the difference of the well investigated /16/ total cross-section (1.9 barn) and the nonelastic cross-section (1.02 $\pm$ 0.06 barn) measured in only one work /23/(1956). Because of the great discrepancy of the experimental data and the lack of information on angular distributions of neutrons elastically scattered in the range 6 - 14 MeV in which a broad 'optical' minimum appears in the cross-sections, the recommended curves at high energies are very unreliable.

The high momentum values are given in tables 11 and 12.

Table 11

Ref.	E, MeV	B_n	Ref.	E, MeV	B_n	Ref.	E, MeV	B_n	Ref.	E, MeV	B_n
[L—6]	0,03	—0,119	[L—6]	0,61	—0,100	[L—6]	1,25	0,070	[L—6]	1,89	0,070
	0,05	0,053		0,69	—0,328		1,33	—0,021		1,97	0,050
	0,130	—0,231		0,77	—0,935		1,41	0,021		2,06	—0,118
	0,210	0,140		0,85	0,023		1,49	—0,115		2,13	—0,116
	0,290	0,446		0,93	0,033		1,57	0,067		2,21	—0,117
	0,370	0,036		1,01	—0,302		1,65	0,088		2,30	—0,112
	0,470	—0,022		1,09	—0,046		1,73	—0,008			
	0, 530	—0,003		1,17	0,129		1,81	—0,089			

Table 12

Ref.	E, MeV	B_n	B_n
[C—16]	14,1	0,373	0,200
[M—8]	14,1	0,554	

$_{11}$Si

1 — [P — 3] — V. I. Popov (1961)
2 — [1ª]; [L — 6] — R. O. Lane (1961)
3 — [1]; [L — 7] — R. O. Lane (1962)
4 — [1]; [L — 3] — G. N. Lovchikova (1962)
5 — [1]; [T — 8] — K. Tsukada (1962)
[T — 9] — S. Tanaka (1964)
6 — [K — 7] — I. A. Korzh (1964)
7 — [C — 16] — R. L. Clarke (1964)
8 — [B — 13] — D. J. Bredin (1964)
9 — [C — 17] — M. Coppola (1965)
10 — [P — 4] — G. A. Petitt (1966)
11 — [B — 20] — R. L. Becker (1966)
12 — [M — 8] — P. W. Martin (1965)

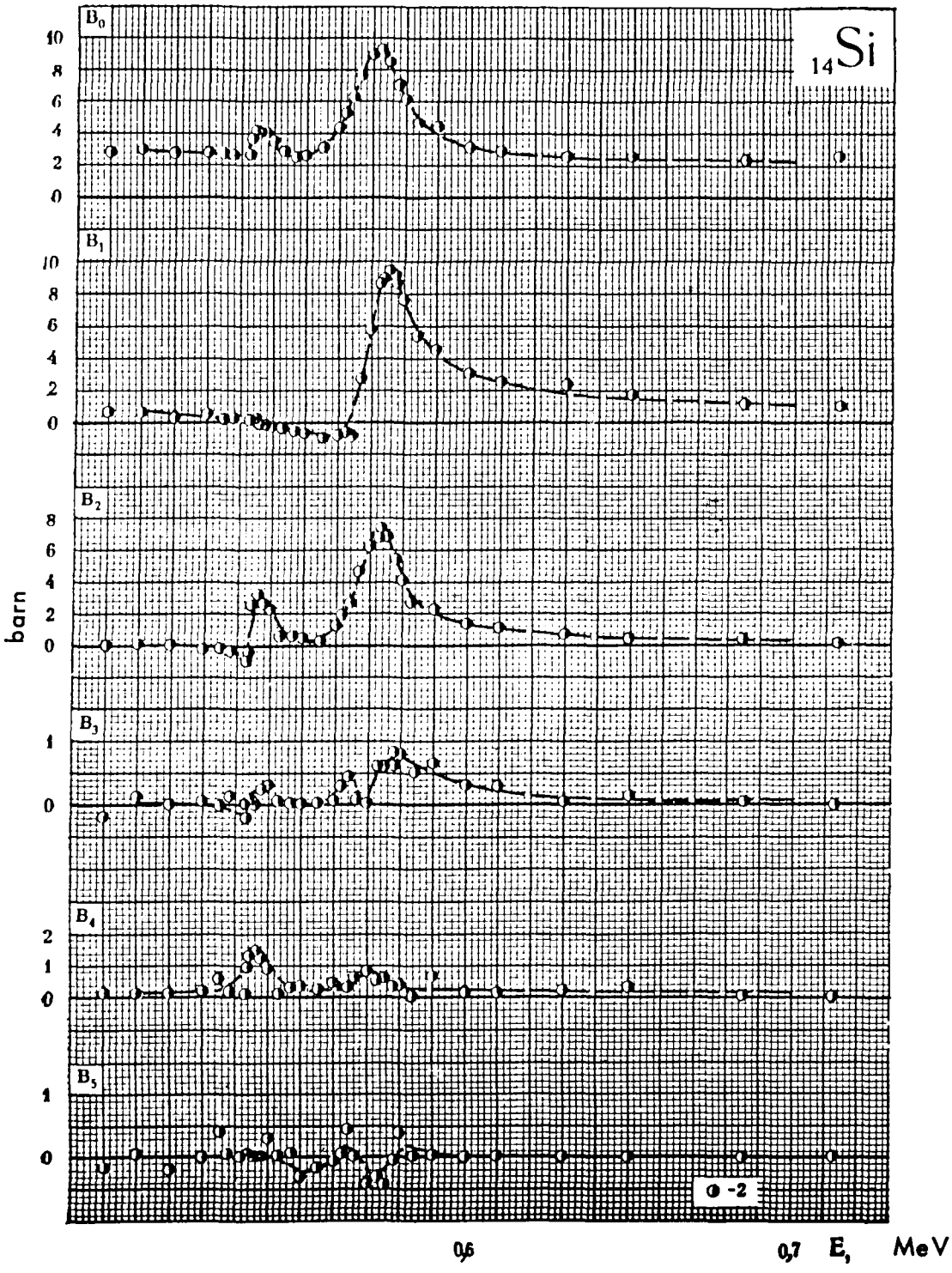
$_{14}$Si
B_0
B_1
B_2
B_3
B_4
B_5
barn
E, MeV
0,6
0,7
-2

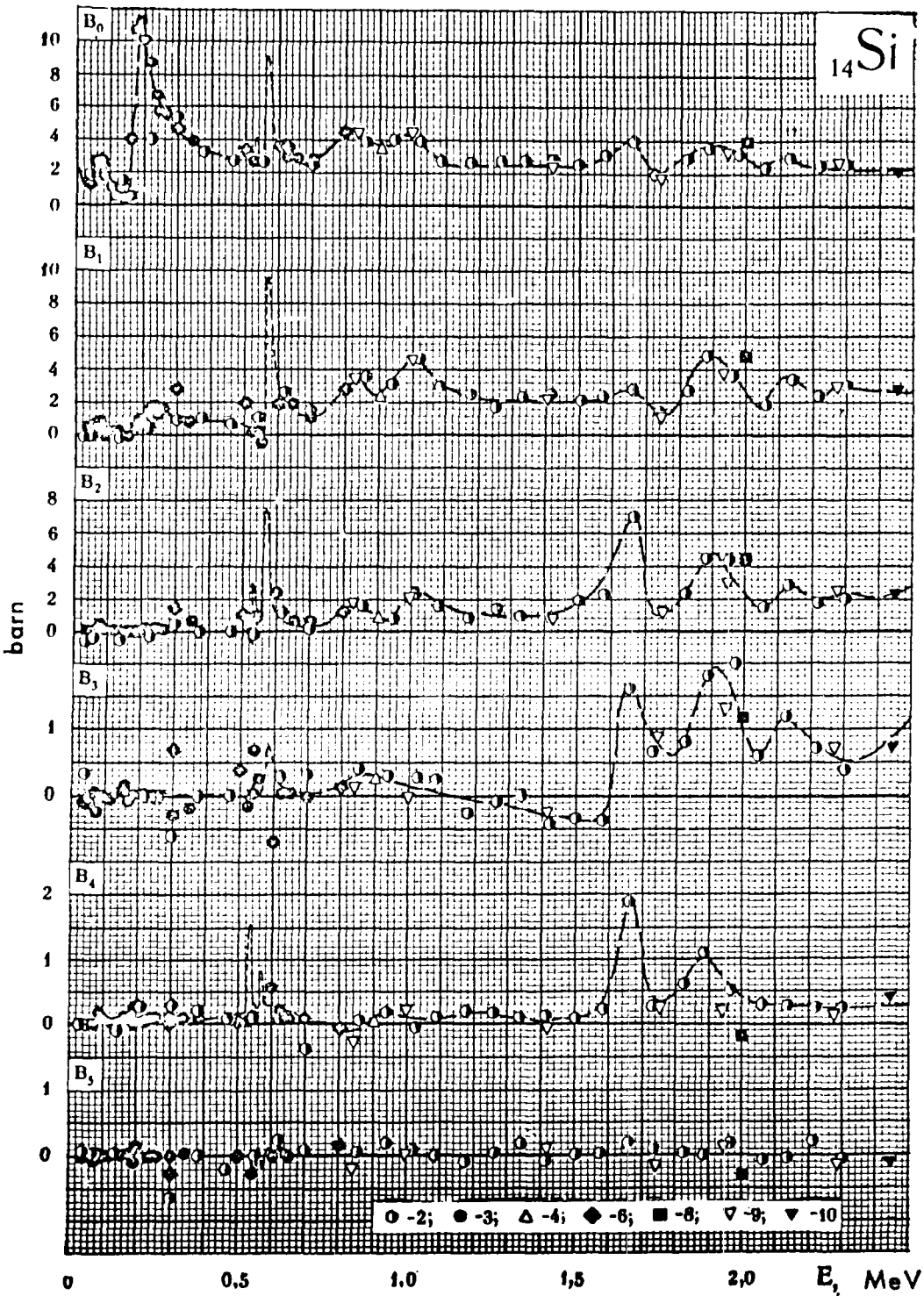
$_{14}$Si
B_0
B_1
B_2
B_3
B_4
B_5
barn
○ -2; ● -3; △ -4; ◆ -6; ■ -8; ▽ -9; ▼ -10
0
0,5
1,0
1,5
2,0
E_p MeV

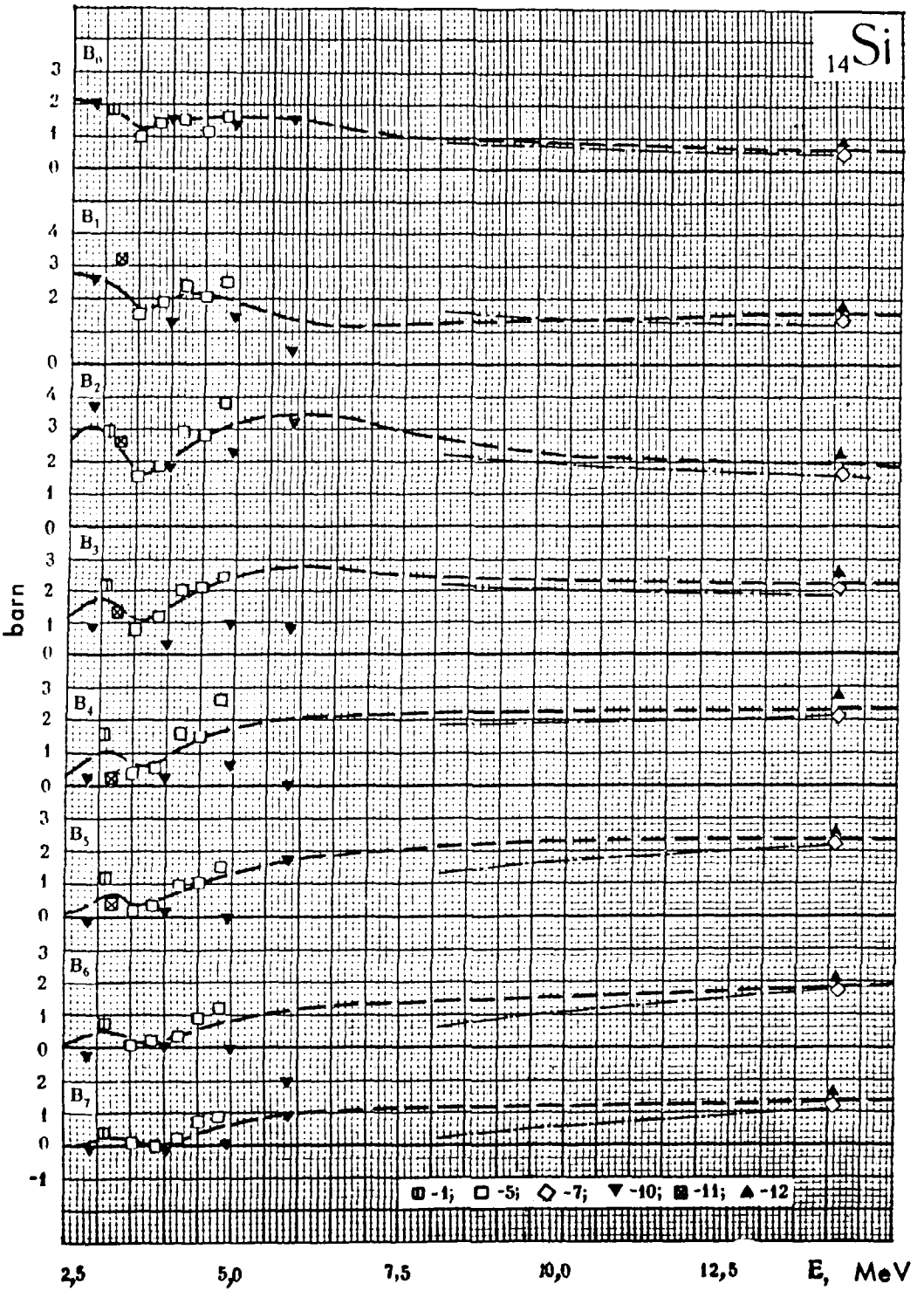
$_{14}$Si
B_0
B_1
B_2
B_3
B_4
B_5
B_6
B_7
barn
-1; -5; -7; -10; -11; -12
2,5
5,0
7,5
10,0
12,5
E, MeV

P H O S P H O R U S

The results by Langsdorf /L-2/(1957) and Elwin et al. /E-3/(1964), which in general agree very well, allow the derivation of the energy dependence of B_ℓ up to 2.2 MeV (Figure 13).

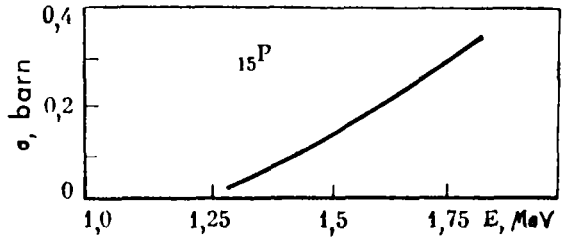

Figure 13. Inelastic neutron scattering cross-section of phosphorus, used for correcting B_o.

In the range 0.7 - 0.9 MeV there is an essential fluctuation of all B_ℓ values in reference /E-3/. One must point out that these fluctuations are in correlation with the total cross-section values obtained in reference /24/ with a resolution of about 35 keV (in references /E-3/ and /L-2/ the resolution was about 100 keV).

The absolute peak cross-sections /24/ are higher than in /E-3/ which was to be expected. In this region there is rather good agreement between B_o and the data of other measurements for the total cross-section, averaged over the interval of 100 keV, values which have been used as orientation when deriving the recommended curve in the range up to 1 MeV.

At 2 MeV the angular distribution of phosphorus has also been measured by Popov et al. /P-6/(see /K-8/); the values of B_o and B_1 obtained from these measurements are considerably higher than in the work /E-3/. This discrepancy could be partly due to the resonances in the cross-section of phosphorus. Since the energy resolution (75 keV) is a little higher in reference /P-6/ than in reference /E-3/, the influence of this fluctuation

should be stronger in the former.

At energies higher than 2.5 MeV results are only available from measurements by Tsukada et al. /T-8/ (E = 3.5 - 4.8 MeV) obtained with the time-of-flight method, and at 14 MeV by Bonazzola et al. /B-14/, and also by Stelson et al. /S-17/. The low value of B_o obtained in /T-8/ at 3.5 MeV corresponds to the big neutron window in the total cross-section /16/ observed at this energy. In the recommended curve this particularity is not reflected since there are not sufficient experimental angular distribution data available in this region.

Unfortunately, in the two references used by us at 14 MeV, no information is given for scattering at angles lower than 24° which, to a considerable extent, decreases the reliability of the extrapolation to lower angles at this energy. The form of the angular distribution when going from 5 MeV to 14 MeV changes essentially, and the interpolation of B_ℓ is, therefore, not very reliable in this range. For deriving B_o in this range we relied on the total cross-sections and the rather scarce data for nonelastic cross-sections (Figure 13). The uncertainty of B_o in the interval 5 - 15 MeV probably amounts to 15 - 20%. The uncertainty of high momenta is, thus, two to three times higher.

The values of B_8 and B_9 at 14 MeV, obtained from the works /B-14/ and /S-17/, amount to 0.574 and 0.592 barn respectively.

$_{15}P$

1 — [1]; [*L* — 2] — A. Langsdorf (1957)
2 — [1]; [*T* — 8] — K. Tsukada (1962)
[*T* — 9] — S. Tanaka (1964)
3 — [*E* — 3] — A. J. Elwyn (1964)
4 — [P — 6] — V. I. Popov (1961)
[*K* — 8] — L. Ya. Kazakova (1965)
5 — [*B* — 14] — G. C. Bonazzola (1965)
[*S* — 17] — P. H. Stelson (1965)

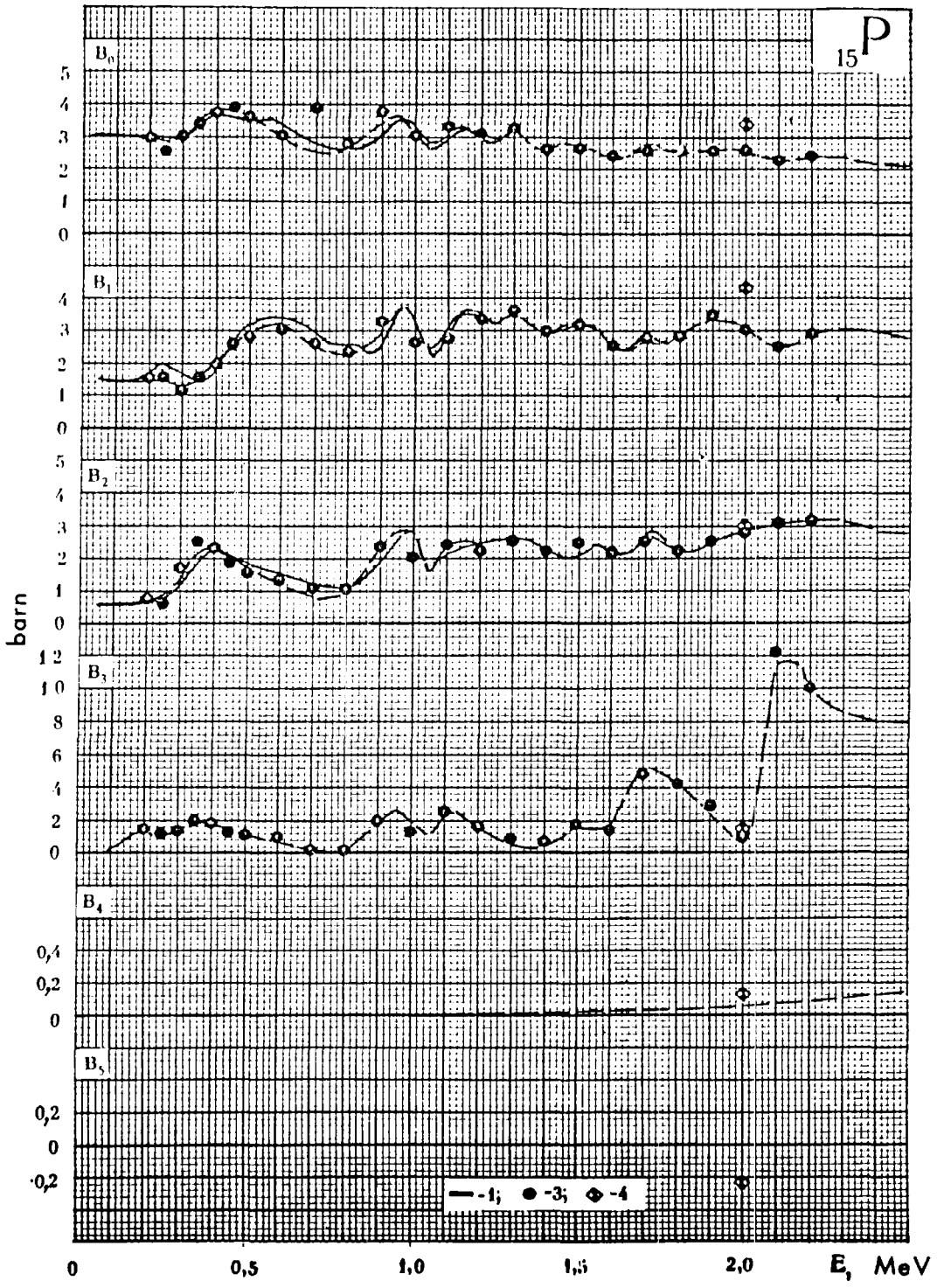
15P
B0
B1
B2
B3
B4
B5
barn
—1; ● -3; ◇ -4
0
0,5
1,0
1,5
2,0
E, MeV

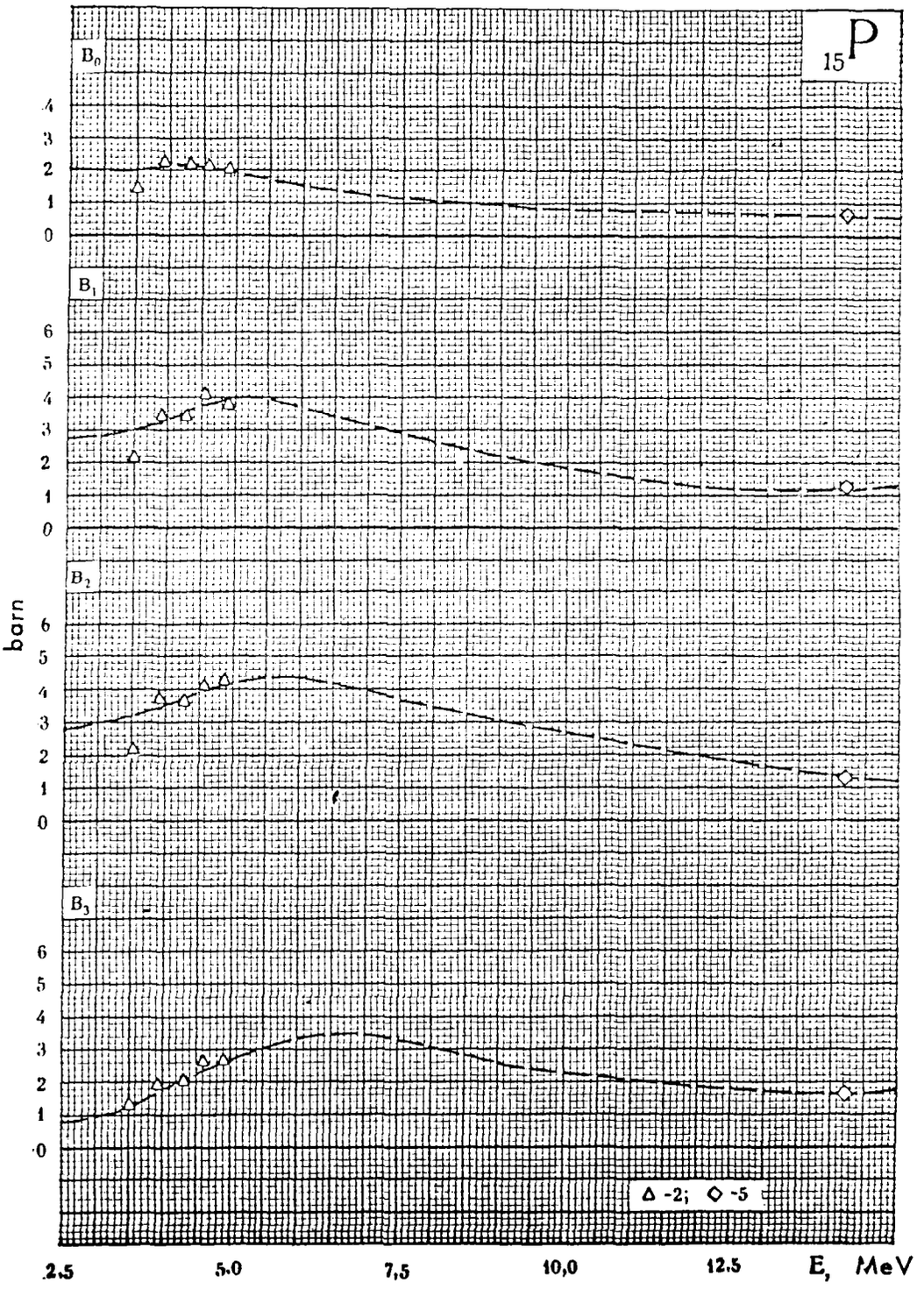
15P
B0
B1
B2
B3
barn
Δ -2; ◇ -5
2.5
5.0
7,5
10,0
12.5
E, MeV

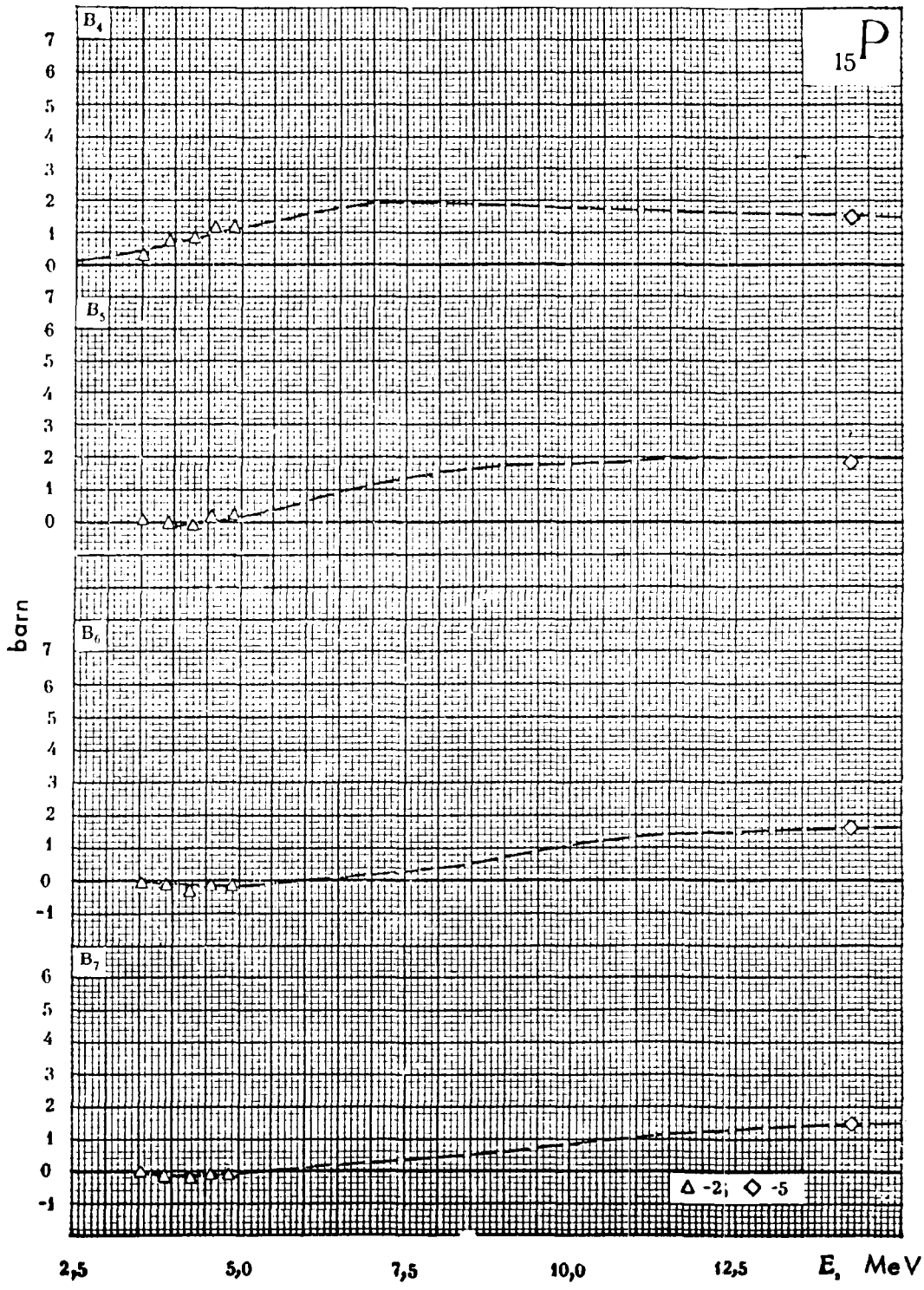
15P
B4
B5
B6
B7
barn
Δ -2; ◇ -5
2,5
5,0
7,5
10,0
12,5
E, MeV

S U L P H U R

At energies below 1.8 MeV, results of detailed measurements of the energy dependence of angular distributions are available /L-2/(1957). The fluctuations of B_ℓ are caused by the bad resolution of the resonances. In reference /L-6/(1961), the results of which appear on a separate sheet, the angular distributions were measured with a high resolution in the vicinity of the resonance around 0.59 MeV. The results of this work are in good agreement with the total cross-sections /13/.

B_o obtained by Langsdorf in the range 0.05 - 0.3 MeV differs from the values obtained by averaging the total cross-sections over the resolution function /L-2/. The maximum of B_o should be found at the large s-wave resonance at 0.11 MeV and not at 0.15 MeV. Therefore, it is suitable to use the total cross-sections for deriving B_o at energies below 0.3 MeV, and the averaged value of the mean cosine of the angular scattering in the range 0.05 - 0.3 MeV obtained from reference /L-2/, and to estimate B_o at lower energies by extrapolation to a value of 0.0206 at $E_n = 0$. In the energy range from 2.5 to 6 MeV, data of a series of authors are available. They agree satisfactorily, but, fit badly the results calculated by the optical model for higher momenta.

It must be mentioned that the comparatively remarkable discrepancy between the calculated and experimental total cross-section values is another indication that the results obtained by the optical model, which we used, are unreliable : the calculated cross-section is 0.4 barn higher at 5 MeV and 0.2 barn lower at 14 MeV than the experimental value. At the same time, the calculated values of B_o are in good agreement with the value of the difference between the total cross-section and the nonelastic cross-section, which has been estimated using the available data /16/. The experimental data in the range 2.5 - 6.0 MeV lie in the mean 0.2 barn below this estimation which is within the accuracy of the latter.

At 14 MeV the difference between the calculated values of B_ℓ and the experimental data is about equal to the uncertainty of the latter. The results of the high momenta are given in tables 13 and 14.

Table 13

Ref.	E, MeV	B_s	Ref.	E, MeV	B_s	Ref.	E, MeV	B_s
	0,587	—0,412		0,5893	—1,43		0,594	0,514
	0,583	—0,344		0,5902	—0,134		0,5954	—0,164
	0,584	—0,321		0,5906	0,130		0,5966	—0,040
[L—6]	0,586	—0,120	[L—6]	0,5914	0,602	[L—6]	0,598	—0,496
	0,5865	0,233		0,5916	—0,009		0,6005	—0,131
	0,588	0,614		0,5922	—0,375		0,603	—0,475
	0,5888	—0,263		0,593	0,715		0,608	—0,564

Table 14

Ref.	E, MeV	B_s	B_p
[1]	14	0,793	0,209
[C—16] [M—8]	14,1	0,745	0,290

$_{16}S$

1 — [1]; [L—1] — R. N. Little (1955)
2 — [1]; [L—2] — A. Langsdorf (1957)
3 — [1]; [M—4] — M. K. Machwe (1959)
4 — [1]; [P—2] — C. St. Pierre (1959)
[E—1] — J. O. Elliott (1956)
[S —10] — V. I. Strizhak (1961)
5 — [1ª]; [L—6] — R. O. Lane (1961)
6 — [1]; [T—8] — K. Tsukada (1962)
[T—9] — S. Tanaka (1964)
7 — [S—18] — D. T. Stewart (1965)
8 — [P— 4] — G. A. Petitt (1966)
9 — [C—16] — R. L. Clarke (1964)
[M— 8] — P. W. Martin (1965)
[C—18] — M. Conjeaud (1965)

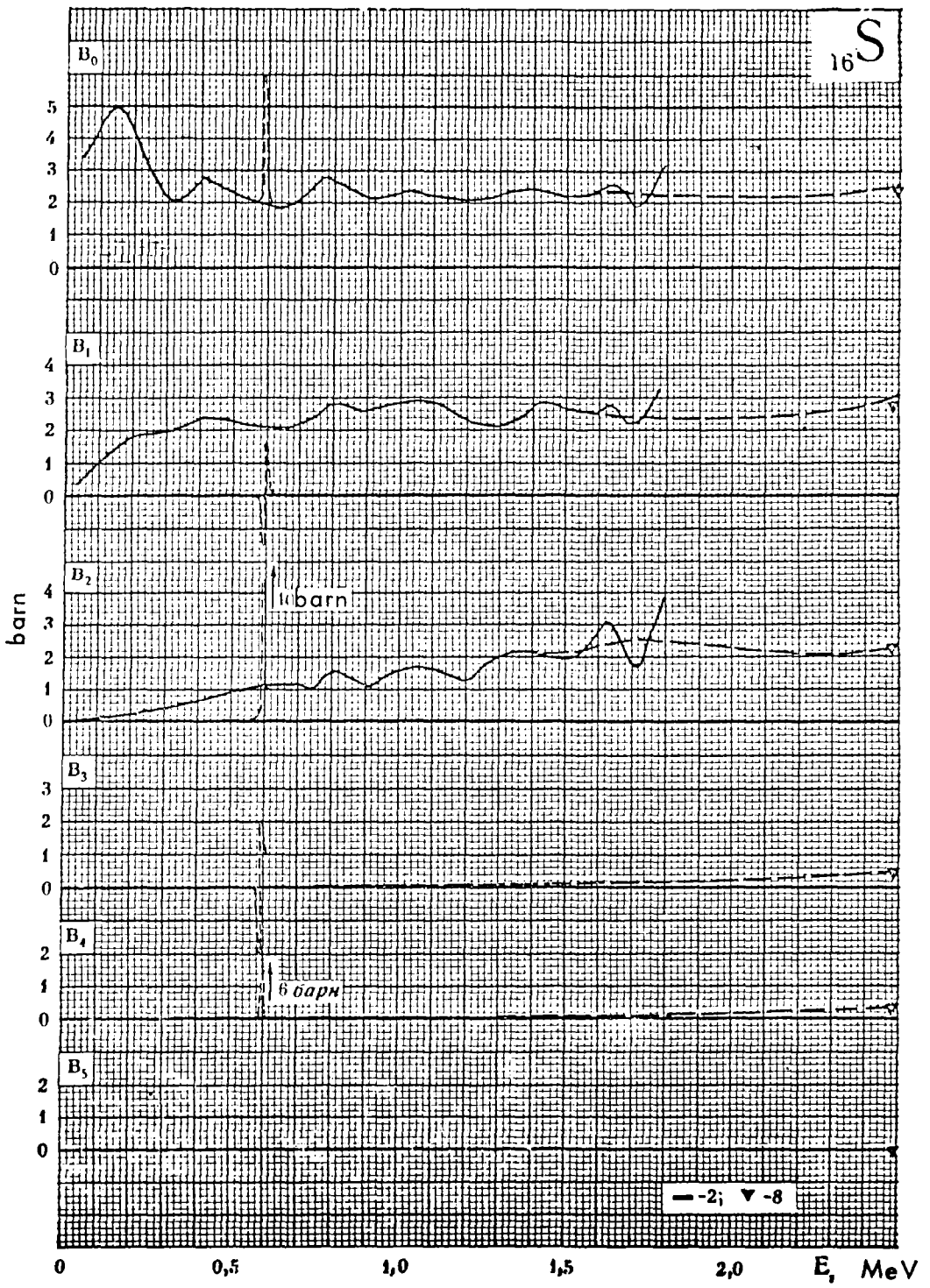
^{16}S
B_0
B_1
B_2
B_3
B_4
B_5
barn
10 barn
6 барн
—2; ▼-8
0
0,5
1,0
1,5
2,0
E_n MeV

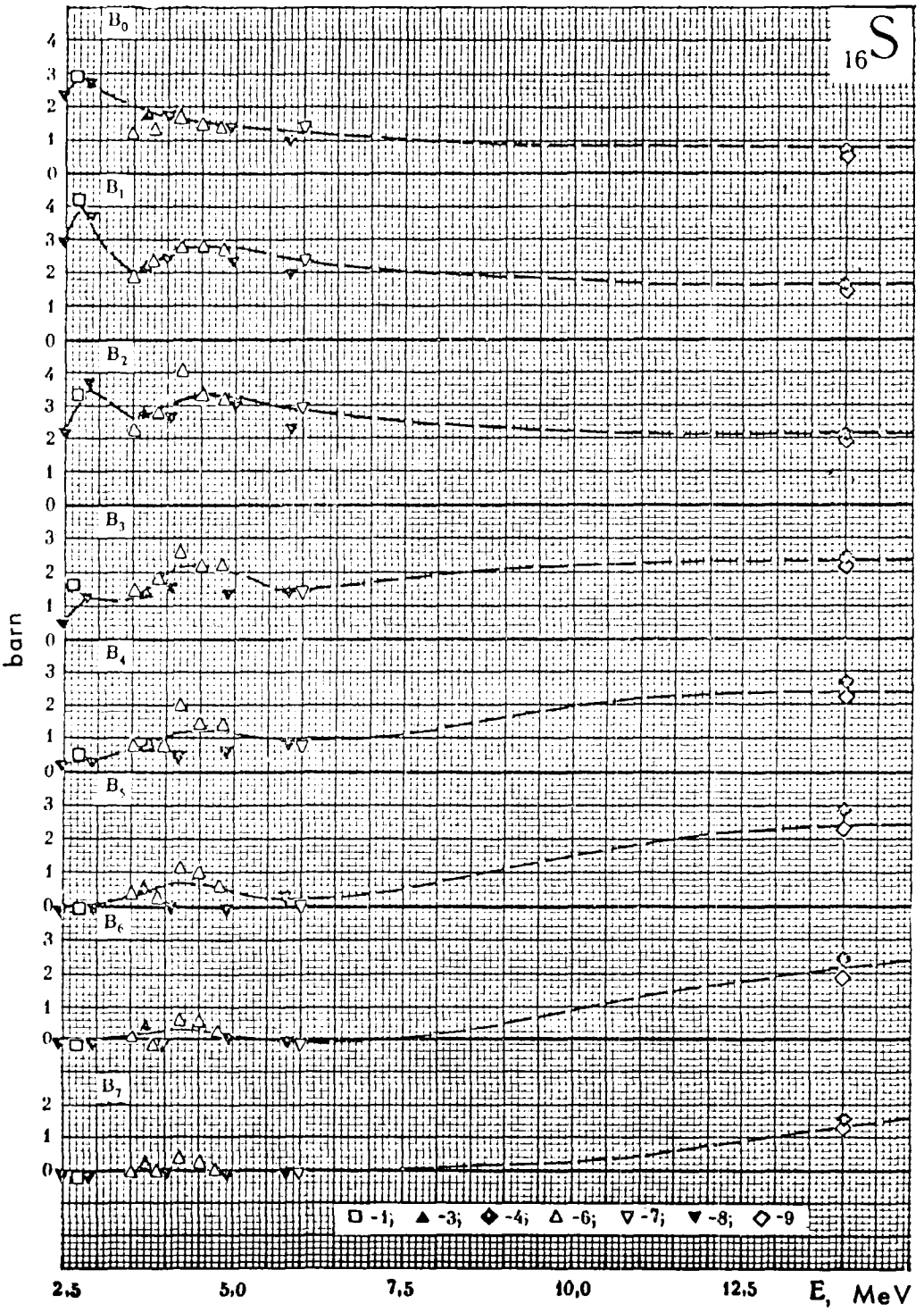
16S
B0
B1
B2
B3
B4
B5
B6
B7
barn
□ -1; ▲ -3; ◆ -4; △ -6; ▽ -7; ▼ -8; ◇ -9
2,5
5,0
7,5
10,0
12,5
E, MeV

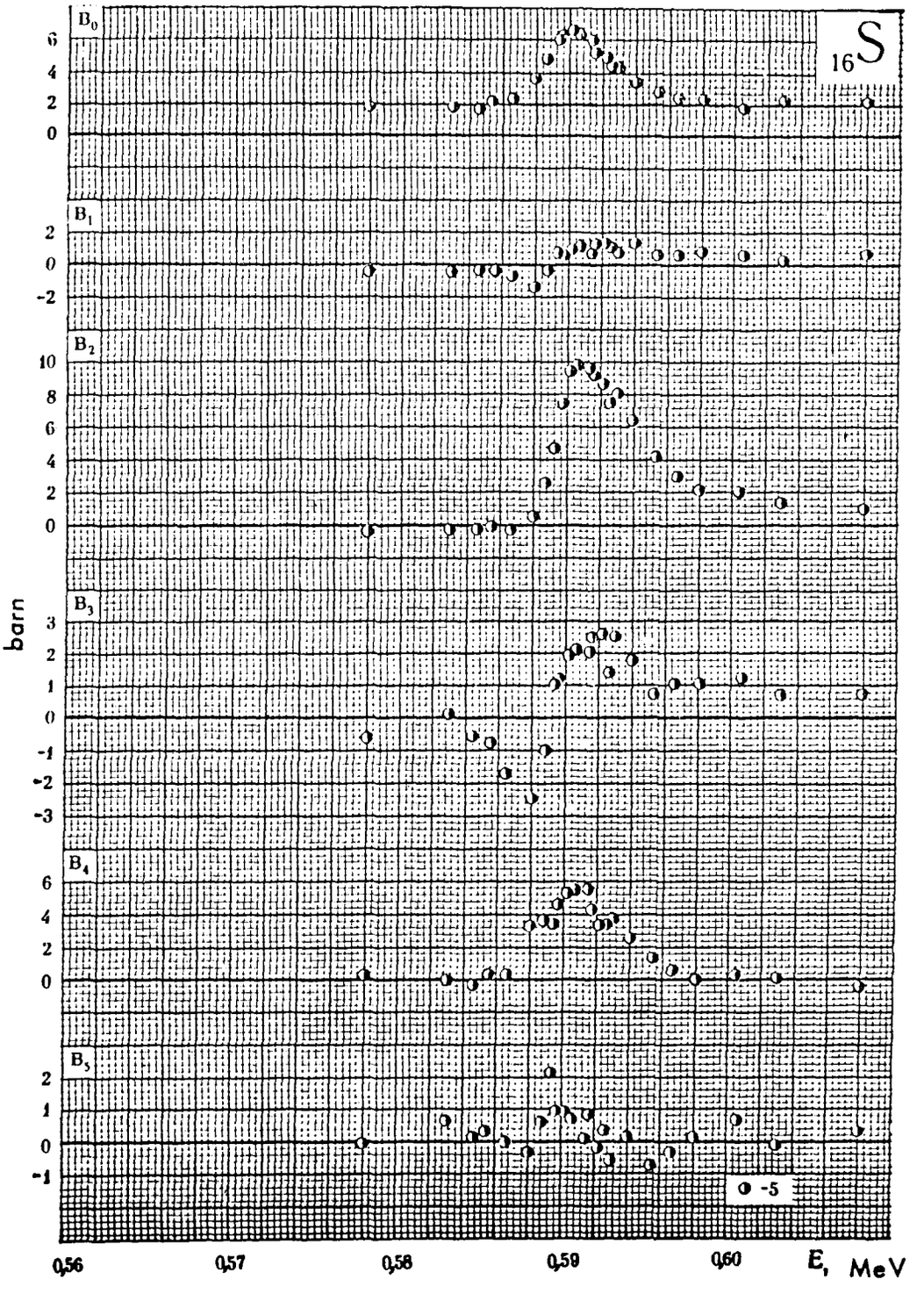
^{16}S
B_0
B_1
B_2
B_3
B_4
B_5
barn
-5
0,56
0,57
0,58
0,59
0,60
E, MeV

P O T A S S I U M

The data by Langsdorf et al. /L-2/ in the energy range below 1.4 MeV fit quite well to the results obtained by Towle et al. /T-11/(1965) at 1.5 MeV, (with the exception of higher harmonics, the derivation of which includes possibly higher uncertainties). The difference between the values of reference /L-2/ and the results of Korsch et al. /K-4/ can be explained by the better resolution used in the latter work; thanks to this, his results show the existence of strong compound nucleus resonances at an energy of 0.3 MeV (see /3/). The data of B_o by Langsdorf and Towle in the energy range up to 2.5 MeV agree with the total cross-section within an accuracy of 0.1 barn. The results of Towle et al. /T-11/ permit the derivation of the energy dependence of B_ℓ up to 4 MeV, where good agreement is observed with the results by Popov /P-3/(1961) and Kent /K-2/(1962) as well as with the available data of the difference between the total and the nonelastic cross-section.

Further data on the angular distribution are only available at 14 MeV /R-9/, /F-7/. We also wish to point out that at small angles the scattering data of references /R-9/ and /F-7/ differ considerably : (B_o = 0.74 /R-9/; B_o = 1.05 /F-7/; B_o = 1.02 /R-9, F-7/. The lack of experimental data at higher energies (4 - 14 MeV) does not permit the derivation of reliable data by interpolation in this energy range. The values of the high momenta are given in table 15.

Table 15

Ref.	E_n·MeV	B_1	B_2
[F—7]	14	1,17	0,246
[R—9]	14	1,3	—

$_{19}K$

1 — [L— 2] — A. Langsdorf (1957)
2 — [P — 3] — V.I.Popov (1961)
3 — [1]; [K— 2] — D. W. Kent (1962)
4 — [K— 4] — I.A. Korzh (1963)
5 — [T—11] — J. H. Towle (1965)
6 — [F— 7] — A. J. Frasca (1966)
7 — [R— 9] — J. Roturier (1966)

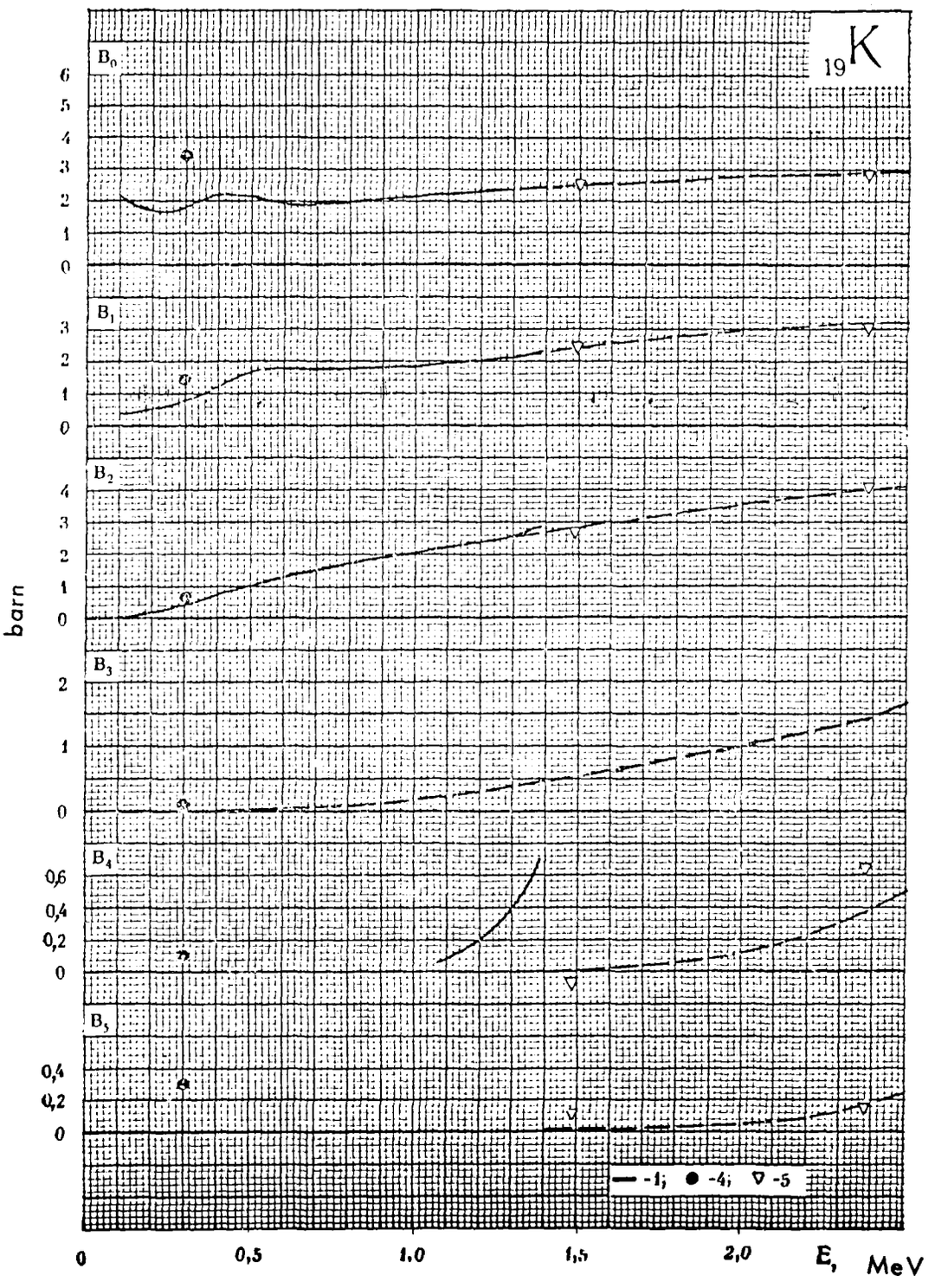
19K
B0
B1
B2
B3
B4
B5
barn
E, MeV
0
0,5
1,0
1,5
2,0
— -1; ● -4; ▽ -5

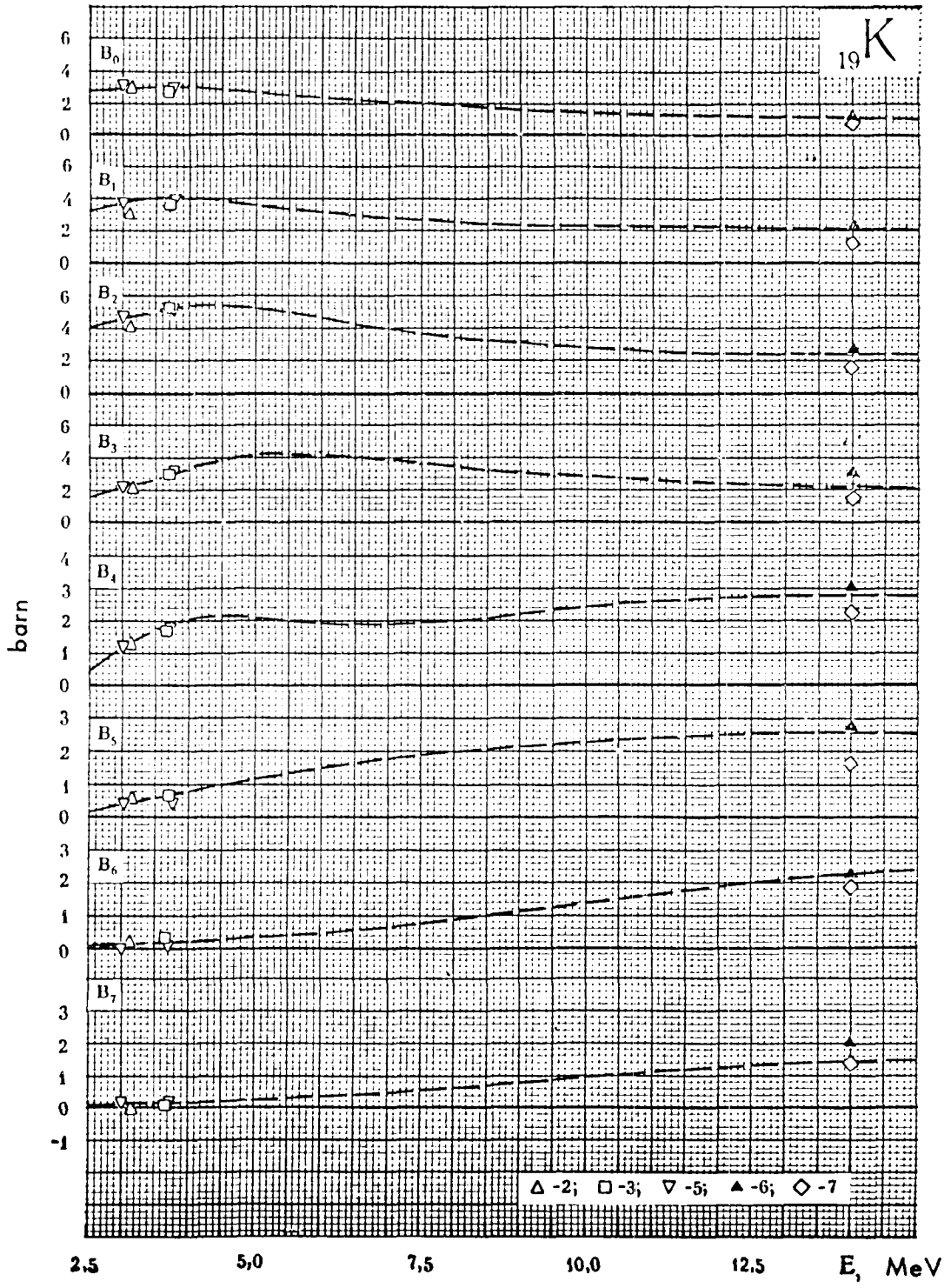
19K
B0
B1
B2
B3
B4
B5
B6
B7
barn
Δ -2; □ -3; ▽ -5; ▲ -6; ◇ -7
2,5
5,0
7,5
10,0
12,5
E, MeV

C A L C I U M

The data by Lane et al. /L-6/(1961), available in the range below 2.3 MeV, have been corrected for a small inelastic scattering contribution and agree with the total cross-section /16/ as well as with the values of B_o obtained in the works /L-4/(1962) and /S-8/(1961) at 1 and 2 MeV, respectively. At these energies, however, the high harmonics differ considerably from the results of reference /L-6/ (in particular, at 2 MeV).

In the energy range 2.5 - 6.0 MeV the available experimental data /P-3/, /S-8/, /K-2/ and /V-1/ do not contradict one another. The observed scatter of the data indicate the uncertainty with which the elastic neutron angular distributions have been measured.

At 14 and 14.6 MeV, the measurements by Cross et al. /C-7/(1960), McDonald et al. /M-7/(1964) and Frasca et al. /F-7/ agree satisfactorily. The interpolation of the data in the range from 6 to 15 MeV can be carried out with good precision : in doing the interpolation for B_o the available total- and nonelastic cross-sections have been taken into account. The values of the high momenta are given in tables 16 and 17.

Table 16

Ref.	E, MeV	B_4	Ref.	E, MeV	B_6	Ref.	E, MeV	B_4
[L—6]	0,05	0,065	[L—6]	0,85	0,065	[L—6]	1,65	—0,090
	0,130	0,305		0,93	—0,014		1,73	—0,140
	0,21	0,159		1,01	—0,227		1,81	—0,180
	0,29	0,123		1,09	0,130		1,89	0,300
	0,37	—0,181		1,17	0,090		1,97	—0,180
	0,45	—0,081		1,25	0,121		2,06	—0,300
	0,53	—0,071		1,33	0,153		2,14	0,000
	0,61	0,066		1,41	—0,213		2,21	0,390
	0,69	0,016		1,49	—0,120		2,29	0,000
	0,77	—0,259		1,57	0,001			

Table 17

Ref.	E, MeV	B_8	B_9	B_{10}	B_{11}
[C—7]	14,6	1,71	0,799	0,358	0,114
[M—7, F—7]	14	1,76	0,893	0,352	0,185

$_{20}$Ca

1 — [1]; [V—1] — L. D. Vincent (1960)
2 — [1]; [C—7] — W. G. Cross (1960)
3 — [P—3] — V. I. Popov (1961)
4 — [1]; [S—8] — J. D. Seagrave (1961)
5 — [L—4] — G. N. Lovchikova (1962)
6 — [1a]; [L—6] — R. O. Lane (1961)
7 — [1]; [K—2] — D. W. Kent (1962)
8 — [M—7] — W. J. McDonald (1964)
[F—7] — A. J. Frasca (1966)
9 — [B—20] — R. L. Becker (1966)

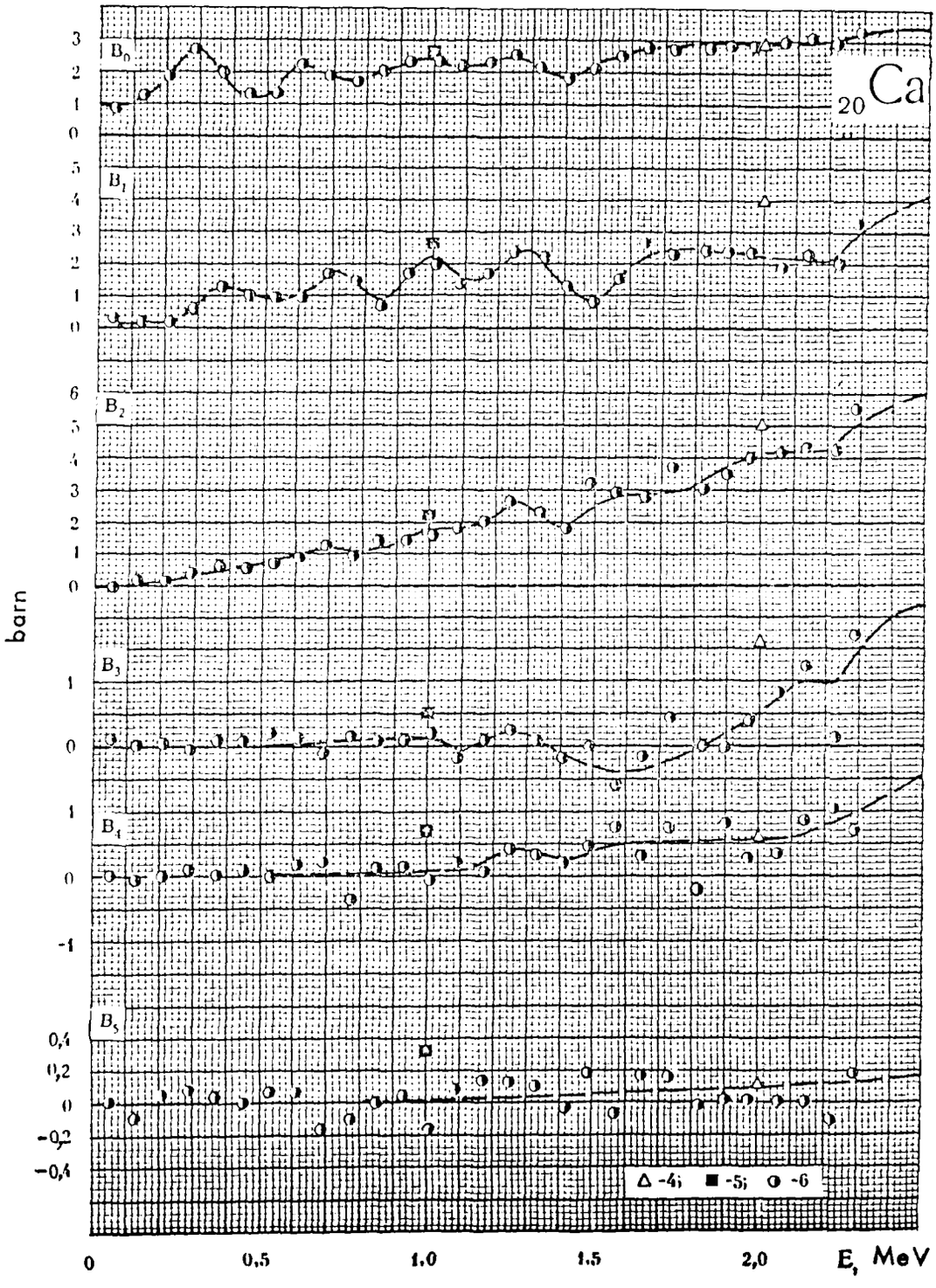
$_{20}$Ca
B_0
B_1
B_2
B_3
B_4
B_5
barn
△ -4; ■ -5; ○ -6
0
0,5
1,0
1,5
2,0
E, MeV

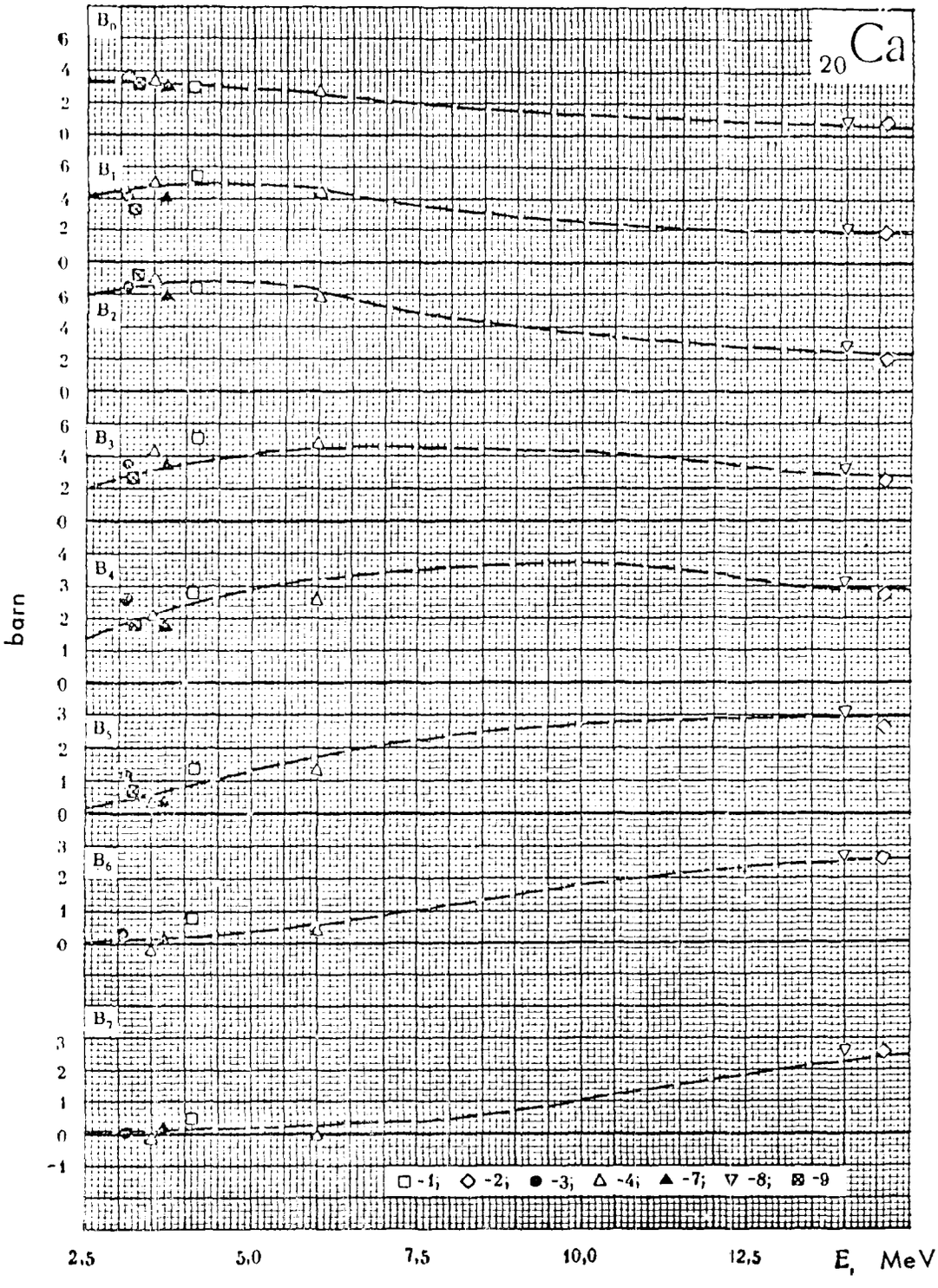
$_{20}$Ca
B_0
B_1
B_2
B_3
B_4
B_5
B_6
B_7
barn
□ -1; ◇ -2; ● -3; △ -4; ▲ -7; ▽ -8; ⊠ -9
2,5
5,0
7,5
10,0
12,5
E, MeV

T I T A N I U M

The data by Langsdorf /L-2/ at 1 MeV are in very good agreement with the results by Lowchikov /L-4/, Walt /W-4/ and Darden /D-2/. The results in reference /L-2/ also agree well with the total cross-sections /13/. The strong increase of B_o in the range below 0.2 MeV is caused by the influence of the strong s-wave resonances of Ti-48, which lie at lower energies, but are touched by the wing of the resolution function. Therefore, one can practically only give recommended values down to about 0.25 MeV. At lower energies, $B_o \sim \delta_T$ and the energy dependence of B_1 can be estimated by linear interpolation of the ratio B_1/B_o from the value at 0.25 MeV to zero at $E_n = 0$. For the ratio B_2/B_o a quadratic interpolation has, of course, to be used.

In the range from 1.5 to 2 MeV no experimental data are available, but here the energy dependence of B_ℓ can be obtained with sufficient reliability by interpolating between the results of reference /L-2/ and the data in the references /P-6/ and /K-8/ at 2 MeV. In the range 2 - 4 MeV, besides the above-mentioned data at 2 MeV, experimental results are available at 2.25 and 2.45 MeV /C-3/, 3.2 MeV /B-20/ and 4.1 MeV /W-5/; they agree well between one another.

At energies higher than 4 MeV, the recommended curve was obtained by interpolation relying on the results calculated by the optical model and the values of the difference between total- and nonelastic cross-sections /Figure 14/. At 14 MeV the calculated results agree with the data of reference /P-2/.

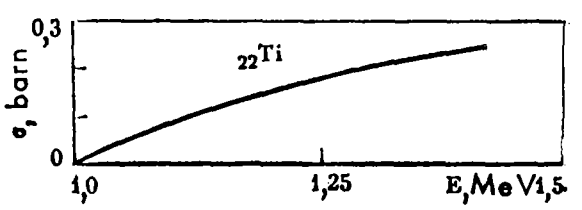

Figure 14. Inelastic neutron scattering cross-section of titanium, used for correcting B_o .

The values of high moments are given in table 18.

Table 18

Ref.	E, MeV	B_s	B_s	B_{1s}
[W—5]	4,1	0,086	—	—
[P—2]	14	1,42	0,652	0,171

$_{22}$Ti

1 — [1]; [W—4] — M. Walt (1954)
[L—4] — G.N.Lovchikova (1962)
[D—2] — S. E. Darden (1955)
2 — [1]; [W—5] — M. Walt (1955)
3 — [1]; [C—3] — L. Cranderg (1956)
[L—2] — A. Langsdorf (1957)
4 — [1]; [P—2] — C. St. Pierre (1959)
5 — [P—6] — V.I.Popov (1965)
[K—8] — L.Ya.Kazakova (1965)
6 — [B—20] — R. L. Becker (1966)
7 — [K—9] — I.A. Korzh (1966)

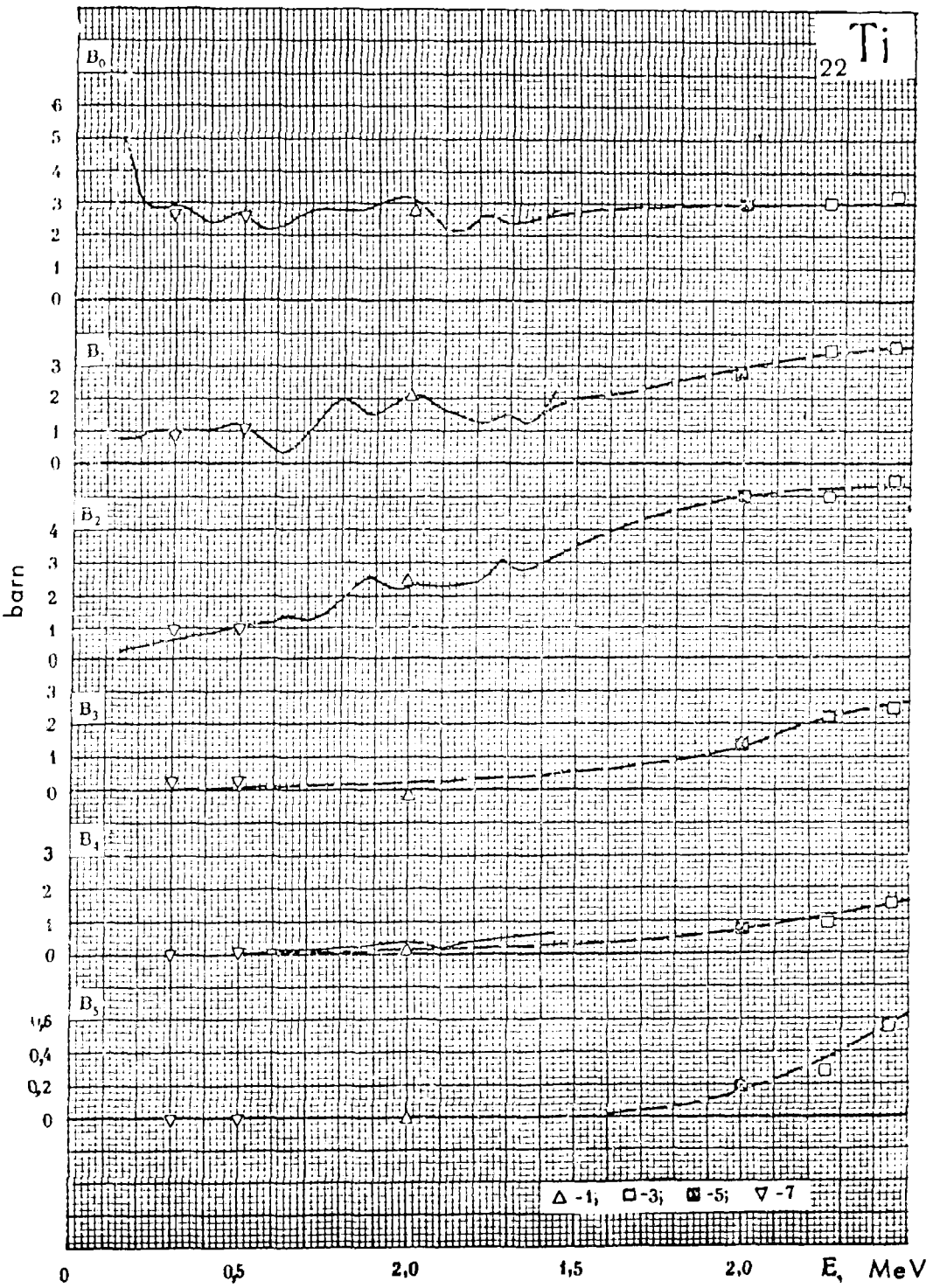
22 Ti
B0
B1
B2
B3
B4
B5
barn
Δ -1; □ -3; ▣ -5; ▽ -7
0
0,5
2,0
1,5
2,0
E, MeV

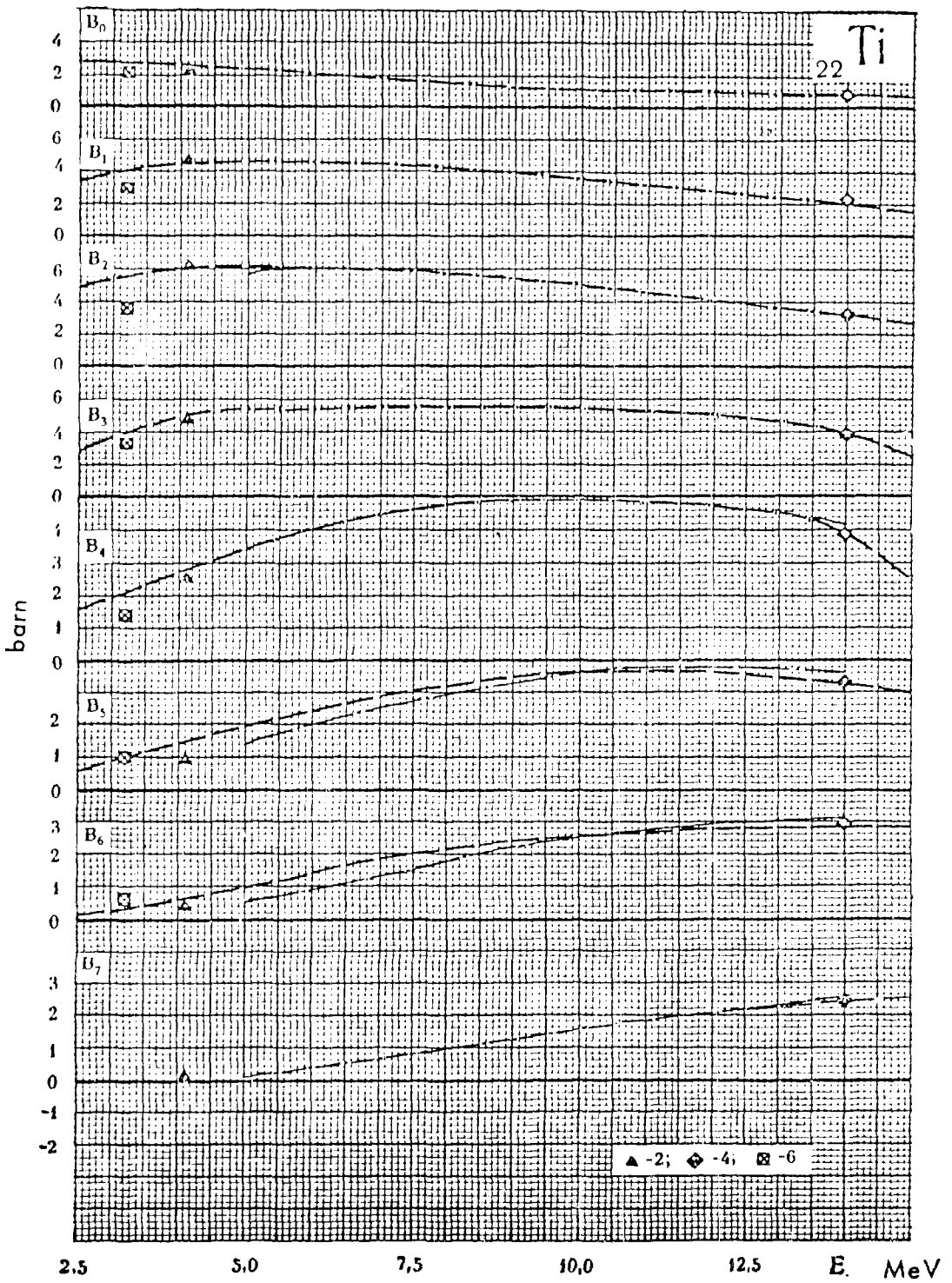
$_{22}$Ti
B_0
B_1
B_2
B_3
B_4
B_5
B_6
B_7
barn
▲ -2; ◆ -4; ⊠ -6
2,5
5,0
7,5
10,0
12,5
E, MeV

V A N A D I U M

The measured value of B_o in reference /L-2/ agrees rather well with the total cross-sections (corrected for the inelastic scattering with the cross-sections mentioned below /Figure 15/). In the interval 0.6 - 1.3 MeV, however, B_o from reference /L-2/ lies 0.5 - 0.7 below σ_T. On the other hand the extrapolation of the quoted inelastic cross-sections yield $\sigma_{in} \approx$ 1 barn at 2.35 MeV.

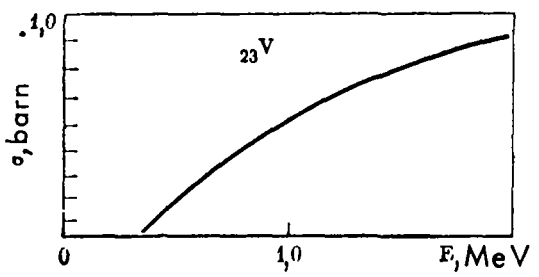

Adding this value to B_o taken from reference /T-10/, we obtain σ_T = 4 barn, which is 0.4 barn higher than the results obtained by direct measurements /13/.

The uncertainty of the recommended curve is, therefore, unlikely to be greater than 0.5 barn in the region below 2.5 MeV.

The angular distribution curve, however, obtained from the relation B_ℓ / B_o has a somewhat better-known accuracy as far as one can judge from the agreement of the results of different authors. At energies below 0.3 MeV B_o converges to σ_T.

The value B_1 in the energy range below 0.15 MeV can be obtained by multiplying σ_T with three times the value of the mean cosine angular scattering. By linear extrapolation from a value of 0.028 at 0.15 MeV it is estimated to be 0.013 at $E_n = 0$.

In the region above 2.5 MeV only one experimental work is available, /B-20/, which is neither at variance with the data given in /L-2/ and /T-10/, nor at variance with the results obtained by optical model calculation. The calculated total cross-section agrees well with the experimental values.

$_{23}V$

1 — [*L*— 2] — A. Langsdorf (1957)
2 — [*T*—10] — J. H. Towle (1965)
3 — [*B*—20] — R. L. Becker (1966)

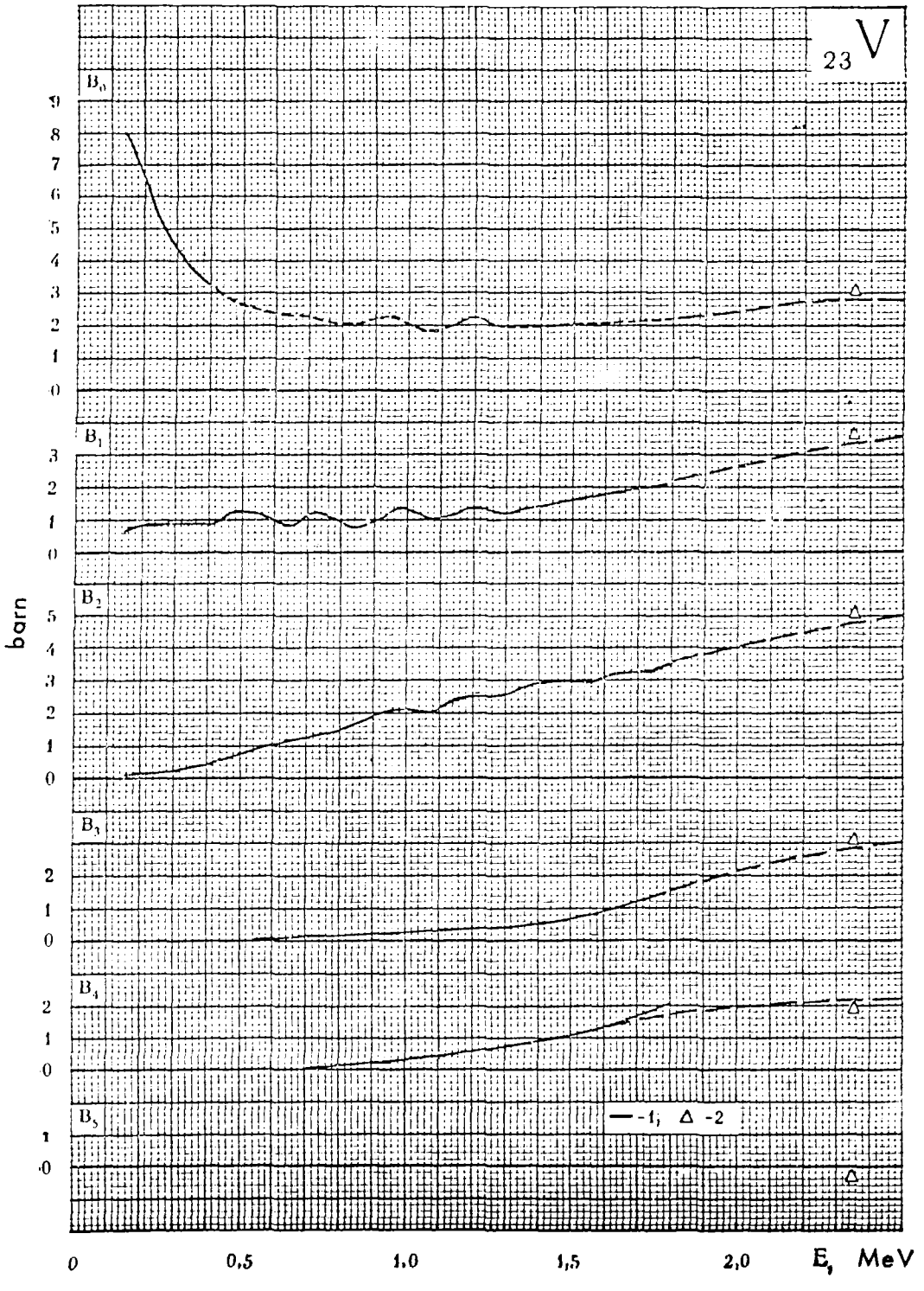
$_{23}$V
B_0
B_1
B_2
B_3
B_4
B_5
barn
— -1; Δ -2
0
0,5
1,0
1,5
2,0
E_γ MeV

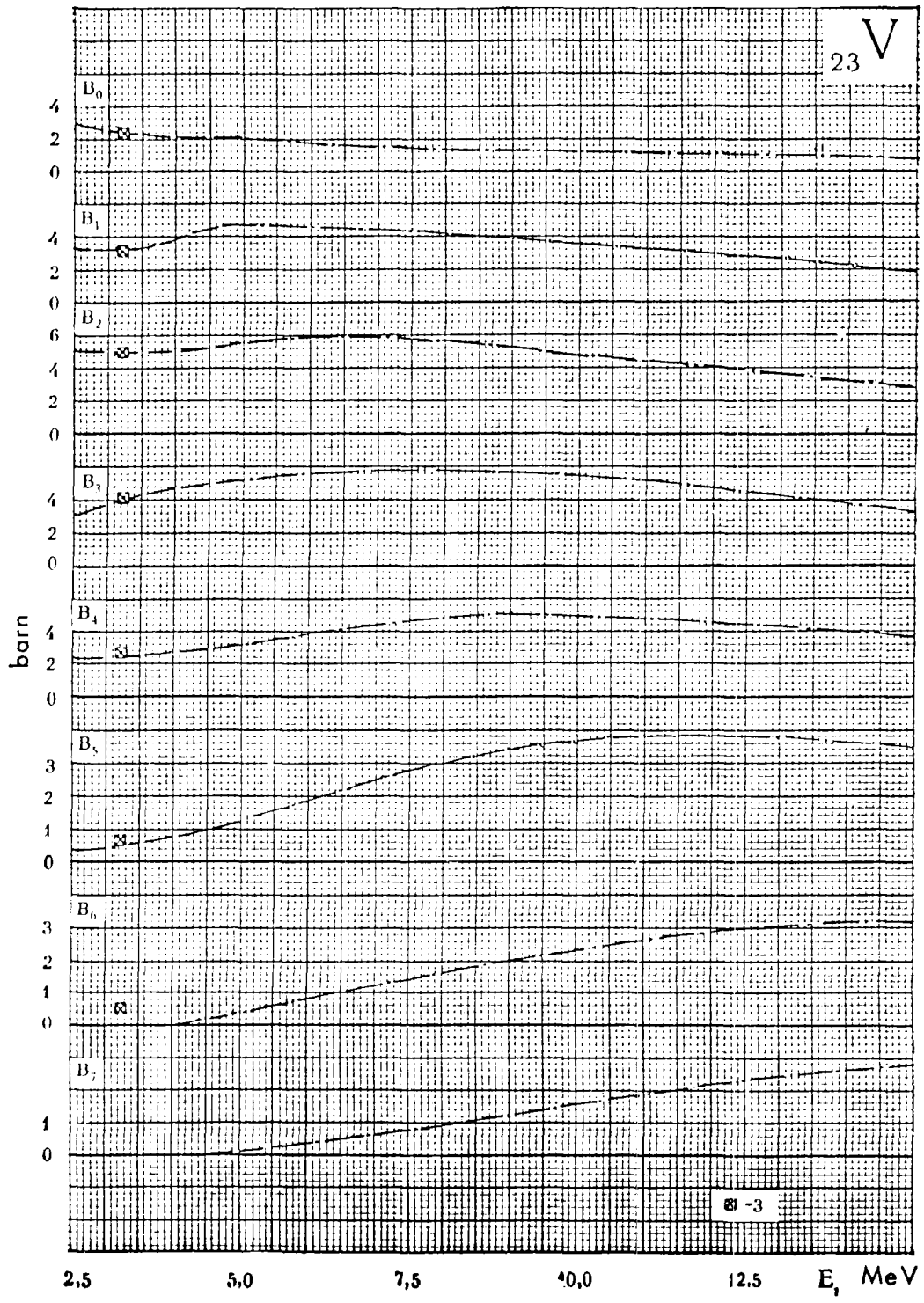
23 V
B0
B1
B2
B3
B4
B5
B6
B7
barn
81 -3
2,5
5,0
7,5
10,0
12,5
E, MeV

C H R O M I U M

In the energy range below 1.8 MeV a sufficiently great number of data agree quite well.

Attention is in particular attracted by the very good agreement of the results obtained with high resolution /L-2/, /K-7/ and the time-of-flight measurements published in /S-14/ and /C-15/. The high resolution used (20 keV) in the latter work, and the large number of points measured (with 8 keV steps) permit a very good resolution of the resonances in the energy range from 0.7 - 1.1 MeV. The results of this work are plotted on a separate sheet. In the energy range 1.1 - 2.5 MeV the angular distribution can be obtained with sufficient reliability by an interpolation between the data of Smith /S-14/ and Langsdorf /L-2/ (with small energy steps) as well as the data by Popov /P-6/ at 2.0 MeV and those of Salnikov /C-4/ at 2.35 MeV.

Unfortunately, in the region above 2.5 MeV no experimental data, except at 3.2 MeV /B-20/ and at 14 MeV /S-17/, are available. The value B_o, obtained in the above-mentioned works agrees well with the difference of the total- and the nonelastic-cross-section (Figure 16). The angular distribution can, in this case, be estimated only on the basis of the optical model.

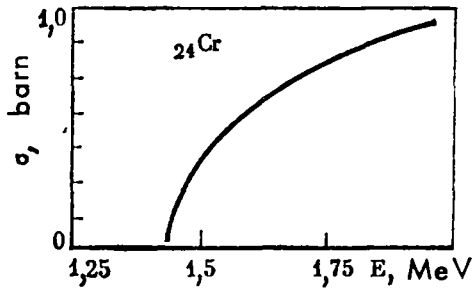

Figure 16 - Inelastic neutron scattering cross-section of chromium, used for correcting B_o.

The calculation of the total cross-section and the compound nucleus cross-section with the adopted potential parameters agrees well with the experimental results.

The values for the moments, B_8 , B_9 and B_{10} at E_n = 14 MeV obtained with the data from reference /S-17/ are 1.97, 1.02 and 0.329 barn, respectively.

$_{24}Cr$

1 — [*L*— 2] — A. Langsdorf (1957)
2 — [2]; [K— 4] — O.A. Kalnikov (1957)
3 — [2]; [*G*— 1] — W. B. Gilboy (1962)
4 — [*S*—14] — A. B. Smith (1964)
5 — [*K*— 7] — I.A.Korzh (1964)
6 — [*C*—15] — S. A. Cox (1964)
7 — [P — 6] — V.I.Popov (1965)
[*K*— 8] — L.Ya.Kazakova (1965)
8 — [*S*—17] — P. H. Stelson (1965)
9 — [*B*—20] — R. L. Becker (1966)

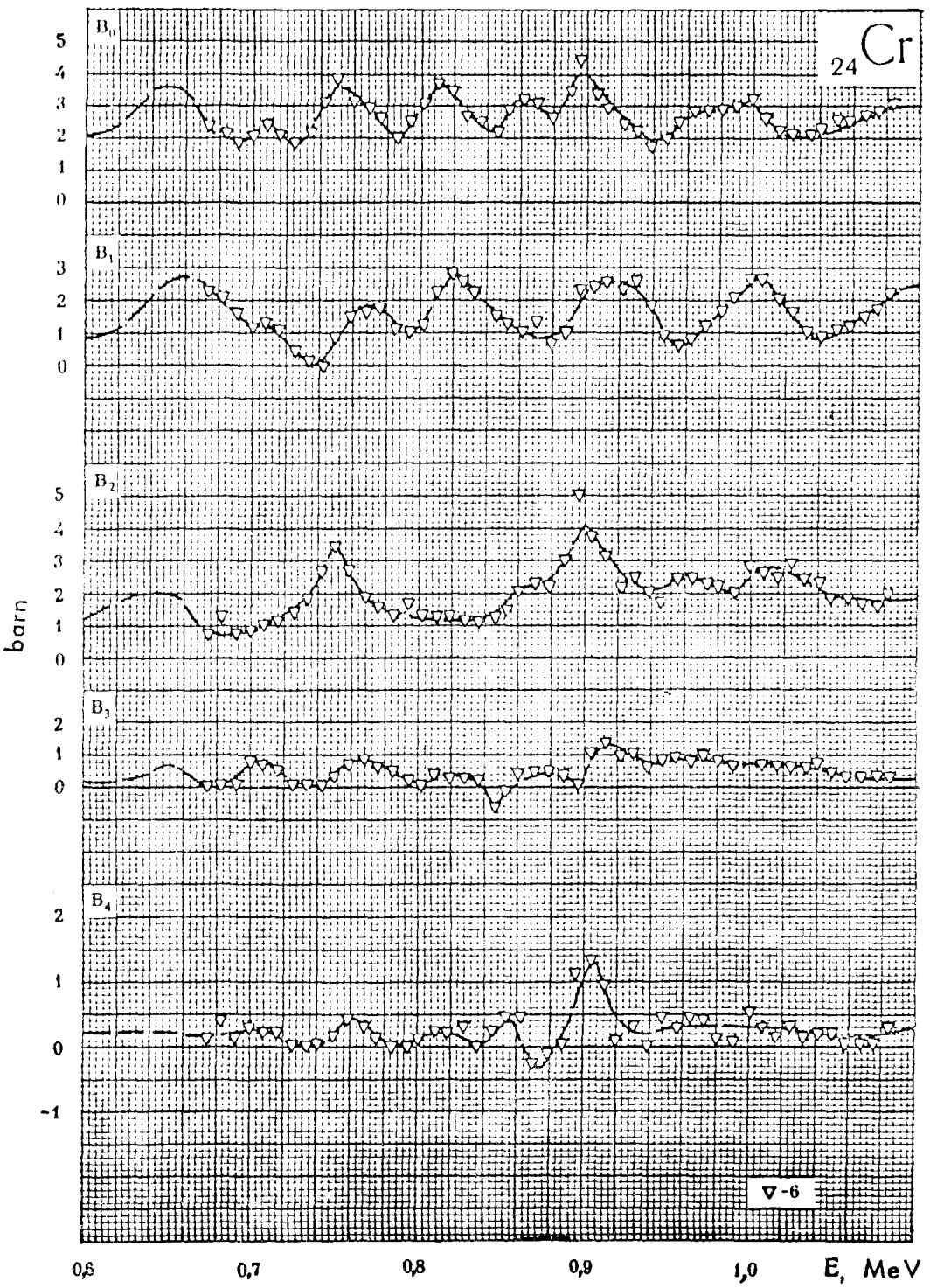
$_{24}$Cr
B_0
B_1
B_2
B_3
B_4
barn
▽-6
0,6
0,7
0,8
0,9
1,0
E, MeV

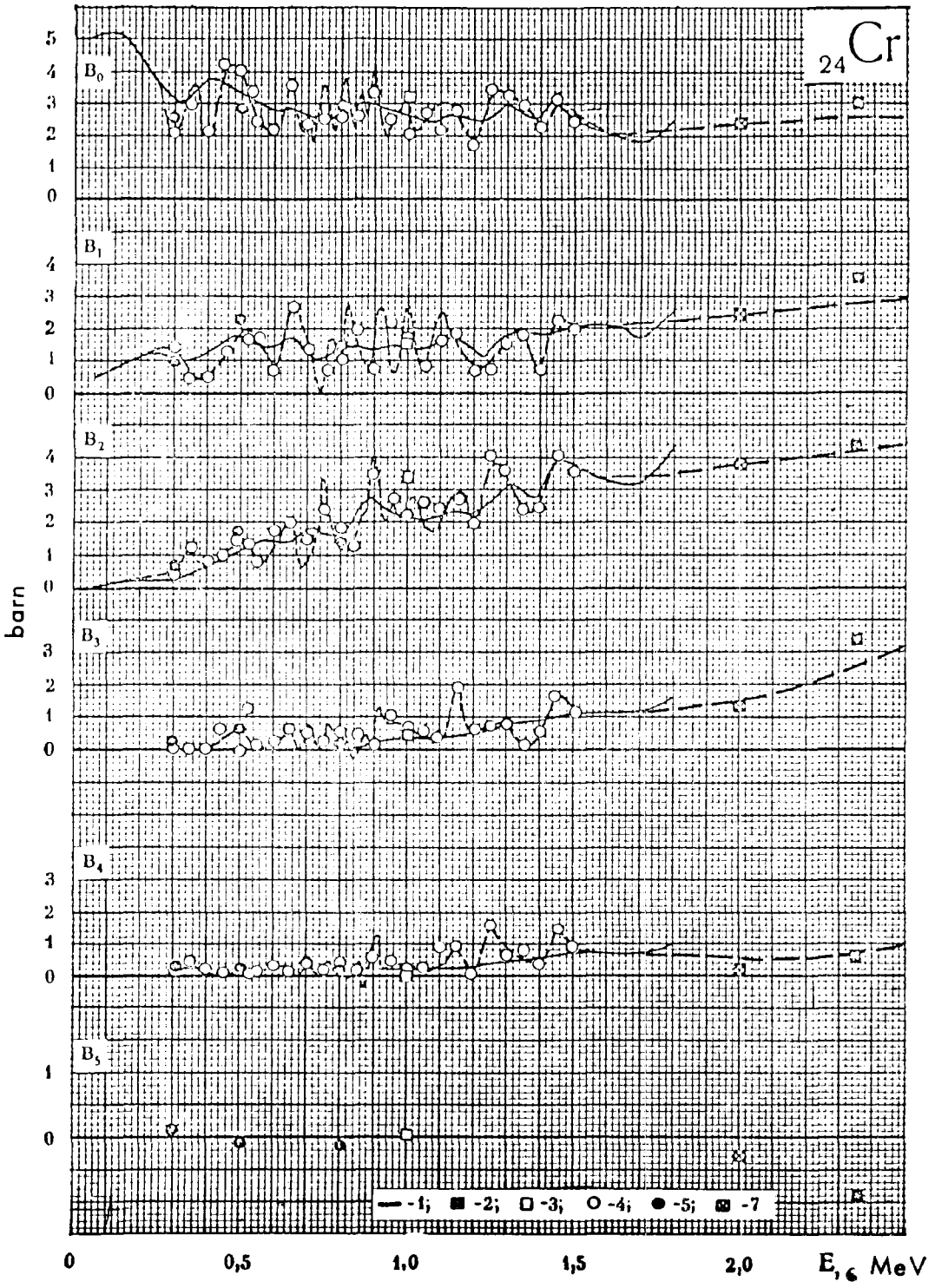
$_{24}$Cr
B_0
B_1
B_2
B_3
B_4
B_5
barn
—1; ■ -2; □ -3; ○ -4; ● -5; ⊠ -7
0
0,5
1,0
1,5
2,0
$E_{n,c}$ MeV

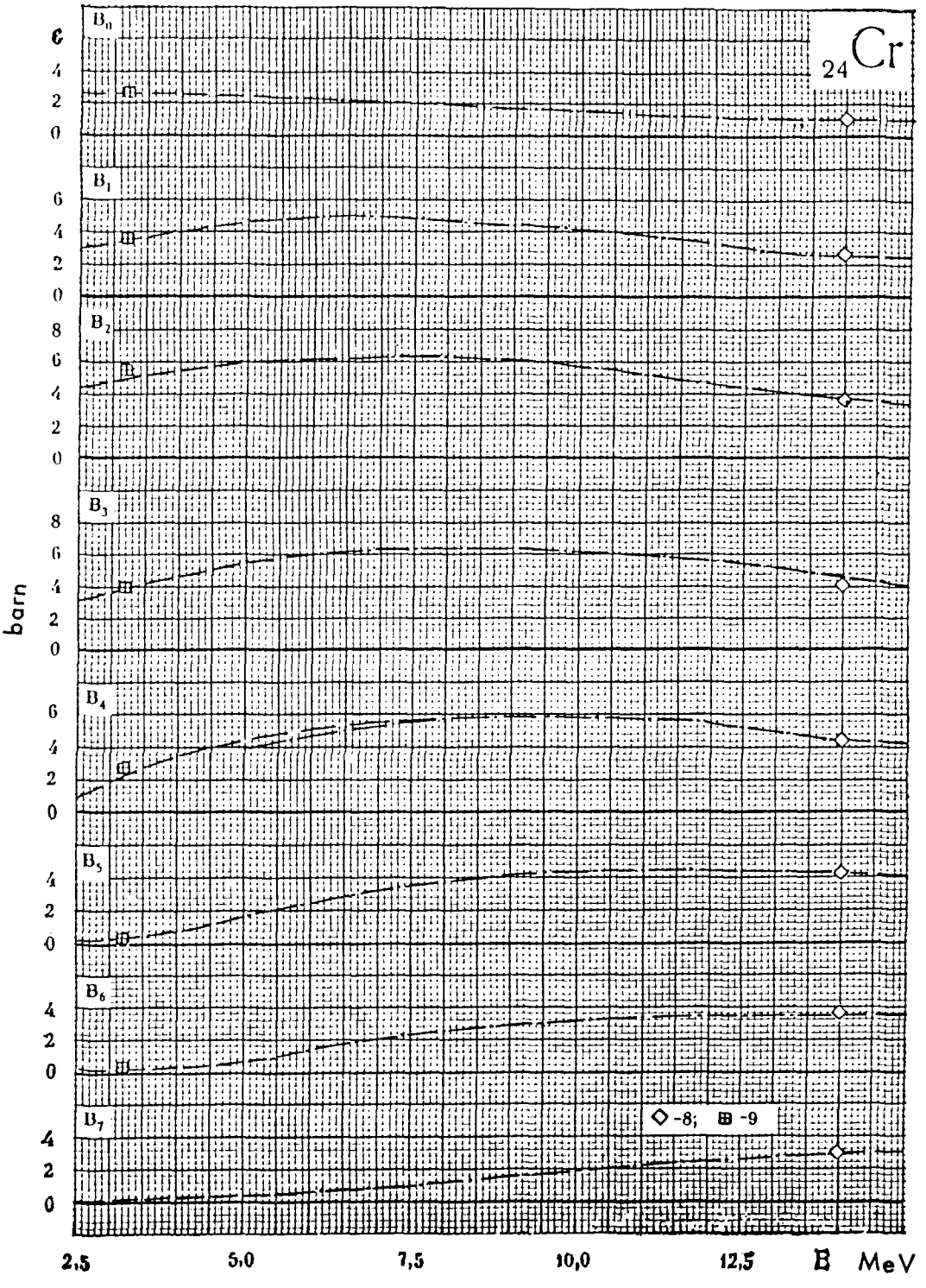
$_{24}$Cr
B_0
B_1
B_2
B_3
B_4
B_5
B_6
B_7
barn
◇ -8; ⊞ -9
2,5
5,0
7,5
10,0
12,5
E MeV

M A N G A N E S E

Information on the neutron angular distribution elastically scattered on manganese is very scarce. Data are only given in the publications by Cox /C-15/, Popov /P-6/, Kazakova /K-8/ and Becker /B-20/. These data permit the representation of the behaviour of B_ℓ only for energies below 3.5 MeV.

At higher energies B_ℓ can only be estimated on the basis of optical model calculations.

$_{25}$Mn

1 — [C—15] — S.A. Cox (1964)
2 — [P — 6] — V.I. Popov (1965)
[K— 8] — L.Ya. Kazakova (1965)
3 — [B—20] — R. L. Becker (1966)

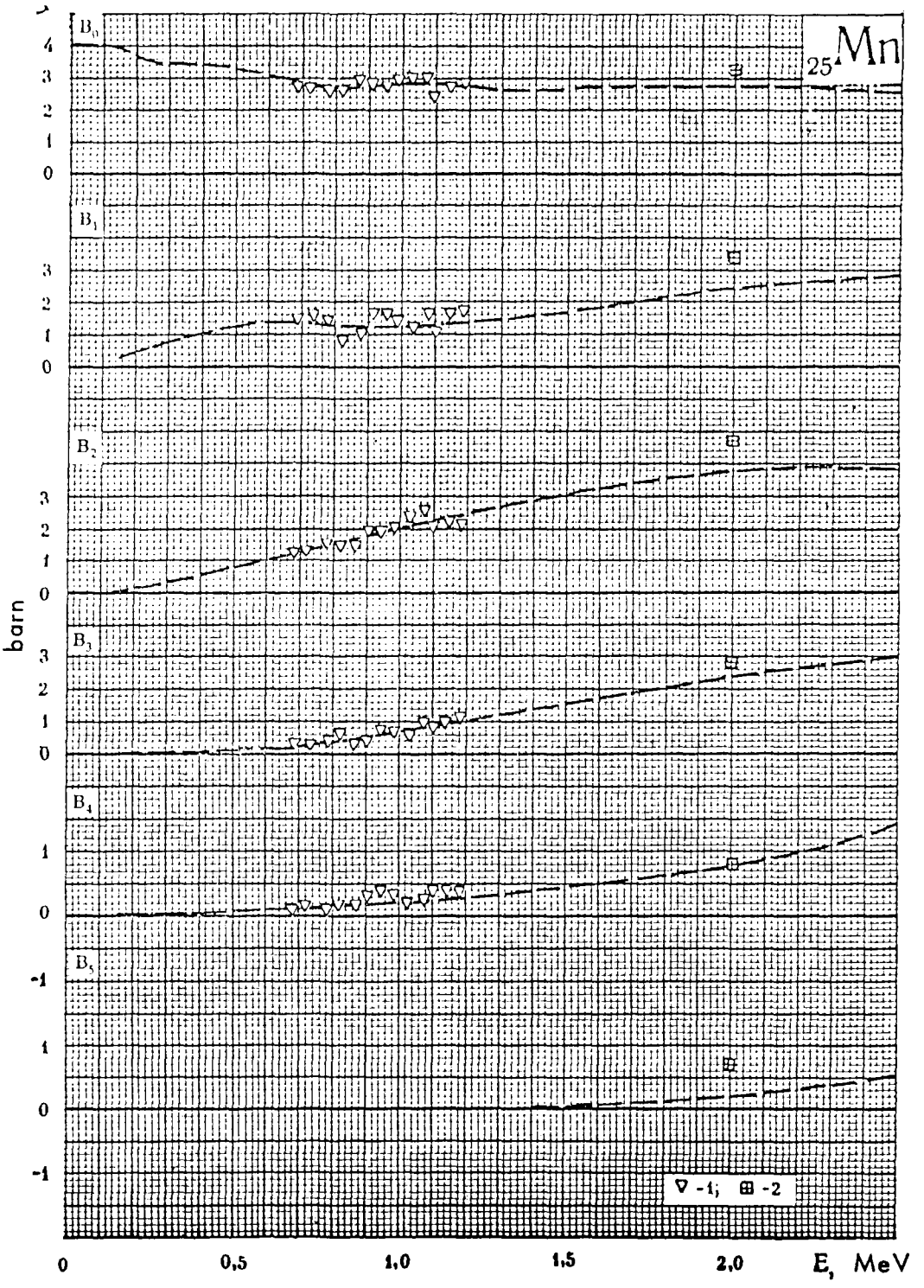
$_{25}$Mn
B_0
B_1
B_2
B_3
B_4
B_5
barn
∇ -1; ⊞ -2
0
0,5
1,0
1,5
2,0
E, MeV

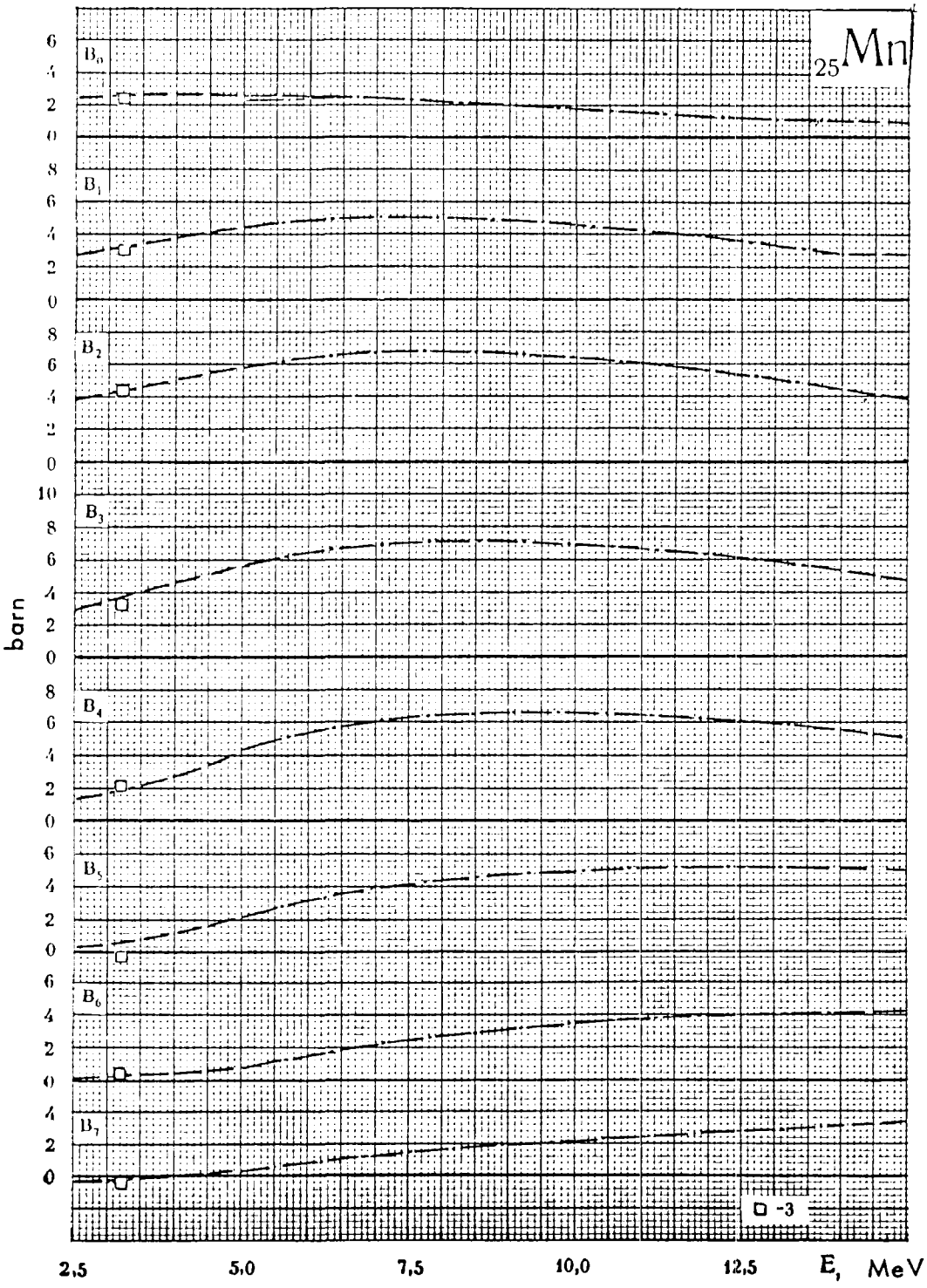
$_{25}$Mn
B_0
B_1
B_2
B_3
B_4
B_5
B_6
B_7
barn
□ -3
2,5
5,0
7,5
10,0
12,5
E, MeV

I R O N

In the energy range below 2.5 MeV many data agree satisfactorily. As in the case of chromium, the results by Smith /S-14/ and Langsdorf /L-2/ agree, on average, very well with the high resolution measurement by Cox /C-14/.

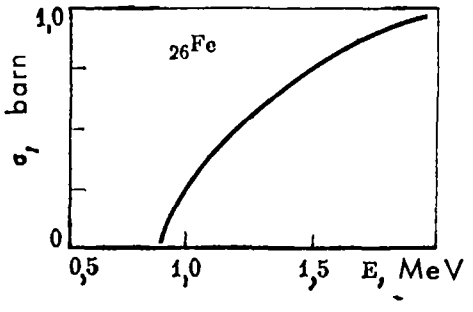

Figure 17 - Inelastic neutron cross-section of iron, used for correcting B_o .

The results by Langsdorf at energies below 0.2 MeV show a great influence of strong, low-lying resonances of iron which is caused by neutrons in the lower energy part of the resolution function. Therefore, we give the recommended curve of B_ℓ (E) only from this energy upwards. The irregularity of points of measurement by Landon /L-3/(1958), Cromberg /C-3/(1956), Salnikov /C-4/(1958) and Beyster /B-2/(1956) could, generally speaking, have been caused by resonance fluctuations : the minima at 2.2 and 2.35 MeV is in correlation with the minima of the total cross-section /13/. The same cause explains the scatter of the values of B_ℓ in the energy range 2.5 - 3 MeV. The discrepancy of the data in reference /B-13/ at 2 MeV and the data obtained in the measurements in the references /P-6/ and /G-3/ can not, however, be explained, since the energy resolution was about the same (100 keV) in all works.

In the high energy region the data by different authors also agree satisfactorily. An exception is the point at 6 MeV /W-12/, /W-13/ which deviates from the smooth energy dependence of B_ℓ . This irregular value is at variance with the total cross-section value as well as with the

value calculated by means of the optical model. We would like to mention that these latter results agree globally with the experimental data at the energies 5, 7 and 14 MeV. The calculated values of the total- and compound nucleus cross-section also agree rather well with the experimental data, on the basis of which we derived our recommended curve in the region 5 - 15 MeV. The values of high momenta are given in Table 19.

Table 19

Ref.	E.MeV	B_1	B_2	B_{10}	B_{11}
[H—2]	5,0	0,311	—	—	—
[B—2]	7,0	0,965	0,343	—	—
[2]	14	2,33	1,31	0,465	0,010

$_{26}$Fe

1 - [2]; [W— 4] — M. Walt (1954)
[L— 1] — G.N.Lovchikova (1957)
[G— 2] — W. B. Gilboy (1965)
[G— 1] — W. B. Gilboy (1962)
[D— 2] — S. E. Darden (1955)
2 — [2]; [W— 5] — M. Walt (1955)
3 — [2]; [M— 3] — C. O. Muehlhause (1956)
4 — [2]; [B— 2] — J. R. Beyster (1956)
5 — [2]; [C— 3] — L. Cranberg (1956)
6 — [2]; [E— 1] — J. O. Elliott (1956)
[Y— 1] — K. Yuasa (1958)
[A— 8] — J. D. Anderson (1958)
[C— 5] — J. H. Coon (1958)
[K— 1] — M.M.Khaletskii (1957)
7 — [L— 2] — A. Langsdorf (1957)
8 — [2]; [P — 1] — V.I.Popov (1957)
9 — [2]; [K— 4] — O.A. Kalnikov (1957)
10 — [2]; [L— 3] — H. H. Landon (1958)
11 — [2]; [P— 2] — M.V.Pasechnik (1958)
12 — [2]; [H— 2] — R. W. Hill (1958)
13 — [2]; [B— 7] — N. A. Bostrom (1959)
14 — [2]; [B— 7] — N. A. Bostrom (1959)
[M— 4] — M. K. Machwe (1959)
[T— 2] — K. Tsukada (1961)
15 — [2]; [L— 2] — G.N.Lovchikova (1960)
16 — [K— 4] — I.A. Korzh (1963)
17 — [C—14] — S. A. Cox (1963)
18 — [P— 5] — M.V.Pasechnik (1964)
19 — [S—14] — A. B. Smith (1964)
20 — [B—13] — D. J. Bredin (1964)
21 — [G— 2] — W. B. Gilboy (1965)
22 — [P— 6] — V.I.Popov (1965)
[K— 8] — L.Ya.Kazakova (1965)
23 — [2]; [W—12] - R. M. Wilenzick (1962)
[W—13] — R. M. Wilenzick (1965)
24 — [J — 1] — A. Jacquot (1966)
25 — [B—20] — R. L. Becker (1966)

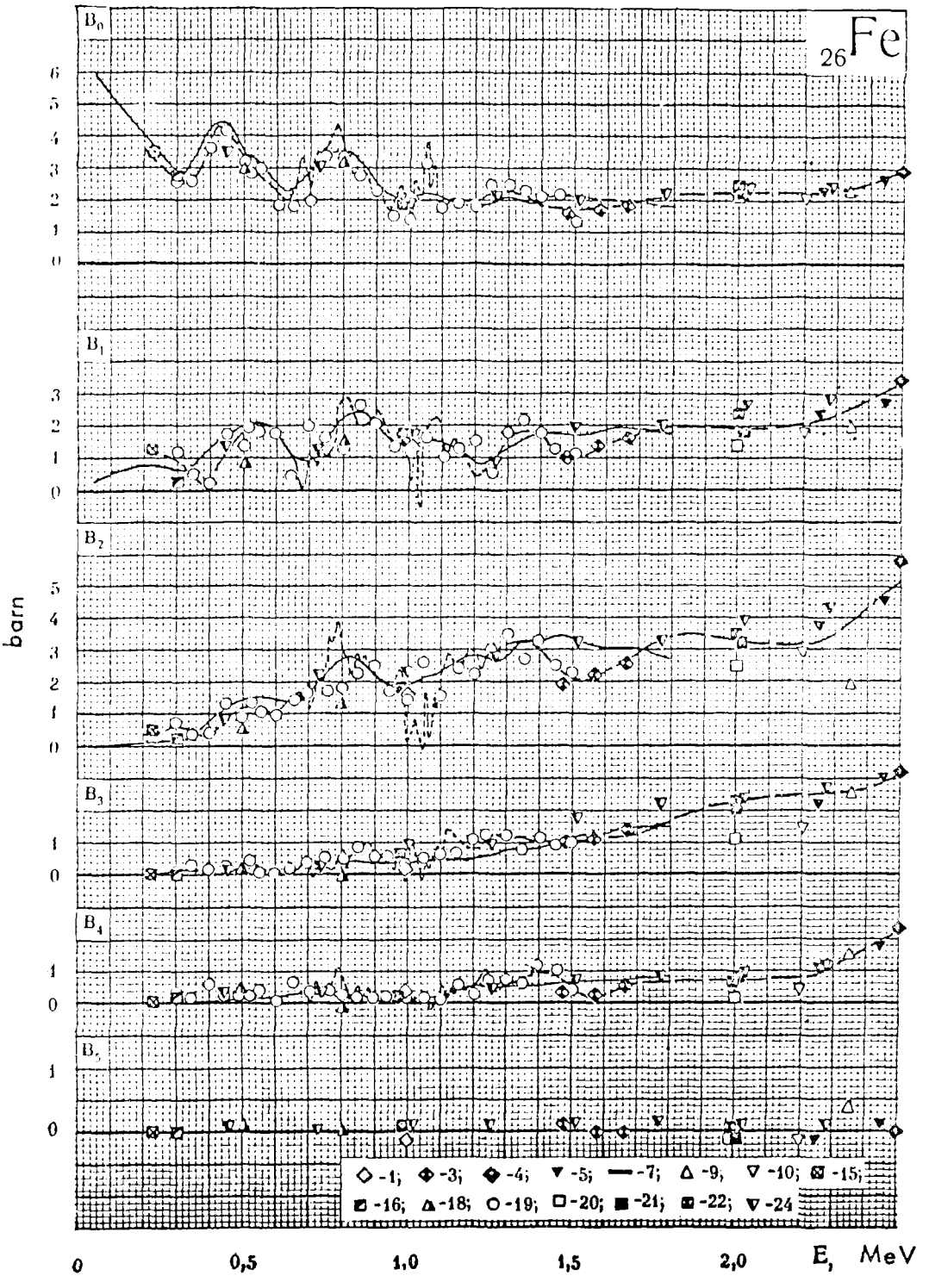
B_0
B_1
B_2
B_3
B_4
B_5
$_{26}$Fe
barn
E, MeV
0
0,5
1,0
1,5
2,0
◇-1; ◆-3; ◆-4; ▼-5; —-7; △-9, ▽-10; ⊠-15;
◩-16; ▲-18; ○-19; □-20; ■-21; ◙-22; ▼-24

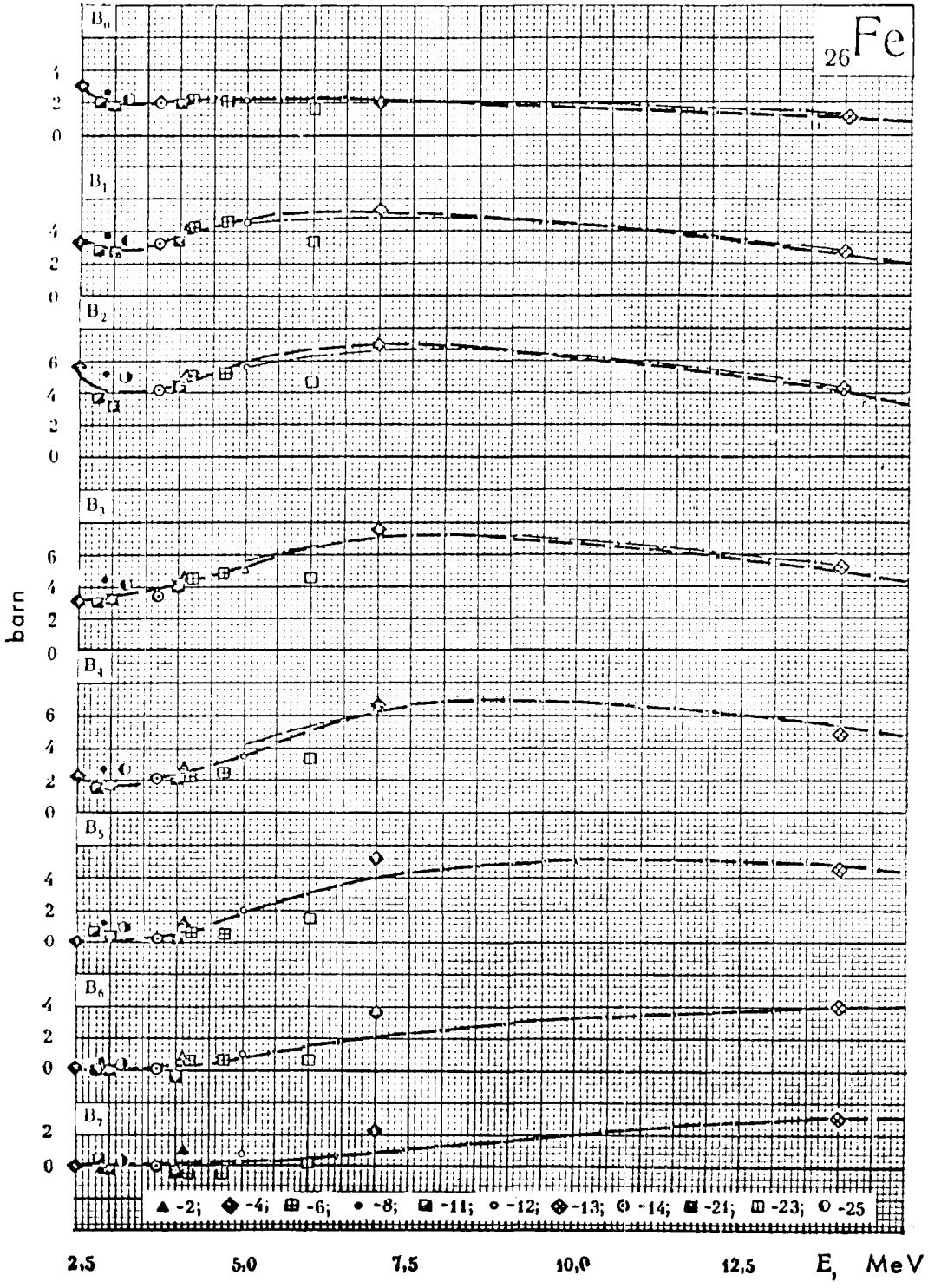
$_{26}$Fe
B_0
B_1
B_2
B_3
B_4
B_5
B_6
B_7
barn
▲ -2; ◆ -4; ⊞ -6; • -8; ■ -11; ○ -12; ◈ -13; ⊙ -14; ▣ -21; ⊡ -23; ○ -25
2,5
5,0
7,5
10,0
12,5
E, MeV

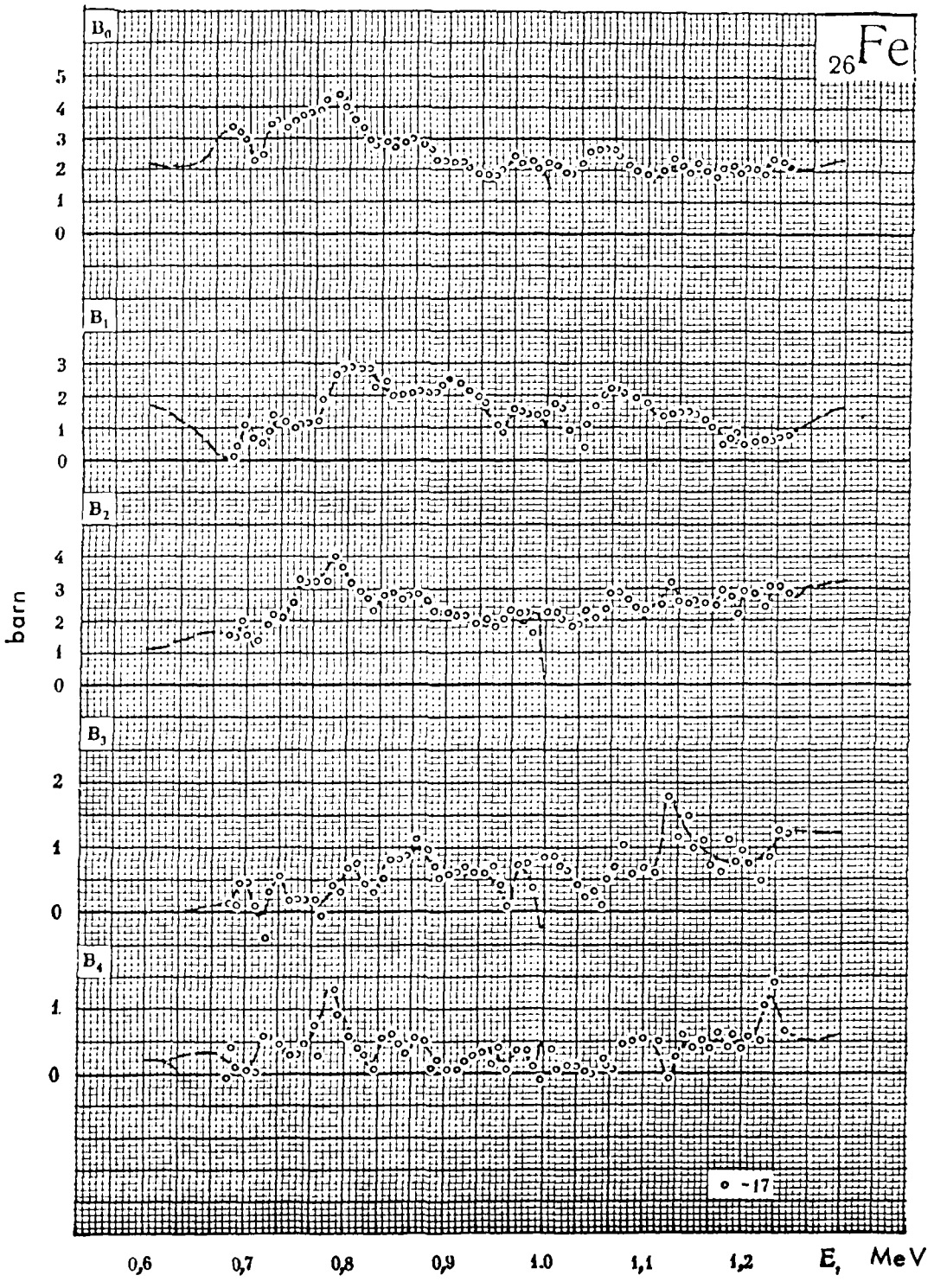
$_{26}$Fe
B_0
B_1
B_2
B_3
B_4
barn
0,6
0,7
0,8
0,9
1.0
1,1
1,2
E_n MeV
o -17

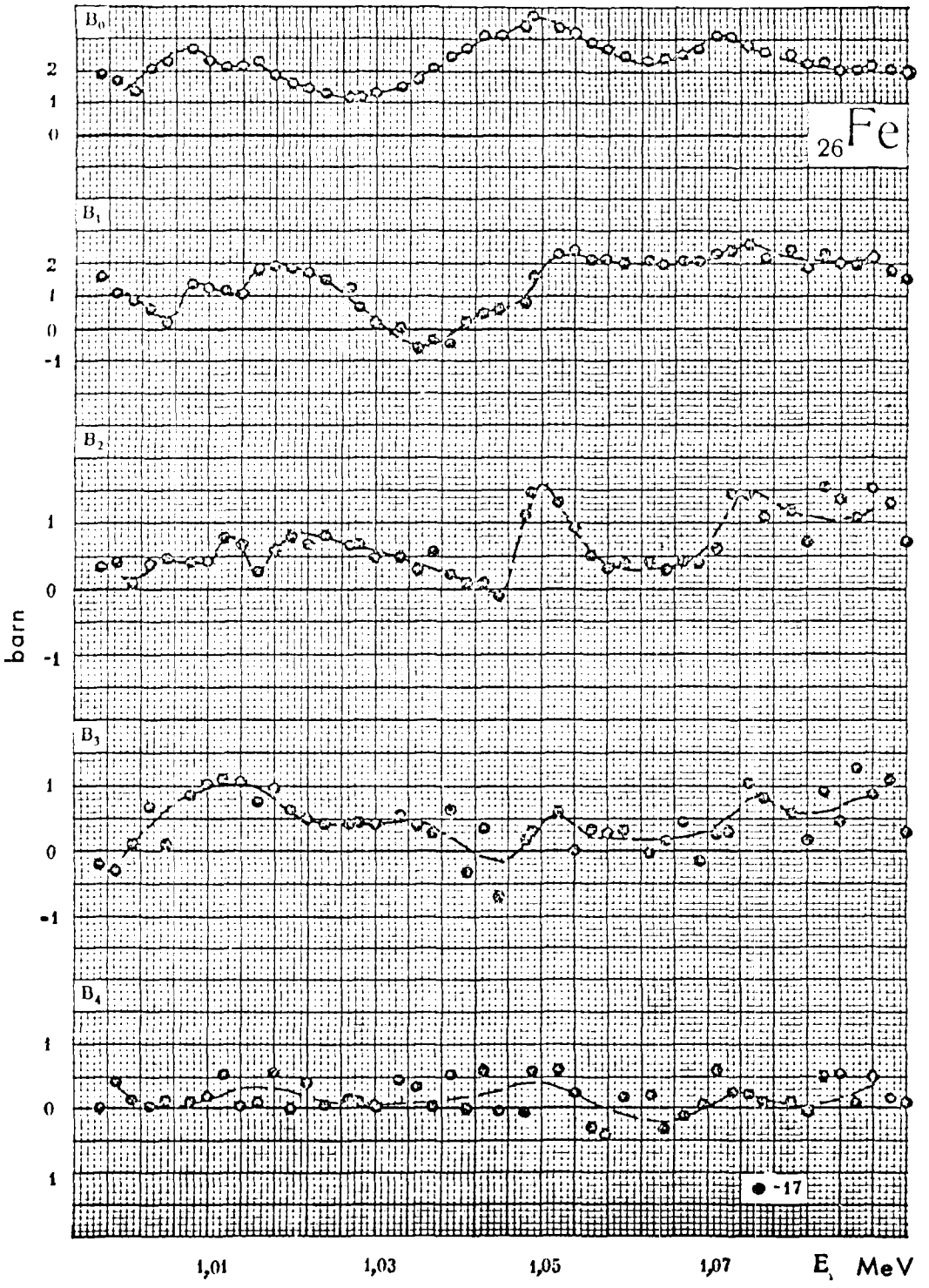
B_0
B_1
B_2
B_3
B_4
$_{26}Fe$
barn
2
1
0
-1
1
0
-1
1
0
-1
1
0
1
● -17
1,01
1,03
1,05
1,07
E_1 MeV

C O B A L T

At energies below 1.5 MeV the data by Cox /C-15/(1964) and Smith /S-14/(1964) agree very well between one another as well as with earlier measurements by Langsdorf /L-2/(1957) and Walt /W-4/(1954). The inelastic scattering cross-section, used for correcting B_o, is presented in Figure 18.

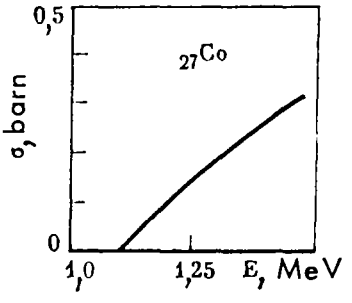

Figure 18 - Inelastic neutron scattering cross-section of cobalt, used for correcting B_o.

The energy dependence of B_l in the energy range from 1.5 - 4.0 MeV can be obtained by means of interpolation between the existing experimental values of references /S-14/(1.5 MeV), /B-13/(2 Mev) - the value of B_o in the latter work is, in fact, too high - /B-20/(3.2 MeV), /M-4/(3.7 MeV) and /G-2/(4 MeV). There is no reason to expect strong irregularities in the energy dependence of B_l in this region.

At energies higher than 5 MeV, a satisfactory estimation of the angular distribution results from the calculation of B_l using the optical model; the results of which fit well with the experimental data at energies of 3.7 and 4.0 MeV on one side, and at 14 MeV on the other. The calculated total cross-section also agrees well with the experimental data.

The values of the moments B_8, B_9, B_{10}, B_{11} and B_{12} at 14 MeV, calculated with the data of reference /P-2/ are : 1.89, 1.06, 0.443,

0.122 and 0.019 respectively.

$_{27}$Co

1 — [1]; [W — 4] — M. Walt (1954)
[L — 2] — A. Langsdorf (1957)
2 — [2]; [M — 4] — M. K. Machwe (1959)
3 — [2]; [P — 2] — C. St. Pierre (1959)
4 — [C — 15] — S. A. Cox (1964)
5 — [B — 13] — D. J. Bredin (1964)
6 — [S — 14] — A. B. Smith (1964)
7 — [G — 2] — G.V.Gorlov (1964)
[G — 3] — G.V.Gorlov (1965)
8 — [B — 20] — R. L. Becker (1966)
9 — [K — 9] — I.A.Korzh (1966)

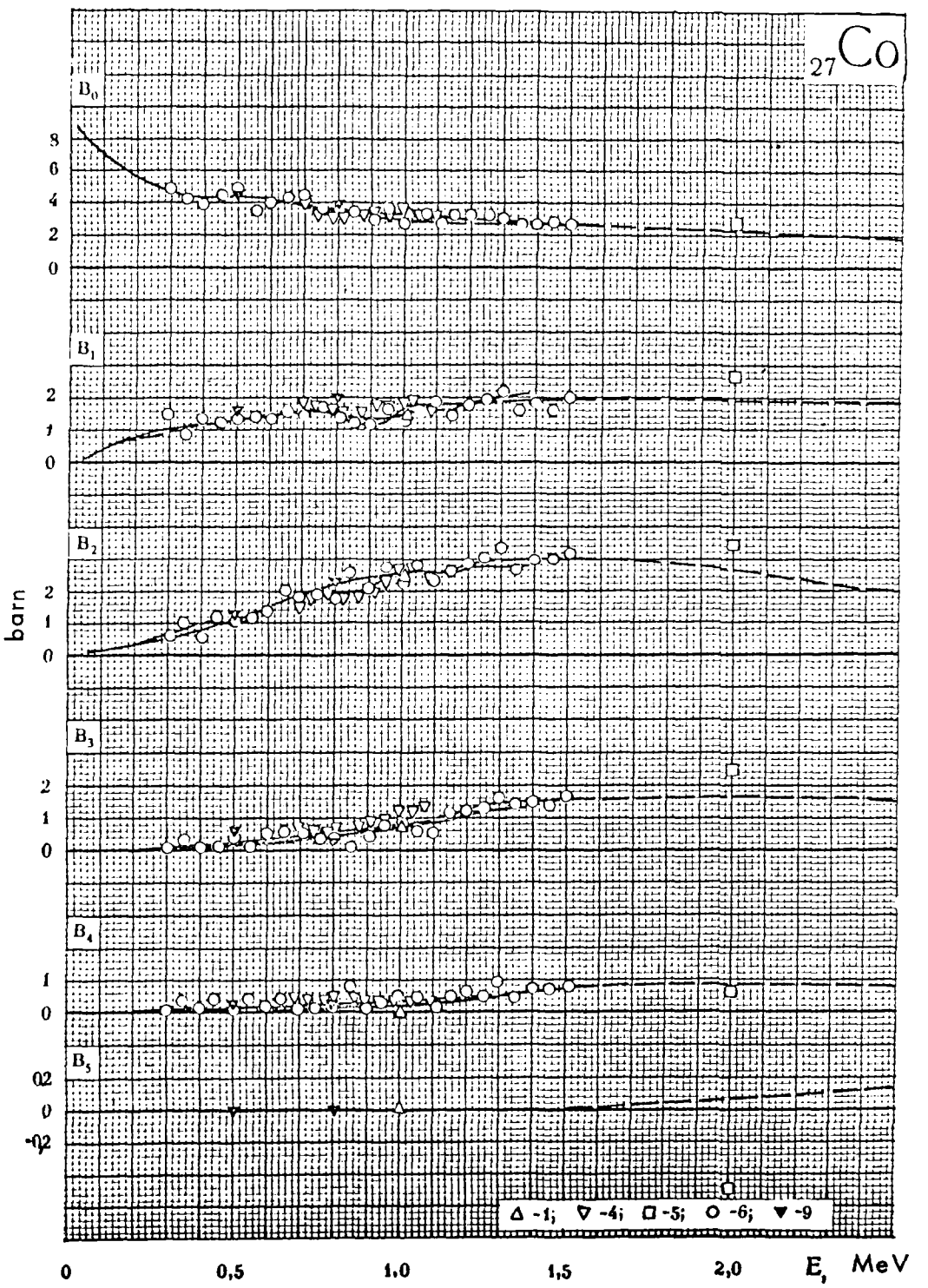
$_{27}$Co
B_0
8
6
4
2
0
B_1
2
1
0
B_2
2
1
0
barn
B_3
2
1
0
B_4
1
0
B_5
0,2
0
-0,2
Δ -1; ▽ -4; □ -5; ○ -6; ▼ -9
0
0,5
1,0
1,5
2,0
E_n MeV

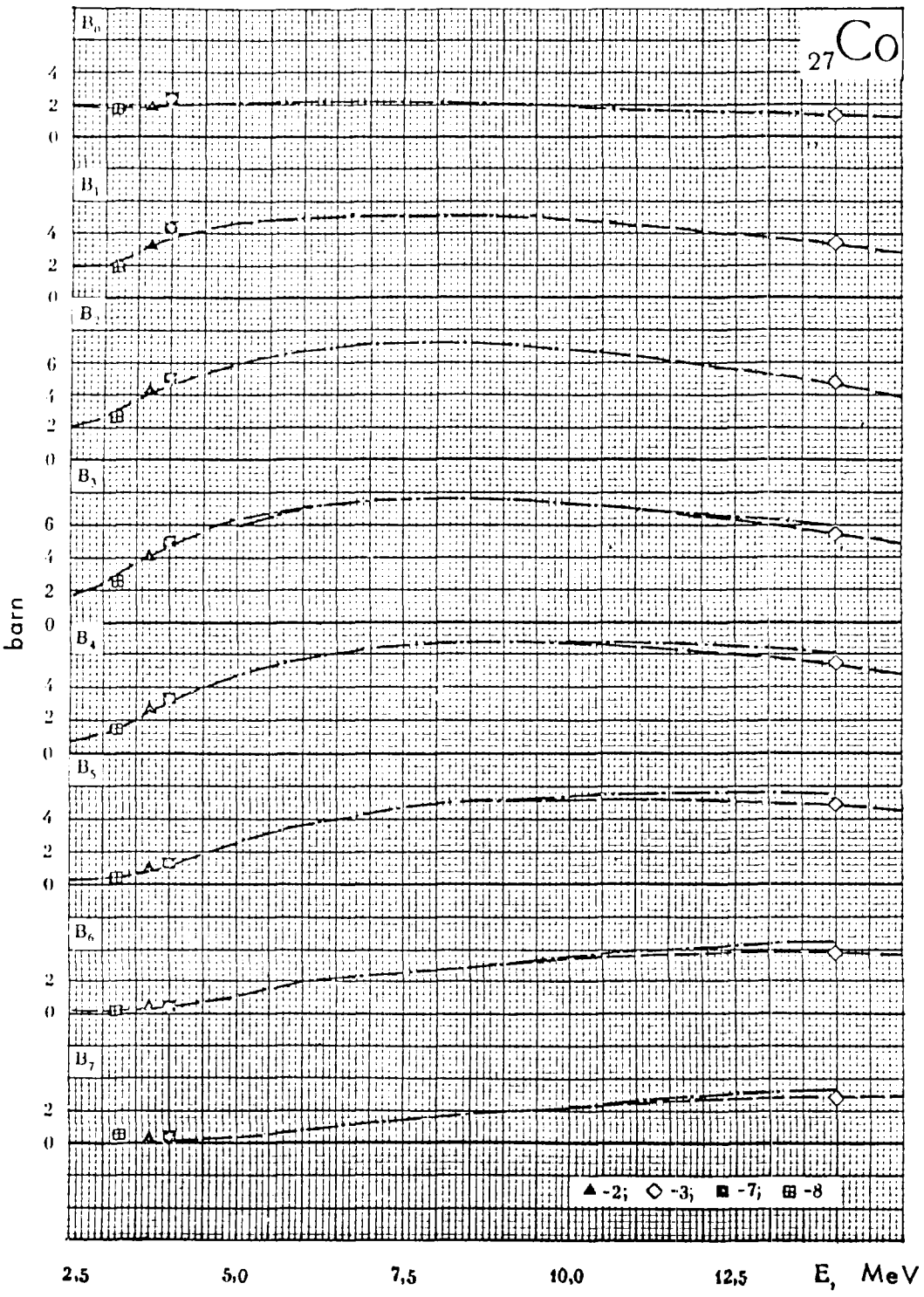
$_{27}$Co
B_0
B_1
B_2
B_3
B_4
B_5
B_6
B_7
barn
▲ -2; ◇ -3; ■ -7; ⊞ -8
2,5
5,0
7,5
10,0
12,5
E, MeV

N I C K E L

In the region below 1.5 MeV the experimental values of B_ℓ are considerably scattered, apparently owing to the resonance structure of the cross-section. There is, however, an indication that the results from different measurements are grouped around the values by Langsdorf et al. /L-2/ and measurements with high resolution, and deviate from them about equally on both sides. The agreement of these data with the difference $(\sigma_T - \sigma_{ne})$ is satisfactory up to 5 MeV.

In the energy interval 2 - 5 MeV experimental results, at six different energies, which can be used for an interpolation are available. However, the value obtained by Strishak et al. /C-8/(1960) at 2.9 MeV, deviates strongly from the general behaviour of B_ℓ. One of the reasons lies in the fact that the value of B_o is too low, it being equal to 1.2 barn in reference /C-8/. The value of the elastic scattering cross-section, estimated by subtracting the nonelastic cross-section from the total cross-section at 3 MeV, is equal to 2.2 barn. However, even by renormalising the data to a higher B_o value an essential difference remains between the values of B_2, B_3 and B_4 obtained by Strishak et al. and results of measurements at energies close to 2.9 MeV. The angular distribution at 5 MeV, measured by Hill /H-2/(1958), gives lower values than those resulting from optical model calculations. As in reference /C-8/, this difference is, to a certain extent, connected with the very low value of B_o (1.75 barn) obtained in reference /H-2/. The subtraction of the nonelastic cross-section from the total cross-section is equal to 2.2 barn at 5 MeV; which is in excellent agreement with the calculated value.

At 14 MeV the calculated value B_ℓ coincides with the data by Bauer /B-9/ and Clarke /C-19/. In the range from 5 to 14 MeV, no other data concerning angular distributions are available, except those obtained by optical model calculations. The energy dependence of B_o in this region is estimated by the difference $\sigma_T - \sigma_{ne}$.

The values of high momenta B_ℓ are given in Table 20.

Table 20

Ref.	E, MeV	B_s	B_p	B_{pp}	B_{pn}
[H—2]	5	0,314	0,048	—	—
[B—9]	14	2,49	1,54	0,696	0,215
[C—19]	14	2,22	0,959	0,468	—

$_{28}$Ni

1 — [2]; [W — 4] — M. Wall (1954)
[L — 3] — G.N.Lovchikova (1962)
2 — [L — 2] — A. Langsdorf (1957)
3 — [2]; [H — 2] — R. W. Hill (1958)
4 — [2]; [M — 4] — M. K. Machwe (1959)
5 — [2]; [S — 8] — V.I.Strizhak (1960)
6 — [B — 9] — R. W. Bauer (1963)
7 — [K — 4] — I.A. Korzh (1963)
8 — [K — 3] — I.A.Korzh (1963)
9 — [K — 5] — I.A.Korzh (1964)
10 — [S — 14] — A. B. Smith (1964)
11 — [P — 6] — V.I.Popov (1965)
[K — 8] — L.Ya.Kazakova (1965)
12 — [G — 3] — G.V.Gorlov (1965)
[G — 2] — G.V.Gorlov (1964)
13 — [C — 19] — R. L. Clarke (1967)
14 — [B — 20] — R. L. Becker (1966)

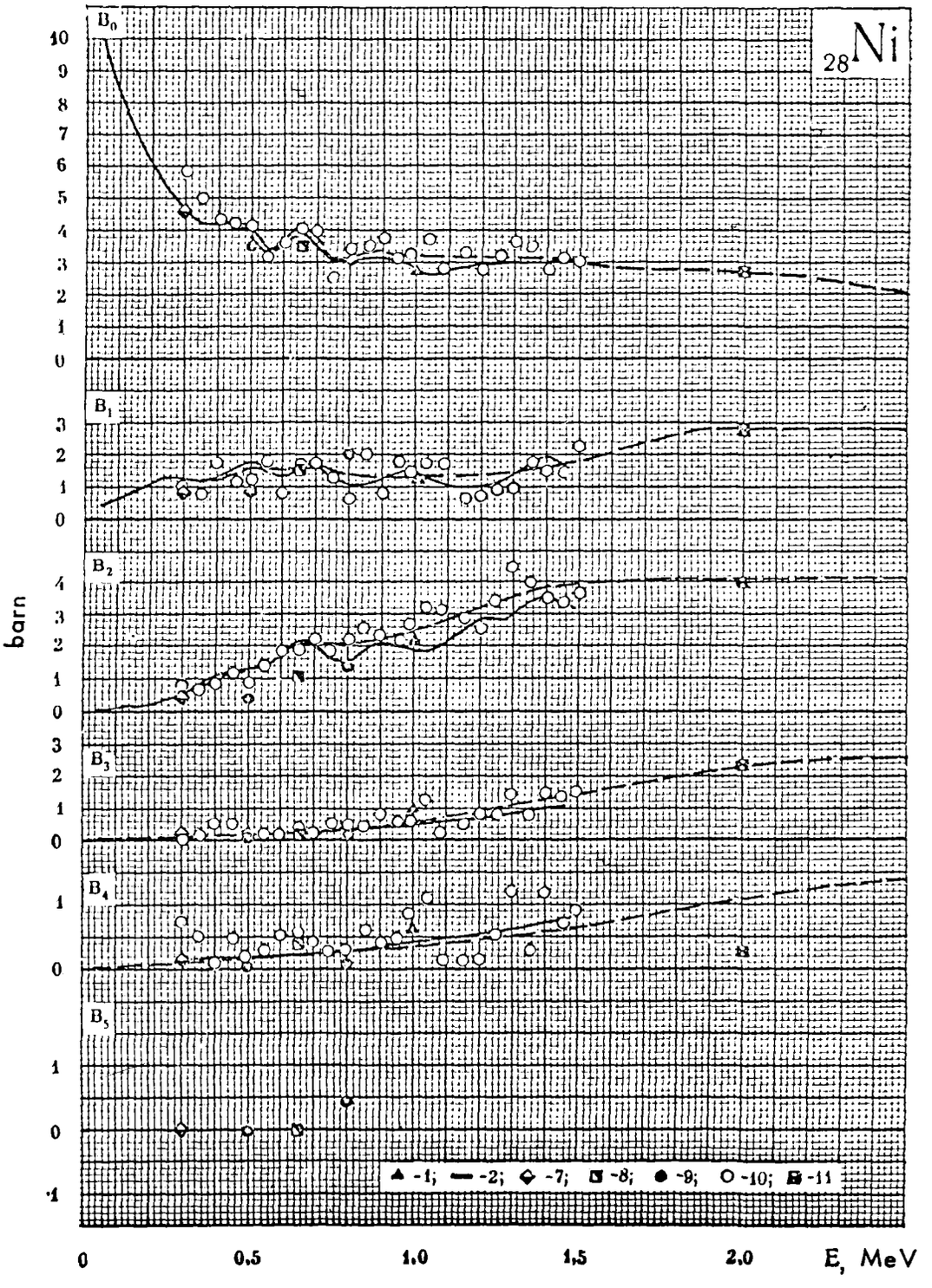
$_{28}$Ni
B_0
B_1
B_2
B_3
B_4
B_5
barn
E, MeV
0
0.5
1.0
1.5
2.0
▲ -1; — -2; ◆ -7; ■ -8; ● -9; ○ -10; ▣ -11

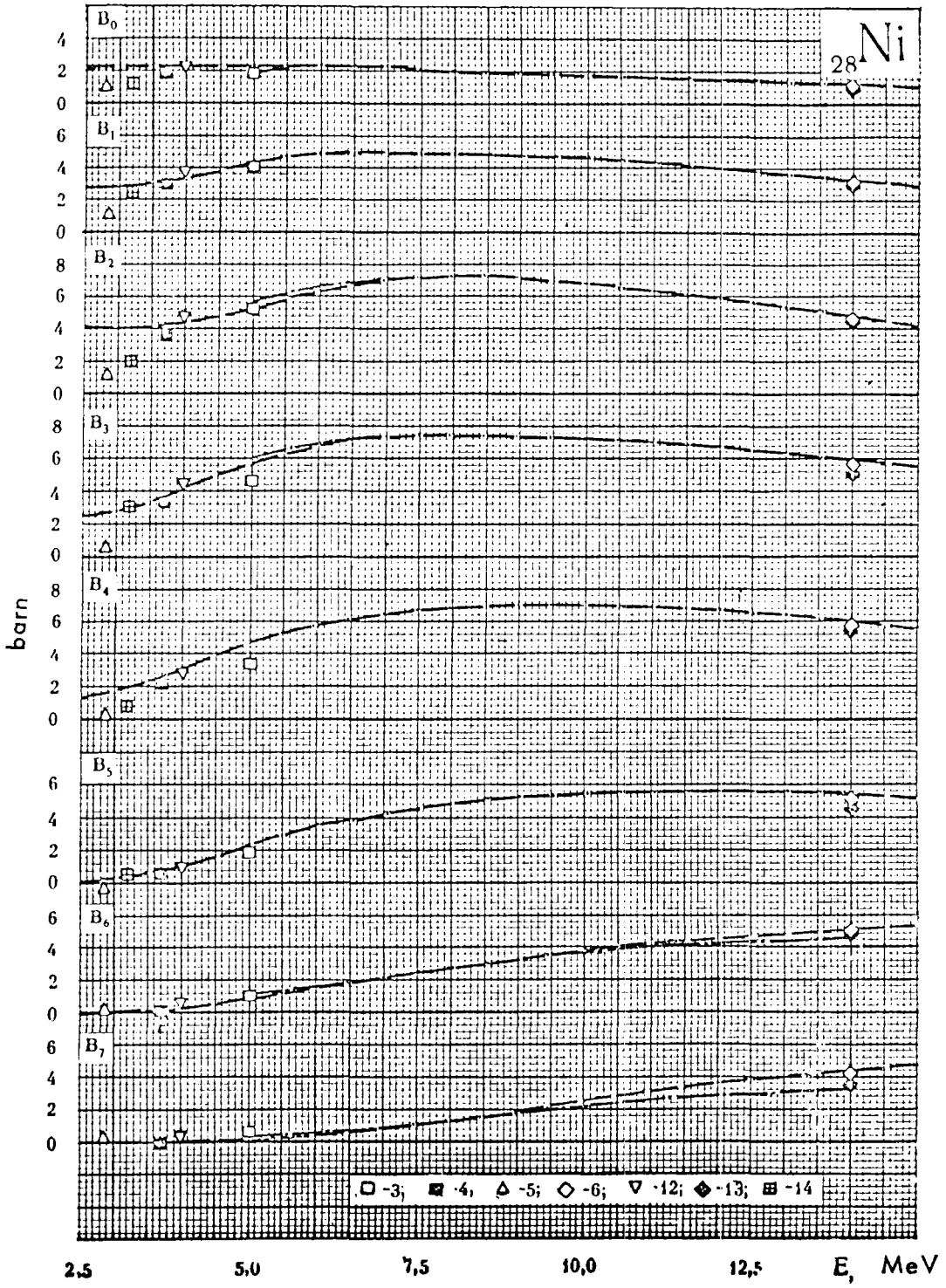
$_{28}$Ni
B_0
B_1
B_2
B_3
B_4
B_5
B_6
B_7
barn
-3; -4; -5; -6; -12; -13; -14
2,5
5,0
7,5
10,0
12,5
E, MeV

C O P P E R

The angular distribution of neutrons scattered on copper have been measured at many energy points below 5 MeV.

Below 1.5 MeV many values of B_ℓ are available from references /S-14/ and /L-6/, and they agree well, but are systematically higher than those of an earlier measurement by Langsdorf /L-2/. However, the difference is not great.

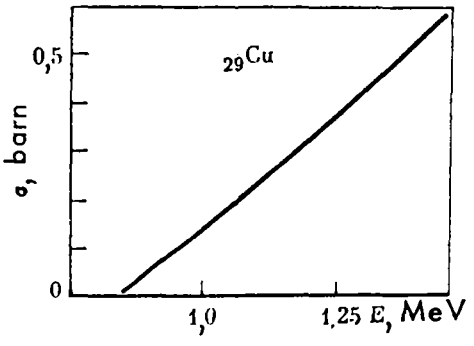

Figure 19 - Inelastic neutron scattering cross-section of copper, used for correcting B_o.

The correction for inelastic neutron scattering contribution was carried out using the values given in Figure 19. The results of different authors agree well on the whole below 2 MeV and describe the energy dependence of B_ℓ in a sufficiently well-defined manner.

In order to interpolate B_ℓ at higher energies, we assumed that the maxima at 2 and 2.5 MeV and the minima at 1.85 and 2.25 MeV (although they exceed - about twice - the experimental accuracy) of the experimental data are most likely due to inaccurate experimental results : the existence of such a structure appears to be unlikely.

The recommended values of B_ℓ are a little higher (up to 0.2 barn) at energies from 2 - 3.5 MeV, and lower (up to 0.2 barn) at energies from 3.5 to 5 MeV than the values $\sigma_T - \sigma_{ne}$ obtained from the available data. At higher energies we derived the curves B_ℓ (E) on the basis of the subtraction $\sigma_T - \sigma_{ne}$.

In the energy range between 5 and 14 MeV the angular distribution has not been measured. In determining the curves B_ℓ (E) ($\ell > 0$) we used the results calculated by means of the optical model, which agree well with the experimental data by Coon /C-5/, Anderson /A-9/ and Gyshovskii /G-1/ at 14 MeV, as well as with the experimental results in the range 4 - 5 MeV.

The values of the moments B_8, B_9, B_{10} and B_{11}, derived from the curves at 14 MeV given in BNL-400/2/ are : 3.02, 1.96, 0.945 and 0.302 barn.

$_{29}$Cu

1 — [2]; [W — 4] — M. Walt (1954)
[D — 1] — S. E. Darden (1954)
[R — 6] — D. Reitmann (1962)
2 — [2]; [R — 2] — A. E. Remund (1956)
3 [L — 2] — A. Langsdorf (1957)
4 — [2]; [P — 1] — V.I.Popov (1957)
5 — [2]; [P — 2] — M.V.Pasechnik (1958)
6 — [2]; [H — 2] — R. W. Hill (1958)
7 — [2]; [C — 5] — J. H. Coon (1958)
[B — 5] — S. Berko (1958)
[A — 9] — J. D. Anderson (1959)
[G — 1] — B.Ya.Gyzhovskii (1961)
8 — [2]; [M — 4] — M. K. Machwe (1959)
[B — 3a] — N. A. Bostrom (1956)
9 — [2^a]; [L — 6] — R. O. Lane (1961)
10 — [K — 5] — I.A.Korzh (1964)
11 — [S — 14] — A. B. Smith (1964)
12 — [P — 6] — V.I.Popov (1965)
[K — 8] — L.Ya.Kazakova (1965)
13 — [A — 12] — B. Antolkovic (1965)
14 — [B — 20] — R. L. Becker (1966)

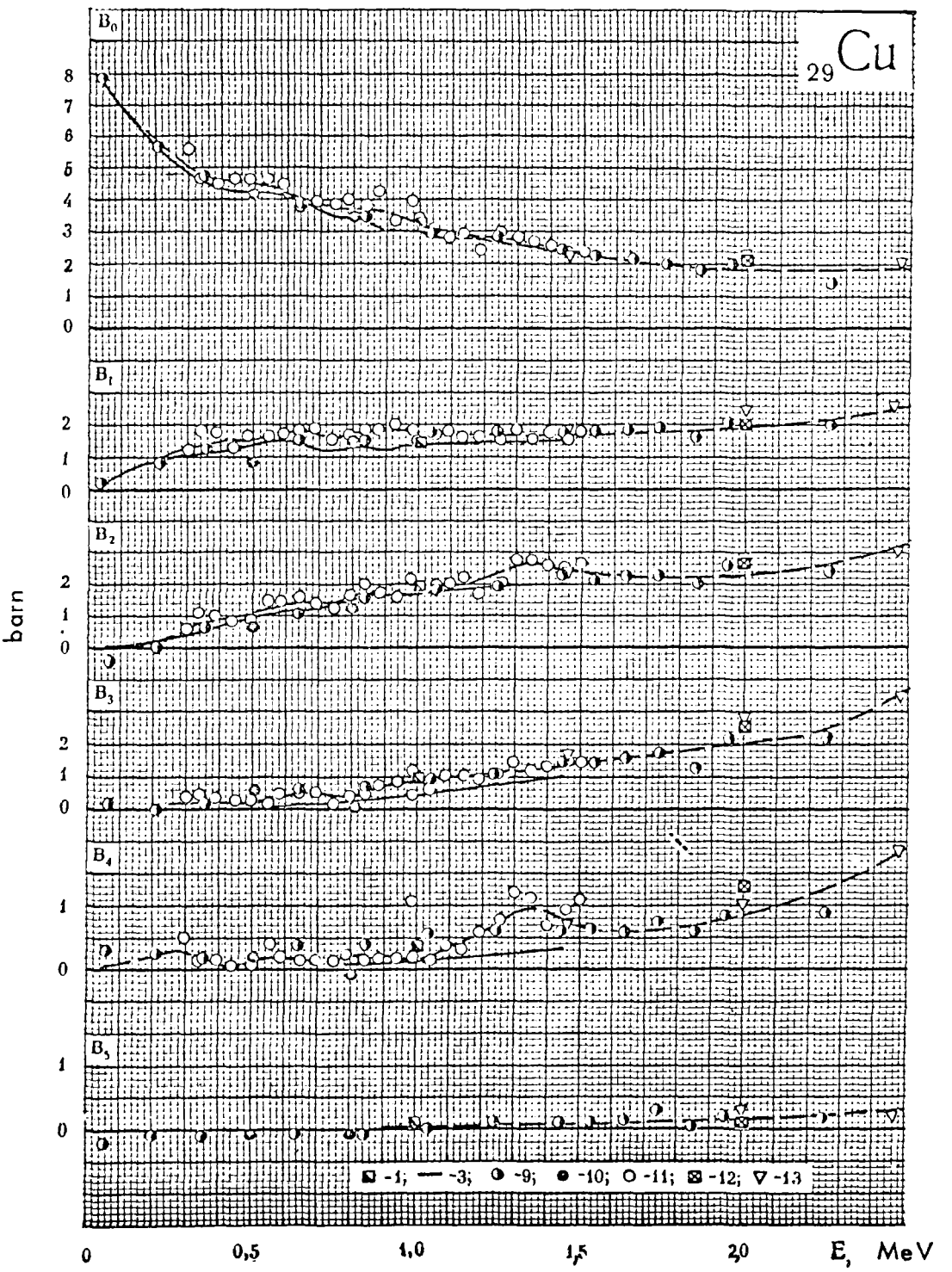
B_0
B_1
B_2
B_3
B_4
B_5
$_{29}$Cu
barn
E, MeV
0
0,5
1,0
1,5
2,0
-1; -3; -9; -10; -11; -12; -13

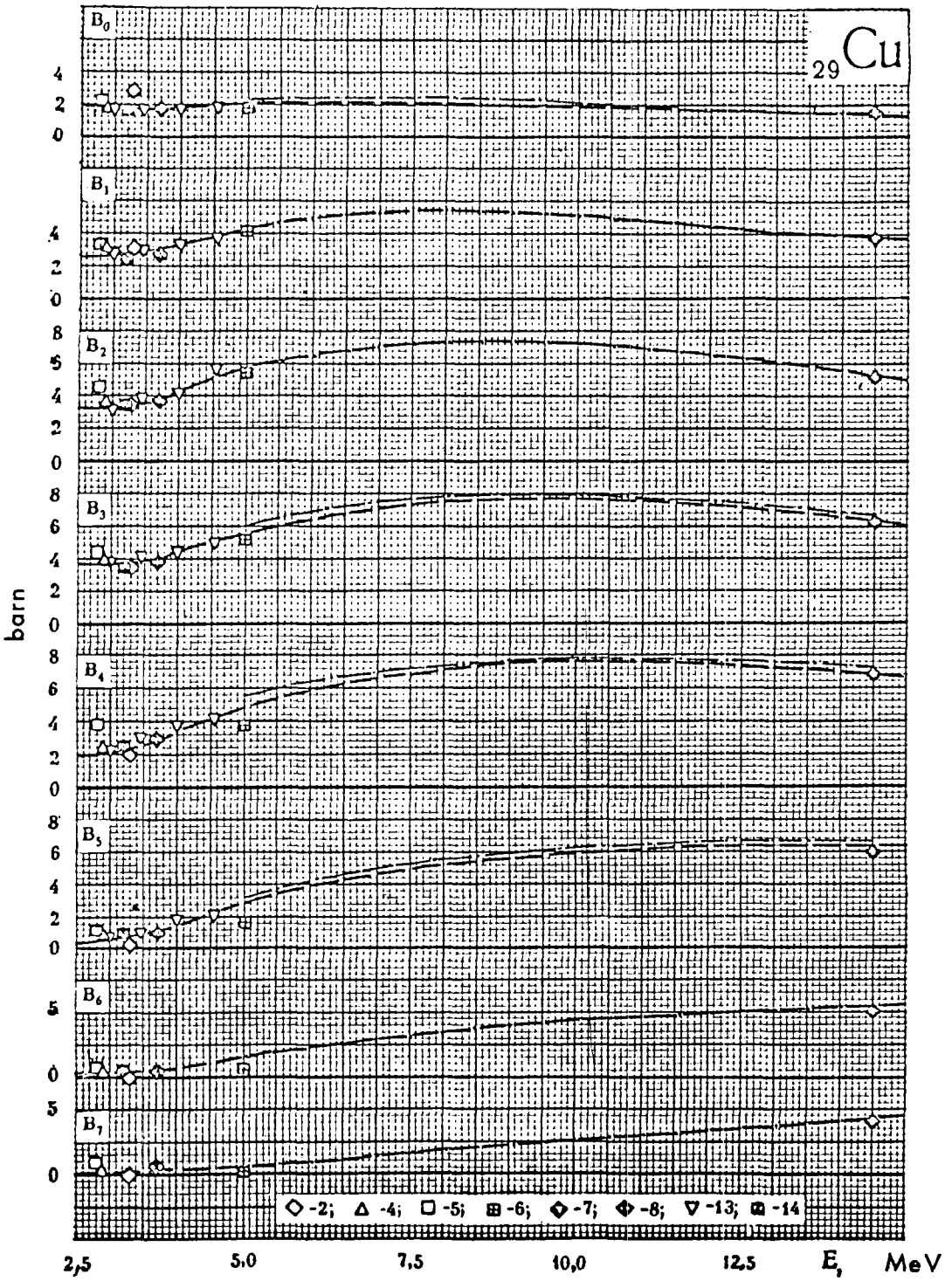
$_{29}$Cu
B_0
B_1
B_2
B_3
B_4
B_5
B_6
B_7
barn
2,5
5,0
7,5
10,0
12,5
E_γ MeV
◇ -2; △ -4; □ -5; ⊞ -6; ◈ -7; ◆ -8; ▽ -13; ⊠ -14

Z I N C

At energies below 1.5 MeV the great number of data available agree satisfactorily for the integrated scattering cross-section B_o. However, the values B_ℓ ($\ell > 0$), in particular B_1, have considerably strong differences. B_1, obtained in reference /S-14/ at energies below 1 MeV, are 20 - 30% higher than the data by Langsdorf /L-2/.

At energies lower than 1.5 MeV, where the inelastic cross-section is low (Figure 20), the curve of B_o agrees well with the total cross-section.

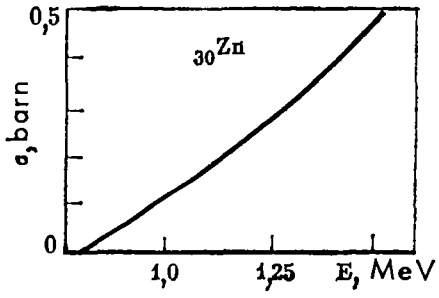

Figure 20 - Inelastic neutron scattering cross-section of zinc, used for correcting B_o.

In the interval 1.5 - 2.5 MeV the experimental values of B_o also agree well with the values of the difference $\sigma_T - \sigma_{ne}$.

In the range from 2.5 - 5 MeV one remarks the rather low values of B_ℓ obtained from the measurements by Tsukada /T-8/ and Tanaka /T-9/. The values of B_o from the latter work range from 1.0 to 1.1 barn in this region, while the values of B_o from the references /M-4/ and /W-5/ range from 1.9 to 2.0 barn : these are in agreement with the values obtained from the difference of the total cross-section minus the inelastic scattering cross-section (see reference /13/). The inelastic scattering cross-section presented in reference /T-8/ also deviates from the data given in reference /13/ by a factor of about 1.8 to 2.0 . As distinct from the other elements,

(Si, P and S), measured in references /T-8/ and /T-9/, the results for zinc obtained by these authors do not agree with the behaviour of the total cross-section. We wish to point out that the sum of elastic- and inelastic scattering cross-sections for aluminium, measured in /T-8/ and /T-9/, is also essentially lower than the total cross-section minus the cross-section of reactions with outgoing charged particles. In the case of aluminium, however, this difference is considerably lower (2 and 2.5 barn). In conclusion, we learned that multiplication, by a factor of 1.9, of all values of B_ℓ from the references /T-8/ and /T-9/ would allow them to coincide with the results of other authors : this confirms that the shape of the angular distribution obtained in these references is correct.

Apart from the above-mentioned discrepancies, the experimental results in the energy range from 1.5 to 5.0 MeV agree within the experimental error and fit sufficiently well to the results of the optical model calculation. In this connection, we wish to stress that the values obtained by optical model calculation are performed at 4 MeV, although the energy at which influence from compound nucleus scattering can be ignored is 5 MeV.

For zinc, the upper energy limit of 4 MeV at which 6 to 8 levels of its isotopes can be excited by inelastic scattering seems to us to be fully justified.

The values of high moments are given in Table 21.

Table 21

Ref.	E, MeV	B_8	B_9	B_{10}	B_{11}
[W—5]	4,1	0,492	0,299	0,144	—
[R—4]	14	3,57	2,40	1,35	0,496

$_{30}Zn$

1 — [2]; [*W* — 4] — M. Walt (1954)
2 — [2]; [*W* — 5] — M. Walt (1955)
3 — [*L* — 2] — A. Langsdorf (1957)
4 — [2]; [P — 2] — M.V.Pasechnik (1958)
5 — [2]; [*M* — 4] — M. K. Machwe (1959)
6 — [2]; [*R* — 4] — L. A. Rayburn (1959)
[*N* — 1] — H. Nauta (1958)
7 — [2]; [*T* — 8] — K. Tsukada (1962)
[*T* — 9] — S. Tanaka (1964)
8 — [P — 4] — V.I.Popov (1963)
9 — [*K* — 4] — I.A. Korzh (1963)
10 — [*K* — 3] — I.A.Korzh (1963)
11 — [P — 5] — M.V.Pasechnik (1964)
12 — [*C* — 15] — S. A. Cox (1964)
13 — [*S* — 14] — A. B. Smith (1964)
14 — [P — 6] — V.I.Popov (1965)
[*K* — 8] — L.Ya.Kazakova (1965)
15 — [Y — 1] — G.B.Yankov (1965)
[*K* — 1] — E.A.Koltypin (1962)
16 — [*B* — 20] — R. L. Becker (1966)

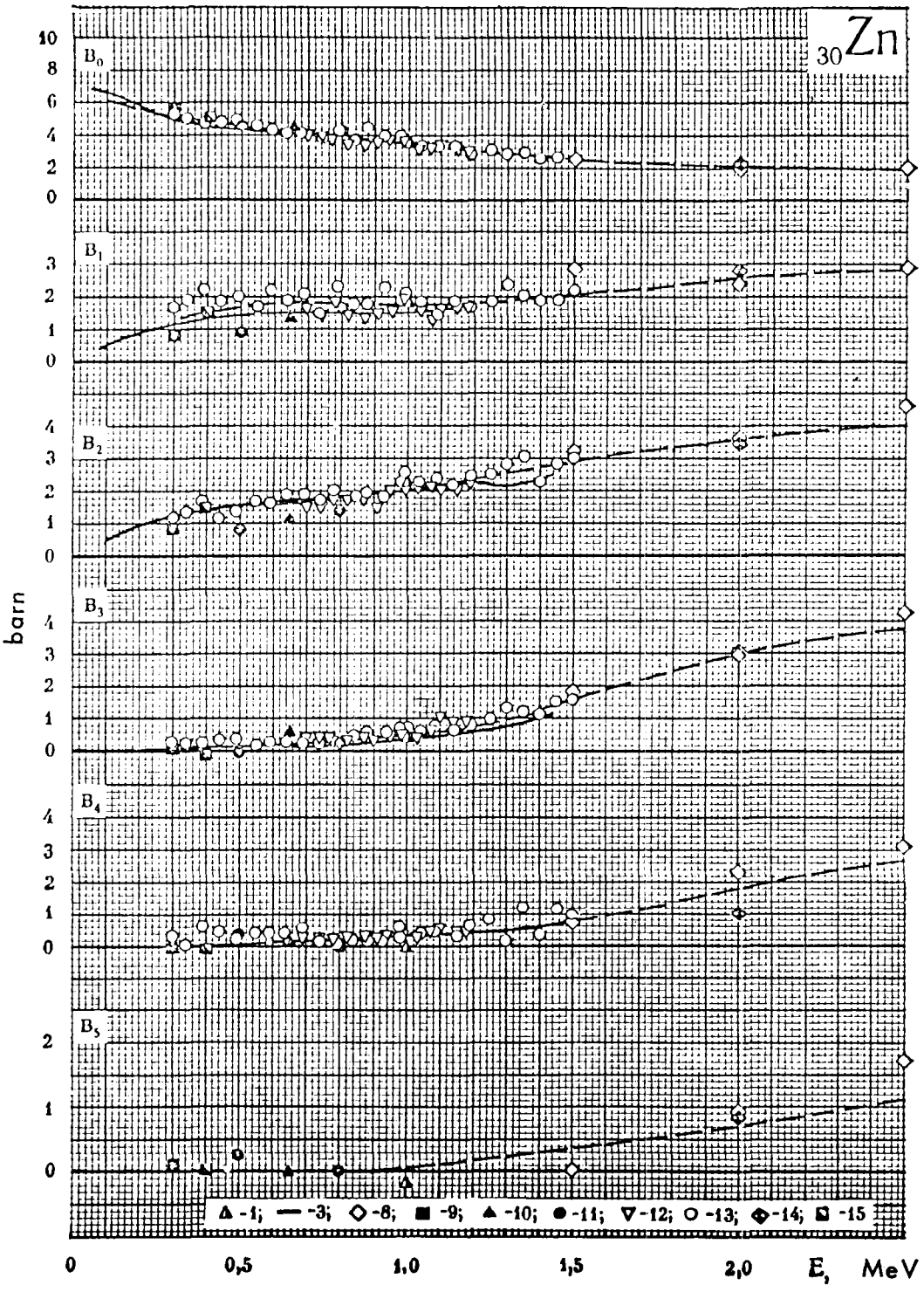
30Zn
B0
B1
B2
B3
B4
B5
barn
▲ -1; — -3; ◇ -6; ■ -9; ▲ -10; ● -11; ▽ -12; ○ -13; ◆ -14; ◘ -15
0
0,5
1,0
1,5
2,0
E, MeV

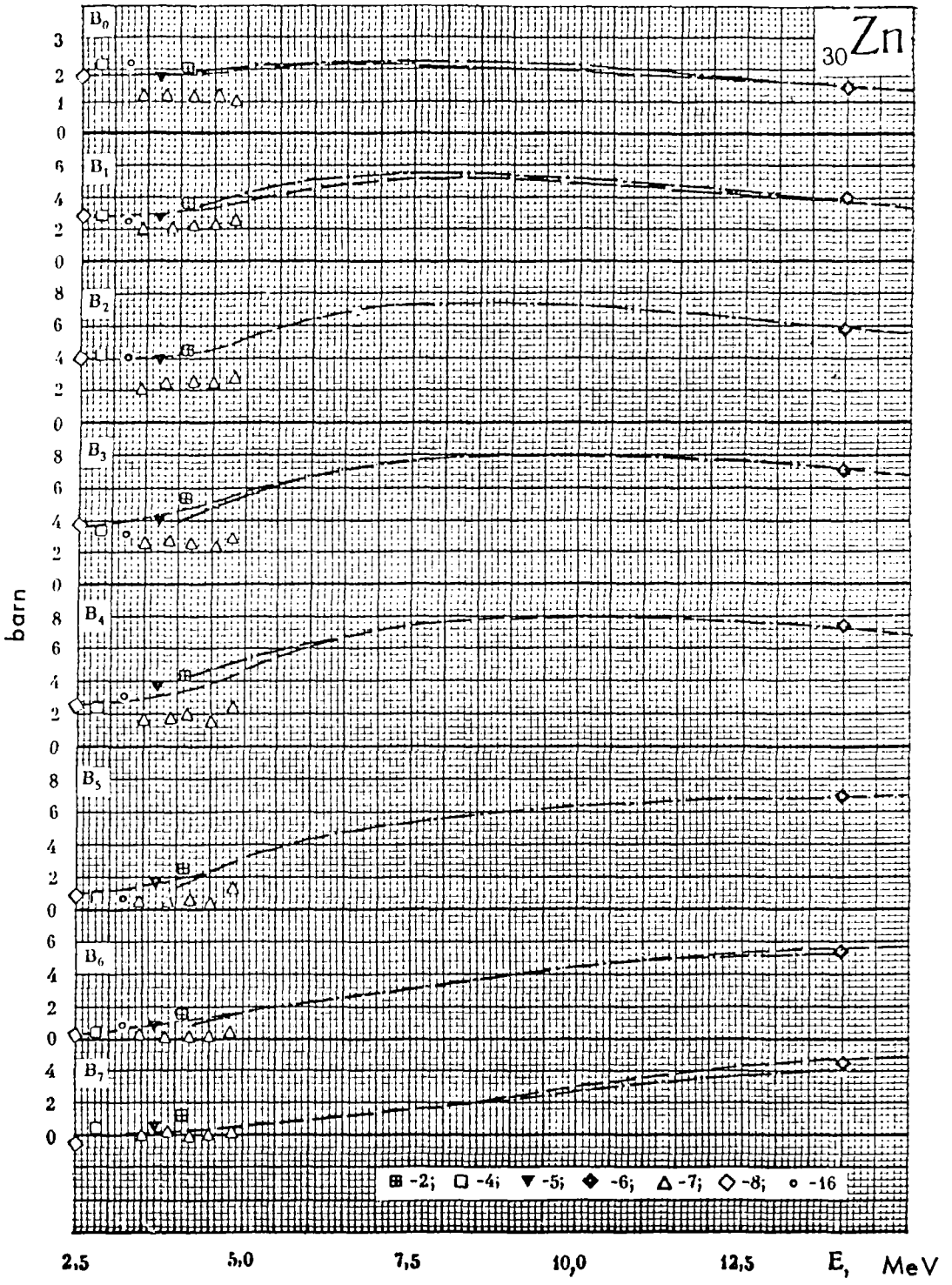
$_{30}Zn$
B_0
B_1
B_2
B_3
B_4
B_5
B_6
B_7
barn
⊞ -2; □ -4; ▼ -5; ◆ -6; △ -7; ◇ -8; ○ -16
2,5
5,0
7,5
10,0
12,5
E, MeV

Y T T R I U M

Data on angular distributions of neutrons scattered on yttrium are scarce. In the work by Bostrom et al. /B-6/(1959) the angular distributions at four energies between 1.45 and 4.7 MeV have been measured. At 1.45 MeV the integrated scattering cross-section obtained is equal to (3.50 ± 0.5) barn which is even a little lower than the value of B_o at 2.2 MeV given in reference /L-3/. This seems to be strange, since the total cross-section (see reference /13/), in passing from 1.5 to 2.2 MeV, decreases by about 1 barn and the increase of the inelastic cross-section should yield a still larger difference in the scattering cross-section at these energies.

At energies below 2 MeV the recommended curve $B_o(E)$ was derived from the available total cross-sections and by extrapolating to low energies, the values resulting from a subtraction of B_o from the total cross-section in the interval from 2 to 6 MeV. According to the available experimental data the mean cosine angular scattering is constant in the energy range from 1.5 to 2.5 MeV, and remains the same down to 0.8 MeV. But, then, the extrapolated values obtained from the available total cross-sections converge smoothly to a value of 0.0075 at an energy equal to zero. As a conclusion this yields unreliable recommended values at energies below 2 MeV.

At energies from 3.7 to 4.2 MeV the values of B_o in reference /B-6/ agree well with the data of reference /T-10/ and are about one-half of the total cross-section. The data of reference /W-13/ show a similar relation between the total cross-section and the elastic scattering cross-section at 6 MeV. The value at 4.7 MeV, which is equal to 2.9 barn /B-6/ is, therefore, too high. The other values of B_ℓ ($\ell > 0$) are approximately the same factor too high at this energy.

The optical model calculations fit rather well to the experimental values which are available for energies from 4 - 5 MeV.

The values of the moments B_8 and B_9 at 6 MeV, obtained from

the results of the references /W-12/ and /W-13/, are : 0.192 and -0.264 barn, respectively.

$_{39}Y$

1 — [2]; [*L* — 3] — H. H. Landon (1958)
2 — [2]; [*B* — 6] — N. A. Bostrom (1959)
3 — [2]; [*W* — 12] — R. M. Wilenzick (1962)
[*W* — 13] — R. M. Wilenzick (1965)
4 — [*T* — 10] — J. H. Towle (1965)
5 — [*B* — 20] — R. L. Becker (1966)
6 — [P — 7] — V. I. Popov (1966)

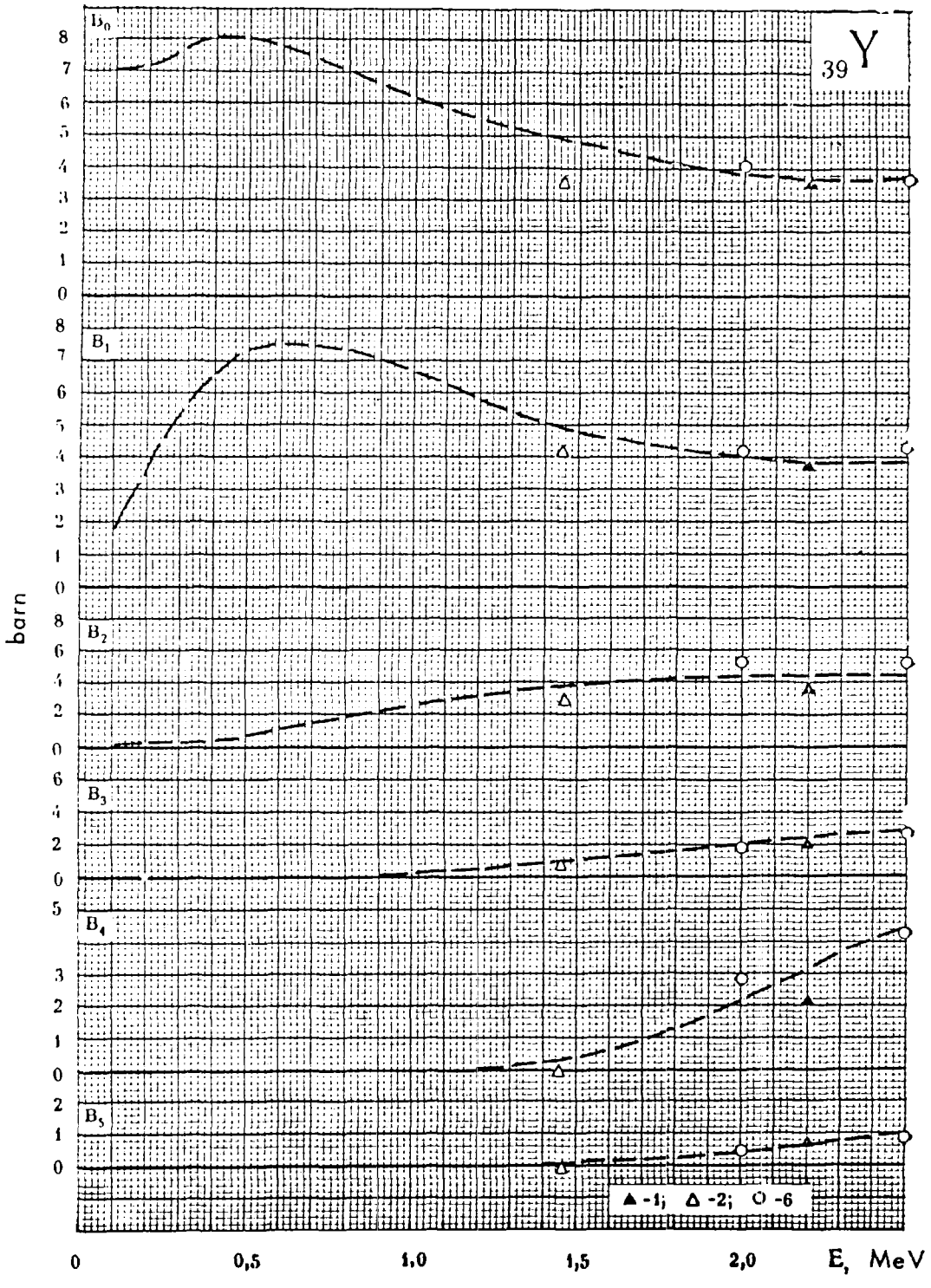
B_0
B_1
B_2
B_3
B_4
B_5
39 Y
barn
▲ -1; Δ -2; O -6
0
0,5
1,0
1,5
2,0
E, MeV

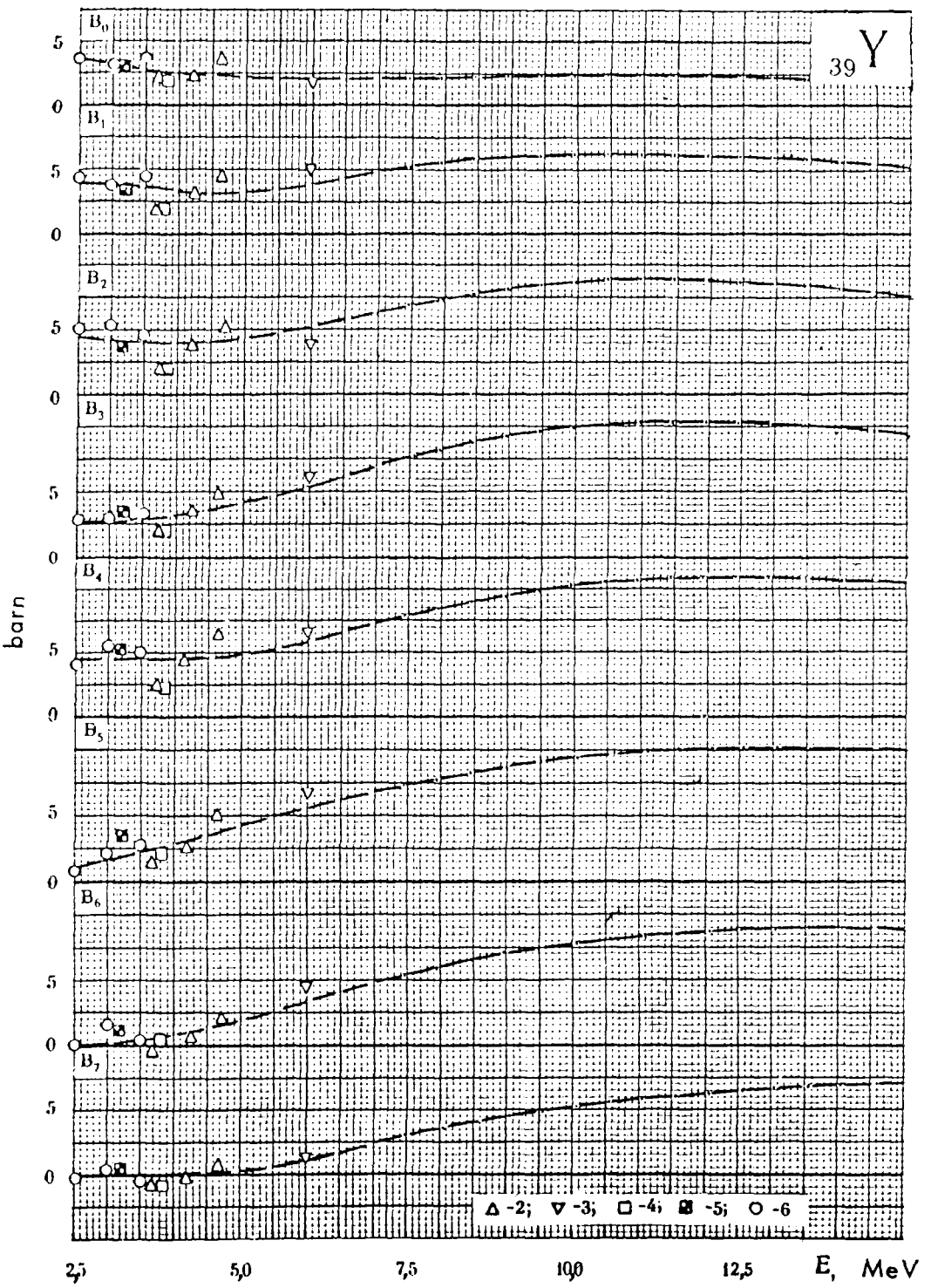
39 Y
B0
B1
B2
B3
B4
B5
B6
B7
barn
5
0
2,5
5,0
7,5
10,0
12,5
E, MeV
△ -2; ▽ -3; □ -4; ▩ -5; ○ -6

Z I R C O N I U M

At energies below 1 MeV the results obtained by using the time-of-flight method /S-14/ are systematically higher than those obtained by Langsdorf /L-2/ and the data by Korsch /K-3, K-7/, Yankov and Koltipin /Ya-1, K-1/ which all agree well with those measured by Langsdorf. The total cross-sections at energies below 1 MeV, where inelastic scattering is not essential (Figure 21), lie between the data of references /S-14/ and /L-2/ on which we relied when deriving the recommended curve. The minimum of B_o at 0.85 MeV coincides with the minimum of the total cross-section. In the range 1 - 1.5 MeV, where the values of B_o from reference /L-2/ are corrected for inelastic scattering, the difference between the results of reference /S-14/ and those of other authors diminish considerably.

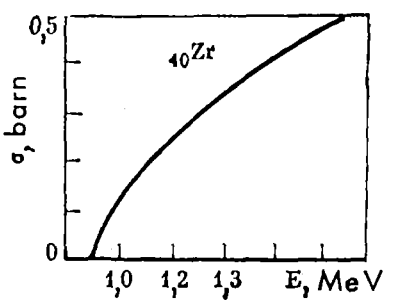

Figure 21 - Neutron inelastic scattering cross-section, used for correcting B_o.

The cross-section of the compound nucleus reaction, obtained by optical model calculation describes the available inelastic scattering data well from 8 MeV upwards. In this region they agree well with the experimental data and the total cross-section. In the region 1 - 8 MeV the calculated total cross-section is about 0.5 barn lower than the experimental value, but the cross-section for the compound nucleus reaction is higher than the inelastic scattering cross-section. One can, therefore, by means of the calculated values recommend the angular distribution only from 8 MeV onwards. We have used these data from 7 MeV onwards in

order to see how closely the calculated results agree with the available experimental data. The comparison at 7 MeV with the value from /B-2/ shows that the fit is sufficiently good. At 14 MeV, however, the calculated values of B_ℓ are considerably higher than the experimental values /C-19, A-8/. At the same time, the calculated value of $B_o = 2.14$ barn is in excellent agreement with the difference of $\sigma_T - \sigma_{in} \sim (2.3 \pm 0.2)$ barn, obtained from several measurements compiled in reference /3/.

The elastic scattering cross-section at 2 MeV, obtained in references /P-6, K-8/, is a little high. At energies from 3 to 5 MeV the value of B_o lies systematically 0.2 - 0.3 barn below the value resulting from the subtraction of the nonelastic cross-section from the total cross-section. At 7 MeV the value of this deviation amounts to 0.4 barn, and at 14 MeV to about 0.5 barn. Possible reasons for this discrepancy are discussed in detail in reference /W-14/ in which the neutron elastic scattering angular distribution of niobium is measured. The observed discrepancy is explained by the fact that the direct inelastic processes, which do not lose much energy are, in the nonelastic cross-section, measured by the sphere-transmission-technique, usually not taken into account.

This explanation might be correct. If one assumes this, then it follows that the inelastic cross-section should also increase at lower energies (although to a lesser degree) so that one obtains agreement between B_o and the values obtained from the subtraction of the inelastic cross-section from the total cross-section.

The values of high moments are given in Table 22.

Table 22

Ref.	E, MeV	B_8	B_9	B_{10}	B_{11}
[B—19]	5	0,575	0,982	0,689	0,230
[B—6]	7	0,867	—	—	—
[A—6, A—8, C—19]	14,1	3,15	1,75	0,973	0,280

$_{40}Zr$

1 — [2]; [*W* — 4] — M. Walt (1954)
[*G* — 1] — W. B. Gilboy (1962)
[*R* — 7] — D. Reitman (1963)
[*D* — 1] — S. E. Darden (1954)
2 — [2]; [*W* — 5] — M. Walt (1955)
3 — [2]; [*B* — 2] — J. R. Beyster (1956)
4 — [2]; [*A* — 6] — S. H. Ahn (1957)
[*A* — 9] — J. D. Anderson (1959)
[*C* — 19] — R. L. Clarke (1967)
5 — [*L* — 2] — A. Langsdorf (1957)
6 — [2]; [*B* — 6] — N. A. Bostrom (1959)
7 — [2]; [*B* — 6] — N. A. Bostrom (1959)
[*K* — 2] — D. W. Kent (1962)
[*H* — 1] — H. S. Hans (1957)
8 — [2]; [S — 8] — V.I.Strizhak (1960)
9 — [*K* — 3] — I.A. Korzh (1963)
10 — [*K* — 7] — I.A.Korzh (1964)
11 — [*S* — 14] — A. B. Smith (1964)
[*R* — 7] — D. Reitman (1963)
12 — [P — 5] — M.V.Pasechnik (1964)
13 — [Y — 1] — G.B.Yankov (1965)
[*K* — 1] — E.A.Koltypin (1962)
14 — [P — 6] — V.I.Popov (1965)
[*K* — 8] — L.Ya.Kazakova (1965)
15 — [*B* — 20] — R. L. Becker (1966)
16 — [*B* — 19] — S. G. Buccino (1966)

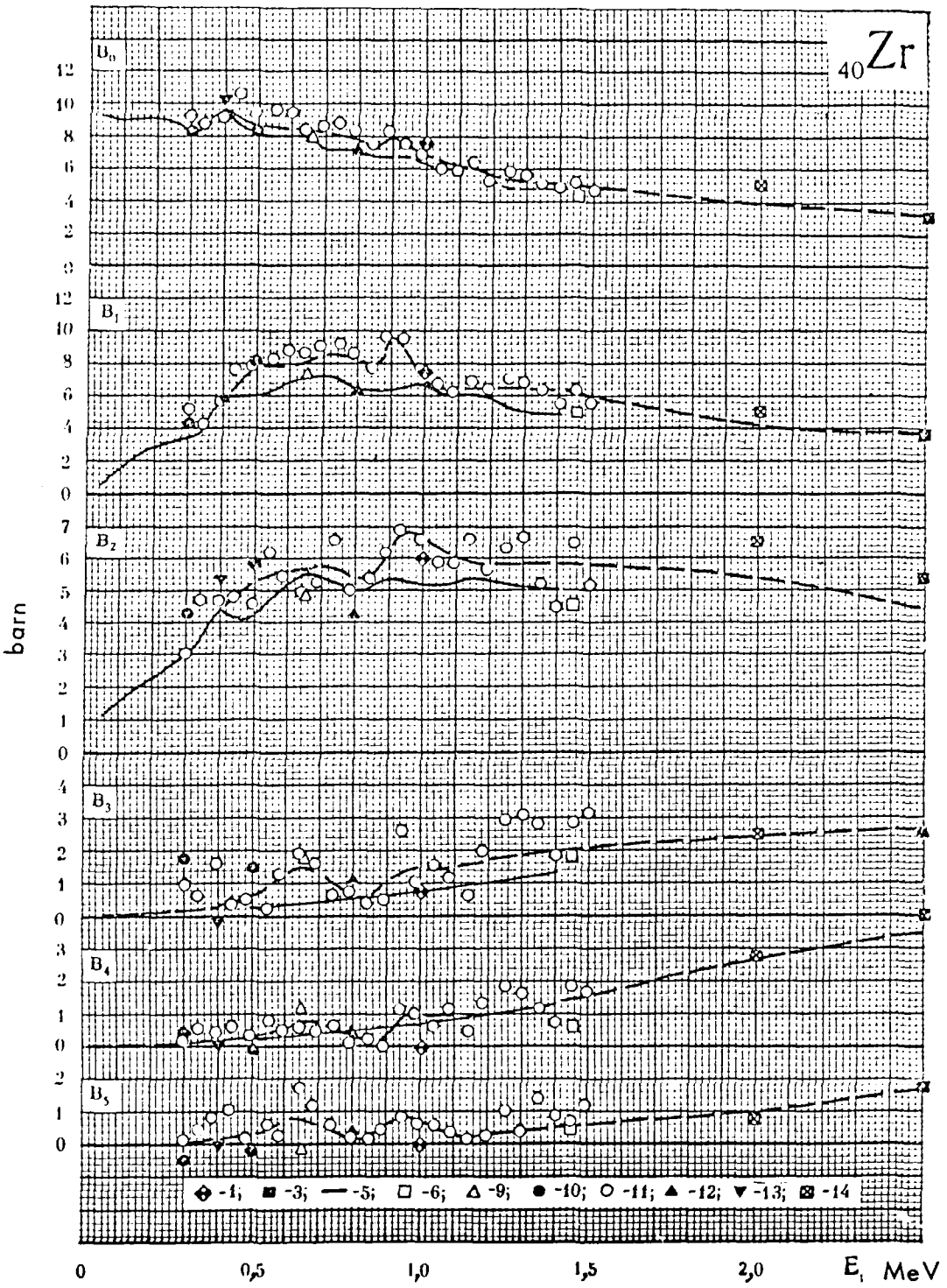
$_{40}Zr$
B_0
B_1
B_2
B_3
B_4
B_5
barn
-1; -3; -5; -6; -9; -10; -11; -12; -13; -14
0
0,5
1,0
1,5
2,0
E_1, MeV

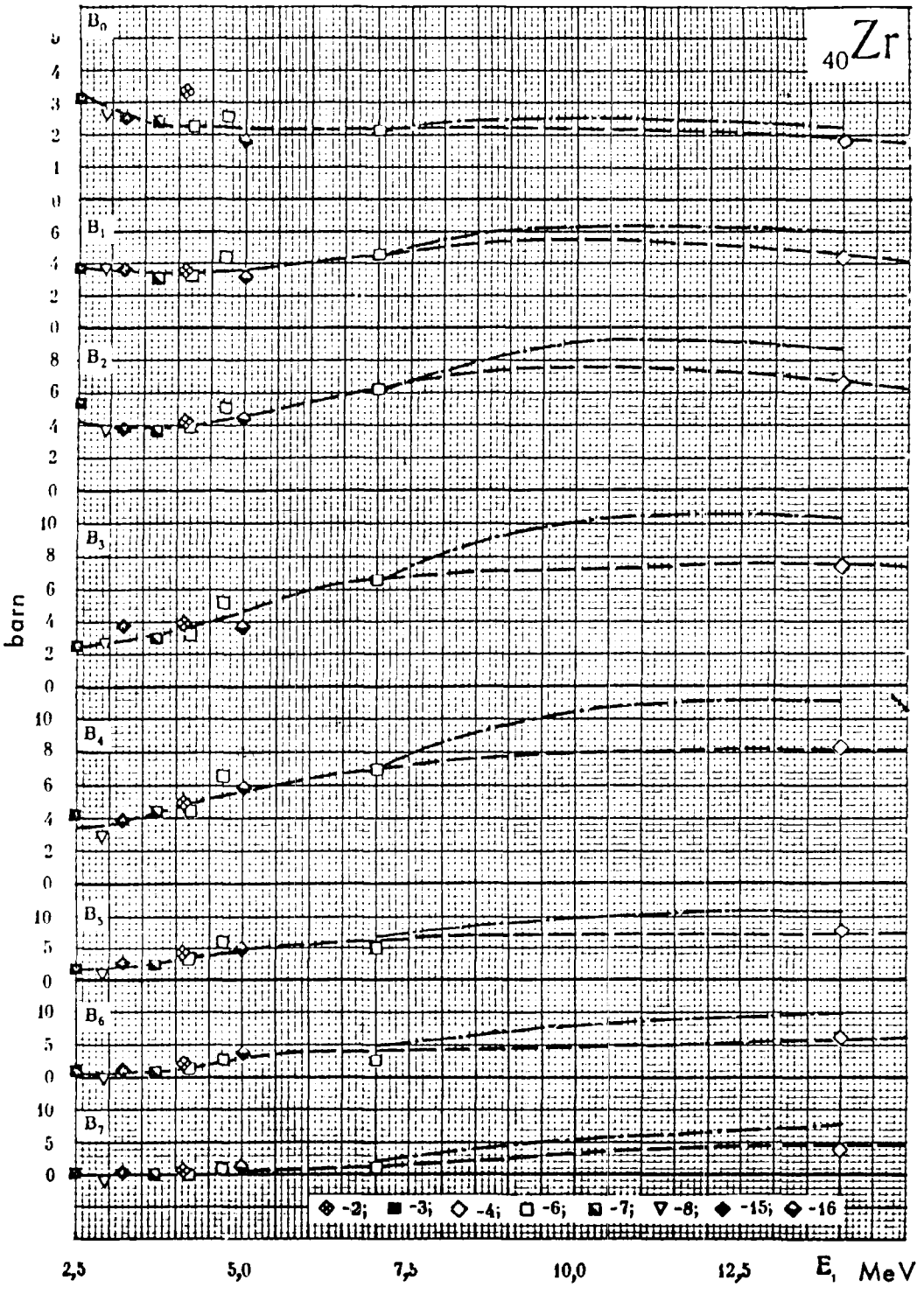
$_{40}Zr$
B_0
B_1
B_2
B_3
B_4
B_5
B_6
B_7
barn
-2; -3; -4; -6; -7; -8; -15; -16
2,5
5,0
7,5
10,0
12,5
E_n MeV

N I O B I U M

Below 1.7 MeV angular distributions have been measured at many energies by Langsdorf /L-2/(1957) and Smith /S-14/(1964).

The results of these experiments agree rather well. They also agree reasonably well with the results by Yankov, Koltipin /Ya-1, K-1/ and Walt /W-4/ as well as with the values $\approx \sigma_T - \sigma_{ne}$ obtained from the available data (Figure 22) /16/.

At higher energies much less information is available.

The data by Popov and Kasakov /P-6, K-8/ are too high : the values of B_o following from their data are considerably higher than the results of $\sigma_T - \sigma_{ne}$ which are sufficiently well known in this energy range. One comes to the same conclusion if one compares their results with the trend of the data of the other authors.

At 14 MeV the experimental values of B_o obtained in reference /W-14/ are considerably lower than the calculated values. The value of the difference $\sigma_T - B_o$ exceeds considerably the value σ_{ne} which can be expected at this energy from systematics of σ_{ne} of neighbouring nuclei.

It should be pointed out that the quoted values of B_ℓ have been obtained by extrapolation of the experimental data into the range of small angles according to results obtained by optical model calculation. A direct fit of the experimental data by the least-squares method yields still smaller values of B_ℓ (e.g., one obtains 1.15 barn for B_o). In reference /W-14/ an analysis of the origin of the above-mentioned discrepancy is given, and it is concluded that in measurements of σ_{ne} the direct inelastic processes leading to small energy losses were not taken into consideration.

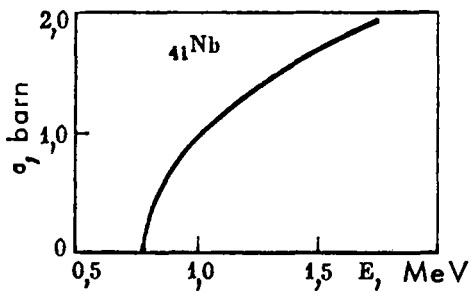

Figure 22 - Inelastic neutron scattering cross-section of niobium, used for correcting B_o.

In the energy range between 5 and 14 MeV the recommended curve $B_o(E)$ has been derived from the subtraction of the nonelastic cross-section from the total cross-section. The nonelastic cross-section has been obtained by interpolating the data at 2 - 2.5 MeV and using the value $\sigma_t - B_o \sim 2.17$ barn obtained from the results of reference /W-14/.

The values of the moments B_8, B_9, B_{10}, B_{11}, B_{12} and B_{13} at 14 MeV obtained from the angular distribution /W-14/ are equal to 4.34, 3.38, 2.24, 1.46, 0.692 and 0.386 barn, respectively.

$_{41}$Nb

1 — [2]; [*W* — 4] — M. Walt (1954)
2 — [*L* — 2] — A. Langsdorf (1957)
3 — [2]; [*T* — 3] — D. B. Thomson (1961)
4 — [G — 2] — G.V.Gorlov (1964)
[G — 3] — G.V.Gorlov (1965)
5 — [*S* — 14] — A. B. Smith (1964)
[*R* — 7] — D. Reitman (1963)
6 — [P — 6] — V.I.Popov (1965)
[*K* — 8] — L.Ya.Kazakova (1965)
7 — [Y — 1] — G.B.Yankov (1965)
[*K* — 1] — E.A.Koltypin (1962)
8 — [*W* — 14] — G. T. Western (1966)
9 — [*B* — 19] — S. G. Buccino (1966)

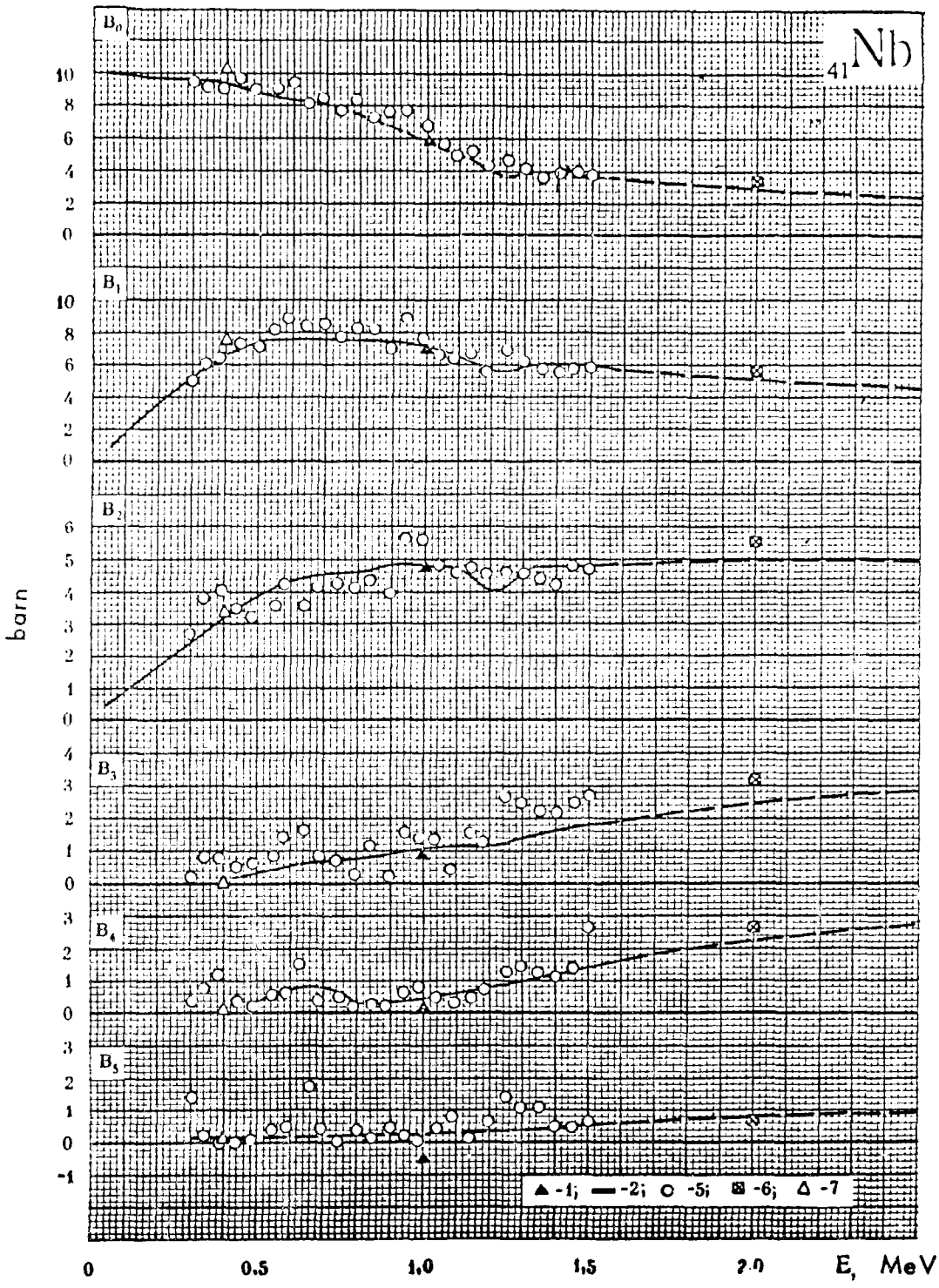
B_0
B_1
B_2
B_3
B_4
B_5
41Nb
barn
▲ -1; — -2; ○ -5; ⊠ -6; Δ -7
0
0.5
1.0
1.5
2.0
E, MeV

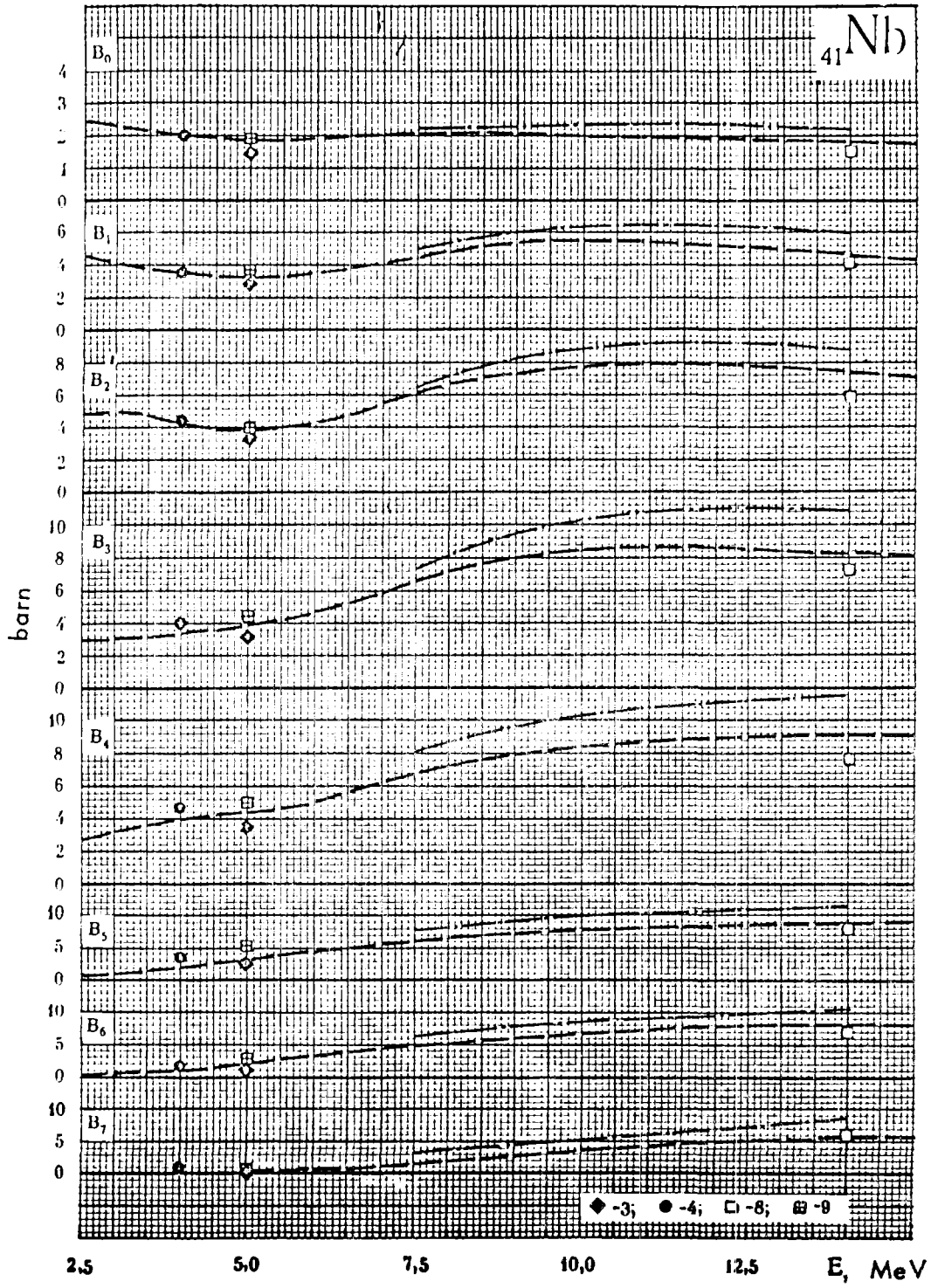
41Nb
B0
B1
B2
B3
B4
B5
B6
B7
barn
◆ -3; ● -4; □ -6; ⊞ -9
2,5
5,0
7,5
10,0
12,5
E, MeV

M O L Y B D E N U M

Results of different works in which the differential cross-section below 1.5 MeV has been measured agree sufficiently well with the exception of the angular distribution obtained in reference /K-6/(1964) at energies of 0.3 and 0.8 MeV. B_ℓ ($\ell > 0$) calculated from these data deviates from the curve around which the results of other authors are lying. The correction for inelastic scattering has been done with the values given in Figure 23. At higher energies the results of different works agree sufficient

Рис. 23. Сечение неупругого рассеяния нейтронов на молибдене, принятое при введении поправки в B_0.

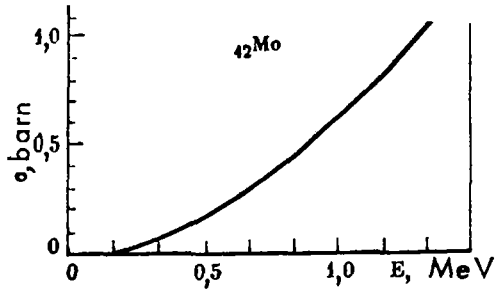

Up to 4 MeV B_o agrees excellently with the values obtained from the subtraction of the compound nucleus cross-section from the total cross-section. At higher energies there are no δ_{ne} available.

One must point out that, for molybdenum, the deviation between experimental and calculated values of B_ℓ at 14 MeV has the same character and order of magnitude as for zirconium and niobium. The values of the moments B_8 and B_9 are presented in Table 23. The values of the moments B_{10}, B_{11}, B_{12}, B_{13} and B_{14} at 14 MeV, obtained in the experiment /C-10/ are 1.64, 0.857, 0.427, 0.264 and 0.118 barn, respectively.

Table 23

Ref.	E, MeV	B_n	B_p	Ref.	E, MeV	B_n	B_p
[B—20]	3,2	—0,762	—	[W—12] [W—13]	6,0	0,300	—0,209
[V—1]	4,1	—0,253	—				
[H—2]	5,0	—0,150	—	[C—10]	14	4,07	2,61

$_{42}$Mo

1 — [12];[W — 4] — M. Walt (1954)
2 — [2]; [H — 1] — H. S. Hans (1957)
3 — [L — 2] — A. Langsdorf (1957)
4 — [2]; [H — 2] — R. W. Hill (1958)
5 — [2]; [V — 1] — L. D. Vincent (1960)
6 — [2]; [S — 8] — V.I.Strizhak (1960)
7 — [2]; [S — 10] — V.I.Strizhak (1961)
8 — [S — 14] — A. B. Smith (1964)
9 — [K — 6] — I.A.Korzh (1964)
10 — [Y — 1] — G.B.Yankov (1965)
[K — 1] — E.A.Koltypin (1962)
11 — [P — 6] — V.I.Popov (1965)
[K — 8] — L.Ya.Kazakova (1965)
12 — [W — 13] — R. M. Wilenzick (1965)
[W — 12] — R. M. Wilenzick (1962)
13 — [B — 20] — R. L. Becker (1966)

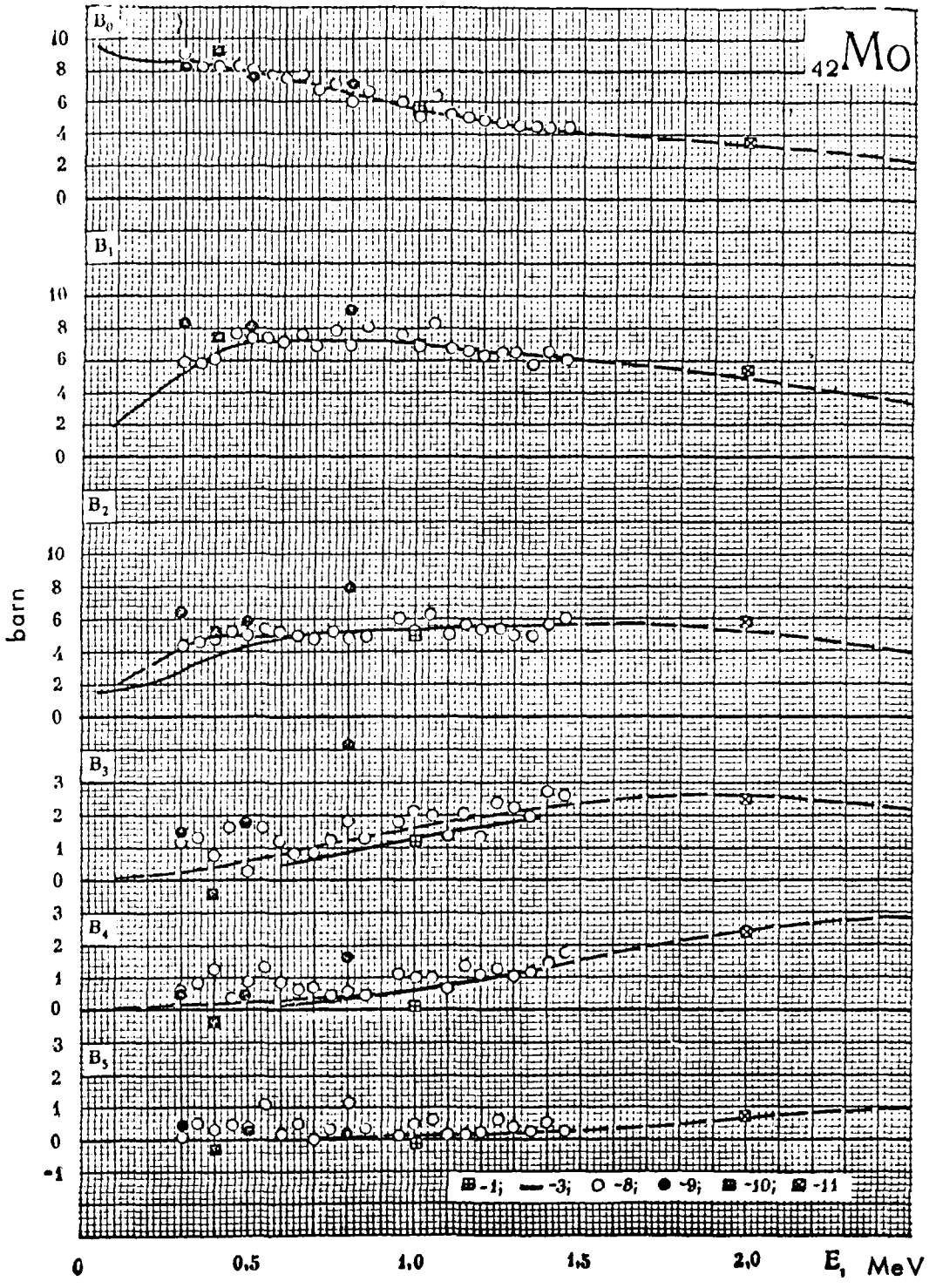
B_0
B_1
B_2
B_3
B_4
B_5
$_{42}$Mo
barn
10
8
6
4
2
0
3
2
1
0
-1
0
0,5
1,0
1,5
2,0
E, MeV
-1; -3; -8; -9; -10; -11

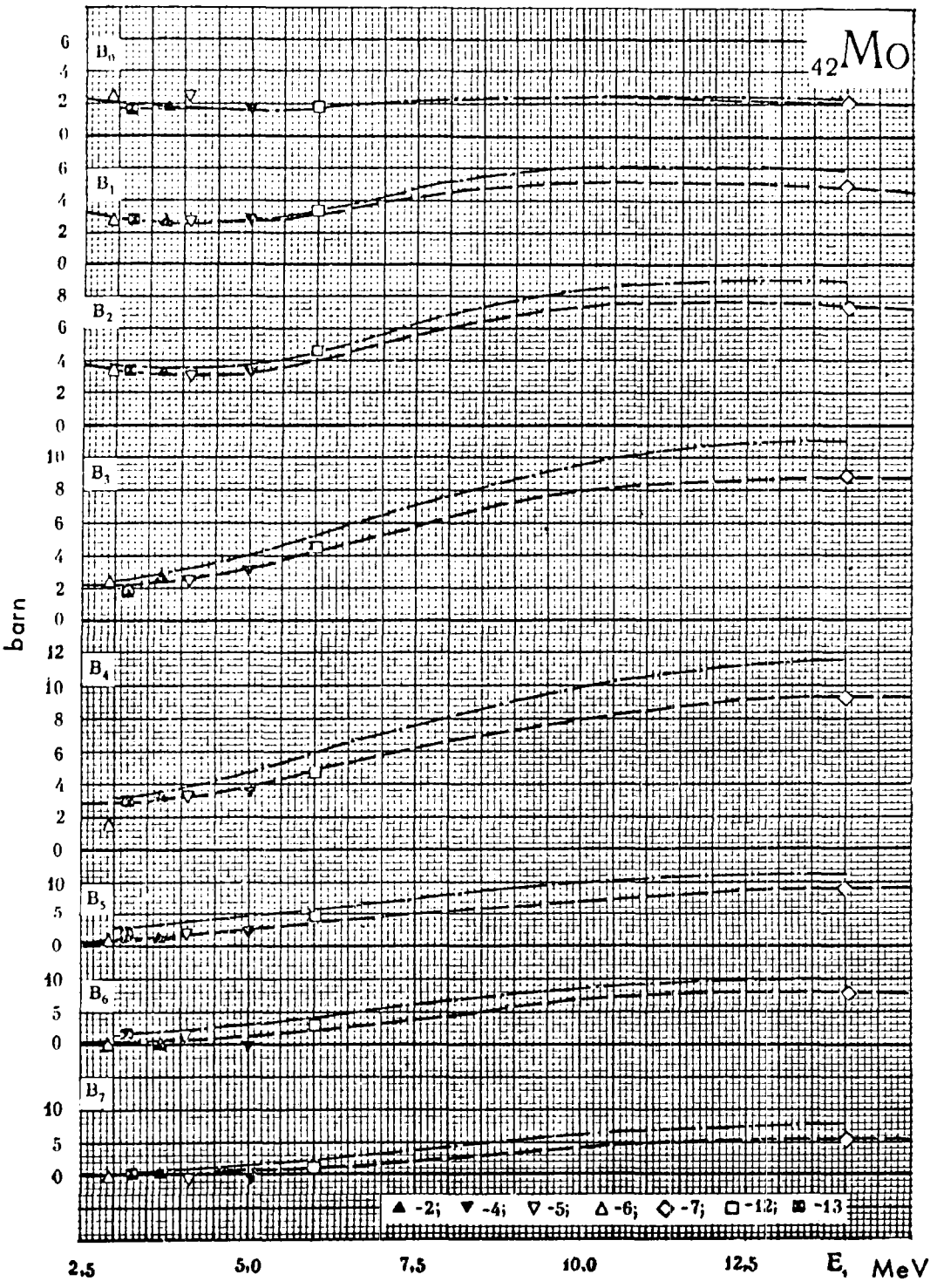
$_{42}$Mo
B_0
B_1
B_2
B_3
B_4
B_5
B_6
B_7
barn
▲ -2; ▼ -4; ▽ -5; △ -6; ◇ -7; □ -12; ▣ -13
2,5
5,0
7,5
10,0
12,5
E, MeV

T I N

The angular distributions of tin are investigated in detail. Many data which are, on the whole, in good agreement determine the energy dependence of B_ℓ up to 2.5 MeV sufficiently well.

Comparing B_o with the total cross-section /13/ and the nonelastic cross-section (Figure 24)/16/ shows, that in the region 0.7 - 2.5 MeV, the experimental values of B_o lie about 0.4 - 0.5 barn below the difference $\sigma_T - \sigma_{ne}$ obtained from the recommended curve of the quoted compilations.

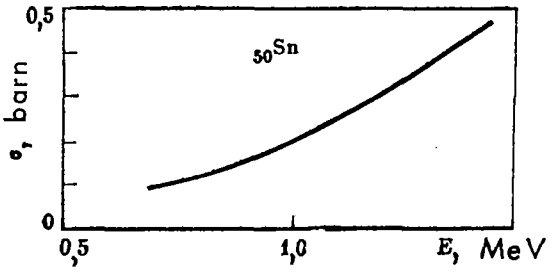

Figure 24 - Inelastic neutron scattering cross-section of tin, used for correcting B_o.

In deriving the curve, it is true that this difference can be removed if one ignores the results obtained in 1956 by Beyster, Walt and Salmo, and if one limits onself only to more recent data. However, a convincing argument for doing this can not be advanced. Moreover, at energies from 0.05 - 0.7 MeV, where the nonelastic interaction is very small, the experimental values of B_o also lie 0.5 barn below the difference $\sigma_T - \sigma_{ne}$. The above-mentioned discrepancies do not, however, advance an argument for the correlation of the concording data of the many authors here quoted, for example, the reliability of these data is higher than the reliability of the data on nonelastic cross-sections as well as the total cross-sections (measured at energies from 0.05 - 2.5 MeV in only two works, and overlapping only in the region 1 - 1.4 Mev) /13/.

At energies > 2.5 MeV the discrepancies of the experimental values of B_ℓ are higher than at lower energies.

However, a systematic deviation of B_o from the difference $\delta_T - \delta_{ne}$ does not exist in this energy region. Our recommended curve for B_o agrees with the trend of the experimental data as well as with the curves of δ_T and δ_{ne} presented in /13/ and /16/. On the whole, the values calculated by the optical model are in satisfactory agreement with the experimental data of B_o and with the difference $\delta_T - \delta_{ne}$.

The values of the moments B_8 and B_9 are represented in Table 24.

Table 24

Ref.	E, MeV	B_8	B_9
[W—5]	4,1	—0,315	—0,07
[W—12] [W—13]	6,0	1,31	0,197
[B—21]	7,0	1,80	0,246
[2]	14	10,08	7,55

The values of the moments B_{10}, B_{11}, B_{12}, B_{13}, B_{14}, B_{15} and B_{16} at 14 MeV, obtained from the angular distribution eye-guide curve presented in BNL-400/2/ are : 5.31, 3.42, 1.87, 1.03, 0.381, 0.193 and 0.024 barn, respectively.

$_{50}Sn$

1 — [2]; [*W* — 4] — M. Walt (1954)
[L — 1] — G.N.Lovchikova (1957)
[*G* — 1] — W. B. Gilboy (1962)
2 — [2]; [*S* — 2] — S. C. Snowdon (1954)
3 — [2]; [*W* — 5] — M. Walt (1955)
4 — [2]; [*B* — 2] — J. R. Beyster (1956)
5 — [*L* — 2] — A. Langsdorf (1957)
6 — [2]; [P — 2] — M.V.Pasechnik (1958)
7 — [2]; [K — 1] — M.M.Khaletskii (1957)
[*R* — 4] — L. A. Rayburn (1959)
[*S* — 11] — P. H. Stelson (1962)
[*C* — 5] — J. H. Coon (1958)
[*A* — 8] — J. D. Anderson (1958)
8 — [2]; [L — 2] — G.N.Lovchikova (1960)
9 — [2^n]; [*L* — 6] — R. O. Lane (1961)
10 — [*K* — 3] — I.A. Korzh (1963)
11 — [*K* — 4] — I.A.Korzh (1963)
12 — [P — 5] — M.V.Pasechnik (1964)
13 — [*S* — 14] — A. B. Smith (1964)
14 — [G — 3] — G.V.Gorlov (1965)
[G — 2] — G.V.Gorlov (1964)
15 — [Y — 1] — G.B.Yankov (1965)
[K — 1] — E.A.Koltypin (1962)
16 — [*W* — 13] — R. M. Wilenzick (1965)
[*W* — 12] — R. M. Wilenzick (1962)
17 — [*B* — 20] — R. L. Becker (1966)

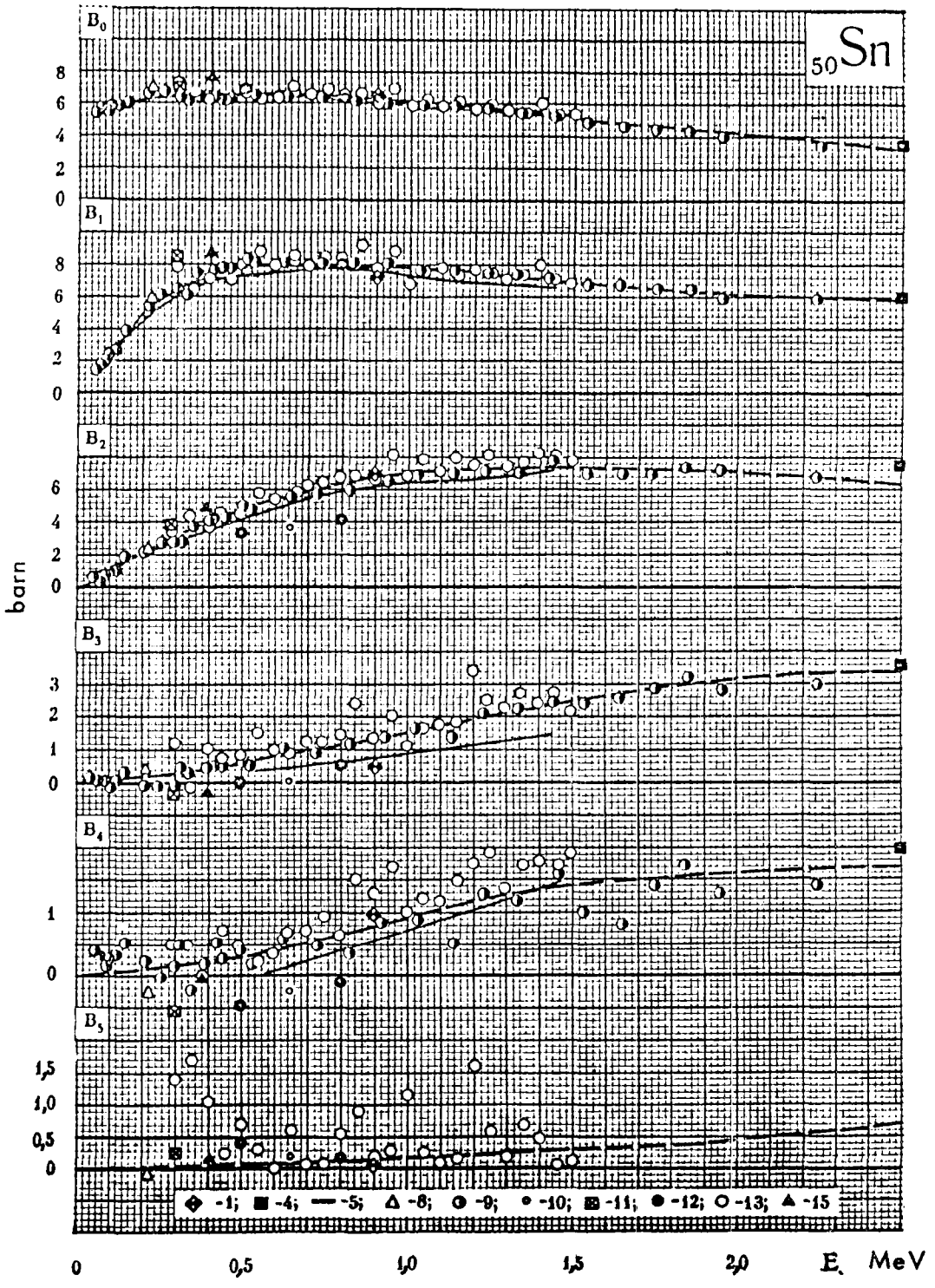
$_{50}$Sn
B_0
B_1
B_2
B_3
B_4
B_5
barn
E, MeV
0
0,5
1,0
1,5
2,0
◆ -1; ■ -4; — -5; △ -8; ● -9; • -10; ⊠ -11; ● -12; ○ -13; ▲ -15

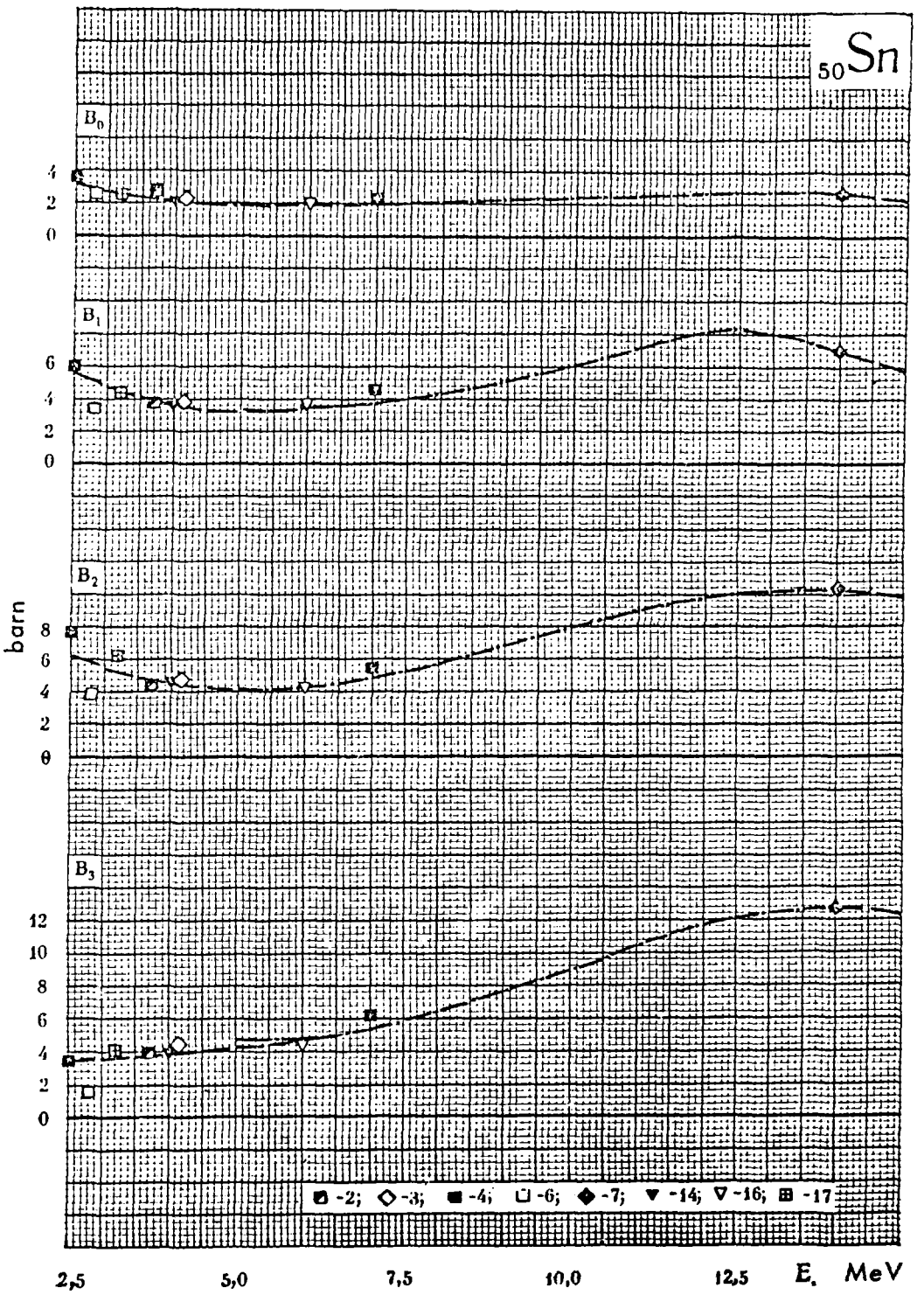
50Sn
B0
B1
B2
B3
barn
4
2
0
6
4
2
0
8
6
4
2
0
12
10
8
6
4
2
0
-2; -3; -4; -6; -7; -14; -16; -17
2,5
5,0
7,5
10,0
12,5
E, MeV

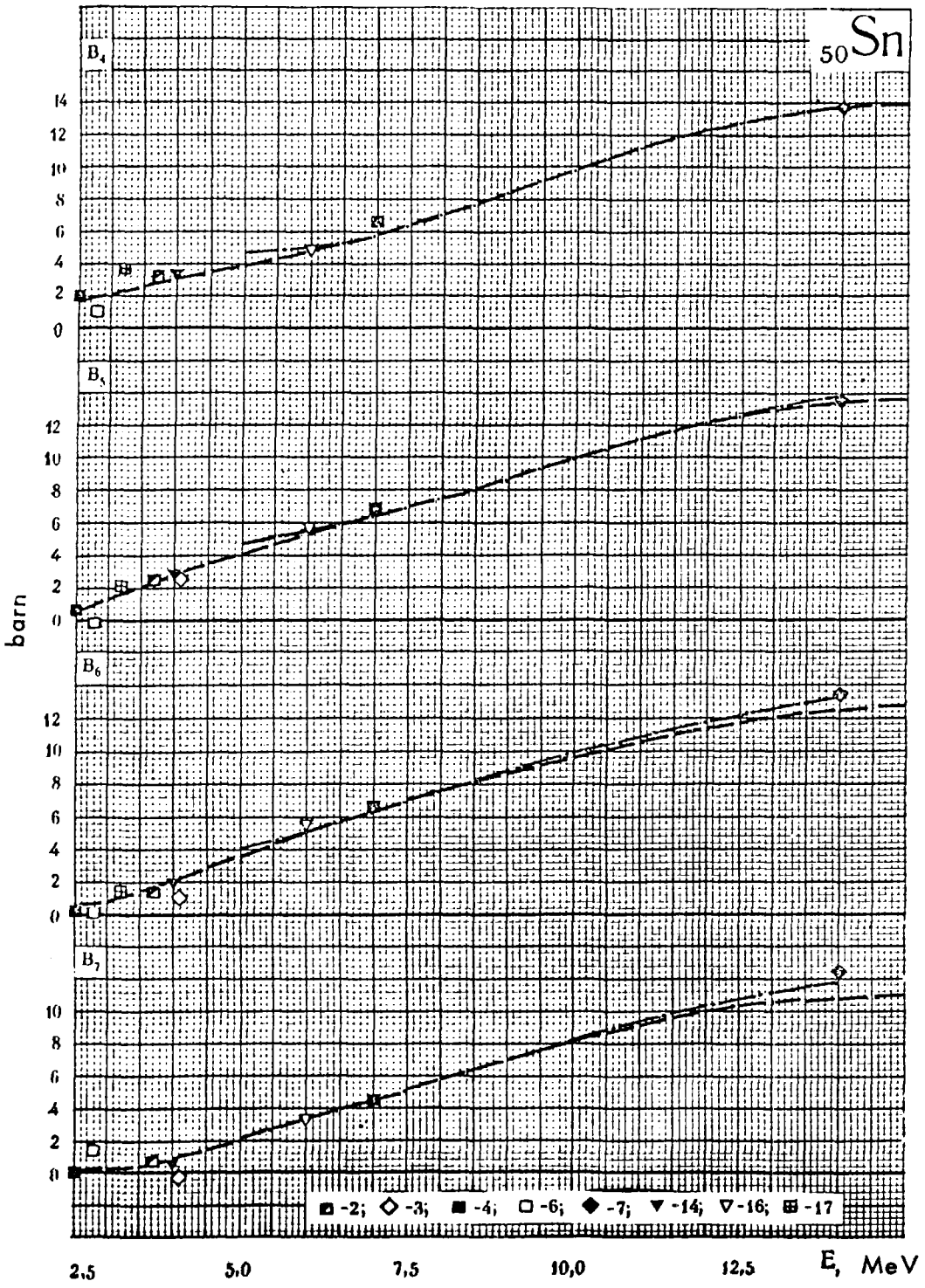
$_{50}$Sn
B_4
B_5
B_6
B_7
barn
14
12
10
8
6
4
2
0
2,5
5,0
7,5
10,0
12,5
E, MeV
-2; -3; -4; -6; -7; -14; -16; -17

T A N T A L U M

At energies below 1.5 MeV the values of B_o derived from the measurement by Smith /S-14/ lie systematically above the values by Langsdorf /L-2/. At 1 MeV the value by Smith is confirmed by the averaged value of a whole group of authors /W-4, D-1, G-1, S-12/. On the other hand, the results by Rogers /R-5/ at 0.7 and 0.9 MeV lie still lower than those by Langsdorf. In order to correct the inelastic scattering contribution we used the cross-section presented in Figure 25.

At present, it is difficult to make a well-founded choice between the available data because the total cross-sections of tantalum are contradictory in the range from 0.1 to 0.65 MeV. The results by Tabon et al., presented in /16/ for the energy range 0.25 - 0.65 Mev, are almost 2 barn lower than earlier total cross-section data /13/. The total scattering cross-sections measured in reference /L-2/ are 0.8 barn above the σ_T obtained by Tabon. Taking the capture cross-section into account, one sees that, σ_T derived from reference /L-2/ lies exactly in the middle of the total cross-sections presented in /13/ and /16/. However, in the range below 0.2 MeV the total scattering cross-sections obtained in /L-2/ agree with σ_T /13/, and, at 0.05 MeV as well as at higher energies the data by Tabon and other authors agree. The insufficiently high resolution in /L-2/ evidently effects the results in the resonance region.

In the region 0.25 - 0.65 MeV if one takes, as we did, the total cross-sections which lie between the results given in /13/ and /16/, i.e., they agree with the measurement by Langsdorf, then, a distinct maximum at 2.5 MeV appears in the total cross-sections. The existence of this maximum is also confirmed in the elastic scattering cross-section calculated by the optical model and in the measured elastic scattering cross-sections as well as in the total cross-section of tungsten.

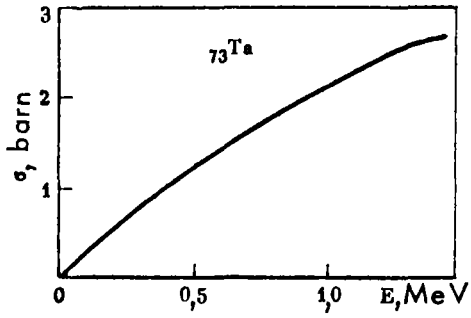

Figure 25 - Inelastic neutron scattering cross-section of tantalum, used for correcting B_o.

We wish to point out that at 2.5 and 7 MeV no discrepancy is observed in σ_{ne} whenever such data are available /13/ and in the total cross-sections /13, 16/ : the values of B_o, following from the results in reference /B-2/, agree with the values of the difference $\sigma_T - \sigma_{ne}$.

The discrepancies between experimental data of B_ℓ and values calculated by the optical model are also comparatively small.

The values of the moments B_8, B_9 and B_{10} are given in Table 25.

The values of the moments B_{11}, B_{12}, B_{13}, B_{14} and B_{15} at 14 Mev, obtained from the angular distribution eye-guide curve in BNL-400/2/ are : 6.77, 4.28, 2.4, 4.9 and 0.486 barn, respectively.

Table 25

Ref.	E, MeV	B_n	B_p	B_α
[B—20]	3,2	—0,625	—0,183	—
[W—5]	4,1	0,954	—	—
[B—19]	5,0	2,10	0,742	—
[B—2]	7,0	4,23	2,44	0,929
[2]	14	12,3	11,3	9,4

$_{73}$Ta

1 — [2]; [W — 4] — M. Walt (1954)
[D — 1] — S. E. Darden (1954)
[G — 1] — W. B. Gilboy (1962)
[S — 12] — A. B. Smith (1962)
2 — [2]; [W — 5] — M. Walt (1955)
3 — [2]; [B — 2] — J. R. Beyster (1956)
4 — [2]; [R — 2] — A. E. Remund (1956)
5 — [2]; [E — 1] — J. O. Elliott (1956)
[R — 3] — L. Rosen (1957)
5 — [2]; [C — 7] — W. G. Cross (1960)
[H — 4] — C. I. Hudson (1962)
6 — [L — 2] — A. Langsdorf (1957)
7 — [2]; [R — 5] — W. L. Rogers (1961)
8 — [S — 14] — A. B. Smith (1964)
9 — [P — 6] — V. I. Popov (1965)
[K — 8] — L. Ya. Kazakova (1965)
10 — [B — 20] — R. L. Becker (1966)
11 — [B — 19] — S. G. Buccino (1966)

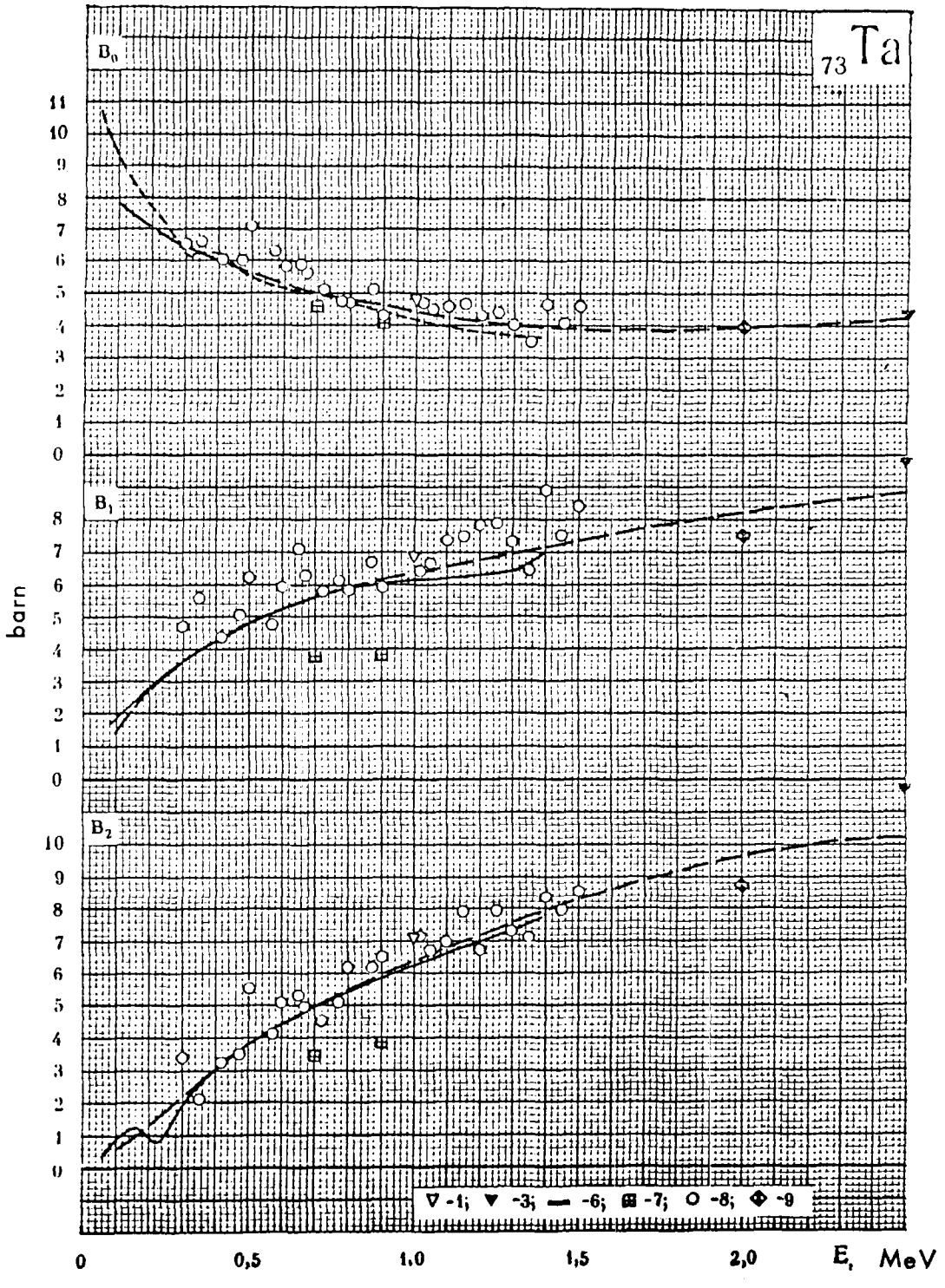
$_{73}$Ta
B_0
B_1
B_2
barn
0
0,5
1,0
1,5
2,0
E, MeV
▽ -1; ▼ -3; — -6; ⊞ -7; O -8; ◈ -9

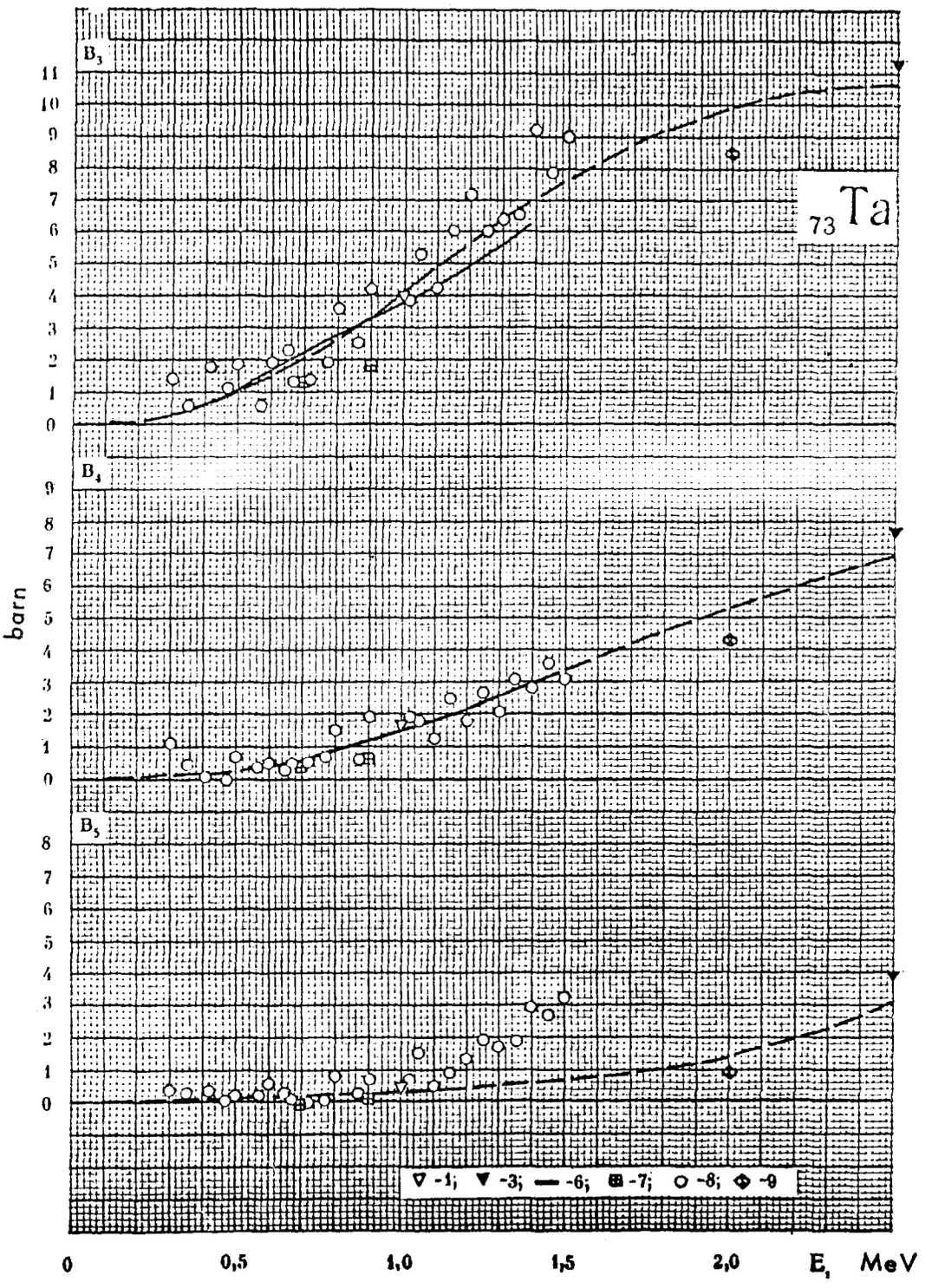
B3
B4
B5
73Ta
barn
0
0,5
1,0
1,5
2,0
E1 MeV
▽ -1; ▼ -3; — -6; ⊞ -7; ○ -8; ◇ -9

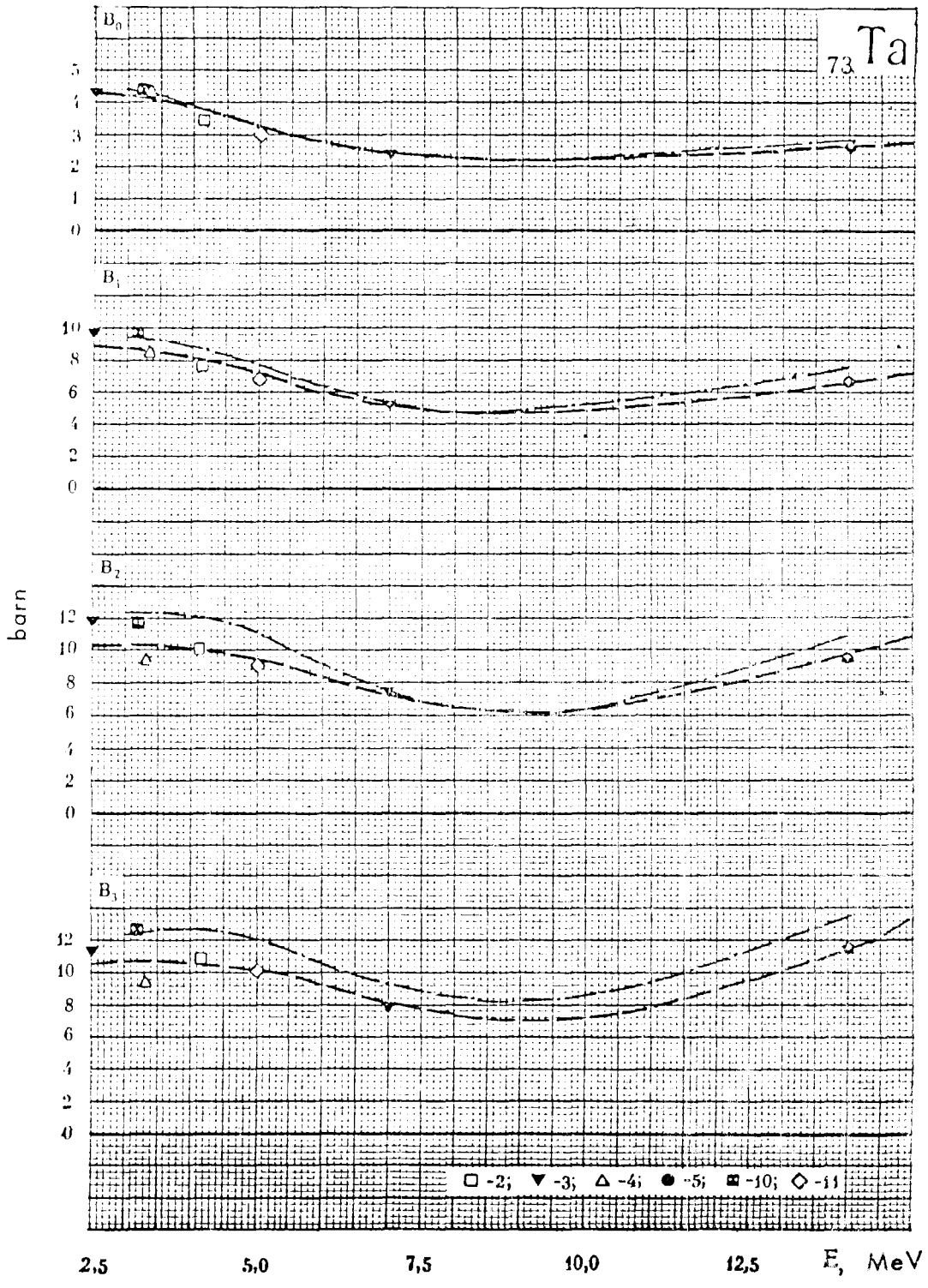
B_0
B_1
B_2
B_3
$_{73}Ta$
barn
□ -2; ▼ -3; △ -4; ● -5; ▣ -10; ◇ -11
2,5
5,0
7,5
10,0
12,5
E, MeV

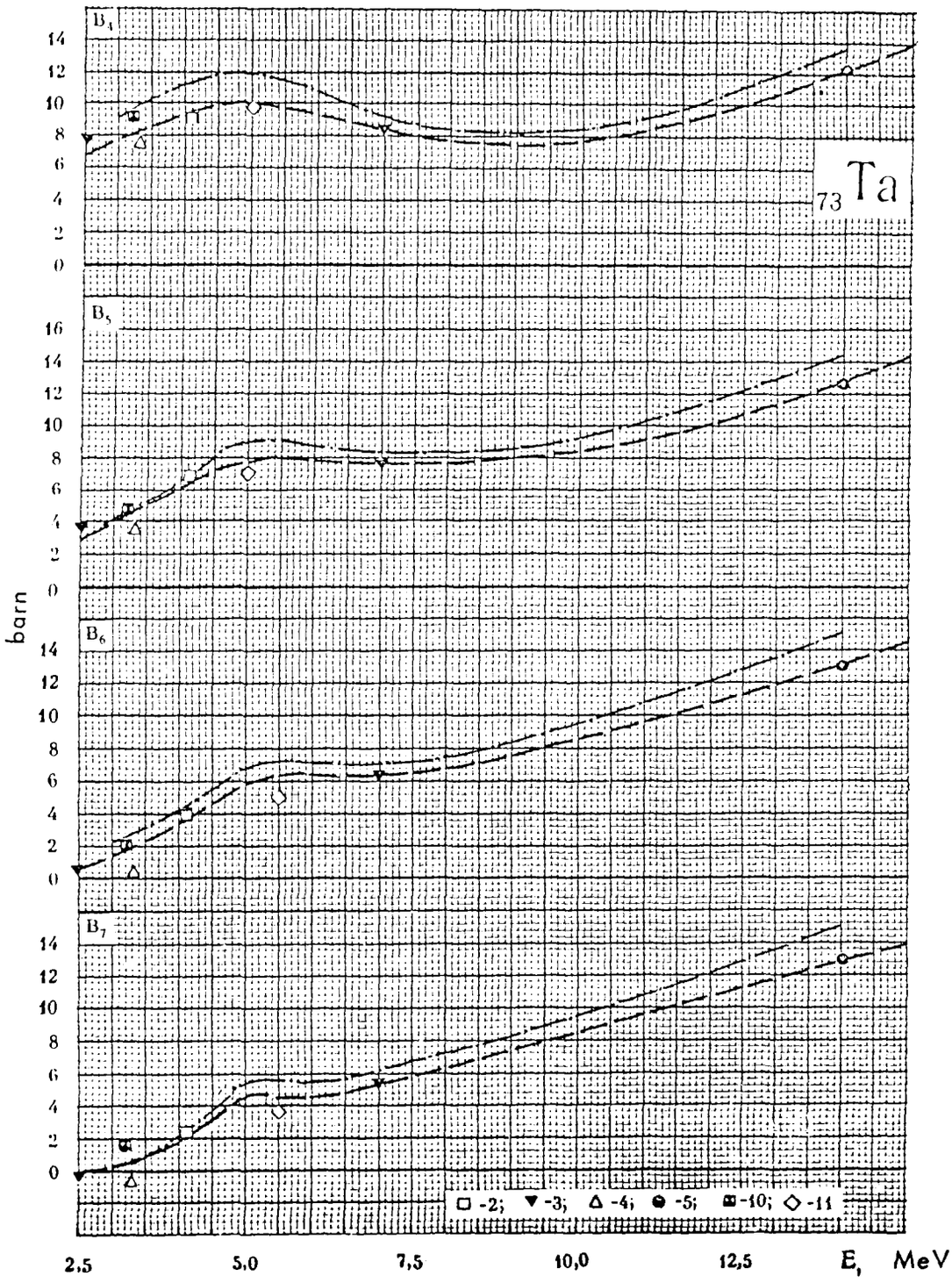
B4
B5
B6
B7
73 Ta
barn
□ -2; ▼ -3; △ -4; ● -5; ■ -10; ◇ -11
2,5
5,0
7,5
10,0
12,5
E, MeV

T U N G S T E N

As in the case of tantalum, the total cross-section values of tungsten in the range 0.2 - 0.6 MeV, presented in the compilations /13/ and /16/ differ by almost 1 barn (the latter lies lower). In the range of low energies ($E_n < 0.2$ MeV) the results /L-2/ are too high., due evidently to the contribution of neutrons with low energies.

The correction for the contribution of the inelastic scattering has been done using the cross-section given in Figure 26.

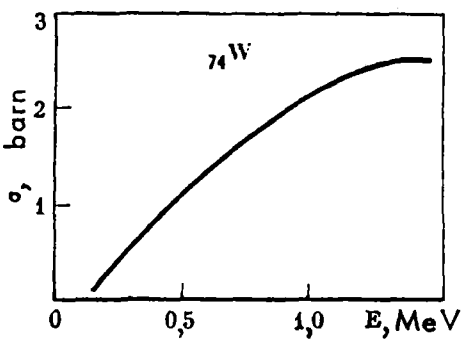

Figure 26 - Inelastic neutron scattering cross-section of tungsten, used for correcting B_o .

The results of B_o by Smith /S-14/ agree with the measurements by Langsdorf. At 1 Mev a consistent value for B_o was also obtained by Walt : the data by Korsch et al. /K-6/ are too high.

In the range 1 - 1.5 MeV, the measured results of B_o lie 0.3 - 0.5 barn lower than the difference $\bar{\nu}_T - \bar{\nu}_{ne}$ estimated from the recommended curves /16/ : this discrepancy is, however, within the limits of the accuracy of this difference estimated on the basis of the available experimental data.

The scatter of the data on B_ℓ ($\ell > 0$) is remarkably higher than for B_o.

In the range 2 - 4 MeV the flat curve derived from the available data /P-6, K-8/, /B-20/ and /W-5/ agrees well with the values of the difference $\delta_T - \delta_{ne}$. The data by Hill /H-2/(1958) at 5 MeV, however, are remarkably low : B_o obtained from them is much lower than $\delta_T - \delta_{ne}$ at this energy, and the data on high moments differ rather strongly from the results measured at energies near to 5 MeV.

At 14 MeV, B_o, following from the results of the work by Nauta /N-1/ agree with the value $\delta_T - \delta_{ne}$ within the limits of the experimental errors.

The recommended curve $B_o(E_n)$ in the region 4 - 14 MeV was derived from the available data on $\delta_T - \delta_{ne}$ /16/. The energy dependence of the high angular moments was obtained in this range by taking the results calculated by the optical model into account. The reliability of the recommended curves is not very high, since, e.g., the calculated energy dependence of B_o deviates quite a lot from the adopted values, i.e. from $\delta_T - \delta_{ne}$.

When experimental results of angular distribution of elastically scattered neutrons with an energy of 8 MeV are available, the reliability of the values of the angular moments in the whole energy range indicated will be considerably increased.

The values of the high moments are given in Table 26.

Table 26

Ref.	E_n, MeV	B_8	B_9	B_{10}	B_{11}	B_{12}	B_{13}
[H—2]	5,0	1,43	0,566	—	—	—	—
[N—1]	14,0	10,73	9,22	6,98	4,39	2,13	0,639

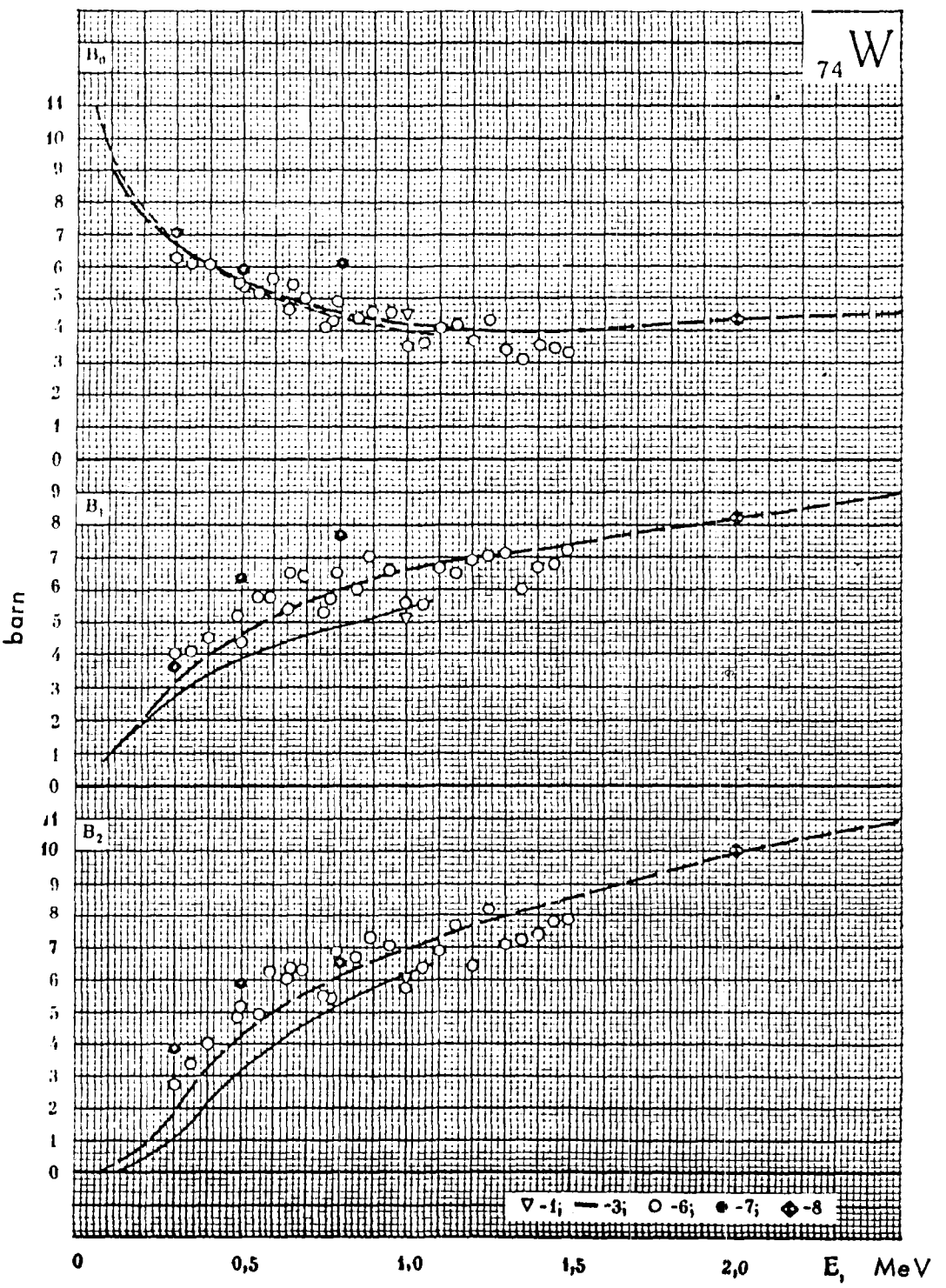
74 W
B0
B1
B2
barn
∇ -1; — -3; ○ -6; ● -7; ◈ -8
0
0,5
1,0
1,5
2,0
E, MeV

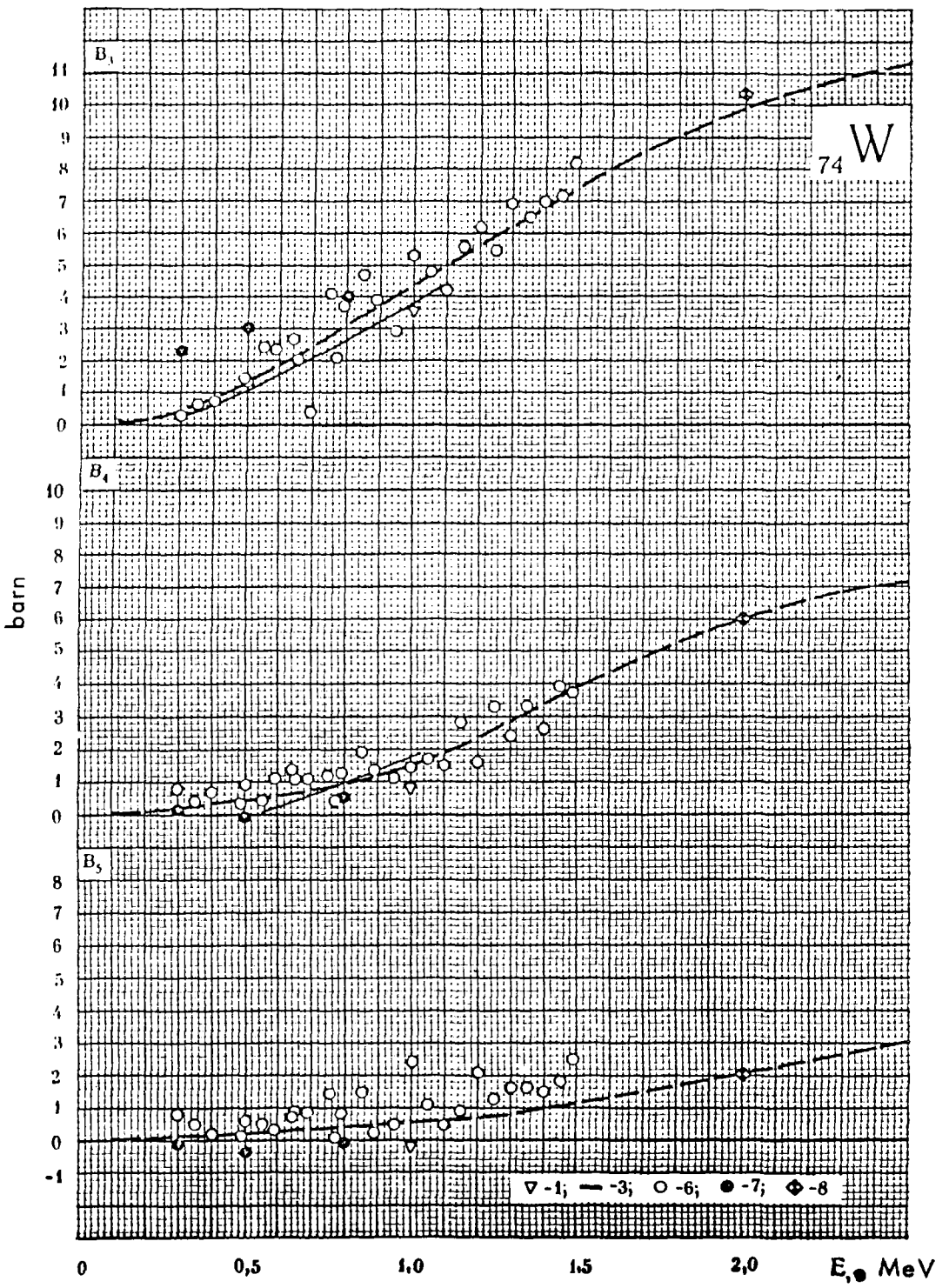
B1
B4
B5
74 W
barn
▽ -1; — -3; ○ -6; ● -7; ◈ -8
0
0,5
1,0
1,5
2,0
E, MeV

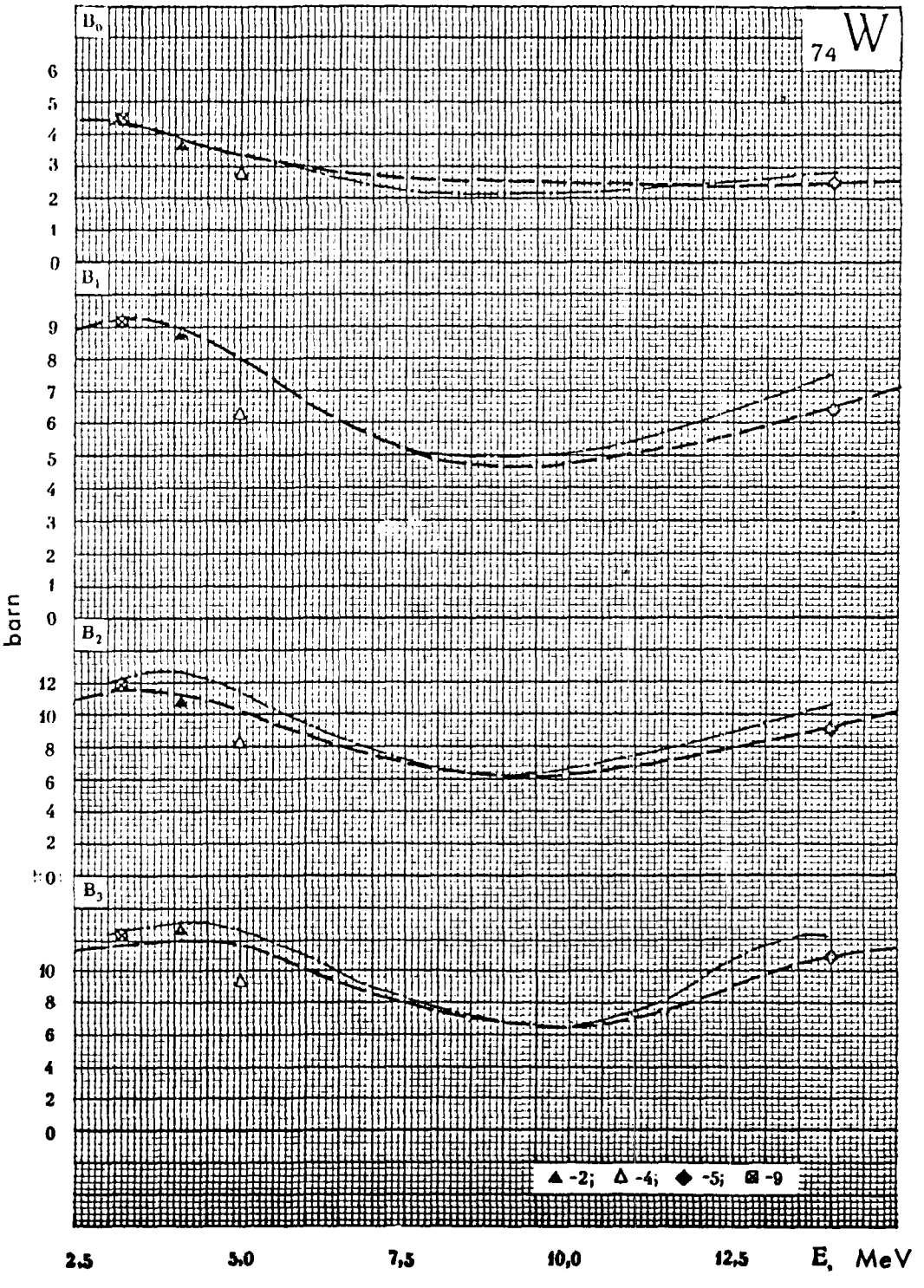
B_0
B_1
B_2
B_3
$_{74}W$
barn
▲ -2; △ -4; ◆ -5; ⊠ -9
2,5
5,0
7,5
10,0
12,5
E, MeV

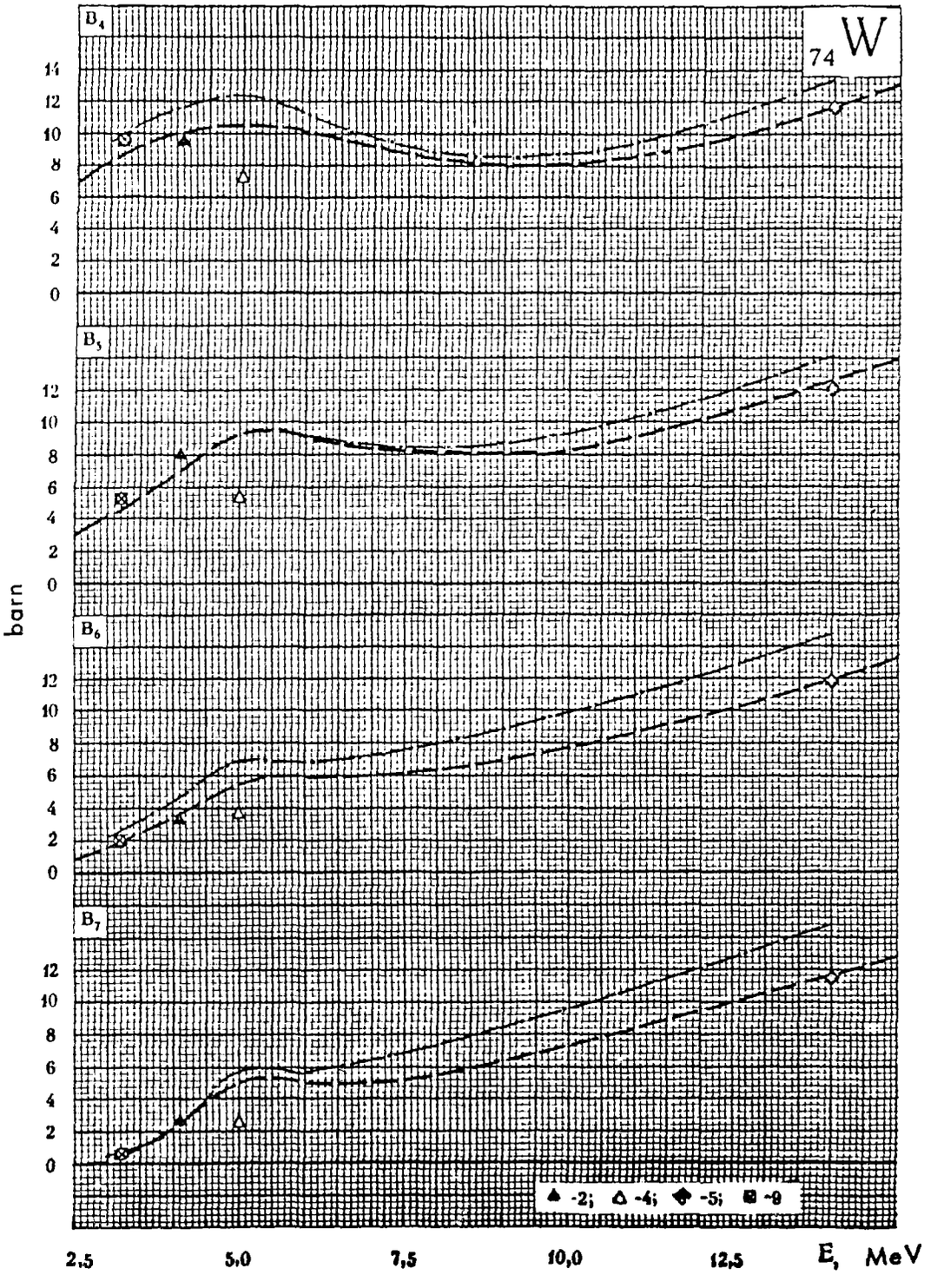
B_4
B_5
B_6
B_7
74 W
barn
14
12
10
8
6
4
2
0
▲ -2; △ -4; ◆ -5; ■ -8
2,5
5,0
7,5
10,0
12,5
E, MeV

T U N G S T E N - 184

The angular distribution of the tungsten - 184 isotope (30.6% in natural tungsten) was only measured in reference /S-14/. The sample was enriched to 94% in W-184. No essential deviation between the neutron angular distribution of natural tungsten and W-184 has been observed.

$_{74}W$

1 — [2]; [W — 4] — M. Walt (1954)
2 — [2]; [W — 5] — M. Walt (1955)
3 — [2]; [L — 2] — A. Langsdorf (1957)
4 — [2]; [H — 2] — R. W. Hill (1958)
5 — [2]; [N — 1] — H. Nauta (1958)
6 — [S — 14] — A. B. Smith (1964)
7 — [K — 6] — I.A.Korzh (1964)
8 — [P — 6] — V.I.Popov (1965)
[K — 8] — L.Ya.Kazakova (1965)
9 — [B — 20] — R. L. Becker (1966)

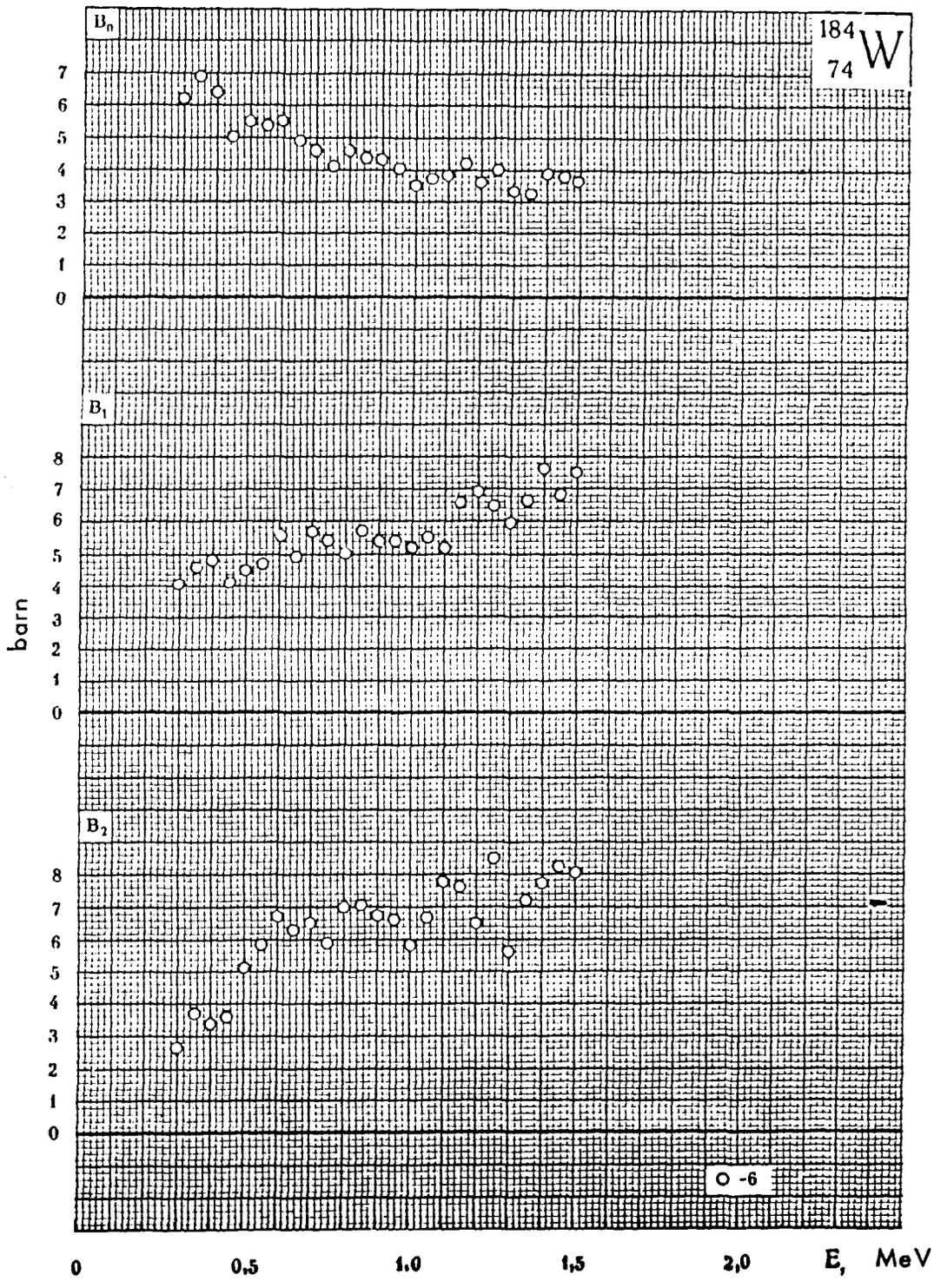
B_0
B_1
B_2
184 74 W
barn
0 -6
0
0,5
1,0
1,5
2,0
E, MeV

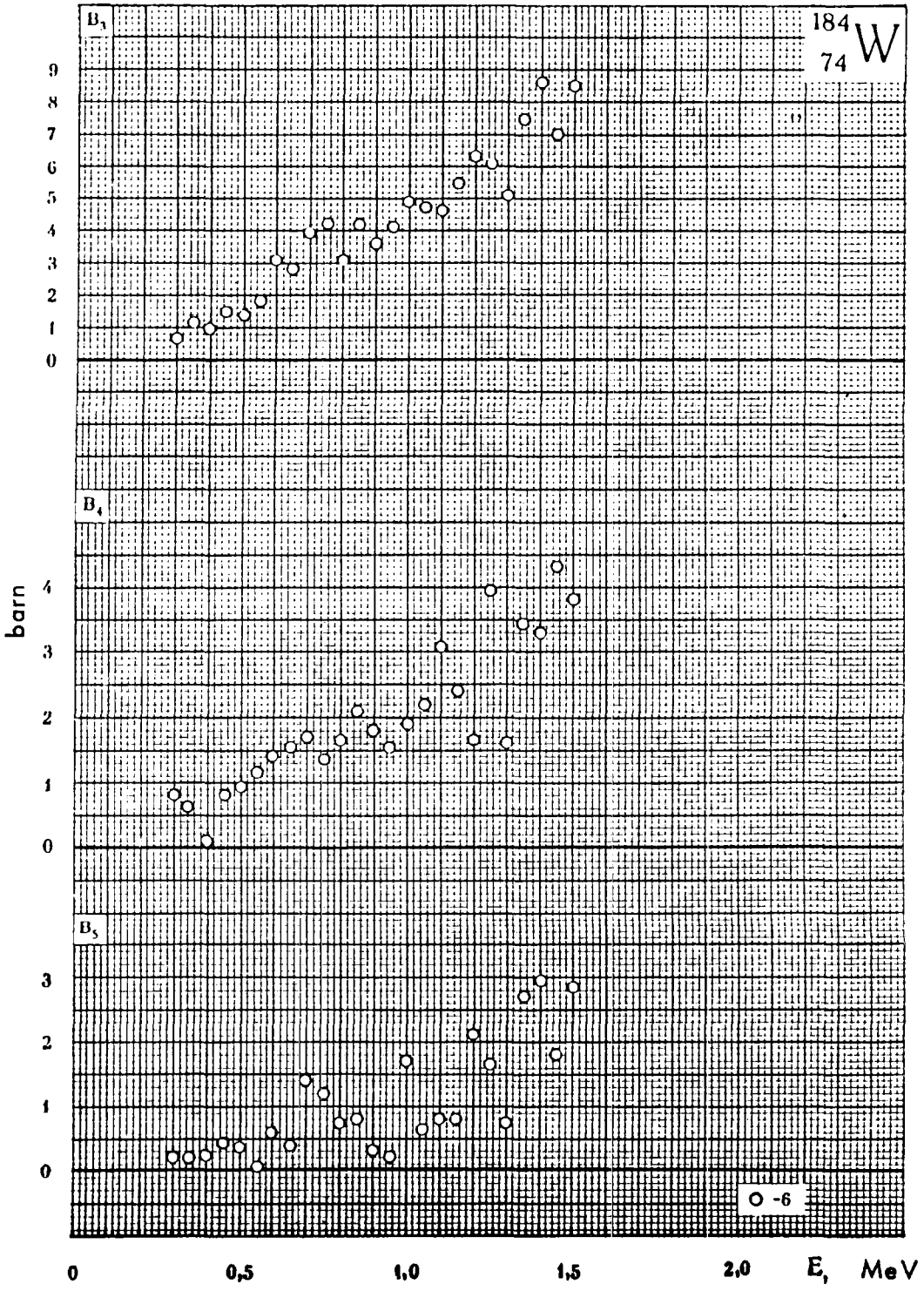
B_3
$^{184}_{74}W$
9
8
7
6
5
4
3
2
1
0
B_4
barn
4
3
2
1
0
B_5
3
2
1
0
O -6
0
0,5
1,0
1,5
2,0
E_n MeV

L E A D

At energies below 1 MeV, where nonelastic scattering is either small or not present (Figure 28), the available data agree comparatively well with one another. At $E_n < 0.4$ MeV, B_o taken from the results of the quoted works, lies considerably above the total cross-section. In this energy range the recommended curve has been derived from the total cross-section in references /13/ and /16/. At very low energies the available data /A-13/ of the ratio B_1/B_o (Figure 27) confirm the linear energy dependence of this value (at few energies) which follows from the theory assuming that no polarized neutrons are present.

In the energy range from 1 to 5 MeV the recommended curve $B_o(E_n)$ derived from the experimental values does not contradict the values resulting from the subtraction of the nonelastic cross-section from the total cross-section.

At 14 MeV, B_o obtained from the curve which is presented in reference /2/ is in good agreement with the difference $\sigma_T - \sigma_{ne}$; all B_l ($l > 0$) derived from this curve are close to results calculated by the optical model.

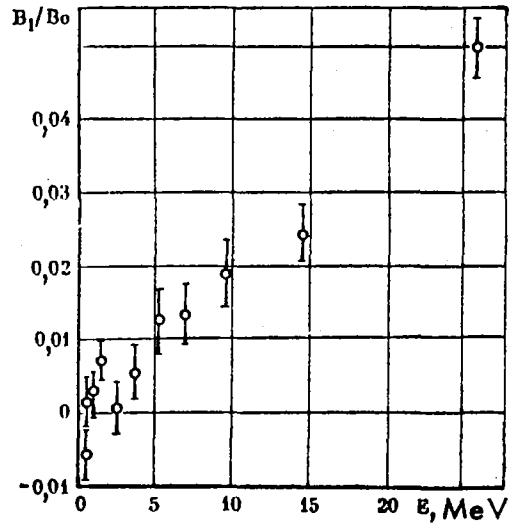

Figure 27 - Neutron energy dependence of the ratio B_1/B_o. The indicated error is the statistical error.

The difference $\beta_T - \beta_{ne}$ /16/ served as a basis for the derivation of the recommended curve of $B_o(E_n)$ in the energy range from 5 to 14 MeV. For high moments, $B_\ell(E_n)$ was derived by interpolating between the calculated and the experimental data.

Table 27

Ref.	E, MeV	B_ℓ	Ref.	E, MeV	B_ℓ	Ref.	E, MeV	B_ℓ
	0,05	0,689		0,437	—0,080		1,24	0,439
	0,07	0,079		0,480	0,455		1,34	0,348
	0,085	1,000		0,487	0,035		1,44	1,132
	0,10	—0,116		0,507	—0,118		1,54	0,778
	0,12	0,138		0,530	0,235		1,65	1,273
[L—6]	0,157	—0,023	[L—6]	0,630	0,076	[L—6]	1,75	1,816
	0,207	0,726		0,730	—0,188		1,85	1,354
	0,257	—0,498		0,830	0,329		1,95	1,145
	0,307	—0,567		0,930	0,113		2,25	2,492
	0,330	—0,264		1,04	0,670			
	0,357	—0,178		1,14	0,106			

Table 28

Ref.	E, MeV	B_ℓ	B_ℓ	$B_{\ell\ell}$	Ref.	E, MeV	B_ℓ	B_ℓ	$B_{\ell\ell}$
[П—2]	2,8	0,711	—	—	[2]	4,1	1,8	—	—
[П—1]	2,9	—	—	—	[2] [B—7a]	4,7	1,24	—	—
[B—20]	3,2	0,754	—	—	[H—2]	5,0	2,59	0,580	—
[2]	3,3	0,585	0,370	0,234	[B—19]	5,0	3,16	0,942	—
[2]	3,7	3,62	2,32	1,08	[2]	14	14,32	13,96	12,68
[Г—2, Г—3]	4,0	1,03	0,22	—					

The values of the moments B_6 to B_{10} are represented in Tables 27 and 28. The values of the moments B_{11}, B_{12}, B_{13} and B_{14} at an energy of 14 MeV obtained from the eye-guide curve of the angular distribution given in BNL-400/2/, are : 9.93, 6.23, 3.02 and 0.924 barn, respectively.

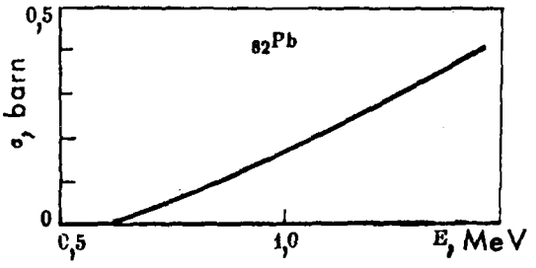

Figure 28 - Neutron inelastic scattering cross-section of lead, used for correcting B_0.

$_{82}$Pb

1 — [2]; [*W* — 4] — M. Walt (1954)
[*R* — 1] — W. J. Rhein (1955)
[*D* — 2] — S. E. Darden (1955)
[*G* — 1] — W. B. Gilboy (1962)
[*L* — 1] — G.N.Lovchikova (1957)
2 — [2]; [*B* — 1] — H. B. Brugger (1955)
[*R* — 2] — A. E. Remund (1956)
3 — [2]; [*W* — 5] — M. Walt (1955)
[*O* — 2] — P. L. Okhuysen (1959)
[*B* — 7a] — N. A. Bostrom (1959)
4 — [2]; [*L* — 2] — A. Langsdorf (1957)
5 — [2]; [*P* — 1] — V.I.Popov (1957)
6 — [2]; [*R* — 4] — L. A. Rayburn (1959)
[*N* — 1] — H. Nauta (1956)
[*S* — 11] — P. H. Stelson (1962)
[*Y* — 1] — K. Yuasa (1958)
[*C* — 5] — J. H. Coon (1958)
[*A* — 8] — J. D. Anderson (1958)
[*B* — 5] — S. Berko (1958)
[K — 1] — M.M.Khaletskii (1957)
[G — 1] — B.Ya.Gyzhovskii (1961)
6 — [2]; [*R* — 1] — W. J. Rhein (1955)
7 — [2]; [*B* — 7a] — N. A. Bostrom (1959)
[*W* — 3] — W. D. Whitehead (1953)
[*R* — 1] — W. J. Rhein (1955)
8 — [2]; [K — 4] — O.A. Kalnikov (1957)
9 — [2]; [P — 2] — M.V.Pasechnik (1958)
10 — [2]; [*H* — 2] — R. W. Hill (1958)
11 — [2]; [*B* — 7a] — N. A. Bostrom (1959)
12 — [2]; [L — 2] — G.N.Lovchikova (1960)
14 — [2]; [*F* — 4] — R. O. Lane (1961)
13 — [2^a]; [*L* — 6] — J. L. Fowler (1962)
15 — [*K* — 3] — I.A.Korzh (1963)
16 — [*K* — 7] — I.A.Korzh (1964)
17 — [P — 5] — M.V.Pasechnik (1964)
18 — [*S* — 14] — A. B. Smith (1964)
19 — [G — 2] — G.V.Gorlov (1964)
[G — 3] — G.V.Gorlov (1965)
20 — [*B* — 19] — S. G. Buccino (1966)
21 — [*B* — 20] — R. L. Becker (1966)

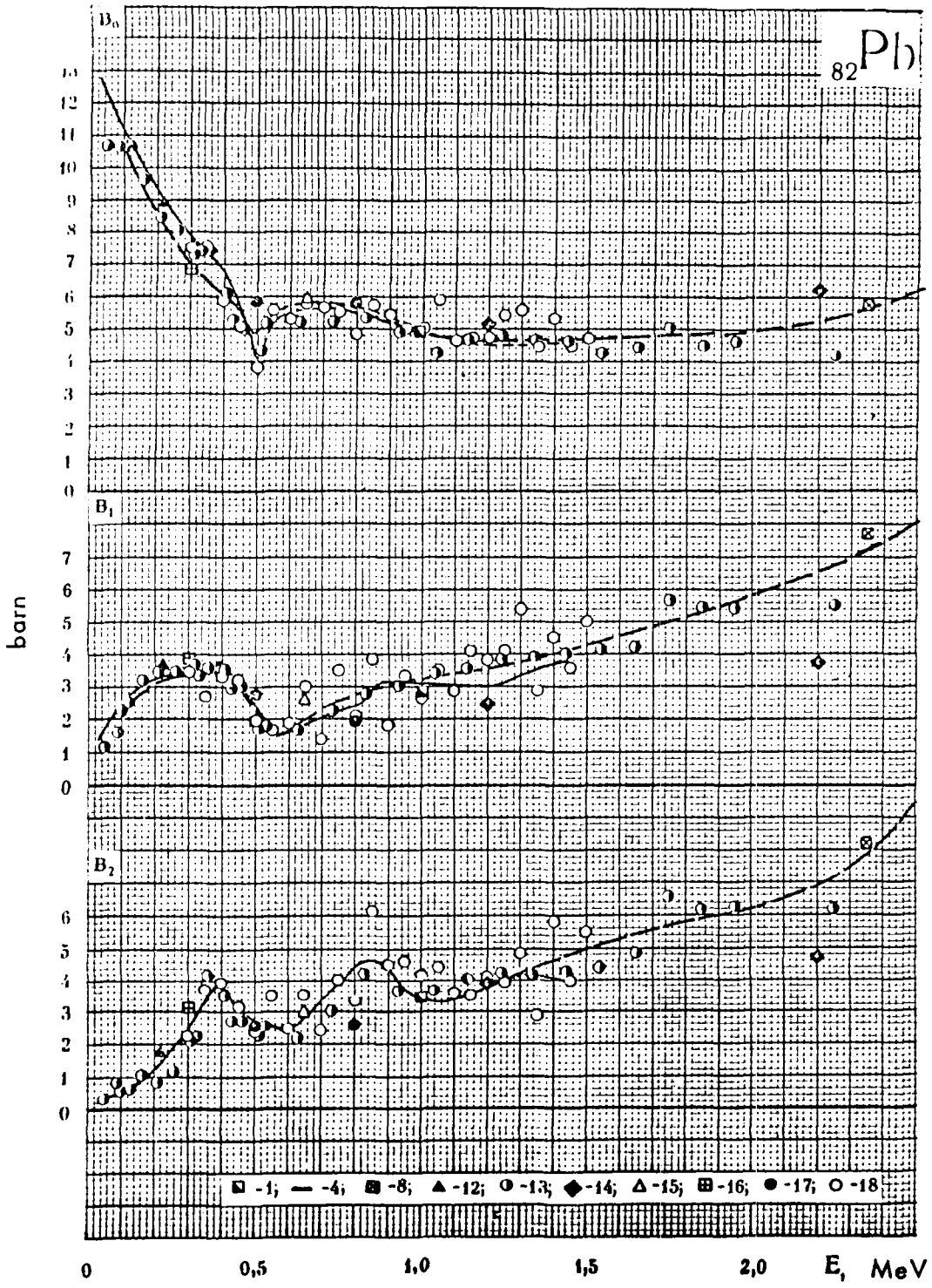
B_0
B_1
B_2
$_{82}Pb$
barn
0
0,5
1,0
1,5
2,0
E, MeV
-1; -4; -8; -12; -13; -14; -15; -16; -17; -18

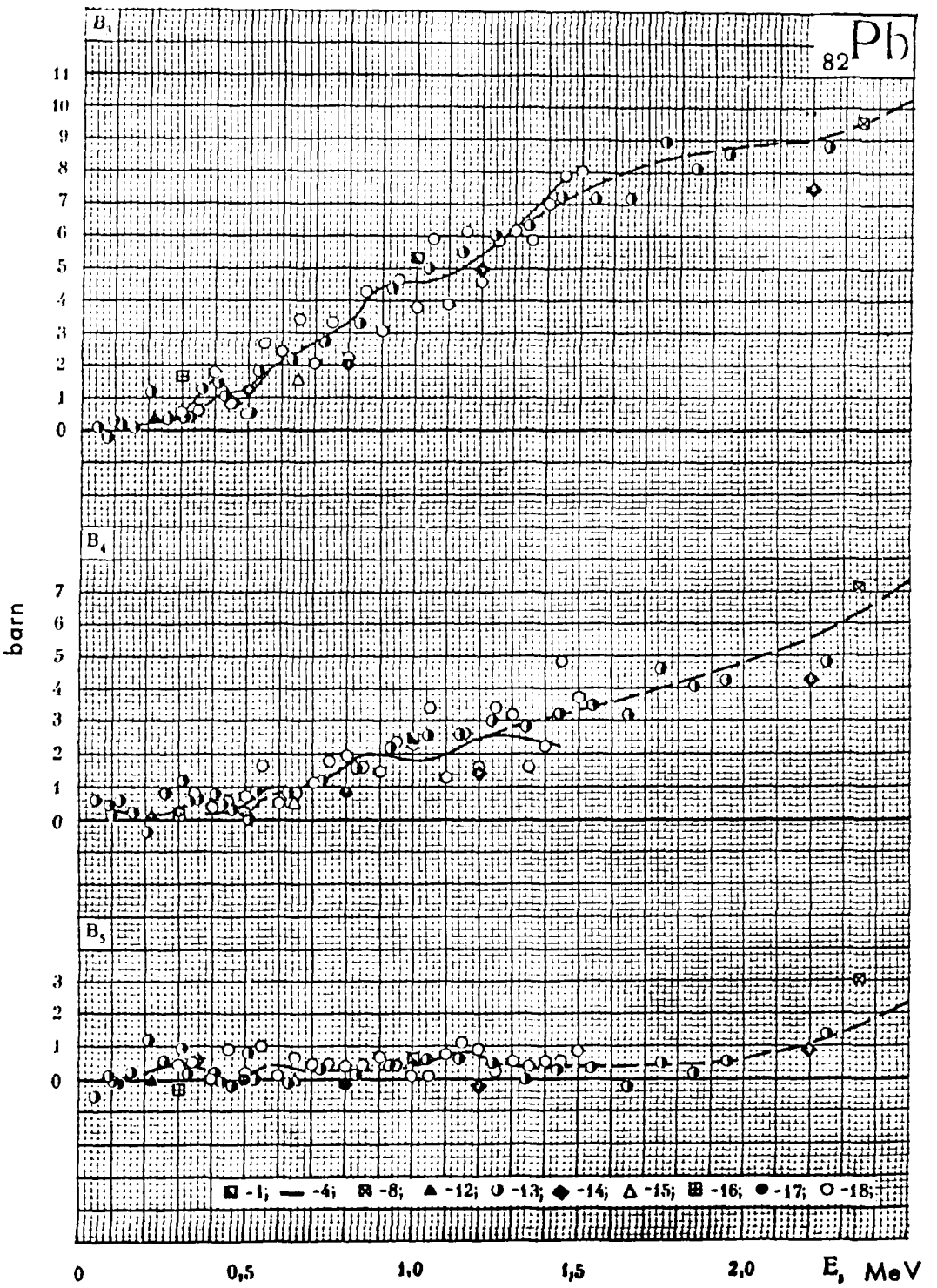
B_1
B_4
B_5
$_{82}Pb$
barn
11
10
9
8
7
6
5
4
3
2
1
0
7
6
5
4
3
2
1
0
3
2
1
0
■ -1; — -4; ⊠ -8; ▲ -12; ◑ -13; ◆ -14; △ -15; ⊞ -16; ● -17; ○ -18;
0
0,5
1,0
1,5
2,0
E, MeV

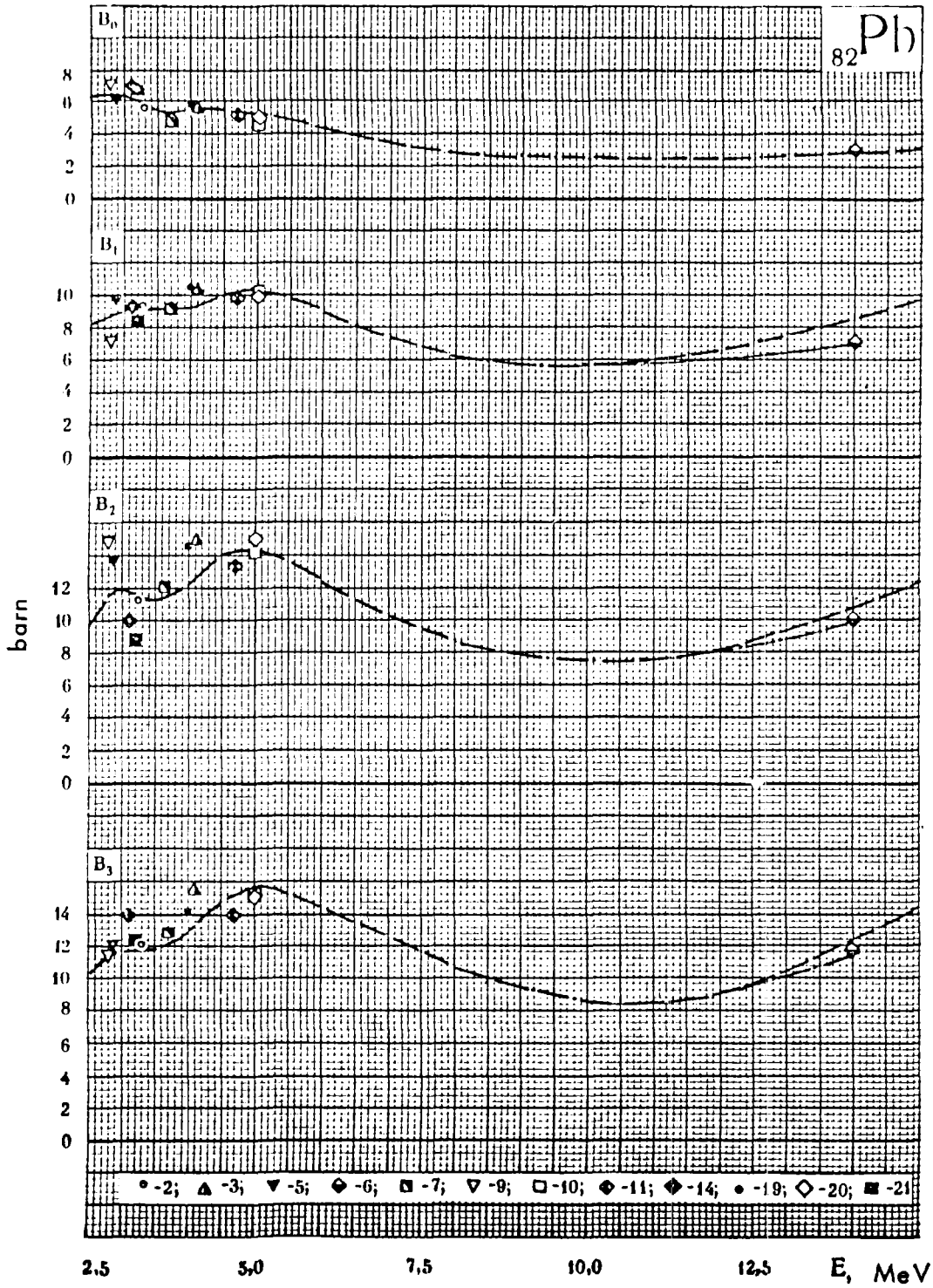
B_0
B_1
B_2
B_3
$_{82}Pb$
barn
E, MeV
2,5
5,0
7,5
10,0
12,5
• -2; ▲ -3; ▼ -5; ◆ -6; ■ -7; ▽ -9; □ -10; ◈ -11; ◆ -14; • -19; ◇ -20; ■ -21

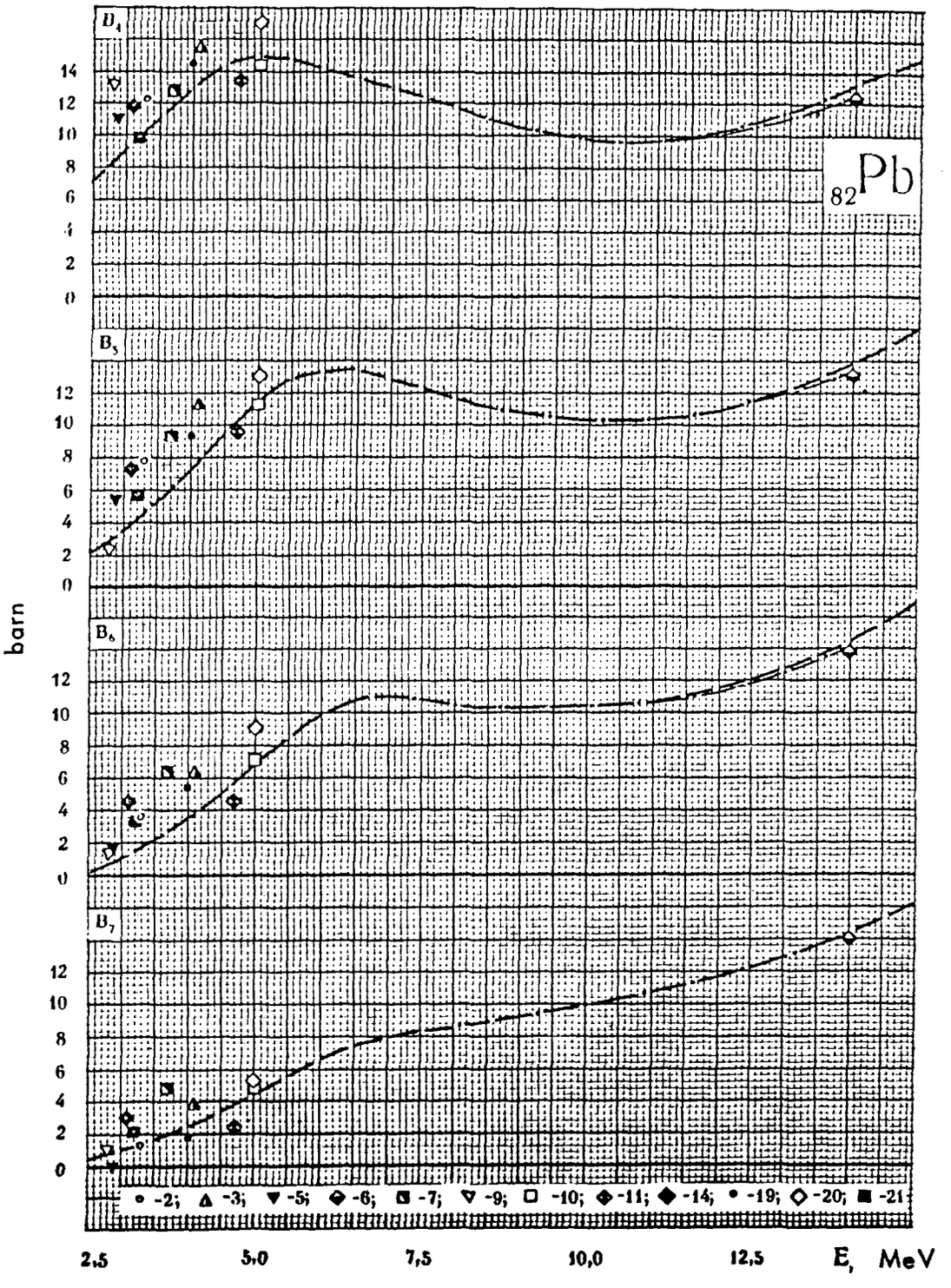
B_4
B_5
B_6
B_7
$_{82}Pb$
barn
E, MeV
2,5
5,0
7,5
10,0
12,5
-2; -3; -5; -6; -7; -9; -10; -11; -14; -19; -20; -21

B I S M U T H

The data by Langsdorf /L-2/ and Smith /S-14/, available in the range around 1.5 MeV, agree well between one another and with the results of references /L-2/, /K-7/, /A-5, D-2/, /P-5/ and /W-4, D-1, L-1/. The contribution of the inelastic scattering to B_o was calculated using the cross-section given in Figure 29.

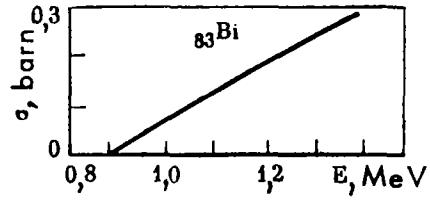

Figure 29 - Inelastic neutron scattering cross-section of bismuth, used for correcting B_o.

The comparison of B_o with the total cross-section which could have been done in this energy range, shows very good agreement. In the energy range from 1.5 to 7 MeV the experimental data do not agree well between one another. This is probably partly due to resonance effects. In this energy range, and up to 15 MeV, the curve $B_o(E)$ has been derived starting from the well-known difference $\sigma_T - \sigma_{ne}$ /13, 16/. At 14 MeV this difference agrees well with B_o which was obtained from the results of a whole group of authors. When evaluating these results, preference has been given to data by Croos /C-7/ and Hudson /H-4/, obtained with highest accuracy . Satisfactory agreement between the energy dependence of $\sigma_T - \sigma_{ne}$ and the results calculated by the optical model permit the derivation of the energy dependence of the high angular moments from the calculated data.

The values of the moments B_8 to B_{12} are given in Table 29.

The values of the moments B_{13} and B_{14} at 14 MeV, corresponding to the angular distribution eye-guide curve in BNL-400/2/ are : 1.79 and 0.38 barn, respectively.

Table 29

Ref.	E, MeV	B_8	B_9	B_{10}	Ref.	E, MeV	B_8	B_9	B_{10}	B_{11}	B_{12}
[П—1]	2,9	—0,421	—	—	[B—6]	4,21	2,46	1,53	0,688	0,143	—
[B—20]	3,2	—0,874	—	—	[W—12, W—13]	6,0	2,36	1,15	—	—	—
[2]	3,3	1,22	1,15	0,669	[B—2]	7,0	4,75	3,23	1,33	—0,26	—0,54
[W—5]	4,1	3,13	1,37	0,398	[2]	14	12,7	11,82	10,15	7,55	4,35
					[Г—2, Г—3]	4,0	3,22	2,05	1,04	0,441	—

$_{83}$Bi

1 — [2]; [S — 2] — S. C. Snowdon (1954)
2 — [2]; [W — 4] — M. Walt (1954)
[D — 1] — S. E. Darden (1954)
[L — 1] — G.N.Lovchikova (1957)
3 — [2]; [W — 5] — M. Walt (1955)
4 — [2]; [A — 5] — R. C. Allen (1956)
[D — 2] — S. E. Darden (1955)
5 — [2]; [B — 2] — J. R. Beyster (1956)
6 — [2]; [R — 2] — A. E. Remund (1956)
[B — 1] — H. R. Brugger (1955)
7 — [2]; [P — 1] — V.I.Popov (1957)
8 — [L — 2] — A. Langsdorf (1957)
9 — [2]; [P — 2] — M.V.Pasechnik (1958)
10 — [2]; [R — 4] — L. A. Rayburn (1959)
[Y — 1] — K. Yuasa (1958)
[R — 3] — L. Rosen (1957)
[E — 1] — J. O. Elliott (1956)
[S — 11] — V.I.Strizhak (1961)
[C — 7] — W. G. Croos (1960)
[B — 5] — S. Berko (1958)
[H — 4] — C. I. Hudson (1962)
11 — [2]; [B — 6] — N. A. Bostrom (1959)
12 — [2]; [L — 2] — G.N.Lovchikova (1960)
13 — [2]; [W — 12] — R. M. Wilenzick (1962)
[W — 13] — R. M. Wilenzick (1965)
14 — [S — 14] — A. B. Smith (1964)
15 — [K — 7] — I.A.Korzh (1964)
16 — [P — 5] — M.V.Pasechnik (1964)
17 — [P — 6] — V.I.Popov (1965)
[K — 8] — L.Ya.Kazakova (1965)
18 — [G — 3] — G.V.Gorlov (1965)
[G — 2] — G.V.Gorlov (1964)
19 — [B — 20] — R. L. Becker (1966)

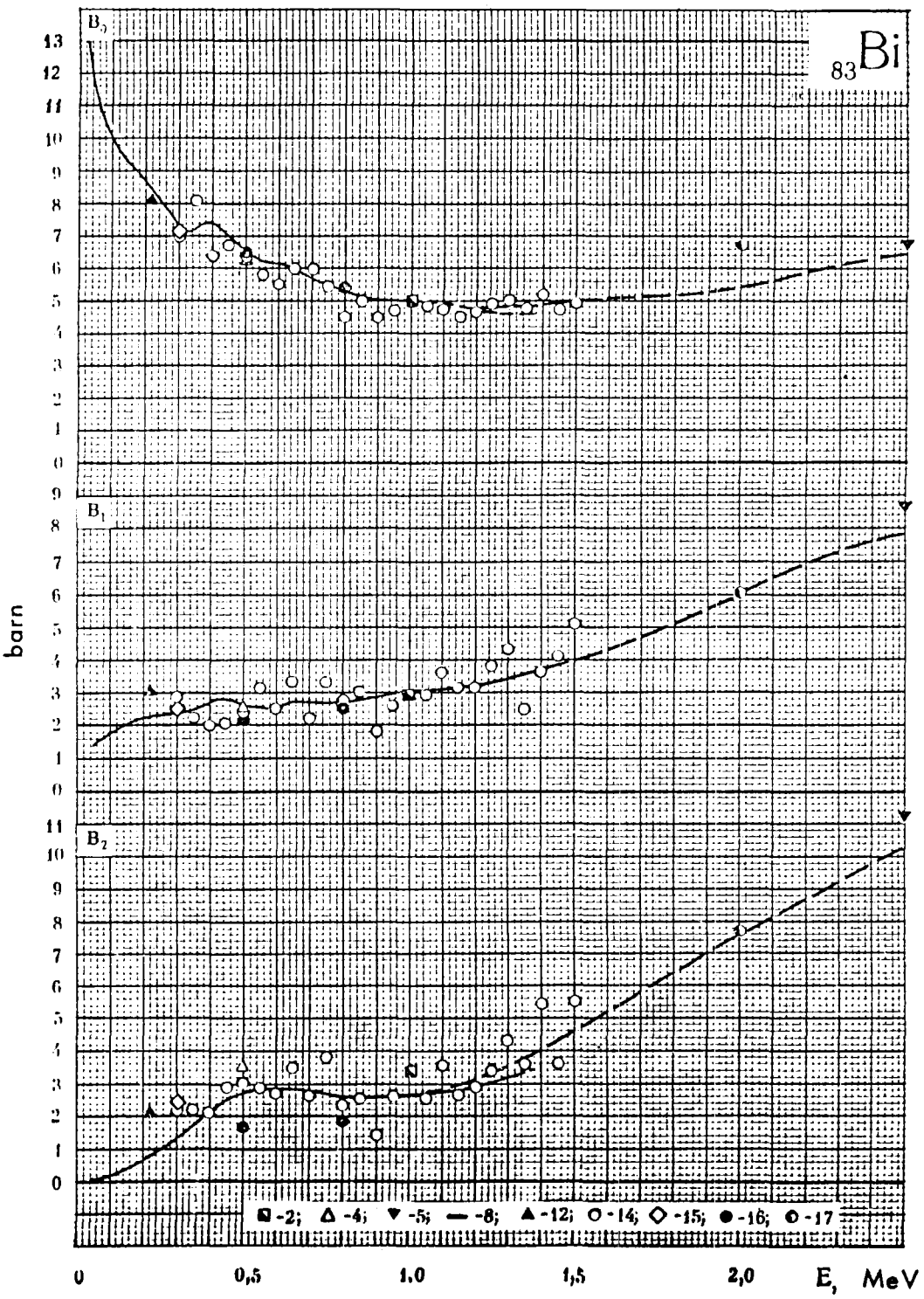
$_{83}$Bi
B_0
B_1
B_2
barn
E, MeV
0
0,5
1,0
1,5
2,0
-2; -4; -5; -8; -12; -14; -15; -16; -17

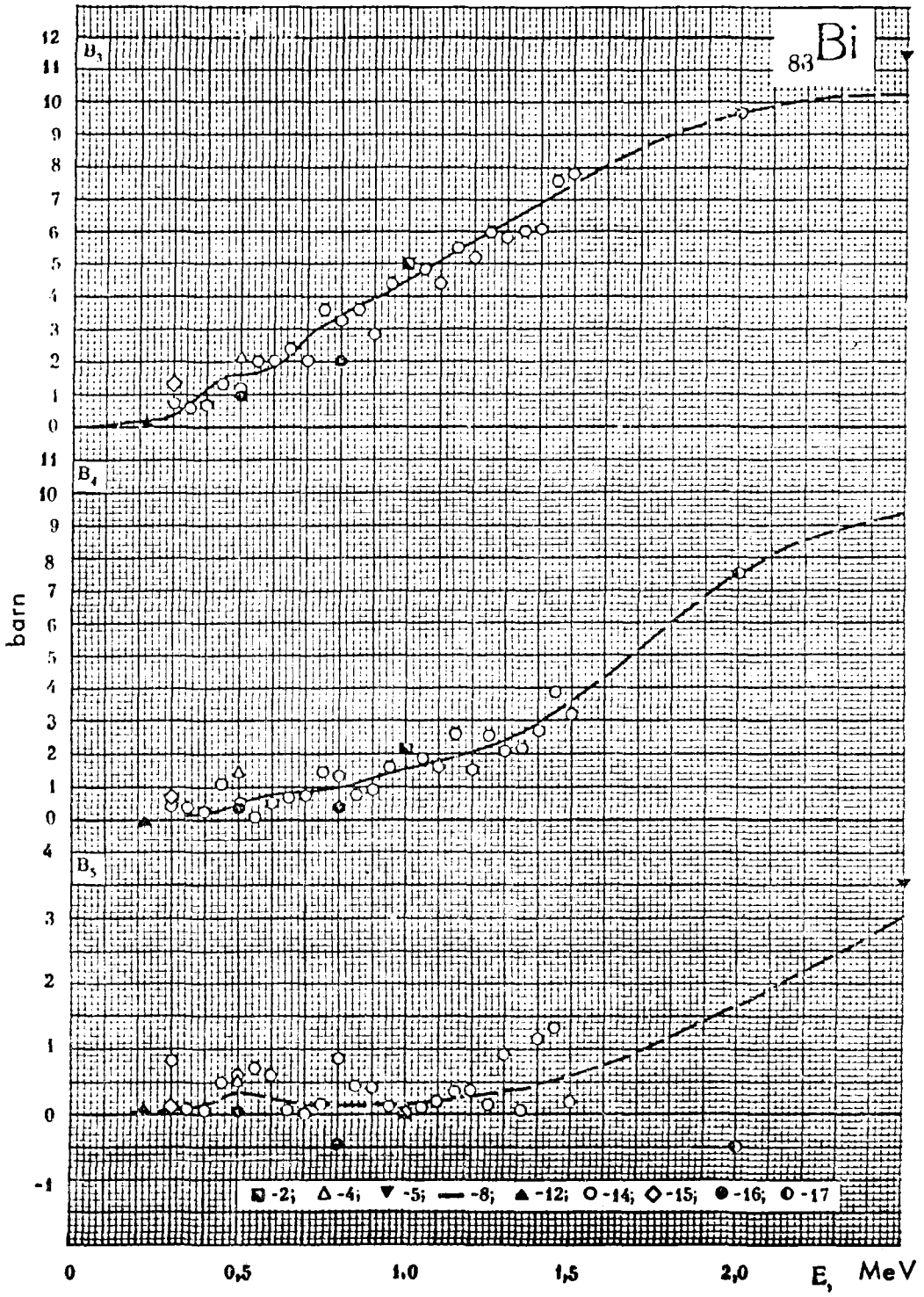
$_{83}$Bi
B_3
B_4
B_5
barn
12
11
10
9
8
7
6
5
4
3
2
1
0
-1
0
0,5
1,0
1,5
2,0
E, MeV
-2; -4; -5; -8; -12; -14; -15; -16; -17

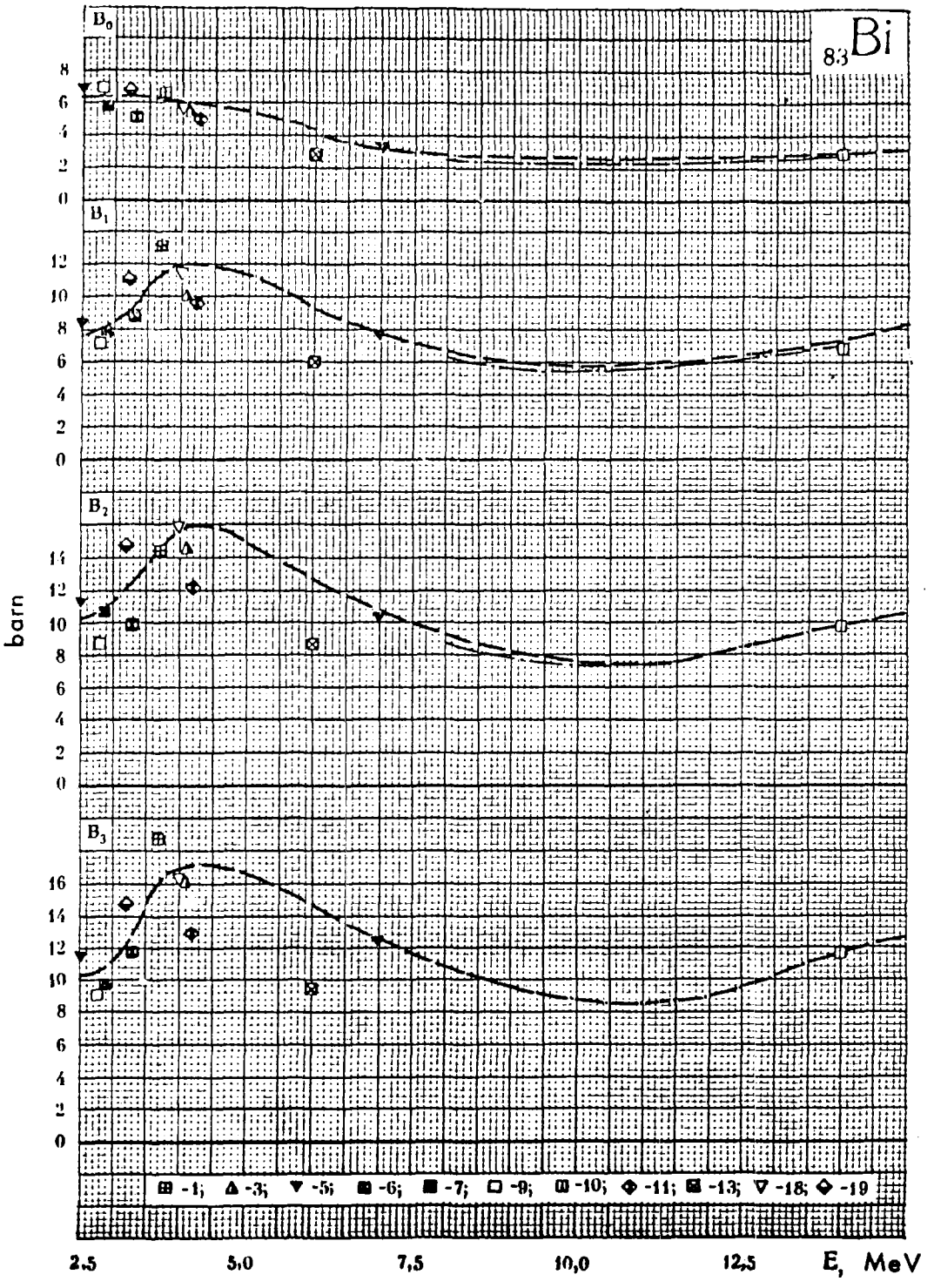
$_{83}$Bi
B_0
B_1
B_2
B_3
barn
E, MeV
2,5
5,0
7,5
10,0
12,5
-1; -3; -5; -6; -7; -9; -10; -11; -13; -18; -19

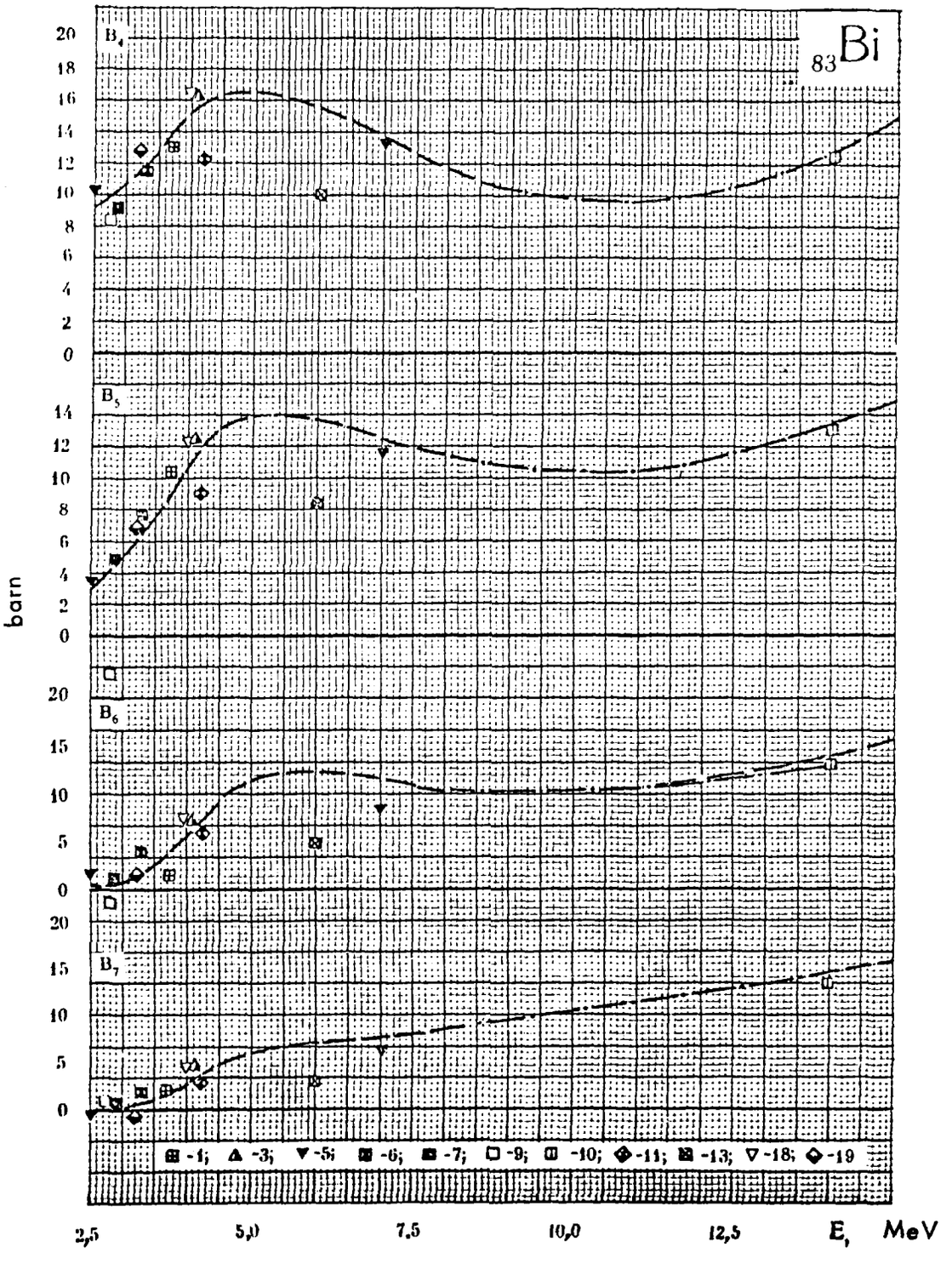
$_{83}$Bi
B_4
B_5
B_6
B_7
barn
20
18
16
14
12
10
8
6
4
2
0
15
5
■ -1; △ -3; ▼ -5; ▣ -6; ■ -7; □ -9; ◫ -10; ◈ -11; ▩ -13; ▽ -18; ◇ -19
2,5
5,0
7,5
10,0
12,5
E, MeV

T H O R I U M

At low energies (1.5 MeV) the data by Langsdorf /L-2/ and Smith /S-14/ agree with one another within the experimental accuracy. The nonelastic cross-section used for correcting B_o is given in Figure 30. Older data given in references /S-10/ and /W-4, D-1/ for the energy range 1.0 - 1.25 MeV appear to be too high. At the same time, in the interval 1.0 - 1.5 MeV the scattering cross-section obtained in reference /L-2/ is a bit lower (about 0.5 barn) than the difference $\sigma_T - \sigma_{ne}$ which can be estimated with the data in references /16/ and /13/ to an accuracy of $\sim$ 0.3 barn. In this range, the values B_o obtained in reference /S-14/ agree better with the values of the above-mentioned difference. At 2 Mev the closely concording results of the references /B-15/ and /P-6/ are also in good agreement with the estimated value $\sigma_T - \sigma_{ne}$. In the range above 2.5 MeV, the data with the highest reliability are obviously that by Batchelor /B-15/(1965). The results of the earlier work by Popov /P-3/ are too low. The results obtained by optical model calculation lie considerably lower than the experimental data. One must point out that the calculated total cross-section values are also 0.5 - 1 barn lower in the range 3 - 5 MeV than the majority of the experimental data /16/.

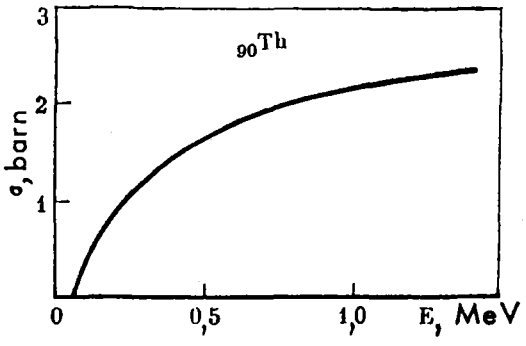

Figure 30 - Inelastic neutron scattering cross-section of thorium, used for correcting B_o.

The values of the high moments are given in Table 30.

Table 30

Ref.	E, MeV	B_8	B_9	B_{10}	B_{11}	B_{12}	B_{13}	B_{14}	B_{15}
[B—15]	3,0	1,44	1,02	0,522	—	—	—	—	—
[B—15]	4,0	3,02	1,07	—	—	—	—	—	—
[B—15]	7,0	9,67	8,28	5,93	3,71	1,95	0,86	—	—
[B—19]	5,0	3,15	1,71	0,517	—	—	—	—	—
[H—4]	15,2	15,2	13,8	13,5	10,9	8,38	4,48	2,34	0,455

$^{232}_{90}$Th

1 — [2]; [W — 4] — M. Walt (1954)
[D — 1] — S. E. Darden (1954)
2 — [L — 2] — A. Langsdorf (1957)
3 — [P — 3] — V. I. Popov (1961)
4 — [2]; [S — 10] — A. B. Smith (1962)
5 — [H — 4] — C. L. Hudson (1962)
6 — [S — 14] — A. B. Smith (1964)
7 — [P — 6] — V. I. Popov (1965)
[K — 8] — L. Ya. Kazakova (1965)
8 — [B — 15] — R. Batchelor (1965)
9 — [B — 19] — S. G. Buccino (1966)

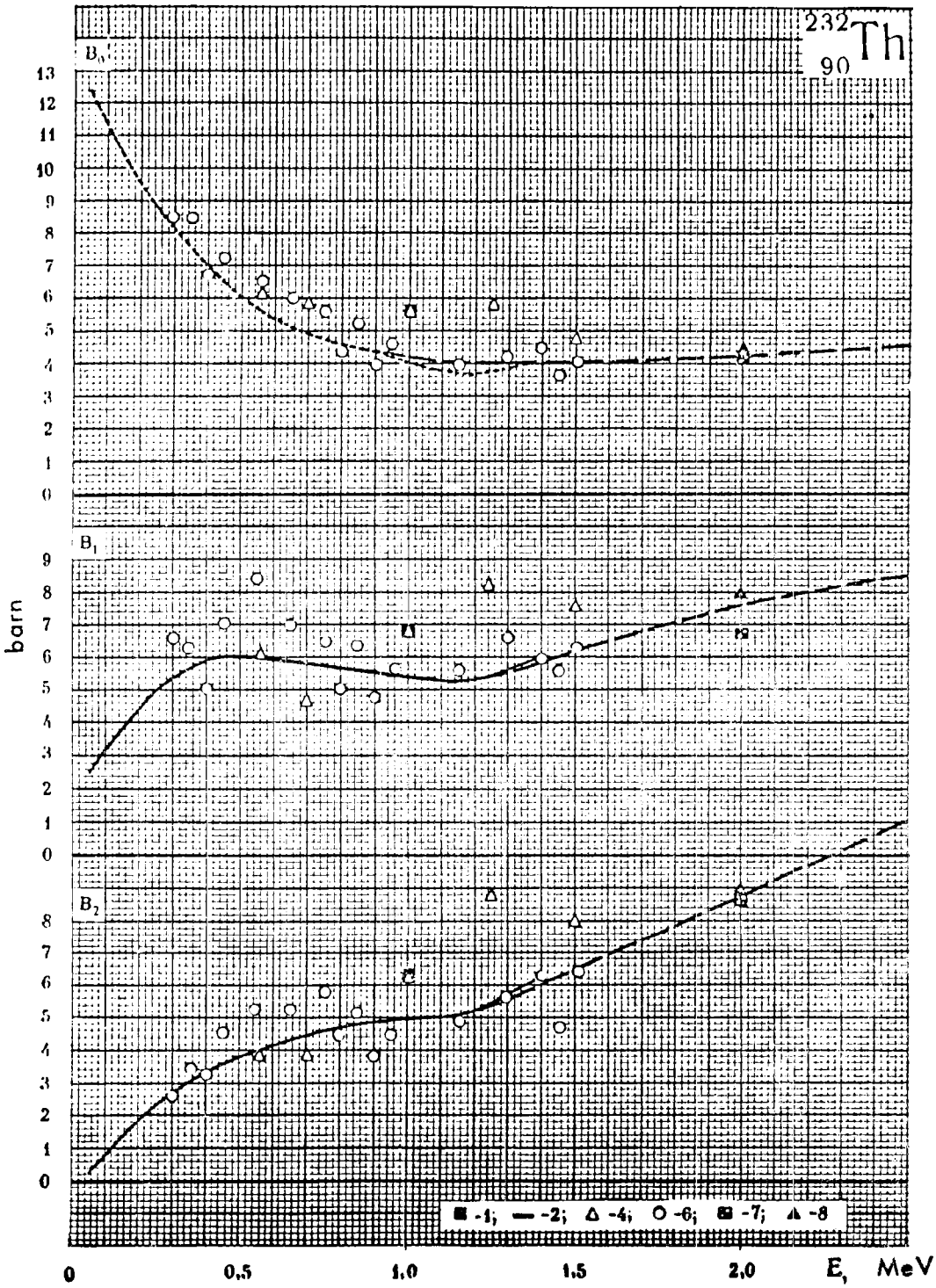
$^{232}_{90}$Th
B_0
B_1
B_2
barn
E, MeV
0
0,5
1,0
1,5
2,0
■ -1; — -2; Δ -4; O -6; ▣ -7; ▲ -8

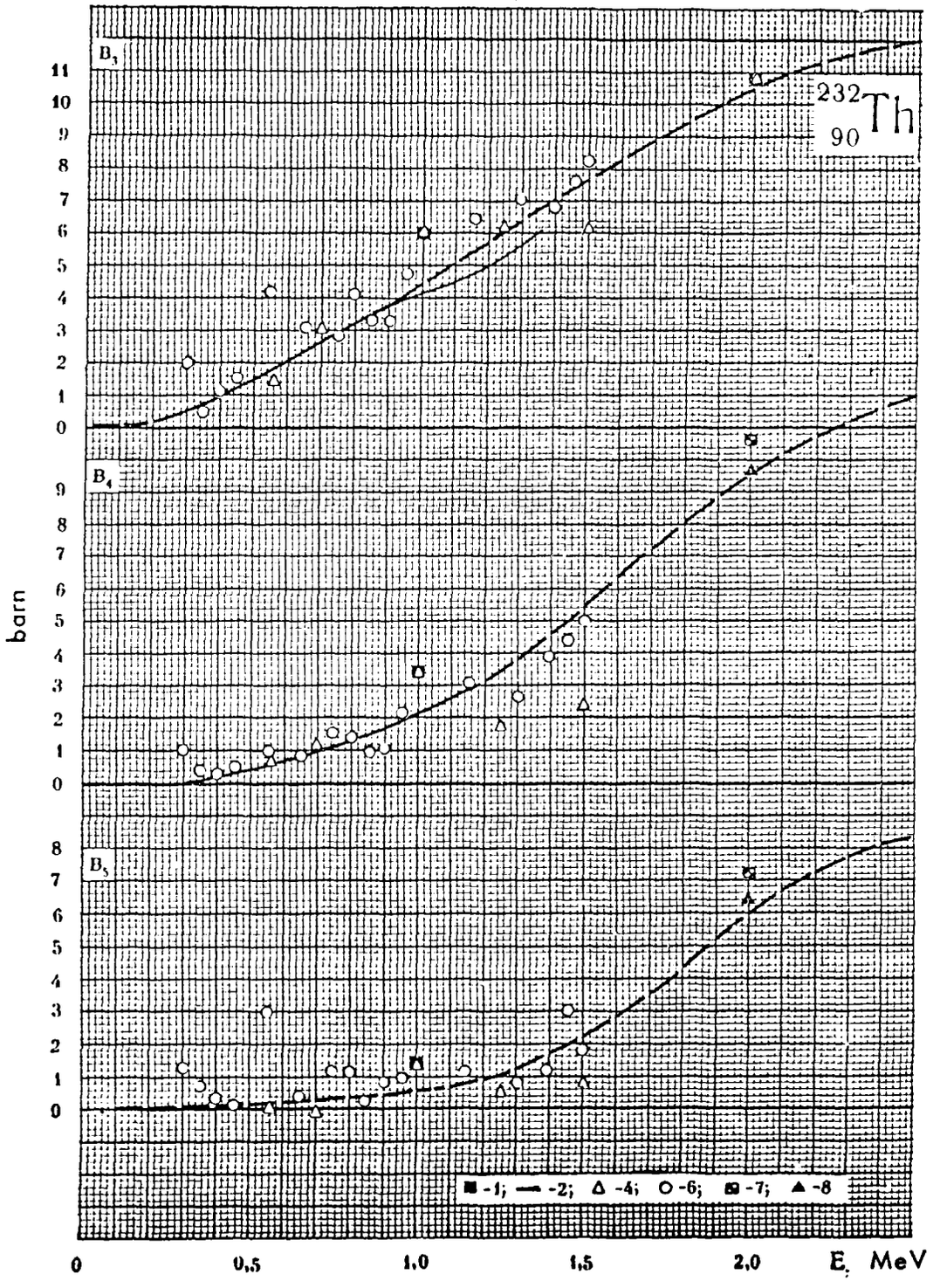
B_3
B_4
B_5
$^{232}_{90}Th$
barn
■ -1; — -2; Δ -4; ○ -6; ⊠ -7; ▲ -8
0
0,5
1,0
1,5
2,0
E, MeV

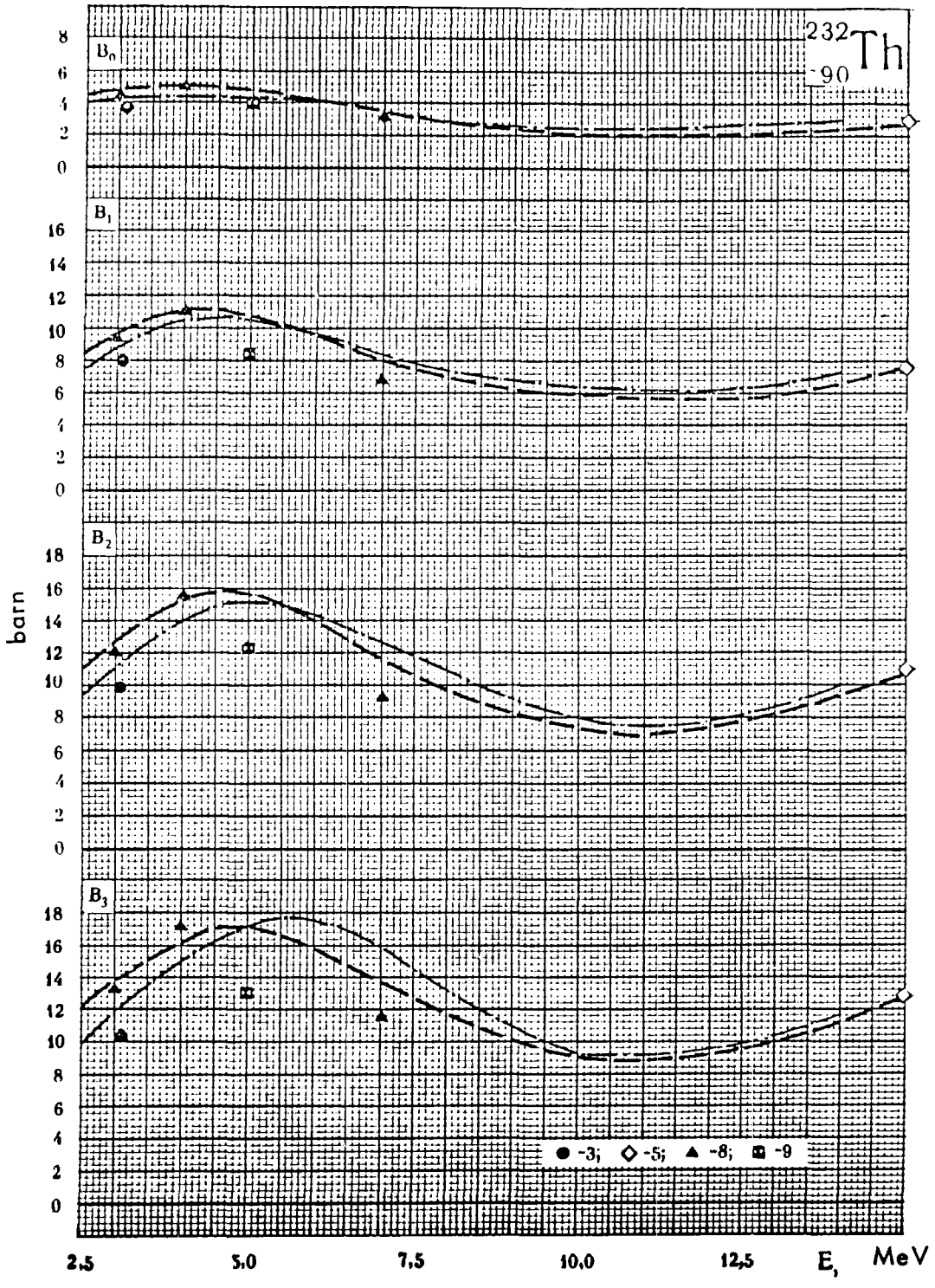
232 90 Th
B0
B1
B2
B3
barn
● -3; ◇ -5; ▲ -8; ⊠ -9
2,5
5,0
7,5
10,0
12,5
E, MeV

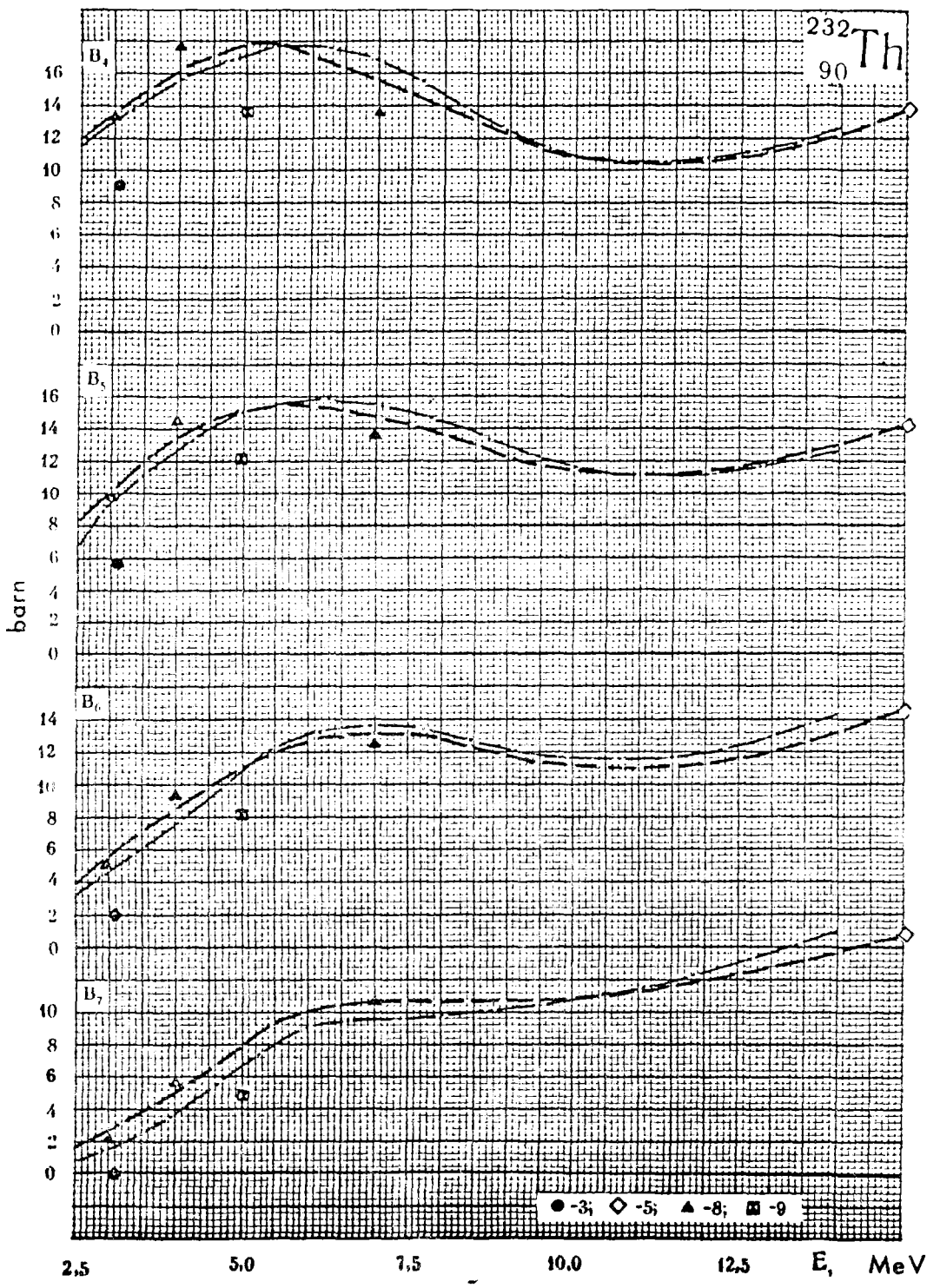
232 90 Th
B4
B5
B6
B7
barn
● -3; ◇ -5; ▲ -8; ⊠ -9
2,5
5,0
7,5
10,0
12,5
E, MeV

U R A N I U M - 235

Experimental data on elastic neutron angular distribution of U-235 are only available for energies below 2 MeV. The results of different works agree well between one another, as well as with the values of the difference $\sigma_T - \sigma_{ne}$ estimated with the data given in references /13/ and /16/. The greatest difference occurs at 2 MeV : B_o from reference /C-6/ is equal to (4.14 ± 0.2) barn, while $\sigma_T - \sigma_{ne} = 3.8$ barn. We would like to point out that, in the range from 2 to 5 MeV, the calculated total cross-sections are 0.3 - 0.8 barn lower than the experimental data, and they merge only at 6 MeV. At higher energies the calculated total cross-section falls more steeply than the experimental data, and in the range 10 - 15 MeV the difference between them is again 0.5 barn. The difference between the calculated and the experimental nonelastic cross-section values is not large.

The recommended curve $B_o(E_n)$ in the energy range above 1 MeV has been derived on the basis of the available data on the difference between the total and the nonelastic cross-section. For the derivation of the remaining curves we relied on the results calculated by the optical model, but, taking into account the difference between the energy dependence of the calculated values of B_o and the difference $\sigma_T - \sigma_{ne}$.

$^{235}_{92}U$

1 — [2]; [A — 5] - R. C. Allen (1956)
[A — 7] - R. C. Allen (1957)
2 — [2]; [C — 6] — L. Cranberg (1959)
3 — [2]; [A — 5] - R. C. Allen (1956)
[A — 7] - R. C. Allen (1957)
[C — 6] — L. Cranberg (1959)
4 — [S — 14] — A. B. Smith (1964)
[S — 15] — A. B. Smith (1964)

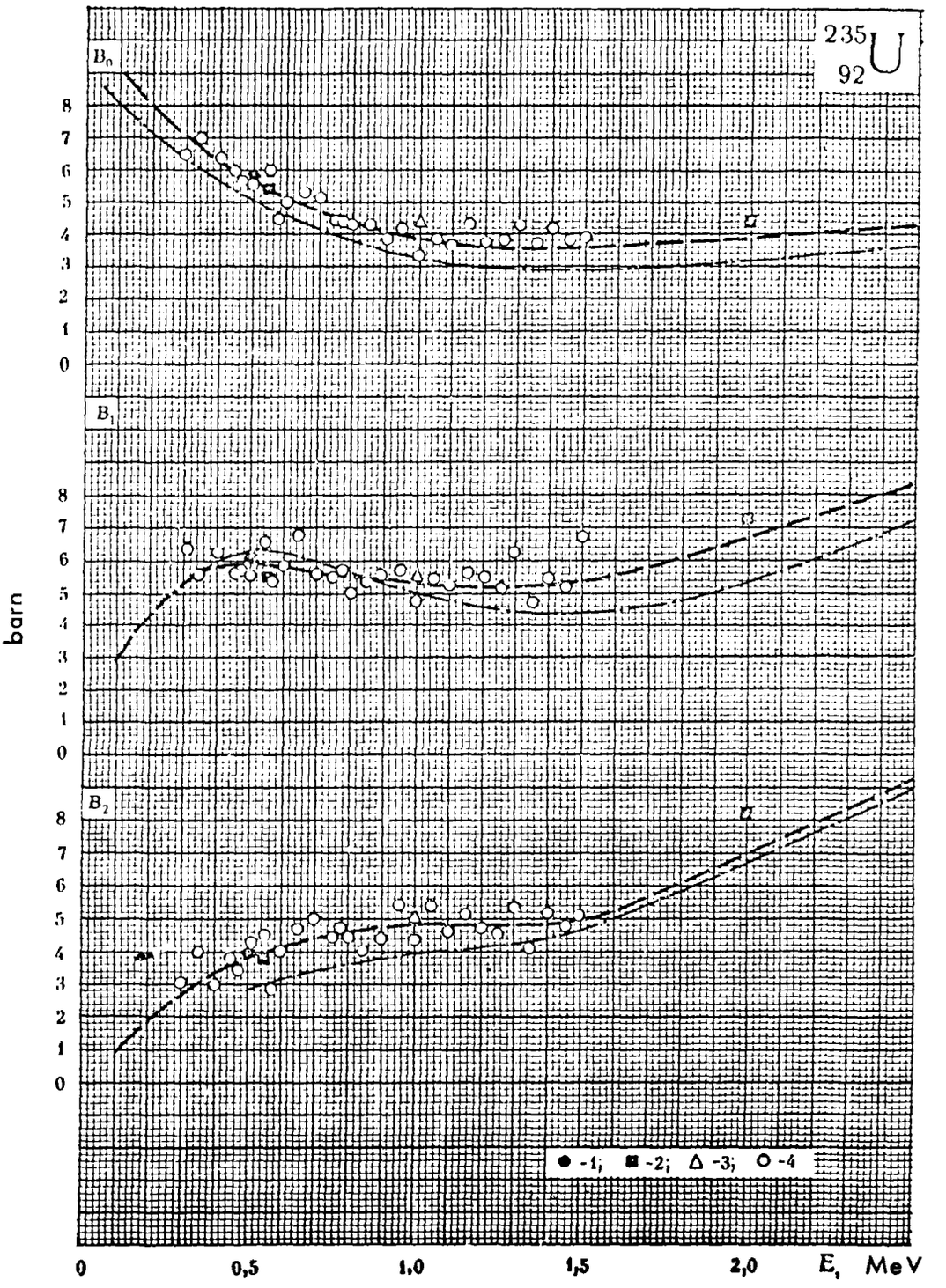
$^{235}_{92}U$
B_0
B_1
B_2
barn
0
1
2
3
4
5
6
7
8
● -1; ■ -2; Δ -3; ○ -4
0
0,5
1,0
1,5
2,0
E, MeV

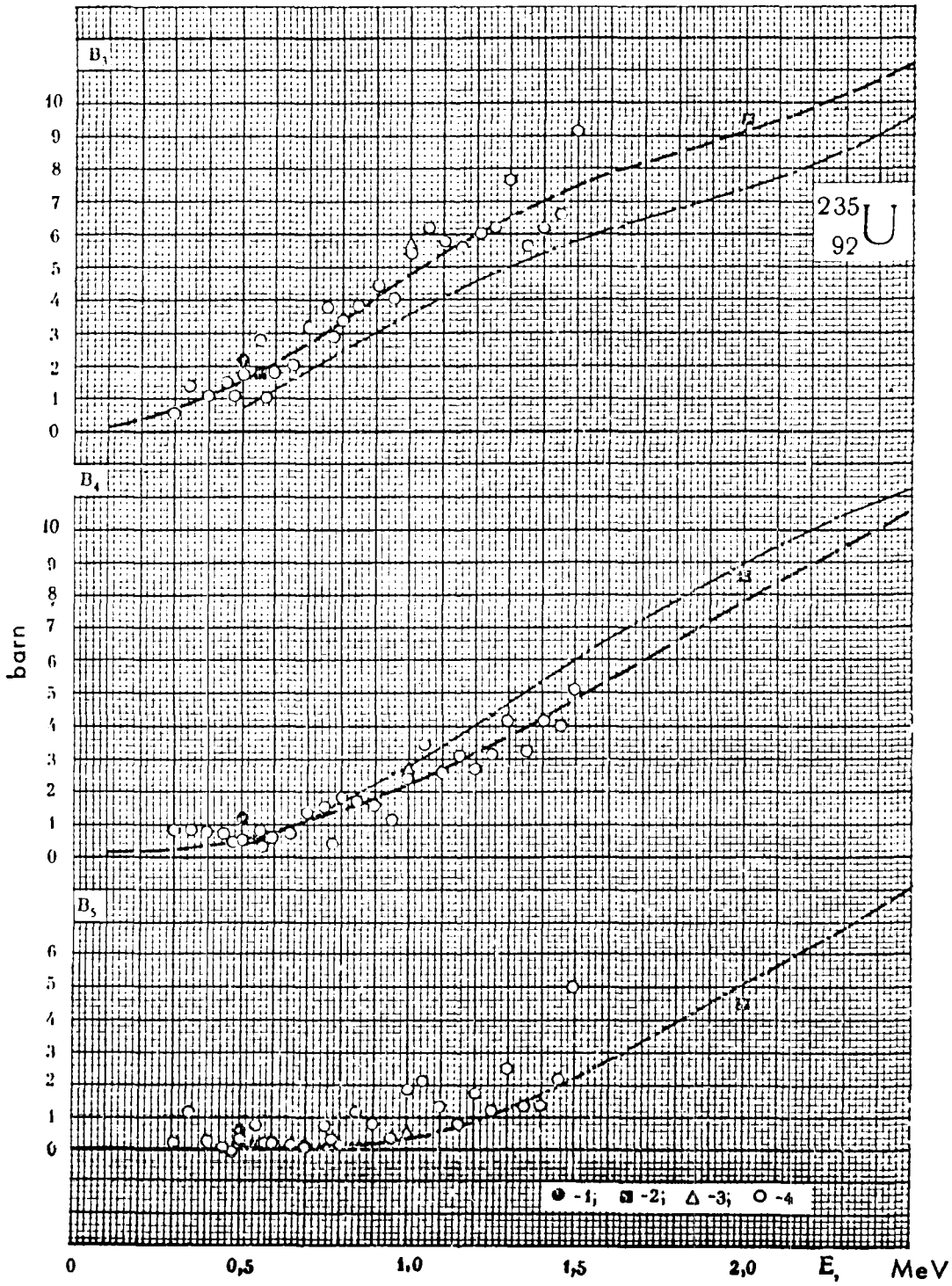
B_3
B_4
B_5
barn
$^{235}_{92}U$
● -1; ■ -2; Δ -3; ○ -4
0
0,5
1,0
1,5
2,0
E, MeV

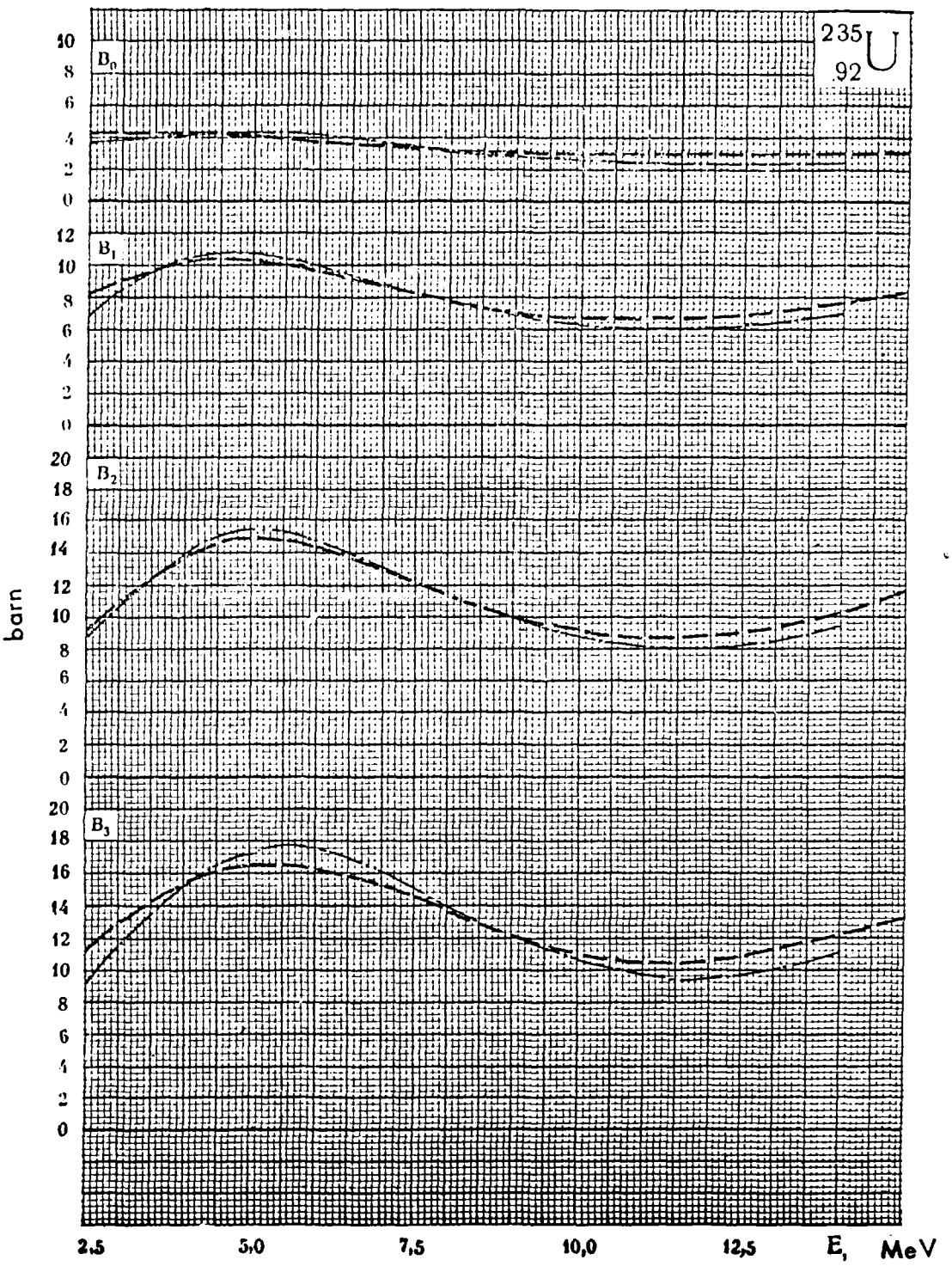
$^{235}_{92}U$
B_0
B_1
B_2
B_3
barn
E, MeV
2,5
5,0
7,5
10,0
12,5

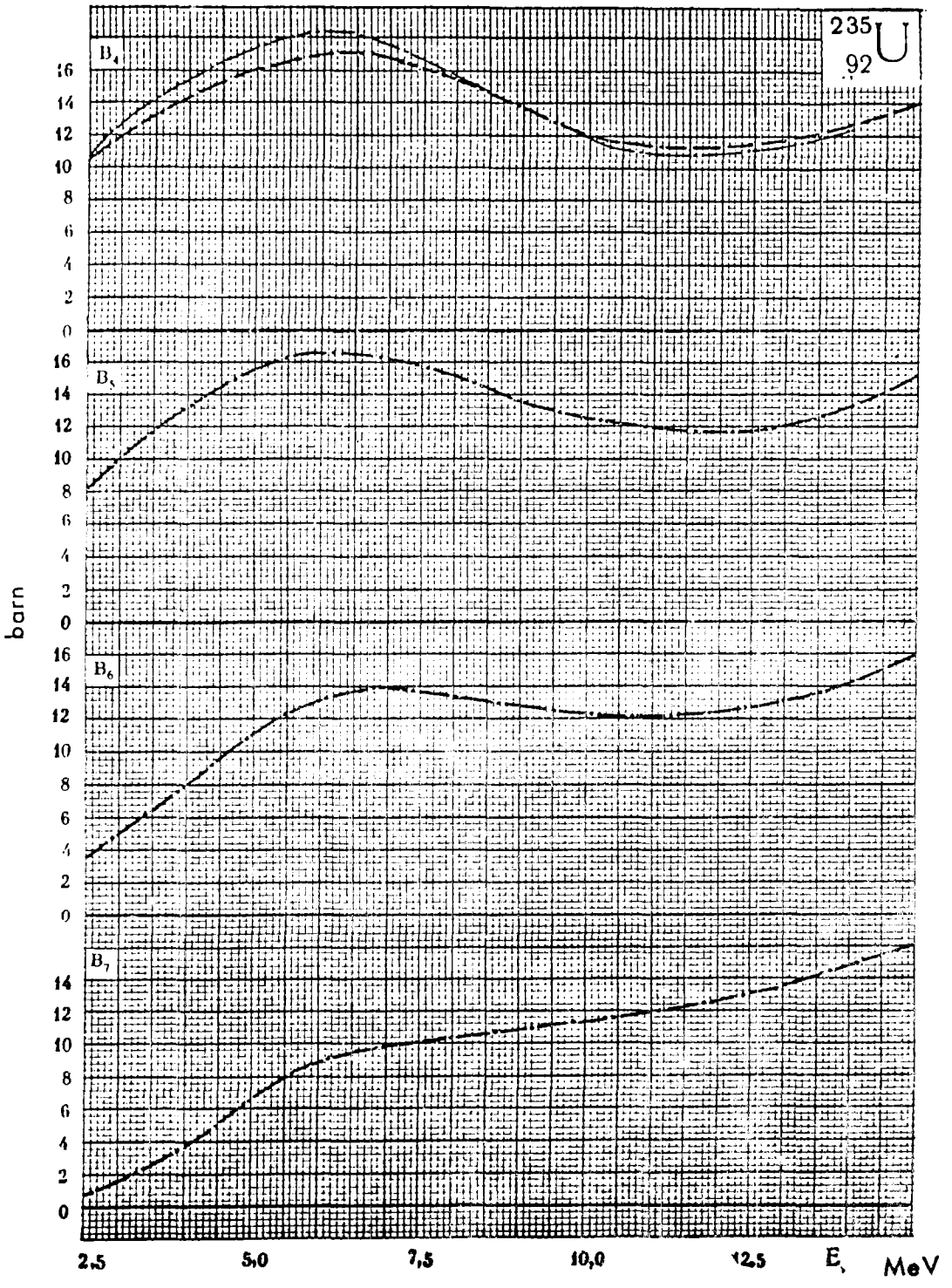
$^{235}_{92}U$
B_4
B_5
B_6
B_7
barn
0
2
4
6
8
10
12
14
16
2,5
5,0
7,5
10,0
12,5
E_n
MeV

U R A N I U M - 238

The most detailed and, obviously the most reliable experimental results of angular distribution of neutrons scattered on U-238 in the energy range below 2 MeV have been obtained by Lane et al. /L-6/.

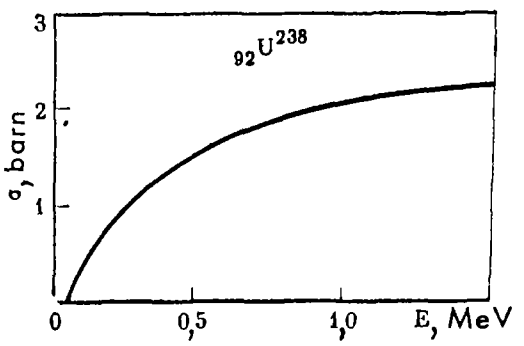

Figure 31 - Inelastic neutron scattering cross-section of U-238, used for correcting B_o.

The results of earlier works by Langsdorf /L-2/(1957) and Smith /S-14/(1964) confirm these results. The results of the majority of other works agree well with his data. In the range 0 - 2.5 MeV the trend of B_o also agrees with the difference $\sigma_T - \sigma_{ne}$ /13/. The inelastic scattering cross-sections used for correcting B_o are given in Figure 31.

At energies above 2.5 MeV information is rare, and the difference $\sigma_T - \sigma_{ne}$ is difficult to estimate because of the absence of experimental data on σ_{ne}. A comparison with the results calculated by the optical model is not very constructive as the calculated total cross-sections in the range 2 - 4 MeV are 0.3 - 0.7 barn below the experimental values.

The values of the high moments are given in Tables 31 - 33.

Table 31

Ref.	E_n, MeV	B_8	B_9	B_{10}	B_{11}	B_{12}	B_{13}	B_{14}	B_{15}
[2]	14	12,90	13,36	11,37	10,79	7,35	5,13	2,22	1,03
[B—15]	7	9,97	8,23	5,85	3,54	1,88	0,666	—	—

Table 32

Ref.	E, MeV	B_n	Ref.	E, MeV	B_n	Ref.	E, MeV	B_n
	0,05	—0,539		0,407	0,359		1,24	0,498
	0,07	—0,647		0,430	0,636		1,34	0,218
	0,085	0,675		0,457	0,061		1,44	0,953
	0,100	—0,913		0,507	0,539		1,54	0,641
	0,120	—0,141		0,530	0,174		1,65	1,42
[L—6]	0,157	—0,372	[L—6]	0,630	0,076	[L—6]	1,75	1,48
	0,207	0,593		0,730	0,424		1,85	1,17
	0,257	—0,056		0,830	0,734		1,95	1,27
	0,307	0,196		0,930	0,178		2,25	2,66
	0,330	0,964		1,04	0,497		—	—
	0,357	—0,238		1,14	0,474		—	—

Table 33

Ref.	E, MeV	B_n	B_p	B_{10}	B_{11}	Ref.	E, MeV	B_n	B_p	B_{10}	B_{11}
[B—15]	2,0	0,168	—	—	—	[B—19]	5,0	2,66	1,68	0,843	—
[B—15]	3,0	1,70	0,729	—	—	[W—8]	7,0	5,48	3,62	1,90	0,587
[B—15]	4,0	3,04	0,603	—0,423	—	[B—15]	7,0	9,97	8,23	5,85	3,54
[W—8]	4,1	3,34	1,70	0,626	—	[2]	14	12,90	13,36	11,37	10,79

$^{238}_{92}U$

1 — [2]; [W — 2] — M. Walt (1953)
[A — 5] — R. C. Allen (1956)
[C — 6] — L. Cranberg (1959)
[G — 1] — W. B. Gilboy (1962)
2 — [2]; [W — 8] — M. Walt (1956)
3 — [2]; [A — 5] — R. C. Allen (1956)
4 — [L — 2] — A. Langsdorf (1957)
5 — [2]; [C — 5] — J. H. Coon (1958)
[G — 1] — B.Ya.Gyzhovskii (1961)
[H — 4] — C. I. Hudson (1962)
6 — [2]; [C — 6] — L. Cranberg (1959)
7 — [2a]; [L — 6] — R. O. Lane (1961)
8 — [S — 14] — A. B. Smith (1964)
[S — 13] — A. B. Smith (1963)
9 — [P — 5] — M.V.Pasechnik (1964)
10 — [K — 6] — I.A.Korzh (1964)
11 — [B — 15] — R. Bachelor (1965)
12 — [B — 16] — E. Barnard (1966)
13 — [B — 19] — S. G. Buccino (1966)

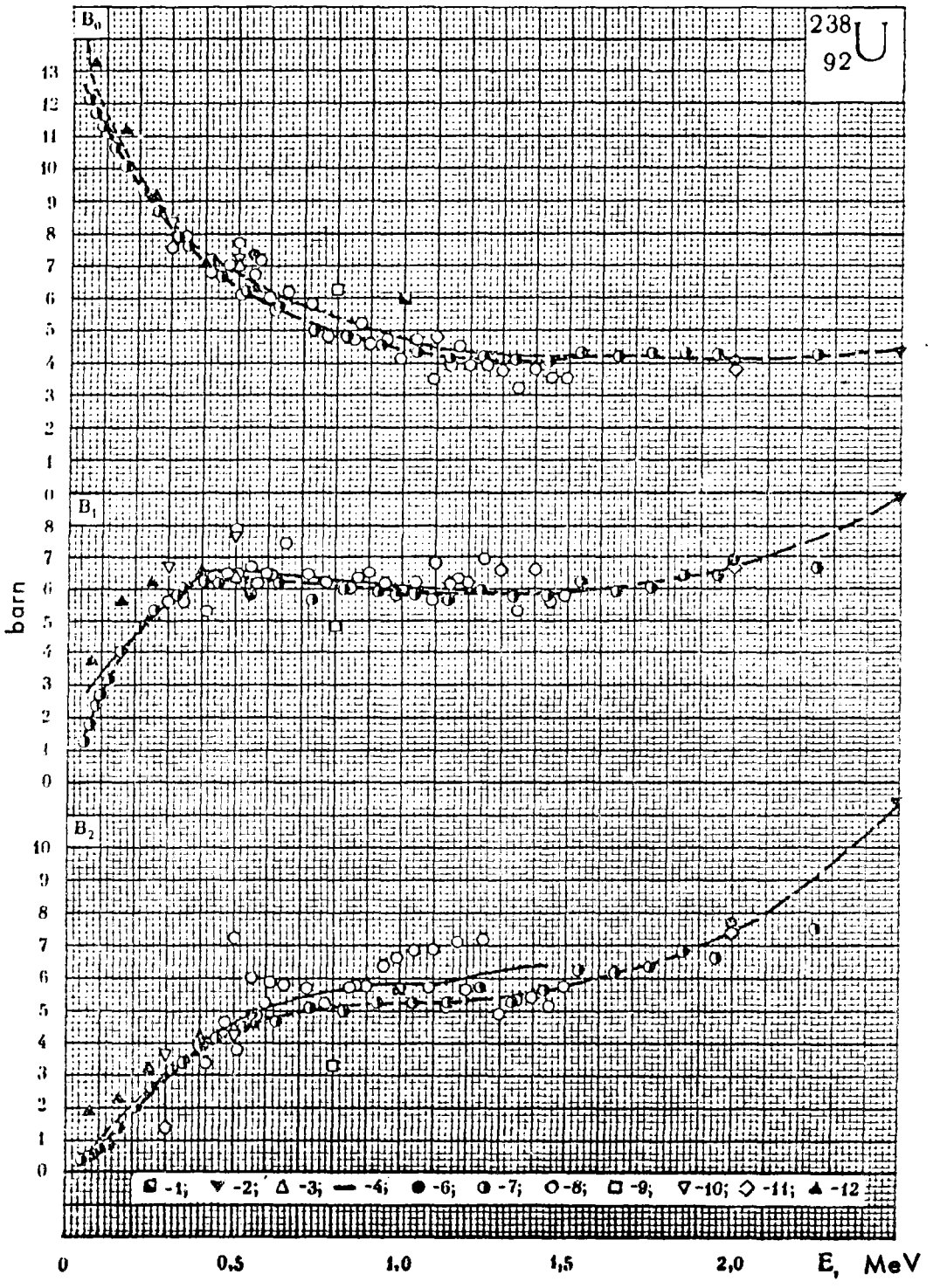
$^{238}_{92}U$
B_0
B_1
B_2
barn
E, MeV
0
0,5
1,0
1,5
2,0
■ -1; ▼ -2; Δ -3; — -4; ● -6; ◑ -7; ○ -8; □ -9; ▽ -10; ◇ -11; ▲ -12

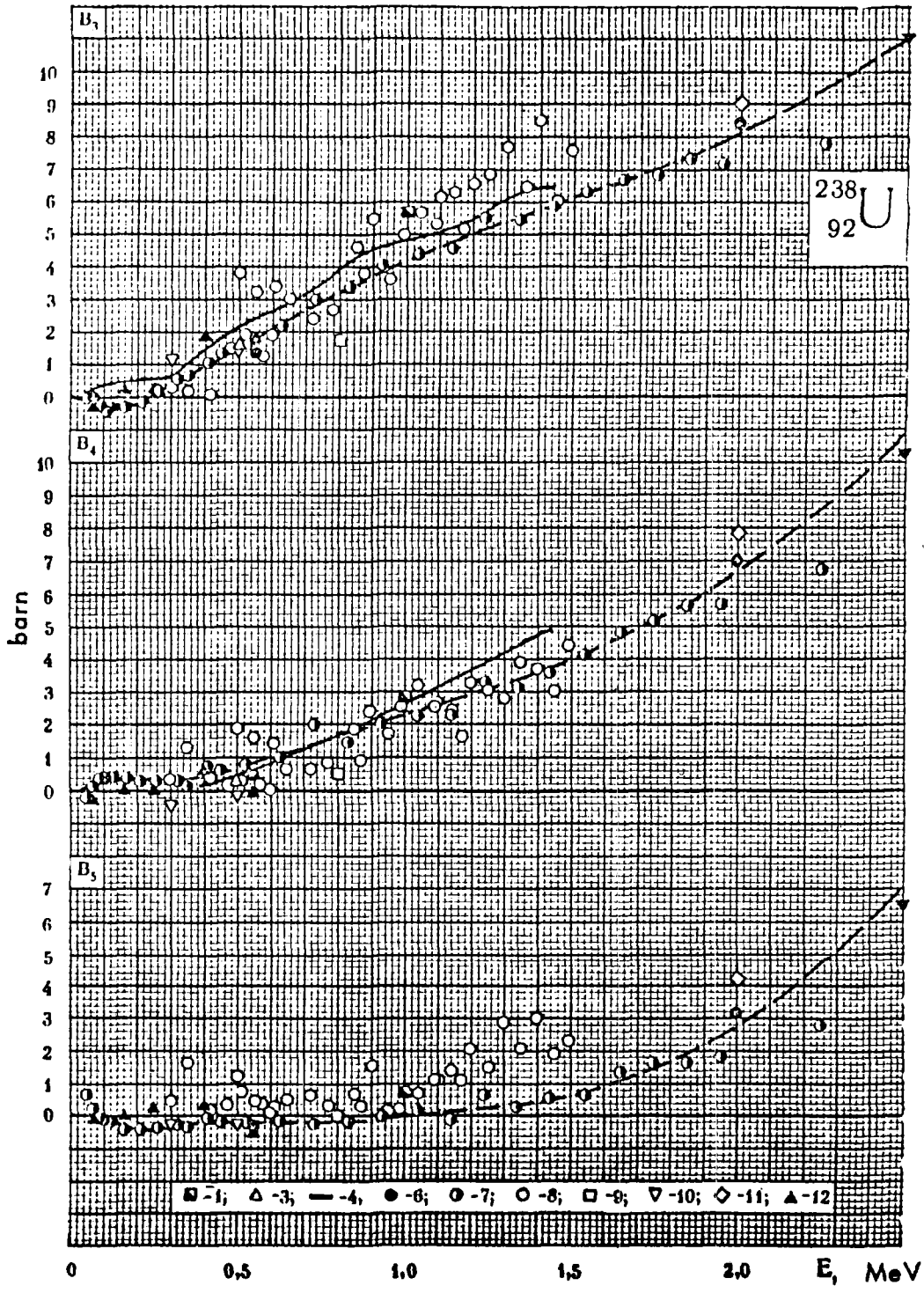
B1
B4
B5
barn
238 92U
1; 3; 4; 6; 7; 8; 9; 10; 11; 12
0
0,5
1,0
1,5
2,0
E, MeV

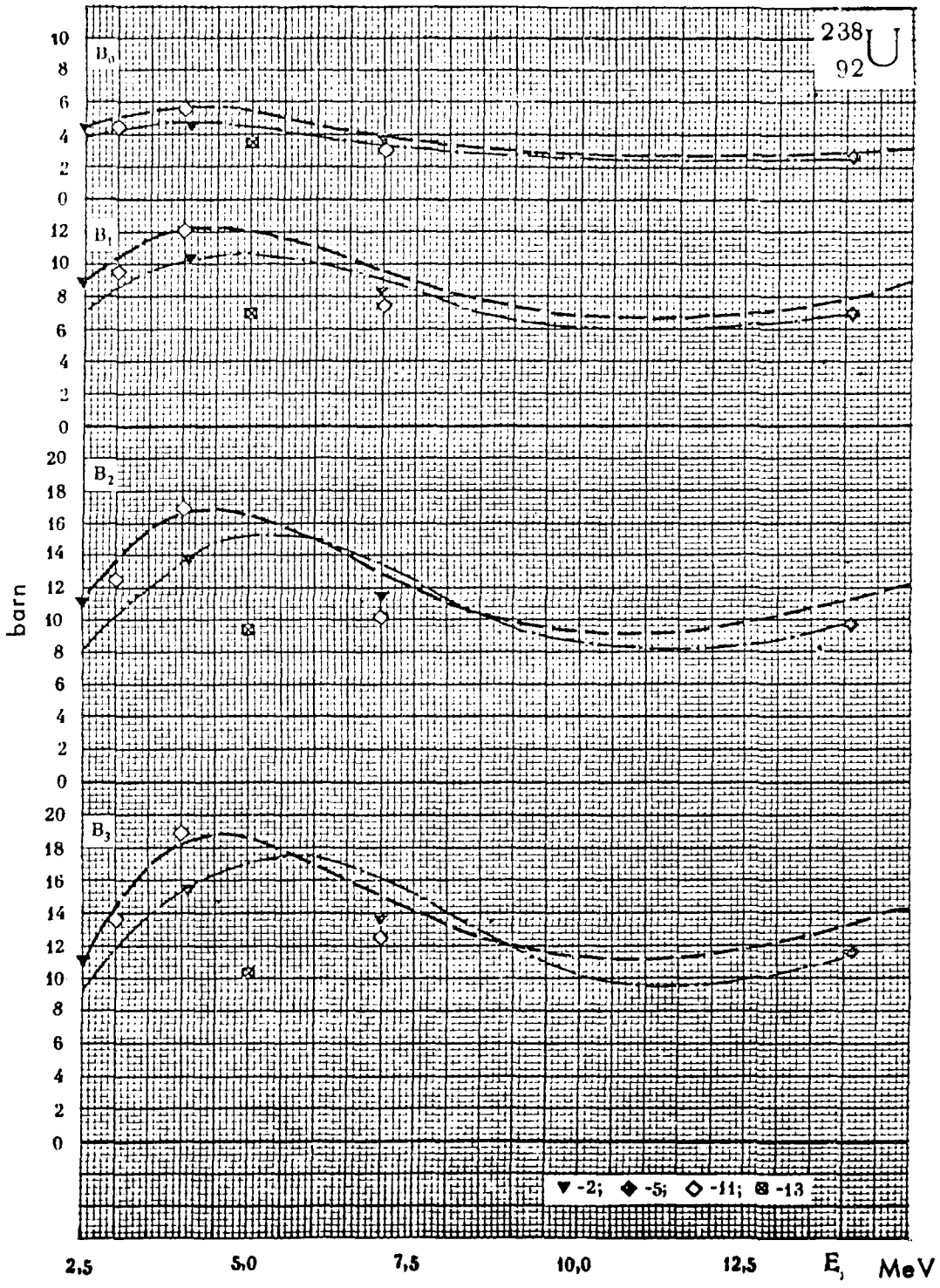
238 92 U
B0
B1
B2
B3
barn
▼ -2; ◆ -5; ◇ -11; ⊠ -13
2,5
5,0
7,5
10,0
12,5
E, MeV

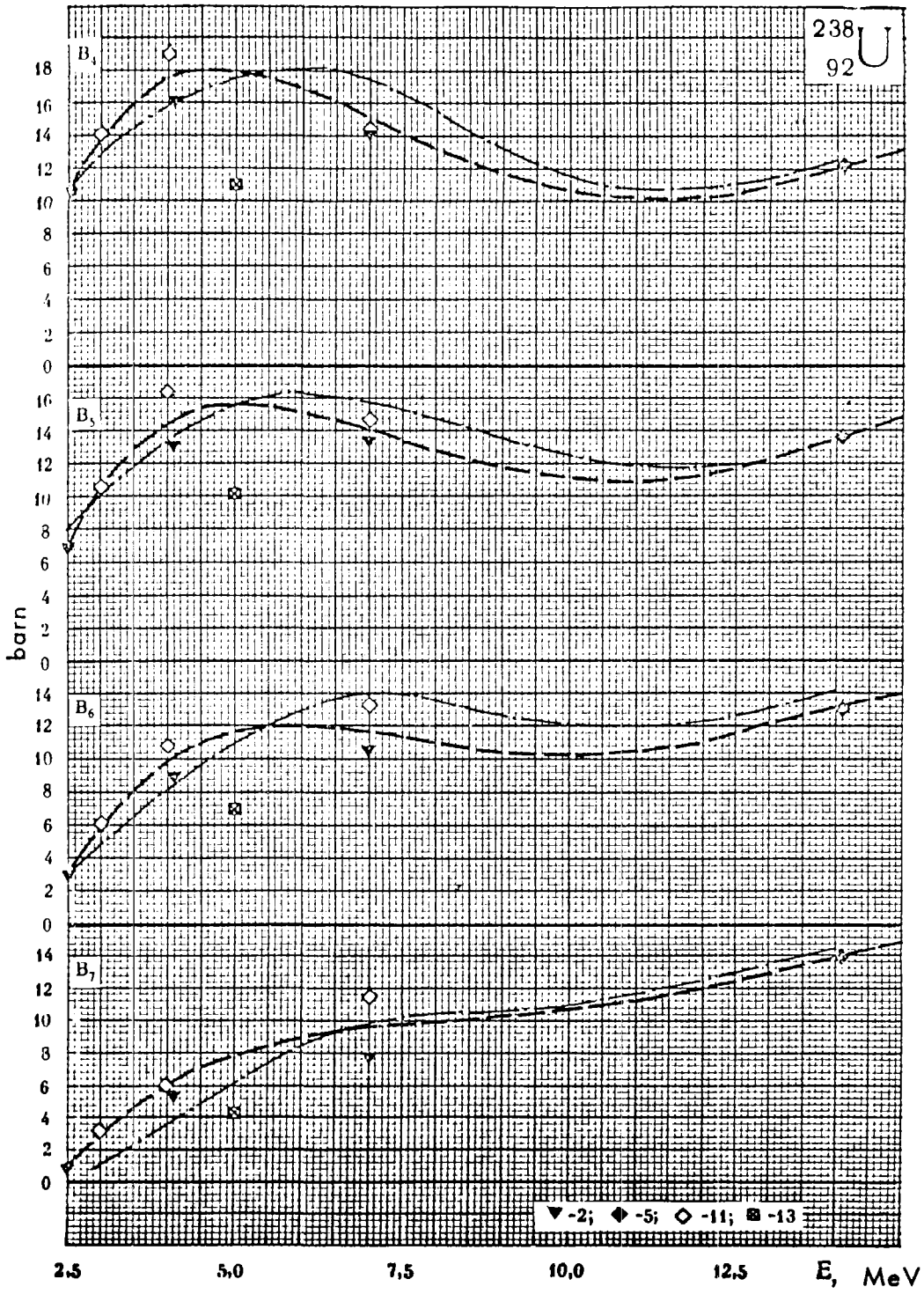
238 92 U
B4
B5
B6
B7
barn
▼-2; ◆-5; ◇-11; ▣-13
2,5
5,0
7,5
10,0
12,5
E, MeV

P L U T O N I U M - 239

Data on angular distribution of neutrons scattered elastically on plutonium are very rare. However, the data available do not contradict one another and permit smooth curves for B_ℓ to be obtained in the energy range 0.5 - 2 MeV : they agree with the data resulting from the subtraction of the nonelastic cross-section from the total cross-section.

The curves for $B_\ell (E_n)$ at $E_n < 0.5$ MeV have been obtained assuming that B_ℓ / B_o concord for U-238 and Pu-239. From the difference between the calculated and the experimental total cross-section one concludes that the data calculated by the optical model in the energy range from 2 to 6 MeV are too low : the uncertainty of B_o at 3 MeV can reach 1 barn. The recommended curve $B_o(E_n)$ in this energy range was derived on the basis of the values $\delta_T - \delta_{ne}$ /13, 16/, the accuracy of which was not high. The curves for the high moments were derived on the basis of the available experimental data and the values calculated by the optical model, taking into account the difference between calculated values of B_o and the difference $\delta_T - \delta_{ne}$.

At 13.9 MeV the values of the high moments derived from reference /D-3/ are : $B_8 = 13.16$, $B_9 = 12.48$, $B_{10} = 11.86$, $B_{11} = 10.42$, $B_{12} = 8.11$, $B_{13} = 5.43$, $B_{14} = 3.25$ and $B_{15} = 1.51$.

$^{239}_{94}Pu$

1 — [2]; [A — 5] — R. C. Allen (1956)
[A — 7] — R. C. Allen (1957)
2 — [2]; [C — 6] — L. Cranberg (1959)
3 — [2]; [A — 5] — R. C. Allen (1956)
[A — 7] — R. C. Allen (1957)
[C — 6] — L. Cranberg (1959)
4 — [D — 3] — D. Didier (1964)

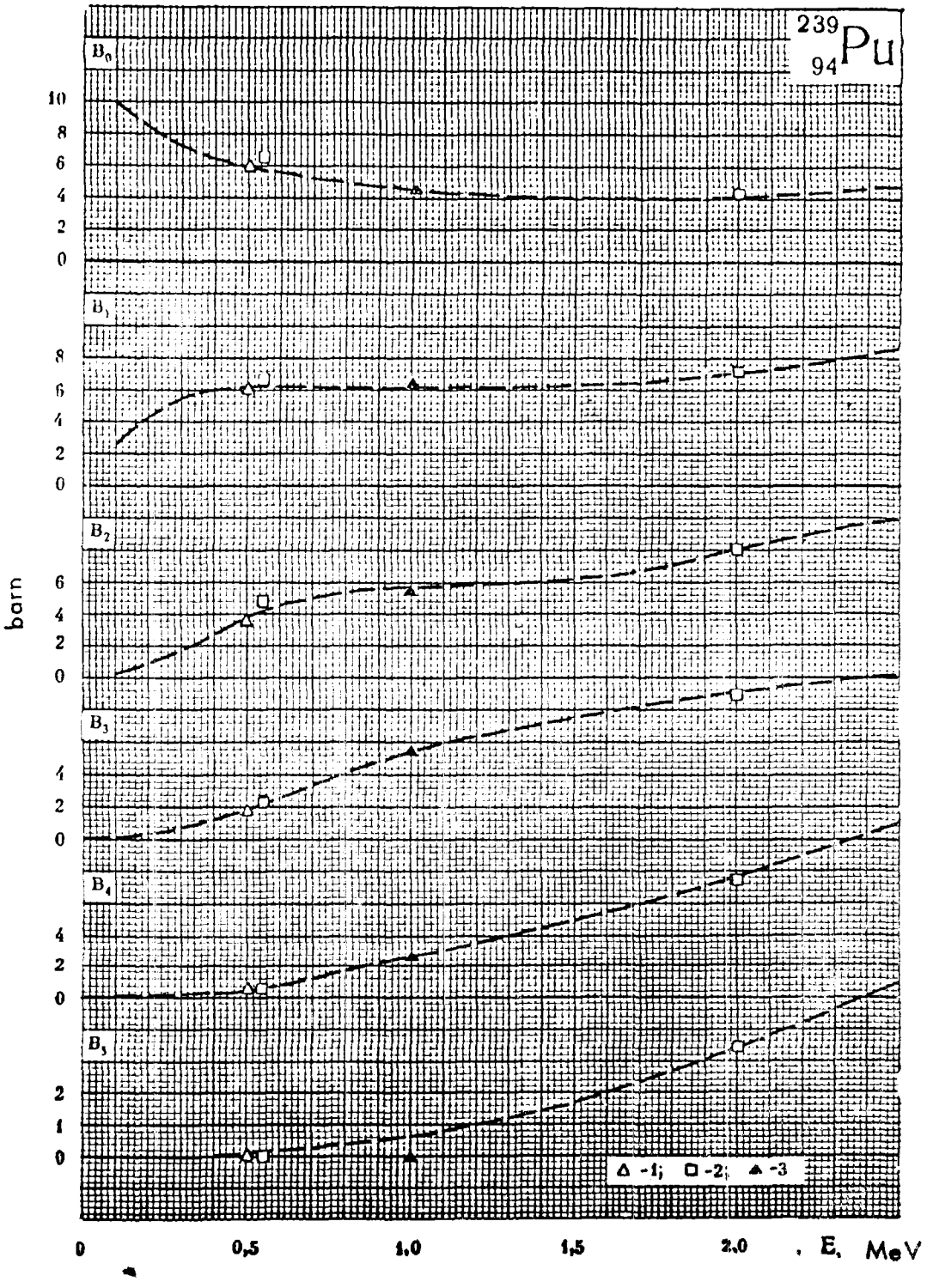
$^{239}_{94}Pu$
B_0
B_1
B_2
B_3
B_4
B_5
barn
Δ -1; □ -2; ▲ -3
0
0,5
1,0
1,5
2,0
E, MeV

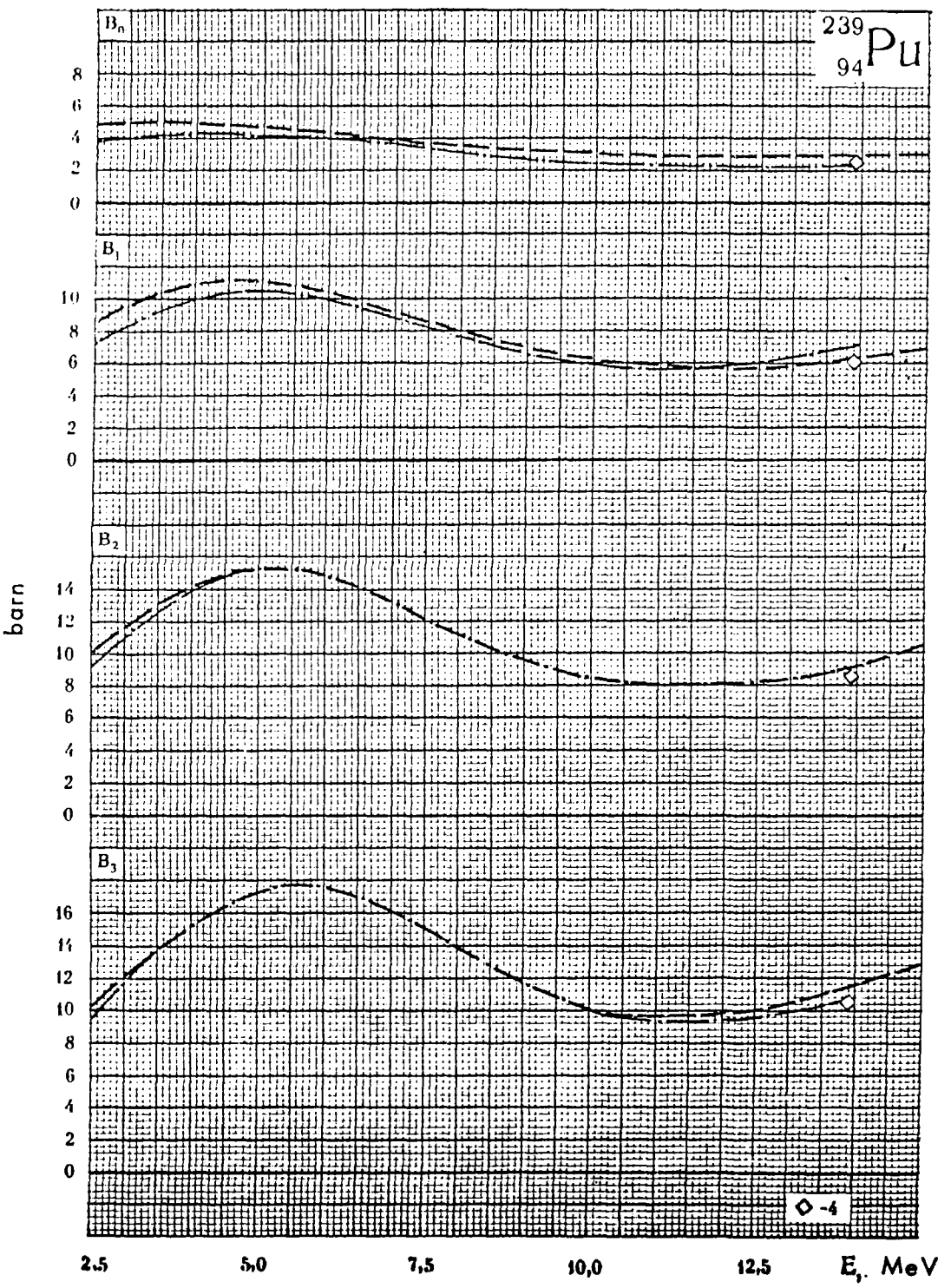
B_n
$^{239}_{94}Pu$
8
6
4
2
0
B_1
10
8
6
4
2
0
B_2
14
12
10
8
6
4
2
0
B_3
16
14
12
10
8
6
4
2
0
barn
◇ -4
2,5
5,0
7,5
10,0
12,5
E_n, MeV

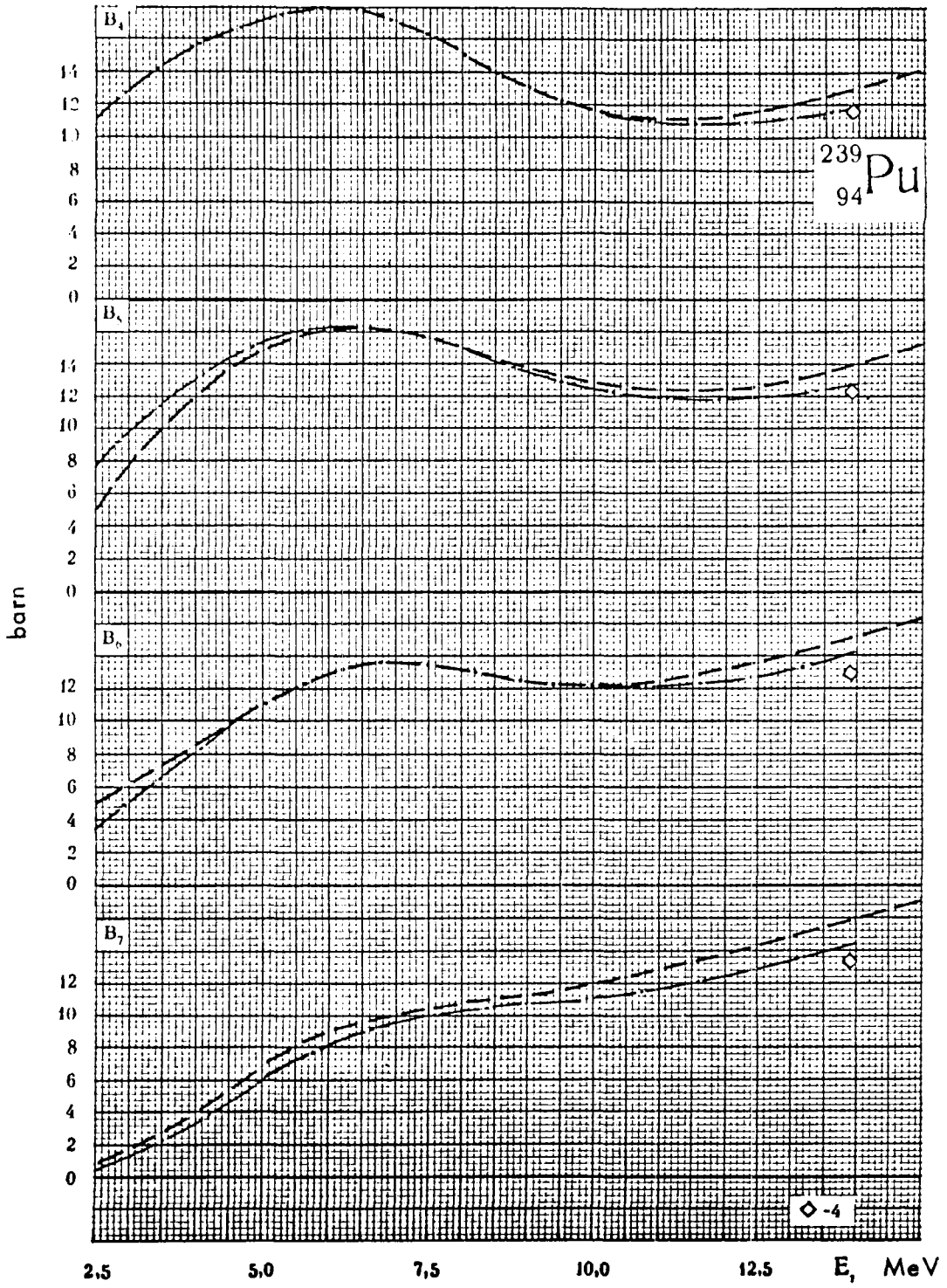
B4
B5
B6
B7
239 94Pu
◇ -4
barn
2,5
5,0
7,5
10,0
12,5
E, MeV

LITERATURE

1. Goldberg M.D., May V.M., Stehn J.P. - Angular Distributions in Neutron-induced Reactions, Vol. 1, Z=1 to 22, BNL-400 , 1962.

2. Goldberg M.D., May V.M., Stehn J.P. - Angular Distributions in Neutron-induced Reactions. Vol. 2, Z=23 to 94, BNL-400 , 1962.

3. Bulletin of the Information Centre on Nuclear Data, N°1, 105 (1964) ; N°2, 112 (1965) ; N°3, 116 (1966) ; N°4, 174 (1967).

4. Bjorklund F.J., Fernbach S. Phys. Rev., 109, 1295 (1958).

5. Blatt J.M., Biedenharn L. C. Rev. Mod. Phys., 24, 258 (1952).

6. Nikolaev M.N., Thesis, MIFI, 1965.

7. Abagyan L.P., Bazazyanz N.O., Bondarenko I.I., Guseinov A.G., Lukyanov A.A., Makhanov U.M., Melentyev V.I., Nikolaev M.N., Orlov V.V., Rabotnov N.S., Suvorov A.A., Usachev L.N., Philippov V.V., Paper N° 357 (USSR) presented at the 3rd International Conference for Peaceful Uses of Atomic Energy, Geneva 1964.

8. Leipunskii A.I. et al., Experimental and Theoretical Investigations in Fast, Neutron Physics. Paper N° 4A/3 presented at the Conference on Fast Reactors, London, 1966.

9. Suvopov A.A., Güseinov A.G., Nikolaev M.N., Atomnaya Energiya 18, 278 (1965).

10. Nikolaev M.N., Bazazyanz N.O., Dovbenko A.G., Vakhromeva V.V., Kolesov V.E., Bulletin of the Information Centre on Nuclear Data, N° 3, 289 (1966).

11. Lukyanov A.A., Interference structure of neutron cross-section. Preprint FEI-78, 1967.

12. Aaron R., Amado R.D., Yam Y.Y., Phys. Rev., 140 , B 1291 (1965).

13. Hughes D.J., Schwartz R.B. Neutron Cross Sections BNL-325. Second Edition, 1958.

14. Ajdačic V. et al. Phys. Rev. Lett., 14, 444 (1965).

15. Thornton S.T. et al. Phys. Rev. Lett., 17, 701 (1966).

16. Goldberg M.D., Mughabghab S.F., Magurno B.A., May V.M. Neutron Cross Sections. Second Edition, Supplement N°2, 1966.

17. Bransden B.H., Hamilton R.A., Robertson H.H. Proc. Phys. Soc., A75, 144 (1960).

18. Bloch I., Hull M.H., Jr., Broyles A.A., Bouricins W.G., Freeman B.E., Breit G. Rev. Mod. Phys., 23, 147 (1951).

19. Freier G., Lampi E., Sleator W., Williams J.H. Phys. Rev., 75, 1345 (1949).

20. Heusinkveld M., Freier G. Phys. Rev., 85, 80 (1952).

21. Joanou G.D., Fenech H. Journ. of Nucl. Energy P. A/B, 17, 425 (1963).

22. Freeman T.M. Phys. Rev. 99, 1446 (1955).

23. Flerov N.N., Talyzin V.M., Atomnaya Energiya 4, 155 (1956).

24. Nikolaev M.N., Philippov V.V., Atomnaya Energiya 15, 493 (1963).

25. Reactor Physics Constants. ANL-5800, Second Edition, 1963.

A P P E N D I X

Comments on the Experiments

* Transliterated names are indicated by an apostroph in the reference code

Reference Code	Author	Reference	Year of publication	Elements studied
A-1	Adair R.K.	Phys. Rev., 86, 155	1952	^{4}He
A-2	Adair R.K. Okazaki A., Walt M.	Phys. Rev., 89, 1165	1953	D
A-3	Allred J. C., Armstrong A.H., Rosen L.	Phys. Rev., 91, 90	1953	D
A-4	Allen W.D, Ferguson A. T. G., Roberts J.	Proc. Phys. Soc., A 68, 650	1955	D
A-5	Allen R.C., Walton R.B., Perkins R.B., Olson R.A., Taschek R.F.	Phys. Rev., 104, 731	1956	Au, Bi, ^{238}U, ^{235}U, ^{239}Pu
A-6	Ahn S.H., Roberts J.H.	Phys. Rev., 108, 110	1957	Zr
A-7	Allen R.C.	Nucl. Sci. and Eng., 2, 787	1957	^{238}U, ^{235}U, ^{239}Pu
A-8	Anderson J.D., Gardner C.C., Nakada M.P., Wong C.	Phys. Rev., 110, 160	1958	Fe, Ag, Cd, Sn, Pb
A-9	Anderson J.D., Gardner C.C., Mc Clure I.W., Nakada M.P., Wong C.	Phys. Rev., 115, 1010	1959	Al, Cu, Zn
A-10	Austin S.M., Barschall H.H., Shamu R.E.	Phys. Rev., 126, 1532	1962	^{4}He
A-11	Armstrong A.H., Gammel J., Rosen L., Frye G.M.	Nucl. Phys., 52, 505	1964	^{6}Li, ^{7}Li
A-12	Antolkovic B., Holmgvist B., Wiedling T.	International Conference on the Study of Nuclear Structure with Neutrons. Paper 143. Antwerpen, Belgium Arkiv fys., 33, 297.	1966	Cu

E_n, MeV	ΔE_n, MeV	Neutron Source	Detector (E_{thr}, MeV)	Interval of θ or cos θ investigated	Remark
0,4-2,73	-	Li(p,n) ; T (p,n)	Recoil proportional counter	~0,5 to -0,8	-
0,22-2,5	0,025	Li(p,n); T (p,n)	Recoil proportional counter	~0,35 to - 0,75	Normalized to σ_t
14,1	0,1	T (d,n)	Nuclear emulsion	46 – 176°	$\Delta\vartheta$ = 5 – 10°
0,1;0,2	0,012	T (p,n)	Recoil proportional counter	0,8 to -0,75	Normalized to σ(H)
0,5 1,0	0,06 0,05	T (p,n)	Biased hydrogen recoil counter ~ 0,45 (E_n = 0,5) ~ 0,9 (E_n = 1,0)	25 – 130°	$\Delta\vartheta$ = 3°. Some inelastic scattering included.
14,1	-	T (d,n)	Nuclear emulsion	20 – 120°	$\Delta\vartheta$ = 8°
0,5 1,0	0,06 0,05	T (p,n)	Biased hydrogen recoil counter E_{thr} = ~ 0,45 for E_n = 0,5; 0,9 for E_n = 1,0	-	Earlier results published in /A - 5/
14,6		T (d,n)	Plastic scintillator (10,8 , 12,1)	90 – 167°	$\Delta\vartheta$ = 2°. Time of flight. Ring geometry.
14,6	-	T (d,n)	E_{thr}: 10,1 Al; 11,3 Cu; 12,3 Zr	85 – 155°	Time of flight. Ring geometry.
2 - 22	0,06-0,60	to { 4,05 T (p,n) 5,97–12 D (d,n) 12,0 T (d,n)	Gas scintillator recoil counter	from (-0,06 ; 0,64 to (-0,82 ; -0,90)	-
14,0	0,1	T (d, n)	Nuclear emulsion	10 – 160°	The angular distribution of Li-7 included inelastic scattering to the 0.48 MeV Level
1,5-4,6	-	-	-	22 – 160°	Time of flight. The angular distribution also represented as $\frac{d\sigma}{d\Omega}(\vartheta_{c.m.}) = \sum A_p P_p(\cos\vartheta_{c.m.})$

Reference Code	Author	Reference	Year of publication	Elements studied
A-13'	Alexandrov Yu., Samosvat G., Sareetar J., Tsoygen-Sor.	Letter to the editor. J. Experim. Theor. Phys.	1966	Pb
B-1	Brugger H.R., Gerber H.J., LUthu B., Remund E.W.	Helv. Phys. Acta, 28, 331	1955	Pb, Bi
B-2	Beyster J.R., Walt M., Salmi E.W.	Phys. Rev., 104, 1319	1956	Al, Fe, Zr, Sn, Ta, Bi, Be, C, Al, Fe, Zr, Sn, Ta, Bi
B-3	Bostrom N.A., Morgan I.L.	Private Communication (Texas) see BNL-400 - Vol. 1.	1956	Al
B-3a	Bostrom N.A., Morgan I.L.	Private Communication (Texas) see BNL-400	1956	Cu
B-4	Bostrom N.A., Morgan I.L., Prudhomme J.T., Sattar A.R.	WADC-TR-57-446	1957	N_7, O_8
B-5	Berko S., Whitehead W.D., Groseclose B.C.	Nucl. Phys. 6, 210	1958	Mg, Al, Ni, Cu, Pb, Bi
B-6	Bostrom N.A., Morgan I.L., Prudhomme J.T., Okhuysen P.L., Hudson O.M.	WADC-TN-59-107	1959	Li C Y, Zr Bi
B-7	Bostrom N.A., Morgan I.L., Prudhomme J.T., Okhuysen P.L., Hudson O.M.	WADC-TR-59-31	1959	Fe
B-7a	Bostrom N.A., Morgan I.L., Prudhomme J.T., Okhuysen P.L., Hudson O.M.	WADC-TN-59-31	1959	Pb
B-8	Braley J.E., Cook C.W.	Phys. Rev., 118, 808	1960	C
B-9	Bauer R.W., Anderson J.D., Christensen L.J.	Nucl. Phys., 48, 152	1963	Ni
B-10	Batchelor R., Towle J.H	Nucl. Phys. 47, 385	1963	^6Li, ^7Li

$E_{n'}$ MeV	$\Delta E_{n'}$ MeV	Neutron Source	Detector (E_{thr}, MeV)	Interval of θ or cos θ investigated	Remark
0,001 - 0,026	-	Pulsed reactor I.B.R.	Boron counter	30 — 150°	Time of flight.
3,45	0,07	D (d,n)	Biased scintillator	30 — 150°	Normalized to σ_t
2,5 7,0	0,20 0,40	T (p,n) D (d,n)	Methan proportional counter (0,8 En)	12 — 150°	-
0,6	-	-	Plastic scintillator	0,99 to -0,88	Ring geometry
3,7	-	-	-	-	Not corrected for inelastic scattering
3,07 — 15,83	-	-	Biased scintillator	from (0,84 ; 0,94) to - (0,80 ; - 0,88)	$\Delta\vartheta$ = 3 - 15°. Ring geometry.
14,7	-	T (d,n)	Plastic scintillator (10 - 11)	from ~20° to (~110; 160°)	Time of flight. Normalized to the theoretical curve. No multiple scattering correction.
1,45;4,21 4,21;4,70 1,45;3,67 4,21;4,70 4,21	-	-	Biased scintillator (0,5)	0,94 to - 0,78	Time of flight.
3,67 ; 4,21 4,7	0,12; 0,1 0,09	-	Biased scintillator (0,5)	from (0,86 ; 0,94) to - 0,78	Time of flight. Normalized to σ(H).
3,67; 4,21 4,7	0,12 0,1 0,09	-	Biased scintillator (0,5)	0,86 to - 0,78	Time of flight. Normalized to σ(H).
5,6	0,06	D (d,n)	Plastic scintillator	34,1 — 152,8°	$\Delta\vartheta$ = 7°
14,0		T (d,n)	Plastic scintillator(11)	16 — 163°	$\Delta\vartheta$ from 2°(ϑ=0) to 5°(ϑ=180) Time of flight.
1,5-7,54	0,08 - 0,115	{up to E_n=4,83 (7,57 D (d,n)	Liquid scintillator (0,5 to 0,7)	30—137°	Time of flight. Normalized to σ(H)

Reference Code	Author	Reference	Year of publication	Elements studied
B-11	Bouchez R., Duclos J., Perrin P.	Nucl. Phys., 43, 628	1963	C
B-12	Bauer R.W., Anderson J.D., Christensen L.J.	Nucl. Phys., 47, 241	1963	$_7N$, $_8O$
B-13	Bredin D.J.	Phys. Rev., 135, 412 B	1964	Al, Si, Fe, Co
B-14	Bonazzola G.C., Chiavassa E.	Nucl. Phys. 68, 369	1965	P
B-15	Batchelor R., Gilboy W.B., Towle J.H.	Nucl. Phys. 65, 236	1965	^{238}U, ^{232}Th
B-16	Barnard E., Ferguson A. T.G., Mc Murray W.R. Van Heerden I.J.	INDSWG-62, Nucl. Phys., 80, 46	1962 1966	^{238}U
B-17	Bonner B.E., Bernard D. L., Popelbaum C., Phillips G.C.	International Conference on the Study of Nuclear Structure with Neutrons. Paper 3. Antwerpen, Belgium.	1965	D
B-18	Bonazzola G.C., Chiavassa E.	Nucl. Phys., 86, 378	1966	^{19}F
B-19	Buccino S.G., Hollandsworth C.E., Bevington P.R.	Z. Phys., 196, 103	1966	C, Zr, Ag, Sb, Ce Pr, Ta, Au, Tl, Radio Pb, Th, U
B-20	Becker R.L., Guindon W.G., Smith G.J.	Nucl. Phys. 89, 154	1966	Al, Si, Ca, Ti, V, Cr, Mn, Fe, Co, Ni, Cu, Zn, Y, Zr, Mo, Sn, Ta W, Bi, Ga, Ge, As, Se Sr, Ag, Cd, In, Sb, Te Ba, La, Ce, Pr, Hg, Tl Pb, Bi
B-21	Bauer R.W., Anderson J. D., Lutz H.F., Wong C. Mc Clure J.W., Pohl B.A	Nucl. Phys. A 93, 673	1967	N
B-22	Blanc D., Cambou F., Niel M., Vedrenne G.	J. phys., 27, N°. 3-4 Suppl., 98	1966	T
B-1'	Bobyr V.V., Strizhak V. I., Totskii I.A.	UKR. Phiz. Journal, 3,836	1958	Fe, Cu, Zn, Cd, Sn, Sb, Hg, Pb, Bi
C-1	Cbon J.H., Bockelman C.K., Barschall H.H.	Phys. Rev., 81, 33	1951	T

$E_{n'}$ MeV	$\Delta E_{n'}$ MeV	Neutron Source	Detector (E_{thr}, MeV)	Interval of θ or cos θ investigated	Remark
14,6	-	T (d,n)	Plastic scintillator	11 — 157°	Time of flight.
14	-	T (d,n)	Stilben scintillator (3,5)	17 — 140°	$\Delta\vartheta$ from 2 (ϑ<20°) to 6° (ϑ~90°) Time of flight. Ring geometry.
1,95	0,09	T (p,n)	Liquid scintillator	30 — 120°	Time of flight. Normalized to σ(H)
14,2	0,7	T (d,n)	Plastic scintillator (7,5)	30 — 160°	Time of flight. Normalized to σ_e (C^{12}) at ~14 MeV
2 3 4 7	0,08 0,07 0,06 0,12	T (p,n) D (d,n)	Organic scintillator	12,5 — 135°	Time of flight. Normalized to σ(H)
0,075 - 0,55	0,005 ~0,008	Li (p,n)	Plastic scintillator	from (0,77 ; 0,865 to (- 0,68 ; - 0,91	Time of flight. Calibration of detector with the incoming beam.
5,635 and 9,035	-	D (d,n)	Plastic scintillator	0,8 to - 0,9	Time of flight.
14	~0,7	T (d,n)	Plastic scintillator	30 — 140°	Time of flight.
5	0,32	D (d,n)	Liquid organic scintillator	20 — 140°	Time of flight. Normalize to σ_t.
3,2	0,1	D (d,n)	Scintillation counter	from 20 to 140 or 150°	Calibration of detector with the incoming beam.
6,78 — 13,96	0,2	D (d,n)	Plastic scintillator (3,5)	15 — 135°	Time of flight.
14	-	T (d,n)	Scintillator recoil counter (solid radiator)	45 — 180°	-
2,8	-	D (d,n)	Spherical methan ionisation chamber	25 — 150°	Ring geometry.
14,3	0,2	T (d,n)	Ionisation chamber and telescope counter.	90 — 180°	$\Delta\vartheta$ =8-12°. Normalized to σ(H) = 50 mbarn/str at 180°.

Reference Code	Author	Reference	Year of publication	Elements studied
C-2	Conner J.P.	Phys. Rev., 89, 712	1953	O
C-3	Cranberg L., Levin J. S.	Phys. Rev. 103, 343	1956	Ti, Fe
C-4	Salnikov O.A.	Atomnaya Energiya3, 106	1957	Cr, Fe, Pb
C-5	Coon J.H., Davis R.W., Felthauser H.E., Nicodemus D.B.	Phys. Rev., 111, 250	1958	C, Al, Fe, Cu, Sn, Pb, U
C-6	Cranberg L., Granberg L., Levin J.S.	La-2177 Phys. Rev., 109, 2063	1959 1958	^{235}U, ^{238}U, ^{239}Pu
C-7	Cross W.G., Jarvis R.G.	Nucl. Phys., 15, 155	1960	Mg, Ca, Cd, Ta, Bi
C-8'	Strizhak V.I., Kozar A. O., Nazarov M.C.	UKR. Phiz. Journal, 5, 704	1960	Ni, Se, Zr, Mo, Te
C-9'	Strizhak V.I., Bobyr V. V., Grona L.YA.	UKR. Phiz. Journal, 5, 702	1960	C, Ag, Cd, Hg
C-10'	Strizhak V.I., Bobyr V. V., Grona L.YA.	M. Experim. I Teoret. Phiz. 41, 313	1961	C, N, S, Mo, Cd, Te
C-11'	Strizhak V.I., Bobyr V. V., Grona L.YA.	M. Experim. I Teoret. Phiz. 40, 725	1961	Ag, Hg, Bi
C-12	Chase L.F., Johnson R. G., Smith R.V., Vaughn F.J., Walt M.	AFSWC-TR-61-15	1961	N, O
C-13	Clarke R.L., Cross W. G.	Private Communication (Chalk River) - see BNL-400. V.1.	1962	C, Mg
C-14	Cox S.A.	WASH-1044	1963	Fe

$E_{n'}$ MeV	$\Delta E_{n'}$ MeV	Neutron Source	Detector (E_{thr}, MeV)	Interval of θ or cos θ investigated	Remark
14,1		T (d,n)	Wilson chamber	0,9 to -0,9	Normalized to σ(H) = 700 mbarn.
2,25 ; 2,45	0,1	T (p,n)	Plastic scintillator (~ 0,5)	0,94 to -0,94	Time of flight. Normalized to σ(H)
2,34		D (d,n)	Nuclear emulsion	30 — 135°	$\Delta\vartheta$ = 10°
14,5	~0,35	T (d,n)	Organic scintillator (13,5 - 14)	5 — 150°	$\Delta\vartheta$ = 1 - 3°. Ring geometry.
0,55 ; 0,98 ; 2,0	-	^{7}Li (p,n) T (p,n)	Plastic scintillator (0,2 at B_n = 0,55	0,93 to - 0,93	$\Delta\vartheta$ = 7°. Time of flight Normalized to σ(H). The cross-section values at 0,98 and 2 MeV contain some inelastic scattering.
14,6	0,1	T (d,n)	Plastic scintillator (10,5)	8 — 130°	$\Delta\vartheta$ = 3°. Mg corrected for inelastic scattering in the case of Ta the angular distribution was only measured up to 80°.
2,9	-	D (d,n)	Ionisation chamber	25 — 150°	Ring geometry.
14	-	T (d,n)	Biased scintillator (11)	Ag, Hg 20—115° C 20 — 140° Cd 15 —160°	$\Delta\vartheta$ = 9°. Ring geometry.
14	-	T (d,n)	Biased scintillator (11)	20 —160° 15 —140°	Ring geometry. No multiple scattering correction.
14,5	-	T (d,n)	Biased scintillator (11)	20 —110°	$\Delta\vartheta$ = 9°.
4,99 — 11,6	0,23- 0,70	-	Biased scintillator	0,93 to - 0,88	Time of flight.
14,1	-	T (d,n)	Biased scintillator (~ 3)	0,97 to - 0,63	Time of flight. Normalized to σ at 30° from ref. /N-2/
0,70 — 1,25 ; ~1 — ~1,09	0,020; 0,036 to 0,07	-	-	22 —160°	Time of flight. All angular distributions represented by Legendre coefficients.

Reference Code	Author	Reference	Year of publication	Elements studied
C-15	Cox S.A.	WASH-1046	1964	Mn, Co, Zn, Cr
C-16	Clarke R.L., Cross W.G.	Nucl. Phys., 53, 177	1964	C, Mg, Si, S
C-17	Coppola M., Knitter H.H.	International Conference on the Study of Nuclear Structure with Neutrons, Paper 146. Antwerpen, Belgium.	1965	Si
C-18	Conjeaud M., Fernandez B., Harar S., Picard J. Souchere G.	Nucl. Phys., 62, 225	1965	S
C-19	Clarke R.L., Cross W. G.	Nucl. Phys., A95, 320	1967	Ni Zr
C-20	Chien J.P., Smith A.B.	Nucl. Sci. and Eng., 26, 500	1966	Be, Na, Al
C-21	Cookson J.A., Dandy D., Hopkins J.C.	Nucl. Phys., A 91, 273	1967	^{6}Li, ^{7}Li
D-1	Darden S.E., Haeberli W., Walton R.B.	Phys. Rev., 96, 836A Private Communication (Wisconsin)	1954 1954	Ti, Ta, Bi, Th, Fe, Ni, Cu, Zn, Zr, Ag, Cd
D-2	Darden S.E., Perkins R.B., Walton R.B.	Phys. Rev., 100, 1315	1955	Sn, Sb, Ce, Ta, Pb, Bi, Th, Ti, Fe, Ni, Cu, Zn, Zr, Ag, Cd
D-3	Didier D., Mouilhayrat G., Perrault F., Thouvenin P.	EANDC 57 "V"	1964	Ni, Ag, U, Pu
E-1	Elliott J.O.	Phys. Rev., 101, 684	1956	Bi, Ta, In, Fe, S
E-2	Elwyn A.J., Lane R.O. Langsdorf A.	Phys. Rev., 128, 779	1962	D

E_n, MeV	ΔE_n, MeV	Neutron Source	Detector (E_{thr}, MeV)	Interval of θ or cos θ investigated	Remark
0,690 - 1,18	0,06	-	-	20 — 160°	Time of flight. The energy resolution is equal to 20 KeV ; results are averages over the interval = 60 KeV;
14,1	0,15	T (d,n)	Plastic scintillator	from (~10 ; 30) to 150°	Time of flight. Normolized to σ(H)
0,84 - 2,28	0,110 0,08	T (p,n)	-	20 — 148°	Time of flight. Normalized to σ(H). Angular distribution given also in form $\frac{d\sigma}{d\Omega}(\vartheta) = \sum_{l=0}^{5} A_l P_l(\cos\vartheta)$
14,6	0,15	T (d,n)	Plastic scintillator	20 — 152°	Time of flight.
14,1	0,90	T (d,n)	Plastic scintillator	15 — 150° 15 — 112°	-
0,3 - 1,5	~0,02	^{7}Li (p,n)	Liquid scintillator	20 — 145°	Time of flight. Normalized to σ(C). Data represented by Legendre polynomials
10	0,04	T (p,n)	Liquid scintillator	27,5 — 151°	Time of flight. $\Delta\vartheta$=0,5°. Cross-section normalized to σ(H). Results for Li-7 include inelastic scattering to the 0,478 MeV level.
1,0	~0,1	^{7}Li (p,n)	Proportional counter (0,66 and 0,79)	8 — 30°	$\Delta\vartheta \sim 1/3\vartheta$. Ring geometry.
0,5 ; 1,00 ; 1,55	~0,1	^{7}Li (p,n)	Proportional counter (0,2 and 0,3) (0,66 and 0,79); (1,1)	8 — 30° 30° 14 and 30°	Ring geometry.
13,9	-	-	-	from (10 ; 20) to (97; 120°)	Time of flight. Data not corrected for multiple scattering, geometry and variation of detector efficiency with energy.
14	-	T (d,n)	Biased scintillator	5 — 55°	$\Delta\vartheta$ = 1 - 3°. Ring geometry.
0,5;1,0 1,95	-	^{7}Li (p,n)	Boron counter in moderator.	22 — 150°	$\Delta\vartheta$ = 3 - 5° Normalized to σ(C)

Reference Code	Author	Reference	Year of publication	Elements studied
E-3	Elwyn A.J., Monahan J.E., Lane R. O., Langsdorf A., Jr.	Nucl. Phys., 59, 113	1964	F, Na, Al, P
F-1	Fowler J.L., Johnson C.H.	Phys. Rev., 98, 728	1955	N
F-2	Fowler J.L., Cohn H.O.	Phys. Rev., 109, 89	1958	O
F-3	Fowler J.L., Cohn H.O. Fowler J.L., Cohn H.O. Fowler J.L.	Bull. Am. Phys. Soc, 305 Bull. Am. Phys. Soc., 4, 385 Priv. Comm. (Oak Ridge)	1958 1959 1961	Be
F-4	Fowler J.L., Campbell E.C.	Phys. Rev., 127, 2192, Bull. Am. Phys. Soc. 5, 443	1962 1960	Pb
F-5	Fasoli U., Zago G.	Nuovo Cimento 30, 1169	1963	^{4}He
F-6	Fowler J.L., Johnson C.H.	ORNL-3582 TID-4500	1964	O
F-7	Frasca A.J., Finlay R. W., Koshel R.D., Cassola R.L.	Phys. Rev., 144, 854	1966	C, B, K, Ca
F-8	Fowler J.L., Johnson C.H., Kernell R.L.	CONF-660303 Book 2, Physics TID-4500	1966	N
F-9	Fowler J.L.	Phys. Rev., 147, 870	1966	^{208}Pb (99,75%)
G-1	Gilboy W.B., Towle J. H.	Private Communication (Aldermaston) see BNL-400. V. 1, 2; Nucl. Phys., 42, 86	1962 1963	Na, Al, Cr, Fe, Zr, Cd, Sn, La, Ce, Pr, Nd, Sm, Gd, Dy, Ho, Er, Yb, Ta, Pb, U
G-2	Gilboy W.B., Towle J.H.	Nucl. Phys., 64, 130	1965	Fe
G-1'	Gyzhovskii - B.YA.	Atomnaya Energiya 11, 395	1961	Pb, Cu, ^{238}U, Pu

$E_{n'}$, MeV	$\Delta E_{n'}$, MeV	Neutron Source	Detector (E_{thr}, MeV)	Interval of θ or cos θ investigated	Remark
0,2 — 2,2	0,10-0,15	^{7}Li (p,n)	Boron counter in moderator	20 — 159°	Normalized to σ(C)
0,8 — 2,36	0,01-0,05	T (p,n)	a) Proportional counter b) Recoil proportional counter	0,85 to -0,7 0,44 to -0,8	Calibration of detector with incoming beam for E_n from 0,8 to 1,54 MeV. Normalized to the theoretical curve, calculated in the article (E_n from 1.35 to 2.36)
0,73 — 2,15	0,05	T (p,n)	Propan recoil counter	0,84 to -0,75	At 1 and 1,21 MeV normalized to σ_e (Be); at 0,73, 1,5, 1,75, and 2,15 MeV normalized to σ_t (0)
0,73 — 2,92	0,05	T (p,n)	Proportional counter	0,87 to -0,79	Normalized to σ_e
1,2 — 3,2	0,05	^{7}Li (p,n)	Proportional counter	0,88 to -0,73	-
14,1	0,1	T (d,n)	Wilson chamber	0,80 to -1,0	Only relative measurement.
3,35 3,77 3,90	0,01	T (p,n)	Stilben scintillator with γ-ray discrimination.	0,95 to -0,9	-
14,0	0,03	T (d,n)	Plastic scintillator	2,0 — 150°	Time of flight. Normalized to σ(H)
1,595 3,207	0,015 0,021	T (p,n)	Stilben scintillator	0,95 to ~ - 0,85	Calibration of detector with incoming beam
0,715 1,765	~ 0,03	^{7}Li (p,n)	Stilben scintillator	~0,9 to ~ - 0,8	Calibration of detector with incoming beam
0,98	0,05 0,10	T (p,n)	Biased liquid scintillator	30 — 137°	Time of flight. Normalized to σ(H)
0,98 — 3,99	0,100 0,065	T (p,n)	Biased liquid scintillator	30 — 137°	Time of flight. Normalized to σ(H)
15,0	0,4	T (d,n)	Organic scintillator	from (10; 16) to (80 ; 155)°	$\Delta\vartheta$ = 1 - 7°

Reference Code	Author	Reference	Year of publication	Elements studied
G-2'	Gorlov G.V., Lebedeva N.S., Morozov V.M.	DOKL. AH CCCP, 158, 574	1964	Be, C, Co, ^{62}Ni, ^{80}Se, Nb, ^{114}Cd, ^{115}In, ^{118}Sn, ^{127}I, Pb, Bi
G-3'	Gorlov G.V., Lebedeva N.S., Morozov V.M.	Private communication	1965	Be, C, Co, ^{62}Ni, ^{80}Se Nb, ^{114}Cd, ^{115}In, ^{118}Sn, ^{127}I, Pb, Bi
H-1	Hans H.S., Snowdon S.C	Phys. Rev., 108, 1028	1957	Zr, Mo
H-2	Hill R.W.	Phys. Rev.. 109, 2105	1958	C, O, Al, Fe, Ni, Cu, Mo, Ba, W, Pb
H-3	Haddad E., Phillips D.D.	Bull. Am., Phys. Soc., 4, 358 Private communication (Los Alamos), see BNL-400 . V.1	1959 1961	C
H-4	Hudson C.I., Walker W. S., Berko S.	Phys. Rev., 128, 1271	1962	Ta, Bi, Th, U
H-5	Hoop B., Jr., Barschall H.H. Hoop B., Barschall H.H.	International Conference on the Study of Nuclear Structure with Neutrons. Paper 78. Antwerpen, Belgium Nucl. Phys., 83, 65	1965 1966	^{4}He
H-6	Hunzinger W., Huber P.	Helv. phys. acta, 35, 351	1962	O
H-7	Hopkins J.C.	CONF-660303 - Book 2, Physics TID-4500	1966	^{6}Li ^{7}Li
K-1'	Koltypin E.A., Yankov G.B.	B.V. "Nuclear Reactions at Low and Intermediate Energies", M., 1st Ed, AH, CCCP	1962	Zn, Se, Zr, Nb, Mo, Cd, In, Sn
K-2	Kent D.W., Snowden S. C., Puril S.P., Bucher W.P.	Phys. Rev., 125, 331	1962	Ca, K, Ge, Se, Sr
K-3'	Korzhl.A., Kopytin N.S. Pasechnik M.V., Pravdivyi N.M., Sklyar N.T. Totskii I.A.	UKR. Phiz. J., 8, 1323	1963	Al, Ni, Zn, Zr, Ag, Sn, Te, Ba, Hg, Pb
K-1''	Khaletskii M.M.	Dokl. AH CCCP, 113, 553	1957	C, Al, Fe, Sn, Pb

$E_{n'}$ MeV	$\Delta E_{n'}$ MeV	Neutron Source	Detector (E_{thr}, MeV)	Interval of θ or cos θ investigated	Remark
4,0	0,05	D (d,n)	Organic scintillator	10 – 170°	$\Delta\vartheta$ =4°. No correction done. Normalized to a absolute measured cross-section (20°)
4,0	0,05	D (d,n)	Organic scintillator	10 – 170°	For information on numerical values see ref. 6-2'
3,7	0,4	D (d,n)	Biased scintillator	18 – 142°	Ring geometry. Detector calibration with incoming beam.
5,0	0,1	D (d,n)	Plastic scintillator	30 – 150°	$\Delta\vartheta$=10°. Detector calibration with incoming beam.
6,0 7,0	-	-	Biased scintillator	0,83 to -0,89	Time of flight. Not corrected for multiple scattering.
15,2	-	T (d,n)	Biased scintillator	0,98 to -0,96	$\Delta\vartheta$ =2°. Time of flight Normalized to the difference ($\sigma_t - \sigma_{ne}$) measured in the same work.
6–30	0,04 at $E_n < 22$	D (d,n) at $E_n < 16$	Gas scintillator	~0,7 to ~ - 0,8	Time of flight.
2–4,11	0,01 0,05	D (d,n)	Nuclear recoil ionisation chamber	~0,7 to ~ - 0,8	Normalized to σ_t. (Except for E_n = 3,61 and 3,70 MeV; which are normalized to σ(H)
4,83 4,83 3,35	~ 0,100	T (p,n)	Plastic scintillator	0,692 to -0,786 0,703 to -0,775	Time of flight. Normalized to σ(H)
0,40		T (p,n)	Hydrogen proportional counter	20 – 150°	Detector calibration with incoming beam.
3,7	0,4	D (d,n)	Scintillation counter.	10 – 150°	Ring geometry. Normalized to σ(H)
0,65	0,05	T (p,n)	Hydrogen proportional counter	30 – 140°	Spherical scatterer used.
14,8	-	T (d,n)	Biased Ring Liquid scintillation counter (~11,5)	from (10; 30) to (70; 95°)	Calibration of detector with incoming beam.

Reference Code	Author	Reference	Year of publication	Elements studied
K-4'	Korzh I.A. - Sklyar N.T.	UKP. Phiz. J. 8, 1383	1963	Na, Mg, Al, K, Fe, Ni, Zn, Cd , Sn, Te, Hg
K-5'	Korzh I.A., Kopytin N.S., Pasechnik M.V., Pravdivyi N.M., Sklyar M.T., Totskii I.A.	Atomnaya Energiya 16, 260	1964	C, Na, Mg, Al, Ni, Cu, Se, Te
K-6'	Korzh I.A., Sklyar N.T. Totskii I.A.	UKR . Phiz. J. 9, 929	1964	Mo, Sb, W, U
K-7'	Korzh I.A., Sklyar N.T. Totskii I.A.	UKR. Phiz. J. 9, 577	1964	Si, Cr, Zr, Pb, Bi
K-8'	Kazakova L.YA., Kolesov V.E., Popov B.I., Salnikov O.A., Sluchenskaya V.M., Trykova V.I.	International Conference on the Study of Nuclear Structure with Neutrons. Antwerpen, Belgium	1965	Na, P, Cl, Ti, Cr, Mn, Fe, Ni, Cu, Zn, Br, Sr, Zr, Nb, Mo, Ag, Cd, Sb I, Ba, Ta, W, Hg, Bi, Th
K-9'	Korzh I.A., Mishchenko V.A., Pradivyi N.M., Prikhodko V.P., Sklyar N.T., Totskii I.A.	UKR. Phiz. J. 11, 563	1966	Ti Co
J-1	Jacquot A., Rousseau C.	Nucl. Phys., 84, 239	1966	Fe
L-1'	Lovchikova G.N.	Atomnaya Energiya 2, 174	1957	Al, Fe, Sn, Pb, Bi
L-2'	Lovchikova G.N.	J. Experim. I Teoret. Phiz.38, 1434	1960	Pb, Bi, Sn, Fe, Al
L-3'	Lovchikova G.N.	Atomnaya Energiya 13, 60	1962	0, Si, Ni
L-4'	Lovchikova G.N.	Atomnaya Energiya 12, 48	1962	Ti, Ca
L-1	Little R.N., Leonard B. P., Prud'homme J.T., Vincent L.D.	Phys. Rev., 98, 634	1955	C, Al, S

$E_{n'}$, MeV	$\Delta E_{n'}$, MeV	Neutron Source	Detector (E_{thr}, MeV)	Interval of θ or cos θ investigoted	Remark
0,30	0,025	T (p,n)	Hydrogen proportional counter	30—140°	Spherical scatterer used
0,5 and 0,8	0,05	T (p,n)	Hydrogen proportional counter	30—140°	Spherical scatterer used $\Delta\vartheta$ = 10°. Data for C only for 0,5 MeV
0,3; 0,5	0,025 —0,05 0,8	T (p,n)	Hydrogen proportional counter	30 — 140° Mo, Sb, W	Mo, Sb, W, V Spherical scatterer used.
0,3 0,5 0,8	0,025 —0,05	T (p,n)	Hydrogen proportional counter	30—140°	Si, Cr, Zr, Pb, Bi; Si, Cr Spherical scatterer used
2,0	0,10	T (p,n)	Biased scintillator	20—160°	$\Delta\vartheta$=6°. Detector calibration with incoming beam.
0,3;0,5 0,5;0,8	-	T (p,n)	Hydrogen proportional counter	30—140°	Spherical scatterer used.
0,45— 2,28	0,14— 0,10			20—140°	Time of flight.
0,900	0,100	Na-γ-Be	Spherical Helium inonization chamber	30—150°	$\Delta\vartheta$ =7—12°. Ring geometry.
0,220		^{24}Na (γ,n) D_2O	Boron counter	30—150°	$\Delta\vartheta$ =10°. Ring geometry.
0,900	0,040	T (p,n)	Spherical hydrogen chamber	30—150°	Ring geometry.
0,900	0,040	T (p,n)	Spherical hydrogen chamber	30—150°	$\Delta\vartheta$ = 3 — 15°. Ring geometry.
2,7	0,04	D (d,n)	Liquid organic scintillator	30—120°	$\Delta\vartheta$ = 5—15°. Ring geometry. Normalized to σ, measured in the same experiment

Reference Code	Author	Reference	Year of publication	Elements studied
L-2	Langsdorf A., Lane R. O., Monahan J.E.	Phys. Rev., 107, 1077	1957	Be, B, C, Na, Mg, Al, P, S, K, Ti, V, Cr, Fe, Co, Ni, Cu, Zn, Se, Zr, Nd, Mo, Pd, Ag, Cd, In Sn, Te, Ta, W, Pt, Au, Tl, Pb, Bi, Th, U, F
L-3	Landon H.H., Elwyn A.J., Glasoe G.N., Oleksa S.	Phys. Rev., 112, 1192	1958	Fe, Y, ^{206}Pb
L-4	Lane R.O., Monahan J.E.	Phys. Rev., 118, 533	1960	Na
L-5	Levin J.S., Cranberg L.	Private communication (Los Alamos) see BNL-400. V.1	1960	Be
L-6	Lane R.O., Langsdorf A.S., Jr., Monahan J.E., Elwyn A.J.	Ann. phys., 12, 135	1961	^{6}Li, (96%), ^{7}Li Be, C, O, Si, S, Ca, Cu Sn, Pb, ^{238}U
L-7	Lane R.O., Elwyn A.J., Langsdorf A.S., Jr.	Phys. Rev., 126, 1105	1962	Si
L-8	Lane R.O., Monahan J.E.	BNL-400. V.1 (appendics) Private communication)	1962	Be
L-9	Lane R.O., Elwyn A.J., Langsdorf A.S., Jr.	Phys. Rev., 133, B 409	1964	Be
L-10	Langsdorf A., Bowen P. H., Cox G.C., Firk F. W.K., Mc Connell D. B., Rose B.	International Conference on the Study of Nuclear Structure with Neutrons. Paper 8, Antwerpen, Belgium	1965	C
L-11	Lister D., Sayres A.	Phys. Rev., 143, 745	1965	C, O
M-2	Meier R. W., Scherer P. Trumpy G.	Helv. Phys. acta, 27, 577	1954	C

E_n, MeV	ΔE_n, MeV	Neutron Source	Detector (E_{thr}, MeV)	Interval of θ or cos θ investigated	Remark
0,06—1,8	0,1—0,6	^{7}Li (p,n)	Boron counter in moderator	24—143°	Includes inelastic scattering. Normalized to σ(C). Data represented in form of Legendre polynomials
2,2	0,12	T (p,n)	Biased scintillator	~0,85 to ~ - 0,7	Time of flight. Normalized to σ(Fe). Not corrected for multiple scattering.
0,2-0,8	0,025	^{7}Li (p,n)	Boron counter in moderator	24—143,7°	Includes inelastic scattering. Normalized to σ(C). Data represented in form of Legendre polynomials
2,48 - 3,46	-	-	Biased scintillator	~0,9 to - 0,9	Time of flight.
0,05 — 2,3	0,04—0,13	^{7}Li (p,n)	Boron counter in moderator	22—145°	Data represented in form of Legendre coefficient. Detailed measurement of B_1 in the resonance region. Heavy nuclei include inelastic scattering. Normalized to σ(C), which was normalised to σ(Sn) at 2MeV
0,2 — 0,7	0,01	^{7}Li (p,n)	Boron counter in moderator	20—150°	Normalized to σ(C). Data represented by Legendre polynomials
0,545— 0,895	~0,01	^{7}Li (p,n)	Boron counter in moderator	0,910 to - 0,860	Energy dependence of $\sigma(\vartheta)$ given.
0,2 — 0,9	~0,01	^{7}Li (p,n)	Boron counter in moderator	0,9 to - 0,86	Data represented by Legendre polynomials
2,08 — 7,8	0,015 at 2,08; 0,080 at 6,3	-	Plastic scintillator	15 — 160°	Time of flight.
3,0 — 4,7	0,018 — 0,025	T (p,n)	Recoil proportional counter	$\vartheta \angle$ 0,65	Normalized to σ(H)
2,4 — 3,65	0,04—0,07	D (d,n)	Biased scintillator	0,8 -0,8	Normalized to σ_t

Reference Code	Author	Reference	Year of publication	Elements studied
M-3	Muehlhouse C.O., Bloom S.D., Wegner H.E., Glasoe G.N.	Phys. Rev., 103, 720	1956	C, Fe
M-4	Machwe M.K., Kent D.W., Snowdon S.C.	Phys. Rev., 114, 1563	1959	S, Fe, Co, Ni, Cu, Zn
M-5	Marion J.B., Levin J.S. Cranberg L.	Phys. Rev., 114, 1584	1959	Be
M-6	Martin J.P., Zucker M. S. Zucker M.S.	Bull. Amer. Phys. Soc., 7, 72 Private communication, see BNL-400 - V.1	1963 1962	O
M-7	Mc Donald W.J., Robson J.M.	Nucl. Phys., 59, 321	1964	Ca
M-8	Martin P.W., Stewart D.T., Martin J.	Nucl. Phys., 61, 524	1965	Si, S
M-9	Merchez F., Nguen Van-Sen Regis V., Bouchez R.	C. r. Acad. sci. Paris, 260, 3922 J. Phys., 27, 3-4, Suppl. 61 and 84	1965 1966	^{6}Li , ^{7}Li
N-1	Nauta H.	Nucl. Phys., 2, 124 Private Communication	1956 1958	Zn, Hg, Pb, W
N-2	Nakada M.P., Anderson J.D., Gardner C.C., Wong C.	Phys. Rev., 110, 1439	1958	Be, C
O-1	Okazaki A.	Phys. Rev., 99, 55	1955	O
O-2	Okhuysen P.L., Prud'homme J.T.	Phys. Rev., 116, 986	1959	Pb
P-1	Poole M.J.	Philos. Mag., 43, 1060	1952	Al
P-2	Pierre C.St., Machwe M. K., Lorrain P.	Phys. Rev., 115, 999	1959	Al, S, Ti, Co
P-3	Phillips D.D.	Private communication (Los Alamos) see BNL-400 - V.1	1961	Be, N, O

E_n, MeV	ΔE_n, MeV	Neutron Source	Detector (E_{thr}, MeV)	Interval of θ or cos θ investigoted	Remark
1,48 ; 1,66	~ 0,075	T (p,n)	Biased scintillator	30 — 140°	$\Delta\vartheta$ =10°. Time of flight. For Carbon, measurement only done at E_n = 1,66 MeV. Normalized to measured σ_e
3,7	0,4	D (d,n)	Scintillation counter	10 — 160°	Ring geometry. Normalized to σ(H)
2,6 — 6,0	0,075 — 0,21	T (p,n) D (d,n)	Biased scintillator	0,926 to - 0,925	$\Delta\vartheta$ =7°. Time of flight.
1,51 — 2,25	0,033 — 0,063	T (p,n)	Biased liquid scintillator	from 20 ; 30° to 165°	$\Delta\vartheta$ = 3,2°. Time of flight. Normalized to σ_t
14,1		T (d,n)	Scintillation counter	20 — 160°	Time of flight. Normalized to σ(H)
14,1	1,2	T (d,n)	Scintillation counter	20 — 140°	Time of flight.
14		T (d,n)	Plastic scintillator	15 — 150°	Time of flight. $\Delta\vartheta$=5°. Data on Li-7 include inelastic scattering to the 0,48 MeV level
14		T (d,n)	Biased liquid scintillator	15 — 125°	Ring geometry.
14		T (d,n)	Biased scintillator	20 — 140°	Ring geometry. Time of flight.
0,410 — 0,493	0,065	^{7}Li (p,n)	Biased scintillator	0,7 to -0,68	Normalized to σ_t, measured in this experiment.
4,2	0,1	D (d,n)	Plastic scintillator	20 — 140°	$\Delta\vartheta$ = 5 — 10°. Time of flight.
2,5			Biased scintillator (0,8)	- 0,15	Ring geometry.
14	≤0,3	T (d,n)	Biased plastic scintillator (10,2 ± 0,4)	10 — 138°	Ring geometry. Contribution for inelastic scattering present.
-	-	-	-	-	-

Reference Code	Author	Reference	Year of publication	Elements studied
P-4	Petitt G.A., Buccino S. G., Hollandsworth C.E., Bevington P.R.	Nucl. Phys. 79, 239	1966	Si, S
P-1'	Popov V.I.	Atomaya Energiya 3, 498	1957	Fe, Cu, Pb, Bi
P-2'	Pasechnik M.V., Bapchuk I.F., Totskii I.A., Strizhak V.I., Korolev A.M., Hoffman YU.V., Lovchikova G.I., Koltypin E.A., Yankov G.B.	Procedure of 2nd International conf. on the Peaceful use of Atomic Energy, Geneva, Vol. 15, p. 18	1959	Fe, Cu, Zn, Cd, Sn, Sb, Hg, Pb, Bi
P-3'	Popov V.I.	In the book entitled "Neutron Physics", M. GOSATOMIZDAT.	1961	Al, Si, K, Ca, Th
P-4'	Popov V.I., Salnikov O.A., Sluchevskaya V. M., Trykova V.I., Pokrovskii A.N.	Private communication See also (K-8)	1961	Zn
P-5'	Pasechnik M.V., Batalin V.A., Korzh I.A., Totskii I.A.	Atomnaya Energiya, 16, 207	1964	Fe, Zn, Zr, Cd, Sn, Ba, Hg, Pb, Bi, U
P-6'	Popov V.I.	Private Communication see also (K-8)	1965	Na, P, Cl, Ti, Cr, Mn Fe, Ni, Cu, Zn, Br, Sr, Zr, Nb, Mo, Ag, Cd, Sb, I, Ba, Ta, W, Hg, Bi, Th
P-7'	Popov V.I.	Private Communication see also (K-8)	1966	B Y
R-1	Rhein W.J.	Phys. Rev. 98, 1300 Private communication (Texas) see BNL-400-V.2	1955 1955	Pb
R-2	Remund A.E.	Helv. phys. acta, 29, 545	1956	Cu, Ta, Pb, Bi
R-3	Rosen L., Stewart L.	Phys. Rev., 107, 824	1957	Ta Bi
R-4	Rayburn L.A.	Phys. Rev., 116, 1571	1959	Zn, Sn, Sb, Pb, Bi

$E_{n'}$ MeV	$\Delta E_{n'}$, MeV	Neutron Source	Detector (E_{thr}, MeV)	Interval of θ or cos θ investigated	Remark
2,45 2,85 4,0 4,9 5,8	0,13 0,12 0,275 0,340 0,240	T (p,n) D (d,n)	Liquid organic scintillator	30—150°	Time of flight. Normalized to σ(C)
2,9	0,10	D (d,n)	Spherical chamber hydrogen ionisation	30 — 150°	Ring geometry. Calibration of detector with incoming beam.
2,8	-	D (d,n)	Spherical chamber hydrogen ionisation	25—140°	Ring geometry.
3,1	-	D (d,n)	Hydrogen ionisation chamber	20 — 150°	Ring geometry.
1,5;2,0 2,5	~0,10	T (p,n)	Biased scintillator	20—160°	$\Delta\vartheta$=6°. Calibration of detector with incoming beam
0,5;0,8	0,05	T (p,n)	Hydrogen proportional counter	30—140°	$\Delta\vartheta$=10°. Spherical scatterer used.
2,0	0,10	T (p,n)	Biased scintillator	20—160°	$\Delta\vartheta$ =6°. Spherical scatterer used.
1,8—3,5 2,0—3,5	0,10	T (p,n)	Biased scintillator	20—160°	$\Delta\vartheta$=6°. Spherical scatterer used.
1,0 3,7 5,0 15,0	0,03 0,28 0,22 0,80	Electrostatic accelerator with different targets	Plastic scintillator	10—150°	$\Delta\vartheta$=10°. Ring geometry.
3,3	-	D (d,n)	Biased scintillator	30—150°	
14	-	T (d,n)	Nuclear emulsion	5 — 150° 5 — 130°	$\Delta\vartheta \leq 8°$
14	≤ 1	T (d,n)	Biased scintillator (~11)	10— 165°	$\Delta\vartheta < 3$ for angles < 50°. Time of flight. Correction for inelastic scattering contribution done.

Reference Code	Author	Reference	Year of publication	Element studied
R-5	Rogers W.L., Garber D.I., Shrader E.F.	Bull. Amer. Phys. Soc., 6, 61 Private communication	1961 1962	F C, Ta
R-6	Reitman D., Smith A.B.	Bull. Amer. Phys. Soc., 7, 334 Private communication (Argonne) see BNL-400. V.2	1962 1962	Cu, Zr, Nb
R-7	Reitman D., Engelbrecht C.A., Smith A.B.	Nucl. Phys., 48, 593	1963	Zr, Nb
R-8	Roturier J., Irigaray J.L. Petitt G.Y.	C. r. Acad. sci., 260, 4491	1965	Be
R-9	Roturier J., Irigaray J.L. Lagardere M., Sonnaert S., Petitt G.Y.	J. de Phys Suppl., 27, 139	1966	K
S-1	Seagrave J.D.	Phys. Rev., 92, 1222	1953	^{4}He
S-2	Snowdon S.C., Whitehead W.D.	Phys. Rev., 94, 1267	1954	Sn, Bi
S-3	Shaw D.F.	Proc. Phys. Soc., A 68, 43	1955	^{4}He
S-4	Seagrave J.D.	Phys. Rev., 97, 757	1955	D
S-5	Seagrave J.D., Cranberg L.	Phys. Rev., 105, 1816	1957	D
S-6	Singletary J.B., Wood D.E.	Phys. Rev., 114, 1595	1959	C
S-7	Seagrave J.D., Cranberg L., Simmons J.E.	Phys. Rev., 119, 1981	1960	T, ^{3}He
S-8	Seagrave J.D., Cranberg L, Simmons J.E.	Private communication (Los Alamos), see BNL-400 - V.1	1961	Ca
S-9	Sayres A.R., Jones K.W. Wu C.S.	Phys. Rev., 122, 1853	1961	^{3}He

Note : For S-8' to S-11' see under C-8' to C-11'

$E_{n'}$, MeV	$\Delta E_{n'}$, MeV	Neutron Source	Detector (E_{thr}, MeV)	Interval of θ or cos θ investigated	Remark
} 0,565 } 1,C } 0,707 } 0,901	0,03	-	-	0,86 to- 0,73 0,86to- 0,54 } 0,86 to - 0,77	Time of flight. Normalized to σ(C)
0,34 — 1,19	~0,02	^{7}Li (p,n)	Biased scintillotor	0,86to- 0,80	Time of flight. Normalized to σ(C). Data represented by Legendre polymonials
0,3 — 1,5	~0,02	^{7}Li (p,n)	Biased scintillator	30 — 145°	Time of flight. Normalized to σ(C). Data represented by Legendre polynomials.
14,07	~ 0,08	T (d,n)	Plastic scintillator	7 — 170°	Time of flight.
14	-	T (d,n)	Plastic scintillator	15 — 150°	Time of flight.
2,61 — 6,50 14,3	0,06 0,10	D (d,n) T (d,n)	Recoil proportional counter	0,4 to- 0,8	Normalized to σ_t
3,7	0,2	D (d,n)	Plastic scintillator	13 — 140°	$\Delta\vartheta$ =10°. Ring geometry.
14,3	-	T (d,n)	Wilson chamber	0,9— 0,1	$\Delta\vartheta$ = 5°
14,1	0,05	T (d,n)	Scintillation telescope counter	0,7to - 0,98	-
2,45 3,27	0,05	T (p,n)	Biased scintillator	0,91 to- 0,97 0,86 to- 0,97	$\Delta\vartheta$ =3°. Time of flight. Normalized to σ(H)
14,1	-	T (d,n)	Nuclear emulsion	0,85 to- 0,88	
1—3,5 6,0	0,1 — 0,2	T (p,n) D (d,n)	Biased scintillator	27 — 161°	Time of flight. Normalized to σ_e.
1—6,0	0,2		Biased scintillator	0,95to- 0,9	Time of flight. Normalized to σ_e
2,6 — 17,5	0,02 — 0,05	E_n: 5Mev T(p,n) 8Mev D(d,n) 17,5 Mev T(d,n)	Proportional counter	48 — 170°	normalized to know σ_t

Reference Code	Author	Reference	Year of publication	Elements studied
S-10	Smith A.B.	Phys. Rev., 126, 718	1962	Th
S-11	Stelson P.H., Robinson R.L.	Bull. Amer. Phys. Soc., 7, 335 Private communication (Oak Ridge), see BNL-400 - V. 2	1962 1962	Sn, Pb "
S-12	Smith A.B.	Private communication (Argonne), see BNL-400 V.2	1962	Ta
S-13	Smith A.B.	Nucl. Phys., 47, 633	1963	U
S-14	Smith A.B., Guenther P.T.	INDSWG-48	1964	Al, Cr, Fe, Co, Ni, Cu, Zn, Zr, Nb, Mo, Ag, Cd, In, Sn, Sb, I, Sm, Gd, Yb, Ta, W, ^{184}W Pt, Au, Hg, Tl, Pb, Bi, Th, ^{235}U, U
S-15	Smith A.B.	Nucl. Sci. and Eng., 18, 126	1964	^{235}U (94% ^{235}U in the sample)
S-16	Smith A.B., Engelbrecht, C.A., Reitmann D.	Phys. Rev., 135, B76	1964	Co, Cu, Zn
S-17	Stelson P.H., Robinson R.L., Kim H.J., Rapoport J., Sachter G.R.	Nucl. Phys., 68, 97	1965	Mg, Al, Si, P, Cr, Ni, Zn, Cd, Sn, Sb, Pb, Bi
S-18	Stewart D., Currie W.M., Martin J., Martin P.W.	International Conference on the Study of Nuclear Structure with Neutrons. Paper 37. Antwerpen, Belgium.	1965	^{32}S, ^{24}Mg
T-1	Thomas R.G., Walt M., Walton R.B., Allen R.G.	Phys. Rev., 101, 759	1956	^{7}Li
T-2	Tsukada K., Tanaka S., Maruyama M.	J. Phys. Sos., Japan, 16, 166 Private communication (JAERI, Japan)	1961 1962	Ti, Fe, Zn

$E_{n'}$, MeV	$\Delta E_{n'}$, MeV	Neutron Source	Detector (E_{thr}, MeV)	Interval of θ or cos θ investigated	Remark
0,57–1,5	-	^{7}Li (p,n)	Biased scintillator (0,2)	20 – 150°	Ring geometry. Normalized to σ(C)
14	-	T (d,n)	Scintillation counter	~0,9 to ~0,5	Time of flight. Ring geometry.
0,35 – 1,1	~0,02	^{7}Li (p,n)	Biased scintillator	~0,7 to ~0,8	Time of flight. Normalized to σ(C)
0,3 – 1,5	~0,02	^{7}Li (p,n)	Liquid scintillator	from (20; 30) to 145°	Time of flight. Normalized to σ(C). Data represented by Legendre polynomials.
0,3 – 1,5	~0,02	^{7}Li (p,n)	Liquid scintillator	20 – 145°	Time of flight. Normalized to σ(C). Data represented by Legendre polynomials.
0,3 – 1,5	0,025 – 0,065	^{7}Li (p,n)	Liquid scintillator	from (20; 30) to 145°	Time of flight. Normalized to σ(C). Data represented by Legendre polynomials.
0,3 – 1,5	0,02 at E_n = =0,5	^{7}Li (p,n)	Liquid scintillator	20 – 145°	Time of flight. Normalized to σ(C). Data represented by Legendre polynomials.
14	0,2 – 0,3	T (d,n)	Plastic scintillator (from 6 to 9)	from (20; 47) to (98; 133°)	Time of flight.
6	-	-	—	30 – 150°	Time of flight.
0,21 – 0,275	0,010 – 0,015	^{7}Li (p,n)	Hydrogen counter	30 – 135°	-
3,4 – 4,6	~0,4	D (d,n), ^{3}He	Biased scintillator	90°	Time of flight.

Reference Code	Author	Reference	Year of publication	Elements studied
T-3	Thomson D.B.	Not published thesis. Private communication (Los Alamos), see BNL-400 - V.2	1960 1961	Nb
T-4	Tesch K.	Nucl. Phys., 37, 417	1962	B, C, S
T-5	Towle J.H., Gilboy W. B.	Nucl. Phys., 32, 610	1962	Na
T-6	Thomson D.B., Granberg L., Levin J.S.	Phys. Rev., 125, 2049	1962	Mg
T-7	Towle J.H., Gilboy W. B.	Nucl. Phys., 39, 300 Private communication (Aldermaston) - BNL-400 - V.1	1962 1962	Al
T-8	Tsukada K., Tanaka S., Maruyama M., Tomita Y.	"Physics of Fast and Intermediate Reactors", Vienna. V.1, p. 75	1962	Al, Si, P, S, Zn
T-9	Tanaka S.	J. Phys. Soc. Japan, 19, 2249	1964	Al, Si, P, S, Zn
T-10	Towle J.H., Gilboy W. B., Owens R.O.	International Conference on the Study of Nuclear Structure with Neutrons. Paper 38. Antwerpen, Belgium.	1965	^{51}V ^{89}Y
T-11	Towle J.H., Gilboy W. B.	Nucl. Phys., 72, 515	1965	K
V-1	Vincent L.D., Morgan I.L., Prud'homme J.T.	WADD TR-60-217	1960	Mo, Ca
W-1	Wantuch E.	Phys. Rev., 84, 169	1951	D
W-2	Walt M., Barschall H.H.	TID-5157	1953	U
W-3	Whitehead W.D., Snowdon S.C.	Phys. Rev., 92, 114	1953	Al, Fe, Pb

E_n, MeV	ΔE_n, MeV	Neutron Source	Detector (E_{thr}, MeV)	Interval of θ or cos θ investigated	Remark
5	-	-	Biased scintillator	0,94to - 0,87	Time of flight.
14,1	-	T (d,n)	Scintillotion counter	20 – 160°	Time of flight.
0,8 – 4,0	-	T (p,n)	Biased organic liquid scintillator	0,85 to - 0,75	Time of flight. Normalized to σ(H)
2 – 4,0 5,0	-	T (p,n) D (d,n)	Plastic scintillator	0,93 to - - 0,876	Time of flight. Normalized to σ(H) at 45° for each E_n
1 – 4	0,1 – 0,06	T (p,n)	Biased liquid scintillator	30 – 137°	Time of flight. Normalized to σ(H)
3,4 – 4,6	0,25; 0,15	D (d,n)	Biased scintillator	~0,9 to ~ 0,9	$\Delta\vartheta$ =7°. Time of flight.
3,5 – 4,8	0,25 – 0,15	D (d,n)	Plastic scintillator	15 – 160°	$\Delta\vartheta$ = 7°. Time of flight.
2,35 3,77	-	T (p,n)	Biased scintillator	0,85 to- 0,72	Time of flight. Normalized to σ(H)
1,49 – 3,76	~0,09	T (p,n)	Biased organic	30 – 136°	Time of flight. Normalized to σ(H).
4,1	0,4	-	Biased scintillator (~0.4)	0,94to - 0,72	$\Delta\vartheta$ = 10°. Time of flight.
4,5 5,5	0,1	D (d,n)	Recoil proportional counter Telescope counter	80 – 180° 70 – 180°	-
1	0,09 – 0,16		Biased proportional counter (0.85)	0,87 to- 0,87	-
3,7	0,2	D (d,n)	Plastic scintilla tor	13 – 127°	$\Delta\vartheta$ =10°. Ring geometry. Some contribution from inelastic scattering : Al < 15%, Fe and Pb < 20%.

Reference Code	Author	Reference	Year of publication	Element studied
W-4	Walt M., Barschall H.H.	Phys. Rev., 93, 1062	1954	Ti, Fe, Co, Ni, Cu, Zn, Se, Sr, Zr, Nb, Mo, Ag, Cd, In, Sn, Sb, Te, Ba, Ce, Hf, Ta, W, Au, Hg, ^{206}Pb, Pb, Bi, Th
W-5	Walt M., Beyster J.R.	Phys. Rev., 98, 677	1955	Be, C, Al, Ti, Fe, Zn, Zr, Cd, Sn, Ta, W, Au, Pb, Bi
W-6	Willard H.B., Bair J.K., Kington J.D.	Phys. Rev., 98, 669	1955	Be, B, ^{10}B, C
W-7	Willard H. B., Bair J.K. Kington J.D., Cohn H.O	Phys. Rev., 101, 765	1956	^{6}Li, ^{7}Li
W-8	Walt M., Beyster J.R.	LA-2061	1956	^{238}U
W-9	Wills J.E., Bair J.K., Cohn H.O., Willard H. B.	Phys. Rev., 109, 891	1958	C, F
W-10	Willard H.B., Bair J.K., Kington J.D., Willard H. B.	Phys. Rev., 94, 786 A. Private communication (Oak Ridge), see BNL-400 - V.1	1955 1962	Li
W-11	Wong C., Anderson J.D. Mc Clure J.W.	Nucl. Phys., 33, 680	1962	Li, ^{6}Li, ^{7}Li
W-12	Wilenzick R.M., Seth K. K., Bevington P.R., Lewis H.W., Wilenzich R.M.	Bull. Am. Phys. Soc., 1, 23 Private communication, (Duke) BNL-400 -V.1,2	1962 1962	C, Fe, Y, Mo, Sn, Bi
W-13	Wilenzick R.M., Seth K. K., Bevington P.R., Lewis H.W.	Nucl. Phys., 62, 511	1965	C, Fe, Y, Mo, Sn, Bi
W-14	Western G.T., Williams J.R., Carter H.G.	CONF-660303, Book 2, Physics. TID-4500	1966	Nb
Y-1	Yuasa K.	J. Phys. Soc. Japan, 13, 1248	1958	Al, Fe, Pb, Bi

$E_{n'}$ MeV	$\Delta E_{n'}$ MeV	Neutron Source	Detector (E_{thr}, MeV)	Interval of θ or cos θ investigated	Remark
1	0,09-0,16	^{7}Li (p,n)	Biased proportional counter (~0.75)	30 — 150°	-
4,1	0,08	T (p,n)	Biased scintillator (~ 3,2)	12,5 — 150°	-
0,54-0,70 0,43-1,2 0,55-1,5	0,008 0,04to 0,015 0,05	^{7}Li (p,n)	Biased proportional counter	0,86 to ~ - 0,80	Be B ^{10}B ; C
0,21-0,3 0,2-0,6	0,02	^{7}Li (p,n)	Biased proportional counter	0,84 to ~ - 0,76	Not corrected for multiple scattering and angular resolution.
2,5;4,1	0,2 ; 0,08	T (p,n)	Biased scintillator (2 and 3,2)	0,97 to -0,94	-
1,45-4,1 0,66-2,92		^{7}Li (p,n) - - E_n < 1,5 T (p,n) - - E_n > 1,5	Biased proportional counter	0,8; 0,6 - 0,8	C(ΔE<0,05 MeV for all E_n, except for 1,45 and for 2,02 MeV, where ΔE 0,1 MeV) F (ΔE not given)
0,260	0,025	^{7}Li (p,n)	Biased proportional counter (0.6 Eń)	-	-
14	-	T (d,n)	Plastic scintillator	20 — 130°	Time of flight.
6	0,23	D (d,n)	Biased liquid scintillator	0,95 to - 0,78	Time of flight. Normalized to σ(C)
6	0,23	D (d,n)	Biased liquid scintillator	20 — 150°	Time of flight. Normalized to σ(C)
14,7	0,30	T (d,n)	-	20 — 140°	Time of flight. $\Delta\sigma$<1
14	-	T (d,n)	Biased scintillator (~10-11)	70 — 170°	$\Delta\sigma$=2-4°. Calibration of detector with incoming beam.

Reference Code	Author	Reference	Year of publication	Elements studied
Y-2	Young P.G., Ohlsen G.G., Okhuysen P.L.	Austral. J. Phys., 16, 185	1963	^{4}He
Y-1'	Yankov G.B.	Private communication	1965	Zn, Se, Zr, Nb, Mo, Cd, In, Sn

$E_{n'}$, MeV	$\Delta E_{n'}$ MeV	Neutron Source	Detector (E_{thr}, MeV)	Interval of θ or cos θ investigated	Remark
1,79	0,05	T (p,n)	Plastic scintillator	25 -- 135°	Normalized to σ_t = 4,5 barn.
0,4	-	T (p,n)	Hydrogen proportional counter	20 – 150°	Calibration of detector with incoming beam.

SUBJECT INDEX

Reproduced by the IAEA in Austria
January 1976
75-10224